

SPIE PRESS



SPIE

Color Vision and Colorimetry

THEORY and APPLICATIONS

Second Edition

Daniel Malacara



Color Vision and Colorimetry

THEORY and APPLICATIONS

SECOND EDITION

Library of Congress Cataloging-in-Publication Data

Malacara, Daniel, 1937-

Color vision and colorimetry : theory and applications / Daniel Malacara. – 2nd ed.

p. cm. – (Press monograph ; 204)

Includes bibliographical references and index.

ISBN 978-0-8194-8397-3

1. Color vision. 2. Colorimetry. I. Title.

QP483.M353 2011

617.7'59–dc22

2011007283

Published by

SPIE

P.O. Box 10

Bellingham, Washington 98227-0010 USA

Phone: +1 360.676.3290

Fax: +1 360.647.1445

Email: Books@spie.org

Web: <http://spie.org>

Copyright © 2011 Society of Photo-Optical Instrumentation Engineers (SPIE)

All rights reserved. No part of this publication may be reproduced or distributed in any form or by any means without written permission of the publisher.

The content of this book reflects the work and thoughts of the author(s).

Every effort has been made to publish reliable and accurate information herein, but the publisher is not responsible for the validity of the information or for any outcomes resulting from reliance thereon.

Printed in the United States of America.

First printing



Color Vision and Colorimetry

THEORY and APPLICATIONS

SECOND EDITION

Daniel Malacara

SPIE
PRESS

Bellingham, Washington USA

Contents

Preface to the Second Edition.....	ix
Preface to the First Edition	xi
Chapter 1 The Nature of Color	1
1.1 Introduction	1
1.2 Newton's Color Experiment.....	4
1.3 Theories and Experiments in Color Vision	4
1.4 Some Radiometric and Photometric Units	8
1.4.1 Radiometric units.....	8
1.4.2 Photometric units.....	10
1.5 Color Sensitivity of the Eye.....	14
1.6 How Materials are Colored or Modify Color	16
1.7 Absorption and Interference Filters	18
References	20
Chapter 2 Light Sources and Illuminants	23
2.1 Introduction.....	23
2.2 Blackbody Radiation and Color Temperature	23
2.3 Tungsten Lamps.....	24
2.4 Gas Discharge and Fluorescent Lamps.....	26
2.5 Light-Emitting Diodes.....	28
2.6 Television and Computer Displays	31
2.7 Standard Light Sources and Illuminants	33
2.8 Color-Rendering Index of Light Sources.....	35
References	38
Chapter 3 The Human Eye	41
3.1 Anatomy of the Eye.....	41
3.2 Eye Resolving Power and Eye Aberrations	44
3.3 Stiles–Crawford Effect.....	45
3.4 Eye Response to Pulsating Light	45
3.5 Visual Detectors in the Retina	47

3.6	Observation of the Human Eye Retina	48
3.7	Cone Fundamentals	51
	References	54
Chapter 4	Trichromatic Theory	59
4.1	Grassmann Laws	59
4.2	Maxwell's Triangle.....	59
4.3	Color-Matching Experiments.....	60
4.4	Color-Matching Functions $\bar{r}(\lambda)$, $\bar{g}(\lambda)$, and $\bar{b}(\lambda)$	63
4.5	Tristimulus Values R , G , B	64
4.6	Chromaticity Coordinates r , g , b	68
	References	72
Chapter 5	CIE Color Specification System	75
5.1	The CIE Color System	75
5.2	Color-Matching Functions $\bar{x}(\lambda)$, $\bar{y}(\lambda)$, and $\bar{z}(\lambda)$	76
5.3	Tristimulus Values X , Y , Z	82
5.4	Chromaticity Coordinates x , y , z	82
5.5	Dominant Wavelength and Correlated Color Temperature.....	85
5.6	The Color of a Transparent or Opaque Body	91
5.7	Color Discrimination Mechanisms	97
5.8	Use of Cone Sensitivities as Color-Matching Functions	99
	References	101
Chapter 6	Uniform Color Systems	103
6.1	Introduction.....	103
6.2	Hue and Chroma in the CIE Diagram.....	104
6.3	The Munsell System.....	105
6.4	The 1960 CIE $L\ u\ v$ Color Space.....	110
6.5	The 1976 CIE $L^*\ u^*\ v^*$ Color Space.....	112
6.6	The Hunter $L\ a\ b$ Color Space.....	114
6.7	The 1976 CIE $L^*\ a^*\ b^*$ Color Space.....	116
6.8	Color-Difference Equation in the CIE $L^*\ a^*\ b^*$ Color Space.....	120
6.9	MacLeod and Boynton Chromaticity Diagram.....	125
6.10	Derrington, Krauskopf, and Lennie (DKL) Color Space	125
6.11	Other Color Spaces.....	127
	References	127
Chapter 7	Color Mixtures and Colorants	131
7.1	Color Addition	131
7.2	RGB Color System for Cathode Ray Tubes.....	133
7.3	Color Subtraction	137

7.4	Metamerism	138
7.5	Colorants	140
7.6	Color Matching and Color Management.....	140
	References	144
Chapter 8	Color Measurements and Color Defects.....	147
8.1	Introduction.....	147
8.2	Visual Chromatic Defects.....	147
8.3	Whiteness and White Standards.....	150
8.4	Pantone® Colors, GretagMacbeth ColorChecker®, and Spectralon® Standards	151
8.5	Optical Configurations to Measure Reflectance	152
8.6	Precision and Accuracy of Measuring Instruments.....	156
8.7	Spectrocolorimeters.....	157
8.8	Tristimulus Photocolorimeters.....	159
8.9	Visual Colorimeters.....	161
	References	162
General References	165	
Index.....	171	
Biography	177	

Preface to the Second Edition

This book has been rewritten, updated, and enlarged, describing the basic principles of color vision and colorimetry. The history of color and the main methods used to measure color and their associated color systems are described. Also, the human eye and its color detectors are explained with some detail. The book has been written with students in an introductory color course in mind. More specialized color techniques, mainly computational color management, are treated only superficially, but there are several excellent books that can be read after studying this book, for example, the books *Computational Color Technology* and *Color Technology for Electronic Imaging Devices*, by H. R. Kang, published by SPIE Press.

Chapter 1 introduces the reader to the main concepts, definitions, and nature of color, including a definition of the main radiometric and photometric units related to color. Chapter 2 describes the main natural and artificial light sources used in colorimetry and the illuminants used as standards in colorimetry. In Chapter 3 the human eye is briefly described, with more emphasis on the retinal detectors—primarily, the role of cones in color vision. In Chapter 4 the history and fundamentals of the trichromatic theory in the r , g , b system are described. In Chapter 5 the CIE x , y , z color specification system is introduced with all of the basic mathematical tools for colorimetry. The mathematical procedure used to transform the r , g , b system to the CIE x , y , z system, a procedure that is not commonly available in most books, is described with some detail. This chapter contains many tables with colorimetric data and standards that can be of use to those working in color-measuring systems. Chapter 6 introduces the readers to the uniform color systems, describing their main differences and limitations. Special emphasis is given to the CIE $L^*U^*V^*$ and CIE $L^*A^*B^*$ uniform color systems, which are now frequently used. In Chapter 7 the principles and mechanisms to produce and predict the color of colorant or pigment mixtures and their use are described, and finally, in Chapter 8 some of the most common methods and instruments used for color measurements are described with their calibration procedures. At the end of each chapter and at the end of the book, a good number of references are given for the benefit of those students who desire to deepen their knowledge of this interesting field.

The author is grateful to Marissa Vásquez Martínez for her efficient secretarial help, Zacarias Malacara for his advice, and especially to my doctoral student Armando Gómez for his help with some technical discussions and proof reading of the manuscript.

*Daniel Malacara
León, Gto., México
May 2011*

Preface to the First Edition

This book is written for those who want to understand the basic principles of color vision and colorimetry but have no previous training in this field. The history of color, the main methods used to measure color, and their associated color systems are described. The human eye and its color detectors are also explained with some detail.

Chapter 1 introduces the reader to the main concepts, definitions, and the nature of color, including a definition of the main radiometric and photometric units related to color. Chapter 2 describes the key natural and artificial light sources used in colorimetry, and the standard illuminants used in colorimetry. In Chapter 3, the history and fundamentals of the trichromatic theory in the r, g, b system are described. In Chapter 4, the CIE color x, y, z specification system is introduced with all the basic mathematical tools for colorimetry. The mathematical procedure used to transform color from the r, g, b system to the CIE x, y, z system, which is not commonly available in most books, is described in some detail. This chapter contains many tables with colorimetric data and standards that can be of some use to those working in color measuring systems. Chapter 5 introduces the reader to the uniform color systems, describing their main differences and limitations. Special emphasis is placed on the CIE $L^*U^*V^*$ and CIE $L^*A^*B^*$ uniform color systems, which are now frequently used. In Chapter 6, the principles and mechanisms to produce and predict the color of colorant or pigment mixtures and their use is described. Chapter 7 covers some of the most common methods and instruments used for color measurements with their calibration procedures. Finally, in Chapter 8 the human eye is briefly described, with emphasis on the retinal detectors, but most importantly on the role of the cones in color vision.

At the end of each chapter, and at the end of the book, a good number of references are given for the benefit of those readers who wish to deepen their knowledge of this interesting field.

The author is grateful to Prof. Donald McCloud, Yobani Mejía and Didia P. Salas for their help and technical discussions.

*Daniel Malacara
March 2002*

Chapter 1

The Nature of Color

1.1 Introduction

Electromagnetic waves can have many different wavelengths and frequencies in a range known as the electromagnetic spectrum, as illustrated in Fig. 1.1. Light is a narrow range of electromagnetic waves that the eye can detect. Different wavelengths of light produce different perceptions of color. The longest wavelengths produce the perception of red, while the shortest ones produce the perception of violet. The spectrum in the visible, ultraviolet (UV), and infrared (IR) regions is classified in Table 1.1.

Humans have been quite interested in color for many centuries. However, the scientific beginning of color studies goes back only to Newton when he performed his classic experiment with a prism, as shown in Fig. 1.2, and as detailed in Section 1.2.

The sensation of color is produced by the physical stimulation of the light detectors—known as *cones*—in the human retina. The color spectrum produced by an ideal prism or a diffraction grating is formed by a display of all of the spectrally pure or monochromatic colors. Each color has a different wavelength. The wavelength values corresponding to each color in the spectrum produced by a prism are quite nonlinear. The diffraction grating produces a more linear spectrum. For illustration purposes we will represent the spectrum with a linear chromatic dispersion, as illustrated in Fig. 1.3. Different spectrally pure colors are said to

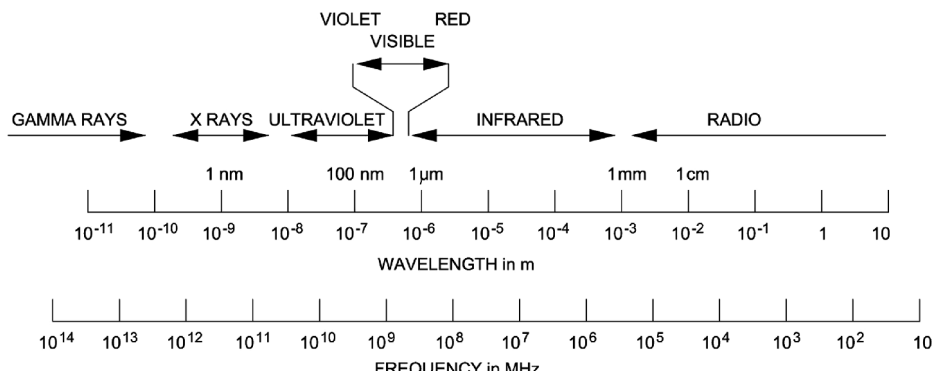
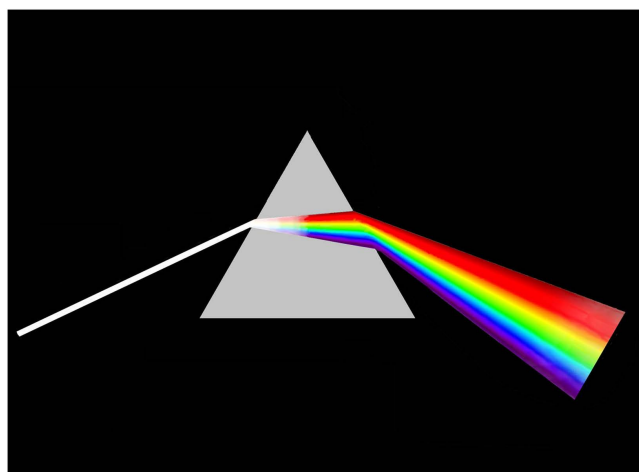
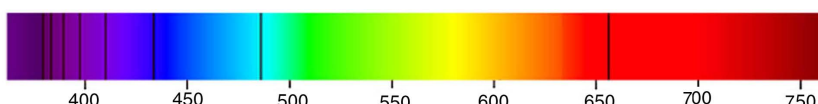


Figure 1.1 Electromagnetic spectrum.

Table 1.1 Ultraviolet, visible, and infrared regions of the electromagnetic spectrum.

Spectral region	Wavelength range (nm)	Subregion
Ultraviolet	100–280	UV-C
	280–315	UV-B
	315–380	UV-A
Visible	380–430	Violet
	430–500	Blue
	500–520	Cyan
	520–565	Green
	565–580	Yellow
	580–625	Orange
	625–740	Red
Infrared	740–1400	Near IR
	1,400–10,000	Far IR

**Figure 1.2** Newton's prism experiment.**Figure 1.3** Color visible spectrum with hydrogen spectral lines as a reference.

have different hues. A spectrally pure or monochromatic color can be produced by a single wavelength. For example, an orange color is associated with a wavelength of 600.0 nm. However, the same color can be produced with a combination of two light beams: one being red with a wavelength of 700.0 nm, and another being yellow with a wavelength of 580.0 nm, and with no orange component with a wavelength of 600.0 nm. In conclusion, when we refer in this book to a spectrally pure light beam it does not mean that it is formed by a single-wavelength beam, as

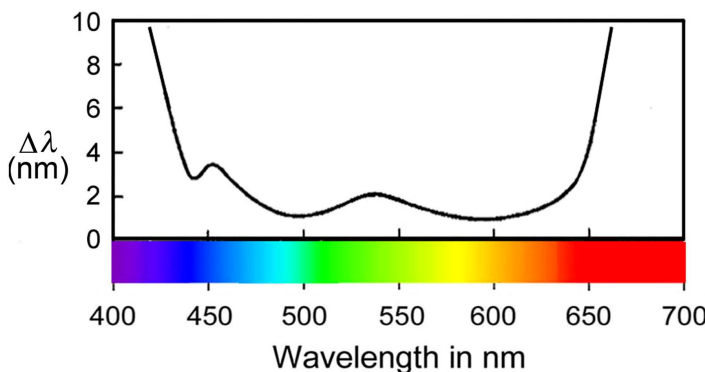


Figure 1.4 Color discrimination in a color spectrum.

in traditional physical or interferometry books (Born and Wolf, 1999). Instead, it means that it has the same color as the single-wavelength light beam matching its color. The two or more components used to produce a color cannot be identified by the eye, only with an instrument called a spectroscope. For this reason we say that the eye is a synthesizer device. In contrast, when the ear listens to an orchestra, the individual instruments producing the sound can be identified. Thus, we say that the ear is an analyzer. An interesting property of the spectrum is that the minimum wavelength separation between two close colors that can be identified as being different is not the same for different parts of the spectrum (Wright and Pitt, 1934). This is illustrated in Fig. 1.4. Colors arise due to the interaction of light with material bodies, for example, chromatic dispersion in glass or water, diffraction, etc. For a complete list of physical phenomena that may produce or modify colors, see Chapter 7 by Nassau in the book edited by Shevell (Shevell, 2003).

Color vision is not exclusive to human beings. Many animals also have this ability. The information contained in the light coming from the world around us is not only in the intensity, but also in its color. For this reason the study of color vision is quite important from an evolutionary point of view, as pointed out by Neitz et al. (2001). The human eye can distinguish about 200 different levels of gray, but the number of different possible combinations that the human eye can discriminate greatly increases with color vision, thereby expanding the amount of information that can be extracted from a scene.

Not all colors in nature are spectrally pure, since they can be mixed with white. In this manner, a mixture of red and white produces a pink color that goes from pure red (100% saturated) to white (0% saturated), depending on the relative amounts of red and white. Colors obtained by mixing a spectrally pure color with white are said to have the same *hue* but different *saturation*. The degree of saturation is called the *chroma*. The relative amounts of a mixture of white and a spectrally pure color determine the color saturation, or chroma.

Combinations of spectrally pure colors and white cannot produce all possible colors in nature. Let us consider two identical samples of a spectrally pure red color. If one of them is strongly illuminated and the other is almost in darkness,

the two colors look quite different. In another example, if a pure red is mixed with some black paint, its appearance is different. In these two examples the difference between the two red samples is its lightness. Therefore, any color has to be specified by three parameters, i.e., hue, saturation (or chroma), and luminance, or any other three equivalent parameters, as will be described later in more detail.

1.2 Newton's Color Experiment

The history of the first color theories and experiments is quite interesting, as described in the review articles by MacAdam (1975), Neil and Steinle (2002), Mollon (2003), and Masters (2011). The first experiment in color, performed with a prism by Newton in 1671, demonstrated color dispersion. He used a triangular prism, as illustrated in Fig. 1.2, in a position so that a narrow beam of sunlight entering into the room passed through the prism. When this beam was projected onto a screen, a band of light with different colors appeared, forming what he called a spectrum (ghost). Newton said that the spectrum was formed by seven colors, i.e., red, orange, yellow, green, blue, indigo, and violet, probably in close analogy with the seven musical notes. This experiment immediately suggested the idea that white light is formed by the superposition of all colors. To prove this idea, Newton used another prism to recombine all colors from the spectrum into a white beam of light. Newton was very careful to state that the spectrum colors are not the only ones in nature. For example, new colors can be obtained by diluting them with the addition of white, thus changing their saturation. New colors can also be produced by increasing or reducing their intensity. In the case of paints, this is equivalent to mixing them with black paint or to increasing the level of illumination.

Newton also tried to recombine only certain parts of the spectrum by blocking out some colors produced by the first prism, by means of diaphragms. When he recombined two different bands of color, a third color appeared, frequently, but not always, matching one between these two. By combining the two ends of the spectrum (red and violet) in different proportions, he was able to obtain a new gamut of purple colors ranging from red to violet. Newton announced his investigations in color to the Royal Society of London in 1672.

The first color diagram was devised by Newton by drawing a circle listing all of the colors of the spectrum. Both spectrally pure colors and purple colors (produced by mixing in different proportions the colors at the ends of the spectrum) were drawn around the circle with white at the center, as shown in Fig. 1.5. Colors formed by a mixture of the pure spectral colors and white are between the center and the circumference. Complementary colors are on opposite points with respect to the center. If this circle is made on a piece of cardboard and placed on the axis of a rotating top, all colors mix to produce the impression of a colorless gray.

1.3 Theories and Experiments in Color Vision

After Newton's experiment, the next important contribution to the understanding of color came when Mariotte (1717) said that three colors are sufficient to produce

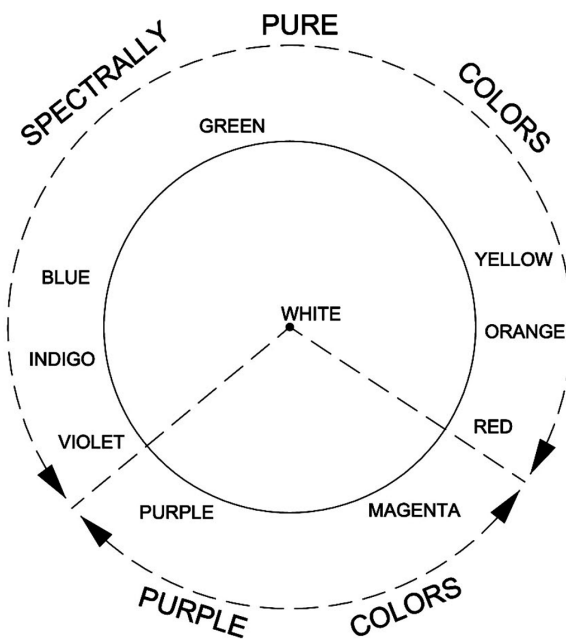


Figure 1.5 Newton's circle.

any color when using the proper combination of them. This concept was formally reintroduced by Palmer (1777) in a manuscript that was discovered in 1956, adding the concept of three different color receptors in the retina. In 1801, probably unaware of the previous work by Palmer, Young (1802) refined the trichromatic theory of color and postulated that all colors in nature could be matched with three different colors, which he called primary colors. He also postulated that the eye has three types of photoreceptors, one for each primary color. The problem with this theory is determining which colors are primary.

This so-called trichromatic theory of color was found satisfactory, but it did not explain many details. About 50 years later von Helmholtz (1852, 1866) revived and improved Young's ideas by adding more details based on experiments. For this reason, the trichromatic theory of light is now known as the Young–Helmholtz theory. Around this time, many other researchers were doing interesting optical color experiments. For example, Peirce (1877), who is considered the first experimental psychologist, made several color experiments that were described in a notebook labeled "Hue," and Rayleigh (1881) studied the matching of colors by many people.

Hering (1964) noticed that yellow and blue appear to be opposite colors. In other words, there is no bluish yellow or yellowish blue. In the same manner, red and green are opposite colors. Hering proposed a theory to explain this with four colors—red, yellow, green, and blue—as primaries. (Later, we will see that although this theory is not correct in detail, it has some interesting concepts that deserve consideration.) Hering assumed that the brain has a detector for yellow and blue light, followed by a classifier to determine the relative luminance of these two

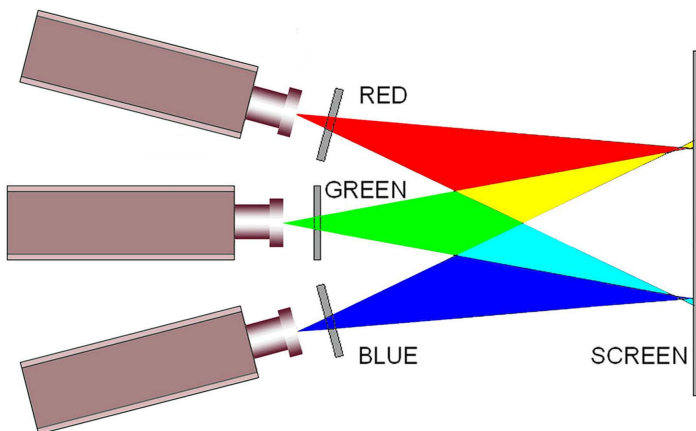


Figure 1.6 Maxwell's experiment.

colors. In the same manner, he assumed another detector for red and green light, followed by another brain classifier to determine the relative quantities of these two colors. Further, he assumed another classifier for white and black.

Almost simultaneously with the work of von Helmholtz (1861), Maxwell (1856, 1857, 1860, 1885) studied the perception of color and performed an experiment, as illustrated in Fig. 1.6, to produce a fully colored image, thus proving the Young–Helmholtz theory. He took three black and white photographs (positive transparencies) of the same scene (a colored ribbon), using three different colored filters in front of each of the three shots. Then, he projected the three pictures simultaneously with three projectors with each of the three colored filters in front of each projector. He assumed that the black and white photographic emulsion was equally sensitive to the three used colors. Unfortunately, his basic assumption was far from being true, since the photographic films used at the time were much more sensitive to the blue light. Evans (1961) describes that Maxwell obtained reasonably good results (with a color deficiency in the red and green) in spite of this because the three colored filters transmitted some light in the ultraviolet. In 1890, König (1903) assumed in a formal manner the previous hypothesis by his predecessors that there are three color detectors in the eye: one for red, one for green, and another for blue light. Frederick E. Ives (1888) repeated Maxwell's experiment using photographic emulsions that were sensitive over the whole luminous spectrum, and set up the main principles that led to modern color photography.

The *zone* color theories combine the opponent and trichromatic models. According to these theories, the trichromatic signals produced by the cones in the retina are sent to the brain, where they are converted into three opponent signals, two of them chromatic and one achromatic. These theories have now been discarded, but not completely, as we will describe in Section 5.7.

Ribe and Steinle (2002) point out that von Goethe (1988) contributed important research in color vision and published a book in 1810 entitled *Theory of Colors*.

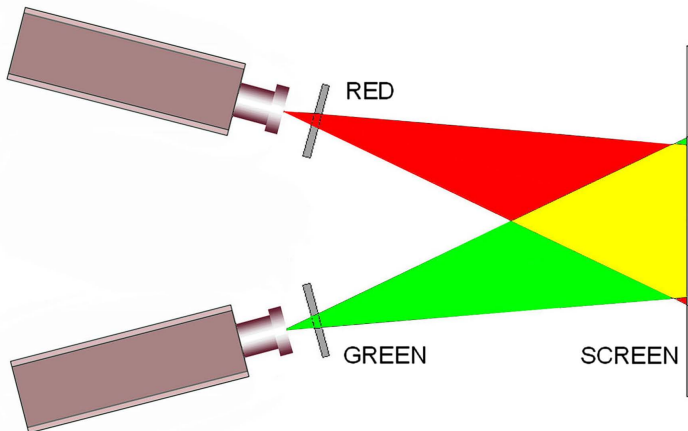


Figure 1.7 Edwin Land's experiment.

Unfortunately, his research was ignored for many years, but recently it has been rediscovered, and many important physicists after him have been fascinated by his book.

A more recent model is the *retinex* theory developed by Land (1977) and described by Kaiser and Boynton (1996) and by Ribe and Steinle (2002). In the 1950s, Land made an impressive modification to the three-projector experiment by Maxwell. Land was able to project a full-color scene with only two colors, such as red and green or even red and white, as shown in Fig. 1.7. According to the trichromatic theory, a picture with only different shades of pink should be observed if only a red and a white projector are used. Land's important conclusion is that the results from the classical trichromatic theory are valid only when the observed color samples are surrounded by a dark environment, and that important deviations from the classical results appear when many colored objects are simultaneously observed. A detailed analysis of this experiment and the theory behind it is found in the articles by Land (1959) and by Judd (1960). Land's theory and experiment can explain our capacity to observe undistorted colors under a large variety of illumination conditions. For example, a white piece of paper appears to be white under daylight illumination and also under an incandescent tungsten lamp. This remarkable process, known as chromatic adaptation, will be described in more detail in Section 5.7 (Judd, 1951, 1952).

To complicate the color vision models even further, it is easy to show that flickering white light, produced by the alternation of bright and dark fields, can produce color sensations that depend on the flickering frequency. If this frequency is sufficiently high—more than ~ 60 Hz—fusion occurs, and no flickering effects are observed. By means of flickering at frequencies smaller than 60 Hz, the so-called subjective or Fetchner colors can be produced. These can be produced with rotating disks with many different patterns. Probably the best known is Benham's disk as shown in Fig. 1.8 (Benham, 1894). Colored rings are observed when the disk is rotated at a speed of 5–10 revolutions per second. Since the pattern is

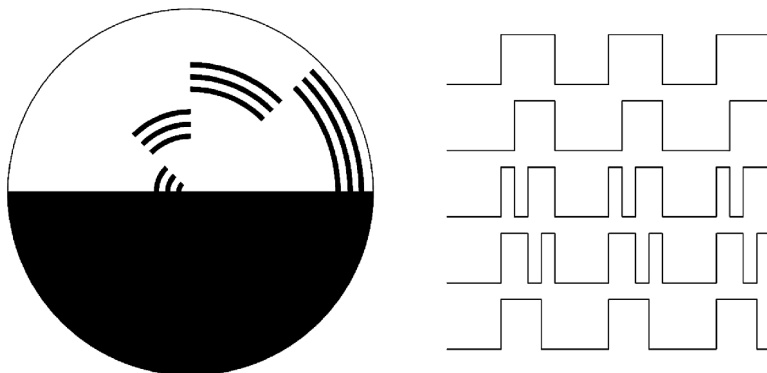


Figure 1.8 Benham's disk with the light-intensity distribution as a function of time.

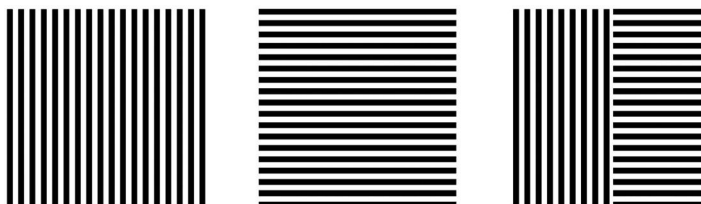


Figure 1.9 McCollough effect. The first and second patterns are observed for about 5–10 min, with alternating fixations of 10 sec. Then, the third pattern is observed. Pale greens appear on the left half and pale reds on the right half.

not rotationally symmetrical, different colors are observed not only for different speeds, but also for different directions of rotation.

Another interesting effect related to flickering is the McCollough effect, as illustrated in Fig. 1.9. The first two patterns, with vertical and horizontal lines, respectively, should be observed for ~10 min in an alternating manner, for ~10 sec each, and then the third pattern is observed. Pale green will be seen where the vertical lines are and pale red where the horizontal lines are. In conclusion, the perception of color is not a purely physical mechanism but also physiological and psychological. Many interesting phenomena related to color appear when studying the psychophysics of the eye, as described in many publications, for example in Chapter 13 in the book by Lee (2005).

1.4 Some Radiometric and Photometric Units

Many concepts in color theory cannot be fully understood without clear definitions of some radiometric and photometric units (Ohno, 2010; Zalewski, 2010). In this section, before going to more interesting matters, we will begin the tedious work of defining some of the most important quantities used in colorimetry studies.

1.4.1 Radiometric units

The most basic definition is that of *radiant flux* ϕ_R , which is the radiant energy per unit time (power) transported by a light beam, measured in watts (J/s). The

irradiance or *radiant incidence* E is the area density of radiant flux received by an illuminated body, integrated for all wavelengths and all directions. It is measured in watts per square meter, and defined by

$$E = \frac{\text{radian flux}}{\text{area}} = \frac{d\phi_R}{dA}. \quad (1.1)$$

The *spectral irradiance* $E(\lambda)$, defined as the irradiance per unit wavelength interval, at the wavelength λ , is related to irradiance E by the relation

$$E = \int_0^\infty E(\lambda) d\lambda. \quad (1.2)$$

Similar to irradiance, or radiant incidence, the *radiant exitance* M of an extended light source, defined as the area density of the total radiant flux emitted and integrated for all wavelengths and all directions, is

$$M = \frac{\text{emitted radiant flux}}{\text{area}} = \frac{d\phi_R}{dA}. \quad (1.3)$$

The *radiant intensity* I of a point light source (or an extended light source observed from a distance much larger than the light source size), defined as the total radiant flux, integrated for the whole area of the source and all wavelengths, emitted per unit solid angle in a given direction, is

$$I = \frac{d\phi_R}{d\Omega}. \quad (1.4)$$

The *spectral radiant intensity* $I(\lambda)$, defined as the radiant intensity per unit wavelength interval, at the wavelength λ , is related to the radiant intensity I by

$$I = \int_0^\infty I(\lambda) d\lambda. \quad (1.5)$$

Thus, the spectral radiant intensity is, in general, a function of the direction as well as of the wavelength.

The *radiance* L of an extended light source, defined as the radiant flux per unit solid angle, per unit of projected area, in a given direction, integrated for all wavelengths, is

$$L = \frac{\text{radian flux per steradian}}{\text{projected area}} = \frac{d^2\phi_R}{dA_P d\Omega} = \frac{1}{\cos \theta} \frac{d^2\phi_R}{dA d\Omega}, \quad (1.6)$$

where the projected area A_P is equal to the area A of the source multiplied by the cosine of the angle θ between the line of sight and the normal to the source. The

Table 1.2 Some radiometric units.

	Name	Formula	Units
Illuminated object	Irradiance = radiant incidence	$E = \frac{d\phi_R}{dA}$	$\text{W} \cdot \text{m}^{-2}$
	Spectral irradiance	$E(\lambda)$	$\text{W} \cdot \text{m}^{-2} \cdot \text{nm}^{-1}$
Light source	Radiant exitance	$M = \frac{d\phi_R}{dA}$	$\text{W} \cdot \text{m}^{-2}$
	Radiant intensity	$I = \frac{d\phi_R}{d\Omega}$	$\text{W} \cdot \text{sr}^{-1}$
	Spectral radiant intensity	$I(\lambda)$	$\text{W} \cdot \text{sr}^{-1} \cdot \text{nm}^{-1}$
	Radiance	$L = \frac{1}{\cos \theta} \frac{d^2\phi_R}{dAd\Omega}$	$\text{W} \cdot \text{m}^{-2} \cdot \text{sr}^{-1}$
	Spectral radiance	$L(\lambda)$	$\text{W} \cdot \text{m}^{-2} \cdot \text{sr}^{-1} \cdot \text{nm}^{-1}$

radiance is a function of the observing direction θ , but for perfectly illuminated diffusing surfaces, called Lambert surfaces, this is a constant.

The *spectral radiance* $L(\lambda)$, defined as the radiance per unit wavelength interval, at the wavelength λ , is related to the radiance L by

$$L = \int_0^\infty L(\lambda) d\lambda. \quad (1.7)$$

Table 1.2 summarizes these units.

1.4.2 Photometric units

When light enters the eye, a luminous stimulus is produced. The *luminous flux* ϕ_v can be considered the basic photometric unit, equivalent to the radiant flux, but evaluated according to the magnitude of the luminous stimulus it produces, measured in lumens (lm). This luminous stimulus is strongly dependent on wavelength, as will be noted later in this section.

The *illuminance* E_v is the area density of luminous flux received by an illuminated body, integrated for all wavelengths and all directions. Its unit is the *lux*, in lumens per square meter, and is defined by

$$E_v = \frac{\text{luminous flux}}{\text{area}} = \frac{d\phi_v}{dA}. \quad (1.8)$$

The *spectral illuminance* $E_v(\lambda)$ is defined as the illuminance per unit wavelength interval, at the wavelength λ , and is related to the illuminance E_v by the relation

$$E_v = \int_0^\infty E_v(\lambda) d\lambda. \quad (1.9)$$

The *luminous exitance* M_v of an extended light source, defined as the area density of the total luminous flux emitted, integrated for all wavelengths and all

directions, is

$$M_v = \frac{\text{emitted luminous flux}}{\text{area}} = \frac{d\phi_v}{dA}, \quad (1.10)$$

which is measured in lumens per square meter (not luxes, which are used only for illuminance). This quantity is rarely used in colorimetry.

The *luminous intensity* I_v of a point light source (or an extended light source observed from a distance much larger than the light source), defined as the total luminous flux, integrated for the whole area of the source and all wavelengths, emitted per unit solid angle in a given direction, is

$$I_v = \frac{d\phi_v}{d\Omega}. \quad (1.11)$$

From the beginning of the nineteenth century, the unit of luminous intensity was the candle. This unit was later adopted as an international standard by the Commission Internationale de l'Éclairage (CIE) in 1921, and in 1979 it was redefined and confirmed in Paris by the Conférence Générale des Poids et Mesures (CGPM) with the Latin name *candela* (cd). A candela is defined as the luminous intensity in a given direction of a source that emits monochromatic light of frequency 540×10^{12} Hz (wavelength equal to 555 nm) and has a radiant intensity in that direction of 1/683 W/sr. This definition, described in detail by Ohno (2010), took into account the average responses of many human eyes; this average is now known as the *standard observer*. With this definition the lumen becomes a secondary unit defined in terms of the candela. So, one lumen is equal to one candela emitted per unit solid angle (steradian, abbreviated as sr).

The *spectral luminous intensity* $I_v(\lambda)$ of a point light source is defined as the luminous intensity per unit wavelength interval, at the wavelength λ , and is related to the luminous intensity I_v by

$$I_v = \int_0^\infty I_v(\lambda) d\lambda. \quad (1.12)$$

The *luminance* L_v of a luminous object is defined as the total integrated luminous flux for all wavelengths, emitted per unit solid angle, per unit of projected area in a given direction, of the luminous surface, as follows:

$$L_v = \frac{\text{luminous flux per steradian}}{\text{projected area}} = \frac{d^2\phi_v}{dA_P d\Omega} = \frac{1}{\cos \theta} \frac{d^2\phi_v}{dAd\Omega}, \quad (1.13)$$

where the projected area A_P is equal to the actual area A of the source, multiplied by the cosine of the angle θ between the line of sight and the normal to the source. As with the radiance, the luminance is also a function of the direction of observation.

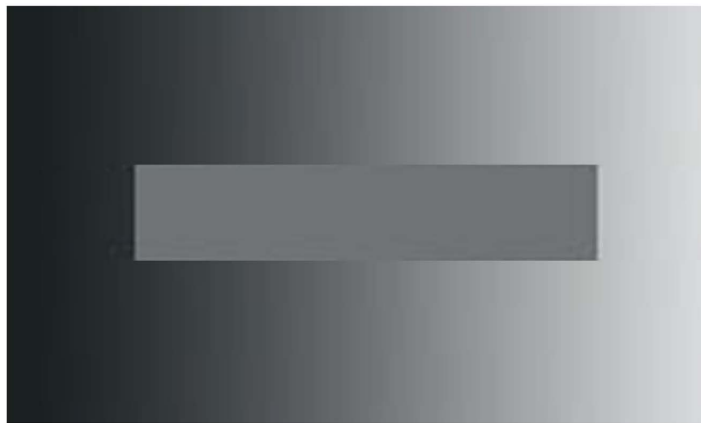


Figure 1.10 A strip with constant luminance but a gradient brightness is surrounded by a field with a gradient luminance [from Cassarly (2008)].

The *spectral luminance* $L_v(\lambda)$, defined as the luminance per unit wavelength interval, at the wavelength λ , is related to the luminance L_v by

$$L_v = \int_0^{\infty} L_v(\lambda) d\lambda. \quad (1.14)$$

Given a certain spectral distribution, the luminance is directly proportional to the radiance, and there is a linear relation between them; however, the eye response is not linear to either of these two quantities. Another quantity, called *lightness*, which is nonlinear to the luminance but linear to the eye response, is sometimes used and will be described in Chapter 5.

The brightness is not a physical unit but a more subjective term related to the perception elicited by the luminance of a luminous object. For example, when observing a sharp frontier between an evenly illuminated surface and a dark field, some fringes called Mach bands are observed. Obviously, in this case, due to the presence of the fringes, the luminance is constant over the whole surface, but the brightness is not. Another example is illustrated in Fig. 1.10, where a strip with constant luminance is surrounded by a field with a gradient in luminance. The inner strip has a gradient brightness but a constant luminance. Table 1.3 summarizes the main photometric units.

The *luminous efficacy* K is defined as the ratio of the luminous flux ϕ_v , measured in lumens, to the radiant flux ϕ , measured in watts:

$$K = \text{luminous efficacy} = \frac{\phi_v}{\phi_R}, \quad (1.15)$$

which can be used as a figure of merit for light sources. It is, for example, an indication of how well a given light source provides visible light for a given amount of electric power.

The *spectral luminous efficiency* $\sigma(\lambda)$ is defined by the ratio of the spectral luminance $L_v(\lambda)$ to the spectral radiance $L(\lambda)$ at the wavelength λ , and thus, it is a

Table 1.3 Some photometric units.

	Name	Formula	Unit
Illuminated object	Illuminance	$E_v = \frac{d\phi_v}{dA}$	lux = lumen · m ⁻²
	Spectral illuminance	$E_v(\lambda)$	lux · nm ⁻¹
Light source	Luminous exitance	$M_v = \frac{d\phi_v}{dA}$	lumen · m ⁻²
	Luminous intensity	$I_v = \frac{d\phi_v}{d\Omega}$	lumen · sr ⁻¹
	Spectral luminous intensity	$I_v(\lambda)$	lumen · sr ⁻¹ · nm ⁻¹
	Luminance	$L_v = \frac{1}{\cos \theta} \frac{d^2\phi_v}{dAd\Omega}$	lumen · m ⁻² · sr ⁻¹
	Spectral luminance	$L_v(\lambda)$	lumen · m ⁻² · sr ⁻¹ · nm ⁻¹

function of the wavelength, as follows:

$$\sigma(\lambda) = \frac{I_v(\lambda)}{I(\lambda)}. \quad (1.16)$$

This function is the same for all light sources, independent of the spectral distribution of the emitted light, and is known as the *luminous sensitivity* of the eye (Gibson and Tyndall, 1923). This function has a peak value located at a wavelength of 555 nm, as described in detail in Section 1.5. In agreement with the definition for the candela, as noted above, 1 W of radiant energy at this wavelength of 555 nm is equivalent to 683 lumens. The *relative spectral luminous efficiency* $V(\lambda)$ is defined as the spectral luminous efficiency divided by its peak value at a wavelength of 555 nm. Then, the maximum value of $V(\lambda)$ is equal to 1. Using this definition, the *spectral luminous efficiency* $\sigma(\lambda)$ of a light source in watts per lumen, per unit wavelength interval, at the wavelength λ , is

$$\sigma(\lambda) = 683 V(\lambda). \quad (1.17)$$

Thus, the spectral radiance $L(\lambda)$ and the spectral luminance $L_v(\lambda)$ are related by

$$L_v(\lambda) = 683 V(\lambda)L(\lambda), \quad (1.18)$$

and hence, the luminance of a polychromatic light source is given by

$$L_v = \int_0^\infty L_v(\lambda)d\lambda = 683 \int_0^\infty V(\lambda)L(\lambda)d\lambda. \quad (1.19)$$

Therefore, the luminous efficacy K of a polychromatic light source can be shown to be given by

$$K = \frac{\int_0^\infty L_v(\lambda)d\lambda}{\int_0^\infty L(\lambda)d\lambda} = 683 \frac{\int_0^\infty V(\lambda)L(\lambda)d\lambda}{\int_0^\infty L(\lambda)d\lambda}. \quad (1.20)$$

The *reflectance* ρ of a diffuse object is the quotient of the total radiant flux, at all wavelengths, reflected from the object in all directions, divided by the total radiant flux incident on the object. Since the object is diffuse, the reflected light travels in all directions, even if the illuminating beam travels in a single direction. The *spectral reflectance* $\rho(\lambda)$ is the reflectance per unit wavelength interval and it is a function of the wavelength. Thus, they are related by

$$\rho = \int_0^{\infty} \rho(\lambda) d\lambda. \quad (1.21)$$

The *luminous reflectance* R is the quotient of the total polychromatic reflected luminous flux divided by the incident luminous flux, assuming a standard illuminant, for example the CIE illuminant D₆₅, to be described in Chapter 2. This luminous reflectance has different values for different standard illuminants. The *spectral luminous reflectance* $R(\lambda)$ is defined as the luminous reflectance per unit wavelength interval, so that

$$R = \int_0^{\infty} R(\lambda) d\lambda. \quad (1.22)$$

The *transmittance* τ of a transparent object is the quotient of the total radiant flux, at all wavelengths, transmitted by the object divided by the total radiant flux incident on the object. The spectral transmittance $\tau(\lambda)$ is the transmittance per unit wavelength interval and is a function of the wavelength. They are related by

$$\tau = \int_0^{\infty} \tau(\lambda) d\lambda. \quad (1.23)$$

The *luminous transmittance* T is the quotient of the total polychromatic transmitted luminous flux divided by the incident luminous flux, assuming a standard illuminant. This luminous transmittance has different values for different standard illuminants. The *spectral luminous transmittance* $T(\lambda)$ is defined as the luminous reflectance per unit wavelength interval, so that

$$T = \int_0^{\infty} T(\lambda) d\lambda. \quad (1.24)$$

With these definitions we are ready to describe the color sensitivity of the eye.

1.5 Color Sensitivity of the Eye

When light enters the eye and arrives at the retina, the energy is absorbed by the photopigments located at the tips of the rods and cones. These cones and rods are at the back of the retina near a black layer known as the choroid. There are 100 million rods and 5 million cones. The center of the retina or fovea is devoid of rods, but the density of cones is greater on the fovea.

The luminous sensitivity, as defined above, is the ratio of the luminance to the radiance and is a function of the wavelength of light. This sensitivity is a constant

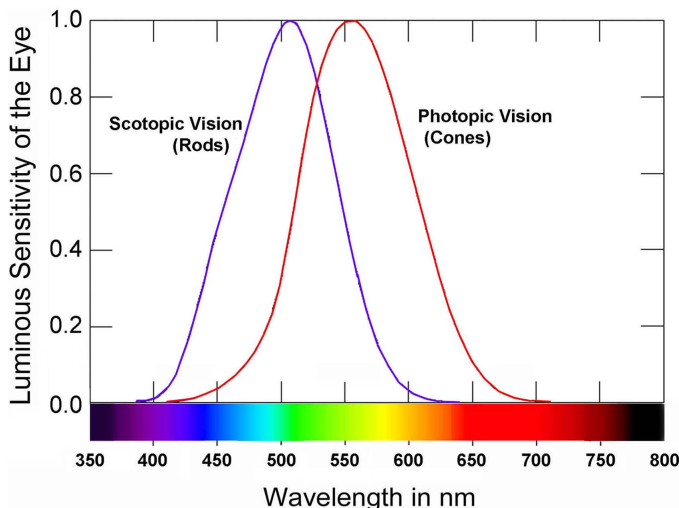


Figure 1.11 Photopic and scotopic luminous sensitivities of the eye.

for all luminance levels. To measure the spectral luminous efficiency of the eye, we must find a procedure to determine when two monochromatic fields with different colors have the same luminance. Then, using the proper procedure, a luminous match is made on a split field with two colors. If the radiance is measured in these two fields using color photometric methods (Abney and Festing, 1886), their *relative luminous efficiency*, or *luminous sensitivity*, for short, is found. A direct brightness match yields unreliable results due to the difference in color and leads to serious additive failures (Uchikawa et al., 1984; Elzingade and Weert, 1986), as described by Boynton (1996). A much better method is to alternate the two fields with different colors at a frequency of $\sim 10\text{--}15$ Hz, and then to change the brightness of one of them until the alternating flickering is minimized. This is known as the flicker method (described in Chapter 3), which was developed by Ives (1912) and is quite reliable.

When performing these measurements, it is found that there are two different luminous sensitivities for low- and high-illumination levels, as shown in Fig. 1.11; one corresponding to the sensitivity of the rods and the other to the sensitivity of the cones. These two eye sensitivities, or luminosity functions, are one for day vision $V(\lambda)$, or photopic vision, and the other for night vision $V'(\lambda)$, or scotopic vision. By definition, these two curves were independently normalized to a maximum value equal to 1.

The *photopic curve* $V(\lambda)$ was measured by several authors; for example, with the flicker methods by Coblenz and Emerson (1918) and with the step-by-step methods of heterochromatic photometry by Hyde et al. (1918). It was shown by Ives (1912) that the two methods give similar results for a field of 2 deg if the wavelength is not below 500 nm. The CIE in 1924 (CIE, 1926) adopted a photopic curve $V(\lambda)$ based on the work by Gibson and Tyndall (1923) and previous researchers. According to more recent measurements, a photopic curve

$V(\lambda)$ slightly different in the violet end of the spectrum was obtained. A corrected version was later proposed by Judd (1951); however, the change has not been made because all present-day photometry has been based on this function for more than half a century (CIE, 1990).

The *scotopic curve* $V'(\lambda)$ was adopted by the CIE in 1951 (CIE, 1951). The measurements were taken with monochromatic stimuli by method of visual comparison with low brightness in a field of 10 deg (Crawford, 1949), and also on visual thresholds viewed eccentrically with more than 5 deg from the fovea (Wald, 1945) with complete dark adaptation. This function is quite sensitive to the age of the observer, who is assumed to be younger than 30 years old. The values for these functions are normalized to a maximum value of 1, as shown in Table 1.4.

We can see that for daylight vision the maximum luminous efficiency is for a color corresponding to a wavelength of 555 nm (yellow), while for night vision this maximum efficiency shifts to the blue at about 505 nm.

1.6 How Materials Are Colored or Modify Color

The color of light emitted by a hot or warm body is defined by its emission spectrum. Every chemical element or compound has a characteristic element that spectroscopists use to identify it. A particular kind of luminous body is the blackbody, which will be studied with some detail in Chapter 2. The brightness and color of the blackbody depends on its temperature. The higher its temperature, the greater its brightness and the bluer the light it emits. At low temperatures the brightness is low and its light is reddish or infrared. This body does not emit any light when it reaches the extremely low temperature of -273.15°C , which is the zero for the scale of “absolute temperatures,” or Kelvin, which is the absolute minimum possible temperature and can be approached but never reached. By definition, this is the temperature at which the entropy becomes zero. Thus, the Kelvin temperature is the Celsius temperature plus 273.15.

Any luminous colored body has a color that can be considered as the superposition of a monochromatic spectrally pure color and white. The wavelength corresponding to the color of the spectrally pure component is said to be the *dominant wavelength*. The temperature of the blackbody with the same dominant color is defined as the *color temperature* of the luminous body. These concepts will be studied with some more detail in Chapter 2.

When an object is illuminated, the light is (a) transmitted, (b) reflected, (c) scattered, or (d) absorbed. These four processes can change the color of the light, since not all wavelengths are equally transmitted, reflected, scattered, or absorbed. If the atoms, molecules, or particles in a body have separations much smaller than the wavelength of light, the scattering process is not present. Then, we have a transparent body, with only the reflection, absorption, and transmission take place. The atoms and molecules forming the material being illuminated have certain resonance frequencies (wavelengths) where they absorb the light and heat the material, instead of reflecting or transmitting it. Most single atoms have their resonances in the visible and ultraviolet. On the other hand, molecules can vibrate

Table 1.4 Relative spectral luminous efficiency functions of the eye.

Wavelength in nm	$V(\lambda)$ Photopic	$V'(\lambda)$ Scotopic	Wavelength in nm	$V(\lambda)$ Photopic	$V'(\lambda)$ Scotopic
380	0.0000	0.0006	585	0.8163	0.0899
385	0.0001	0.0011	590	0.7570	0.0655
390	0.0001	0.0022	595	0.6949	0.0469
395	0.0002	0.0045	600	0.6310	0.0331
400	0.0004	0.0093	605	0.5668	0.0231
405	0.0006	0.0185	610	0.5030	0.0159
410	0.0012	0.0348	615	0.4412	0.0109
415	0.0022	0.0904	620	0.3810	0.0074
420	0.0040	0.0966	625	0.3210	0.0050
425	0.0073	0.1436	630	0.2650	0.0033
430	0.0116	0.1998	635	0.2170	0.0022
435	0.0168	0.2625	640	0.1750	0.0015
440	0.0230	0.3281	645	0.1382	0.0010
445	0.0298	0.3931	650	0.1070	0.0007
450	0.0380	0.4550	655	0.0816	0.0004
455	0.0480	0.5130	660	0.0610	0.0003
460	0.0600	0.5670	665	0.0446	0.0002
465	0.0739	0.6200	670	0.0320	0.0001
470	0.9010	0.6960	675	0.0232	0.0001
475	0.1126	0.7340	680	0.0170	0.0001
480	0.1390	0.7930	685	0.0119	0.0000
485	0.1693	0.8510	690	0.0082	0.0000
490	0.2080	0.9040	695	0.0057	0.0000
495	0.2586	0.9490	700	0.0041	0.0000
500	0.3230	0.9820	705	0.0029	0.0000
505	0.4073	0.9980	710	0.0021	0.0000
510	0.5030	0.9970	715	0.0015	0.0000
515	0.6082	0.9750	720	0.0010	0.0000
520	0.7100	0.9350	725	0.0007	0.0000
525	0.7932	0.8800	730	0.0005	0.0000
530	0.8620	0.8110	735	0.0004	0.0000
535	0.9148	0.7330	740	0.0002	0.0000
540	0.9540	0.6500	745	0.0002	0.0000
545	0.9803	0.5640	750	0.0001	0.0000
550	0.9949	0.4810	755	0.0001	0.0000
555	1.0000	0.4020	760	0.0001	0.0000
560	0.9950	0.3288	765	0.0000	0.0000
565	0.9786	0.2639	770	0.0000	0.0000
570	0.9520	0.2076	775	0.0000	0.0000
575	0.9154	0.1602	780	0.0000	0.0000
580	0.8700	0.1212			

or rotate, moving atoms with respect to each other within the molecule. Due to their relatively large mass, they frequently have resonances in the infrared or even microwave regions, but may also have resonances in the visible (Weisskopf, 1968).

In general, materials are formed by many different kinds of atoms and molecules. This gives them a characteristic spectral transmission or reflection. Thus, each opaque or transparent material has its own characteristic color when illuminated with white light.

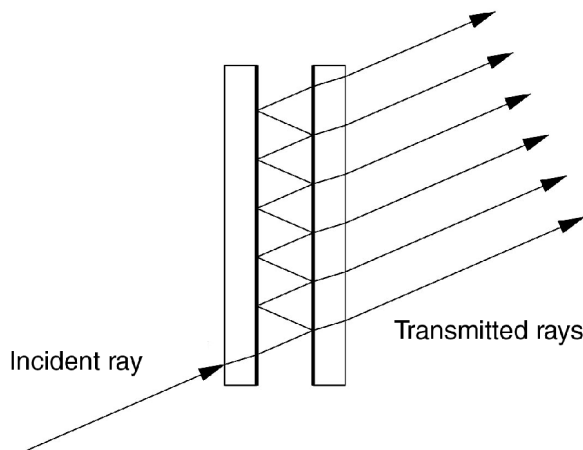


Figure 1.12 A Fabry–Perot interferometer.

1.7 Absorption and Interference Filters

When a beam of light passes through a transparent body, some of the light is transmitted, some is reflected, and some is absorbed. These three processes are a function of the wavelength. A transparent plate made out of a material with absorption for some visible, infrared, or ultraviolet wavelengths is an absorption filter. These filters are usually made out of a colored glass or plastic, which in turn is made by adding a dye to the material. The optical quality of plastic filters is lower than that of glass filters, but plastic filters are less expensive. The gelatin Wratten filters, invented by Wratten, and sold to Kodak in 1912, were very popular and inexpensive. The most common colored glass filters now available are made out of colored Schott glass. These filters are more costly, but are high quality and possess a large diversity of transmittance curves that can be classified as follows:

- Color temperature conversion filters that can lower (reddish filters) or elevate (bluish filters) the color temperature of light sources, for example, tungsten lamps.
- Heat-absorbing filters, used in illumination systems to block out the heating infrared radiation without attenuating the visible light by any noticeable amount.
- Long- and short-wavelength pass filters, whose edges are not sharp, as in the interference filters to be described later.
- Bandpass filters, with a wide wavelength transmission band.
- Interference filters (see Born and Wolf, 1999) transmit part of the light and reflect the rest, like a bandpass filter; however, they can be considered in a class of their own, since they have a narrow bandpass. Their working principle is based on the Fabry–Perot interferometer, as illustrated in Fig. 1.12. The multiple-light-beam reflections between the two flat and partially reflecting surfaces produce many transmitted beams. These beams interfere, producing a very characteristic spectral distribution on the transmitted beams as well

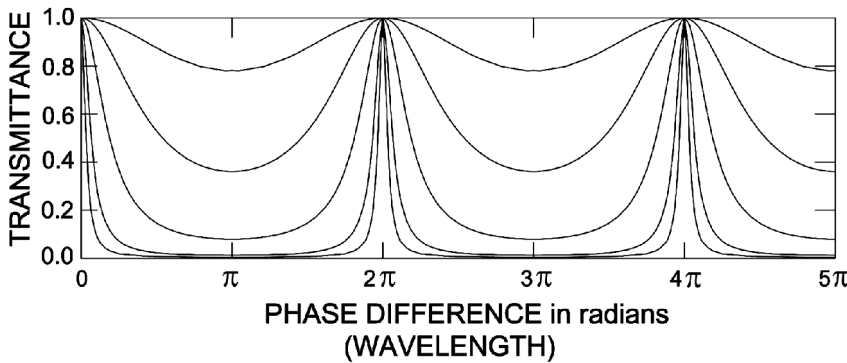


Figure 1.13 Spectral transmittance curves for a Fabry–Perot interferometer, with different values of the reflectivity of the partially reflecting mirrors. The optical path difference is that between two consecutively reflected beams, which is a function of the wavelength.

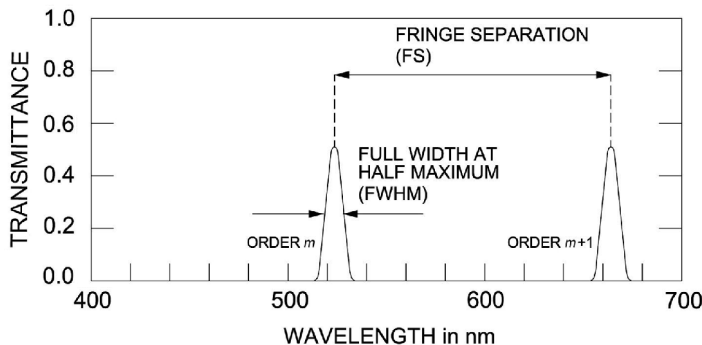


Figure 1.14 Typical spectral transmittance curves for an interference filter.

as on the reflected beams. Due to the energy conservation principle, at any wavelength, the energy on the transmitted beam plus the energy on the reflected beam equals the energy on the incident beam. The spectral transmittance of these filters is shown in Fig. 1.13.

We see that the spectral transmittance is formed by a series of spectral lines with different orders of interference m spaced with equal wavelength intervals. This separation $\Delta\lambda$ between the lines depends on the separation d between the two partially reflecting mirrors, as given by

$$\Delta\lambda = \frac{\lambda^2}{2nd}, \quad (1.25)$$

where n is the refractive index for the medium between the two flat semireflecting mirrors. A typical spectral transmission for an interference filter is illustrated in Fig. 1.14. Absorption and interference filters can be combined to isolate a single spectral line.

References

- Abney, W. D. W. and Festing, E. R., “Colour photometry,” *Philos. Trans. Roy. Soc. London* **177**, 423–456 (1886).
- Benham, C. E., “Notes,” *Nature (London)* **51**, 113–114 (1894).
- Born, M. and Wolf, E., *Principles of Optics*, 7th ed., Cambridge University Press, Cambridge, U.K. (1999).
- Boynton, R. M., “History and current status of a physiologically based system on photometry and colorimetry,” *J. Opt. Soc. Am. A* **13**, 1609–1621 (1996).
- Cassarly, W. J., “High-brightness LEDs,” *Opt. Photonics News* **January**, 19 (2008).
- Coblentz, W. W. and Emerson, W. B., “Relative sensibility of the average eye to light of different colors and some practical applications to radiation problems,” *Bull. Bur. Stand.* **14**, 167–236 (1918).
- CIE, *Proc., 1924 Commission Internationale de l’Éclairage*, Cambridge University Press, Cambridge, U.K. (1926).
- CIE, *Proc., 1951 Commission Internationale de l’Éclairage*, CIE, Paris, 1, Sec. 4; Vol. 3, 37 (1951).
- CIE, “CIE 1988 2 deg spectral luminous efficiency function for photopic vision,” Publication 86, CIE, Vienna (1990).
- Crawford, B. H., “The scotopic visibility function,” *Proc. Phys. Soc. London* **B62**, 321–334 (1949).
- Elzinga, C. H. and de Weert, C. M. M., “Spectral sensitivity functions derived from color matching: implications of intensity invariance for color vision models,” *J. Opt. Soc. Am. A* **3**, 1183–1191 (1986).
- Evans, R. M., “Maxwell’s color photograph,” *Sci. Am.* **205**, 112–128 (1961).
- Gibson, K. S. and Tyndall, E. P. T., “Visibility of radiant energy,” *Sci. Pap. Bur. Stand.* **19**, 131–191 (1923).
- Hering, E., Hurvich, L. M. and Jameson, D., Eds., *Outlines of a Theory of the Light Sense*, Harvard University Press, Cambridge, MA (1964) (translation).
- Hyde, E. P., Forsythe, W. E., and Cady, F. E., “The visibility of radiation,” *Astrophys. J.* **48**, 65–88 (1918).
- Ives, H. E., “Studies in the photometry of lights of different colours. I. Spectral luminosity curves obtained by the equality of brightness photometer and flicker photometer under similar conditions,” *Philos. Mag.* **24**, 149–188 (1912).
- Judd, D. B., Report of the U.S. Secretariat Committee on Colorimetry and Artificial Daylight, in *Proc. of the 12th Session of the CIE, Stockholm*, Technical Committee No. 7, Commission Internationale de l’Éclairage, Paris (1951).

- Judd, D. B., "Object-color changes from daylight to incandescent filament illumination," *Illuminating Engineering* **47**, 221–233 (1952); reprinted in *Selected Papers in Colorimetry—Fundamentals*, MacAdam, D. L., Ed., SPIE Press, Bellingham, WA (1993).
- Judd, D. B., "Appraisal of Land's work on two-primary color projections," *J. Opt. Soc. Am.* **50**, 254–268 (1960); reprinted in *Selected Papers in Colorimetry—Fundamentals*, MacAdam, D. L., Ed., SPIE Press, Bellingham, WA (1993).
- Kaiser, P. K. and Boynton, R. M., *Human Color Vision*, 2nd ed., Optical Society of America, Washington, DC (1996) p. 508.
- König, A., *Gesammelte Abhandlungen zur Physiologischen Optik*, Barth-Verlag, Leipzig (1903).
- Land, E. H., "Experiments in color vision," *Sci. Am.* **200**, 84–94 (1959).
- Land, E. H., "The retinex theory of color vision," *Sci. Am.* **237**, 108–128 (1977).
- Lee, H.-C., *Introduction to Color Imaging Science*, Cambridge University Press, Cambridge, U.K. (2005).
- MacAdam, D. L., "Color essays," *J. Opt. Soc. Am.* **65**, 483–493 (1975).
- Mariotte, E., *Oeubres*, Van de Aa, Leyden, The Netherlands (1717).
- Masters, B. R., "A history of color vision from Newton to Maxwell," *Opt. Photonics News* **January**, 43–47 (2011).
- Maxwell, J. C., "Theory of the perception of colors," *Phil. Trans. Roy. Scottish Soc. Arts* **4**, 394–400 (1856); reprinted in *Selected Papers in Colorimetry—Fundamentals*, MacAdam, D. L., Ed., SPIE Press, Bellingham, WA (1993).
- Maxwell, J. C., "The diagram of colors," *Trans. Roy. Soc. Edinbrgh* **21**, 275–298 (1857); reprinted in *Selected Papers in Colorimetry—Fundamentals*, MacAdam, D. L., Ed., SPIE Press, Bellingham, WA (1993).
- Maxwell, J. C., "On the theory of compound colours and the relations of the colours of the spectrum," *Philos. Trans. Roy. Soc. London* **150**, 57–84 (1860).
- Maxwell, J. C., "Experiments on colours, as perceived by the eye, with remarks on colour-blindness," *Trans. Roy. Soc. Edinburgh* **21**, 275–298 (1885).
- Mollon, J. D., "The origins of modern color science," in *The Science of Color*, Shevell, S., Ed., 2nd ed., Elsevier, Oxford, U.K. (2003).
- Neil, R. and Steinle, F., "Exploratory experimentation: Goethe, Land, and color theory," *Phys. Today* **55**, 43 (2002).
- Neitz, J., Carroll, J., and Neitz, M., "Color vision, almost reason enough for having eyes," *Opt. Photonics News* **January**, 26–33 (2001).
- Newton, I., "New theory about light and colors," *Philos. Trans. Roy. Soc. London* **80**, 3075–3087 (1671); reprinted in *Selected Papers in Colorimetry—Fundamentals*, MacAdam, D. L., Ed., SPIE Press, Bellingham, WA (1993).

- Ohno, Y., *Radiometry and photometry for vision optics*, in *Handbook of Optics*, Vol. II, Optical Society of America, Washington, DC (2010).
- Palmer, G., *Theory of Colors and Vision*, Leacroft, London (1777) pp. 41–47; reprinted in *Selected Papers in Colorimetry—Fundamentals*, MacAdam, D. L., Ed., SPIE Press, Bellingham, WA (1993).
- Peirce, C. S., “Note on the sensation of color,” *Am. J. Sci. Arts* **13**, 247–251 (1877).
- Rayleigh, L., “Experiments on colour,” *Nature* **25**, 64–66 (1881).
- Ribe, N. and Steinle, F., “Exploratory experimentation: Goethe, Land, and color theory,” *Phys. Today* **July**, 43–49 (2002).
- Shevell, S. K., Ed., *The Science of Color*, 2nd ed., Optical Society of America, Washington, DC (2003) Elsevier, Amsterdam.
- Uchikawa, K., Uchikawa, H., and Kaiser, P. K., “Luminance and saturation of equally bright colors,” *Color Res. Appl.* **9**, 5–14 (1984).
- von Goethe, J. W., Miller, D. E., Ed., *Scientific Studies*, Suhrkamp, New York (1988) (translation).
- von Helmholtz, H., “Physiological optics,” in *Handbuch der Physiologischen Optik*, (1866); reprinted in *Selected Papers in Colorimetry—Fundamentals*, MacAdam, D. L., Ed., SPIE Press, Bellingham, WA (1993).
- von Helmholtz, H., “On the theory of compound colours,” *Philos. Mag. Ser. 4* **4**, 519–534 (1852).
- Wald, G., “The spectral sensitivity of the human eye: a spectral adaptometer,” *J. Opt. Soc. Am.* **35**, 187–196 (1945).
- Weisskopf, V. F., “How light interacts with matter,” *Sci. Am.* **219**, 60–71 (1968).
- Wright, W. D. and Pitt, F. H. G., “Hue discrimination in normal color vision,” *Proc. Phys. Soc. London* **46**, 459–473 (1934).
- Young, T., “On the theory of light and colours,” *Philos. Trans. Roy. Soc. London* **92**, 20–21 (1802); reprinted in *Selected Papers in Colorimetry—Fundamentals*, MacAdam, D. L., Ed., SPIE Press, Bellingham, WA (1993).
- Zalewski, E. F., *Radiometry and photometry*, in *Handbook of Optics*, Vol. II, Optical Society of America, Washington, DC (2010).

Chapter 2

Light Sources and Illuminants

2.1 Introduction

The perceived color of an illuminated object depends not only on its intrinsic color or spectral reflectivity, but also on the power spectrum of the light source. In this chapter, we will study some of the most important light sources used in colorimetric studies. General descriptions of light sources can be found in many publications (Elenbaas, 1972; Eby and Levin, 1979; Malacara and Morales, 1988; LaRocca, 1995; IESNA, 2000).

2.2 Blackbody Radiation and Color Temperature

Any nonmonochromatic light source can be characterized by its spectral power distribution, which is the total amount of power that it emits in a small unit interval of wavelength or frequency. Different curves are obtained in both of these cases, but the most frequently used is the power per unit of wavelength interval. A blackbody is one that has no color, that is, one that looks black because it absorbs all of the light that falls on its surface, such as a piece of carbon. A blackbody at the temperature of absolute zero (0 K on the Kelvin scale, or -273.15°C) looks perfectly black, since it emits no light.

If a blackbody is heated, it will become luminous, with a radiance and color that depends on the temperature. It looks red at about 1000 K (727°C), yellow at about 1500 K (1227°C), white at 4500 K (4227°C), and bluish-white at about 6500 K (6227°C). Further details are described in Chapter 5 in Fig. 5.10. Figure 2.1 shows how the spectral radiance and the color of a blackbody change with the temperature, as given by the well-known blackbody radiation law. Its spectral radiance $L(\lambda)$ is given by

$$L(\lambda) = \frac{2\pi hc^2}{\lambda^5} \frac{1}{e^{ch/\lambda kT} - 1}, \quad (2.1)$$

where h is Planck's constant, k is Boltzmann's constant, c is the speed of light, λ is the wavelength, and T is the absolute temperature. The wavelength at which the peak of radiation occurs is given by Wien's displacement law, which can be

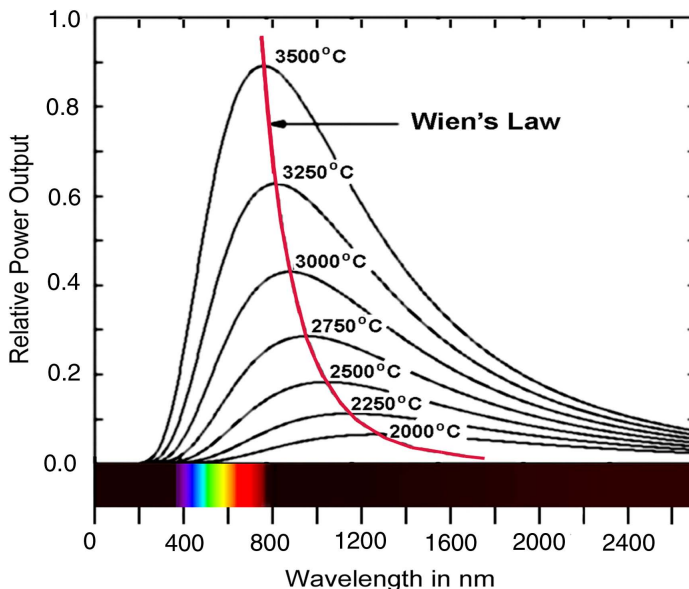


Figure 2.1 Blackbody spectral radiance function and Wien's law.

derived from the blackbody radiation law

$$\lambda_m T = \frac{ch}{4.965k} = 0.0028978 \text{ m} \cdot \text{K}, \quad (2.2)$$

and is represented by the red line in Fig. 2.1. Using this law, the temperature of an incandescent body, such as a star or an object in an oven, can be estimated from its color.

If a light source has the same color as a blackbody with a temperature T , we say that its *color temperature* is T . However, this is not the real temperature, unless the light source is a blackbody. If the color is not exactly the same as that of the blackbody, but it is close to it, we say that the *correlated color temperature* (CCT) is T . This concept will be discussed in more detail in Section 5.5.

In the case of an incandescent temperature lamp with a white glass bulb, the source is closer to being a blackbody than in the case of a lamp with a colored glass bulb. A fluorescent lamp is far from being a blackbody. An ordinary noncolored incandescent lamp has a color temperature of about 2850 K, while a “cool white” fluorescent lamp has a color temperature of about 4100 K.

Daylight does not have a constant color temperature, since it depends on many factors even on a clear day. Its color temperature is lower, or redder, at sunrise and sunset and higher, or bluer, at noon.

2.3 Tungsten Lamps

A tungsten lamp emits light with a high temperature by means of an incandescent filament. The spectral emission of the incandescent tungsten in the visible range

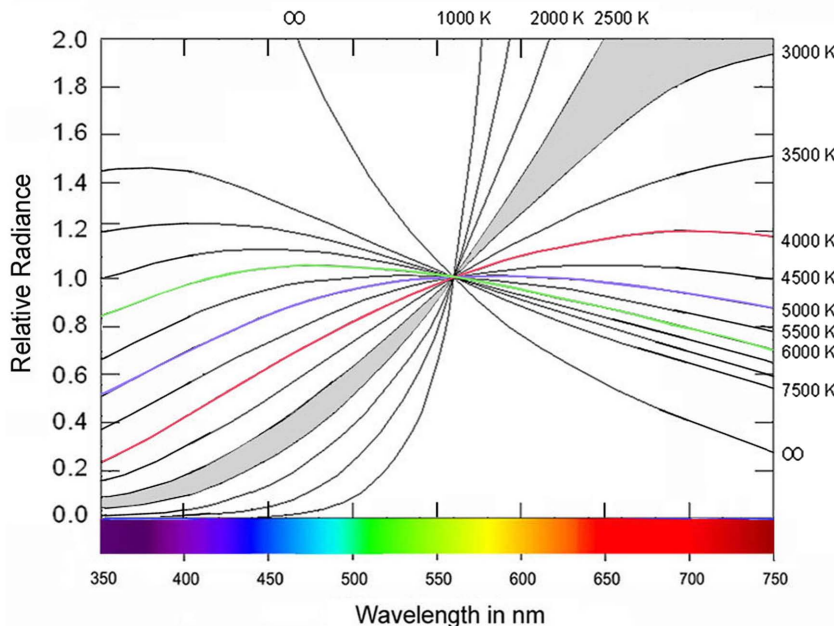


Figure 2.2 Emission spectral radiance curves of a blackbody in the visible range, normalized so that they have the same value at the wavelength of 560 nm. These curves approach those of a tungsten lamp, which operates in the range of color temperatures from 2500 to 3000 K.

is quite similar to that of the blackbody, only multiplied by a constant efficiency factor. The peak of the emission spectrum is also in the infrared, but is slightly shifted toward shorter wavelengths, with respect to the peak of the blackbody with the same temperature.

Figure 2.2 plots the blackbody spectral radiance $L(\lambda)$ for different temperatures, where each radiance function is multiplied by a proper constant, so that they all have the same value at a wavelength of 560 nm (normalized to 1 at 560 nm). As shown in this figure, the blackbody emits a white color and is almost constantly radiant in the visible interval when the temperature is ~ 5500 K, which is close to the sun's temperature. Thus, this temperature would give the light source the maximum luminous efficiency as defined in Section 1.4. However, this is not the proper temperature for a tungsten lamp, because at such a high temperature the tungsten would rapidly evaporate. The luminous power efficiency is defined as the luminous flux in lumens divided by the electrical power supplied to the lamp in watts. This luminous power efficiency is maximized (~ 20) for temperatures between 2500 K and 3000 K, as shown in the shaded area in Fig. 2.2.

The spectral radiance emitted by the lamp is equal to the spectral radiance emitted by the tungsten, multiplied by the spectral absorption of the glass envelope. The temperature of the filament depends on several factors, mainly the working voltage and the electric current. Thus, the characteristic color and the spectral

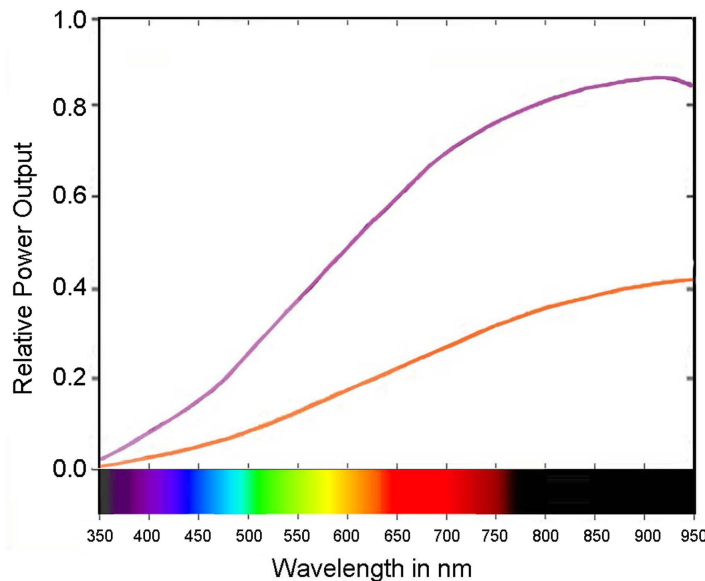


Figure 2.3 Emission spectra for two tungsten incandescent lamps with different temperatures.

radiance are dependent on this temperature. Figure 2.3 illustrates the emission spectra for two tungsten lamps with different temperatures.

A halogen lamp is an incandescent lamp, whose transparent envelope is filled with an inert gas and a small amount of a halogen such as iodine or bromine. The purpose of this gas is to increase the lifetime of the lamp by means of a process known as the halogen cycle, which redeposits the evaporated tungsten back onto the filament. This process not only increases the lifetime of the lamp, but also avoids darkening the glass envelope with the evaporated tungsten.

For this process to operate, the lamp temperature must be higher than in a conventional tungsten lamp. This higher temperature requires that the transparent envelope be made out of fused silica (quartz) instead of glass. The higher operating temperature of the lamp increases its efficacy and also shifts its spectral distribution toward the blue.

It must be noted that any contamination—mainly fingerprints in the glass envelope—can damage the quartz when heated, after turning on the lamp. If the lamp is touched, it must be cleaned with alcohol and dried before operation.

2.4 Gas Discharge and Fluorescent Lamps

A gas discharge lamp is a glass tube containing electrodes to which an electrical current is applied. The tube contains a low-pressure gas such as hydrogen, argon, or neon, or a vaporized metal, such as mercury vapor, whose emission spectrum is in Fig. 2.4. When an electrical discharge excites the gas or metal vapor, light is emitted with a spectrum formed by a series of spectral lines, which is characteristic of the gas or vapor, unlike the continuous spectrum of an incandescent lamp. Gas

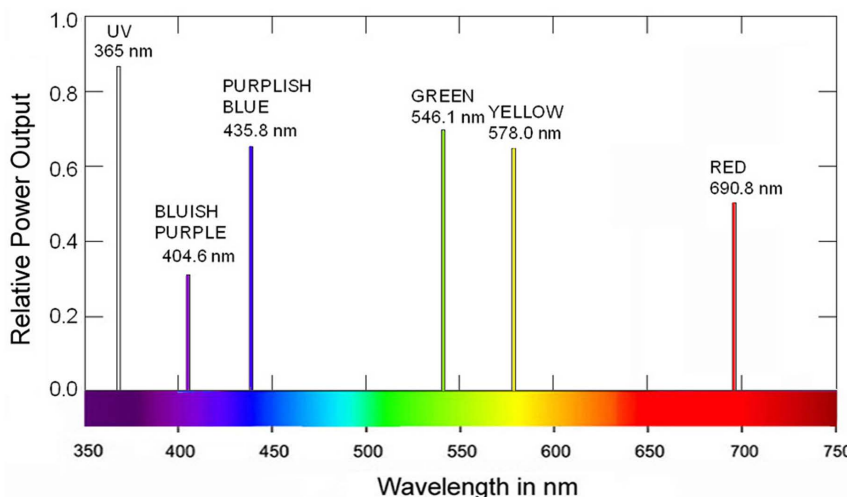


Figure 2.4 Emission spectrum of mercury vapor.

discharge lamps with mercury vapor or sodium are used for street illumination. In the mercury lamp the vapor discharge is blue and contains much ultraviolet, which can be blocked out if desired with the proper glass envelope. A sodium lamp's discharge is an orange-yellow color. The spectrum of gas or vapor discharge lamps is greatly dependent on the internal pressure of the gas or vapor.

The flashlamp is a gas discharge lamp that produces an extremely intense white light for a very short duration. The gas pressure is of the order of a few hundred Torrs. Higher pressures produce greater output efficiency with a whiter color. The gas is xenon, krypton, argon, or neon. The electrodes of the lamp are connected to a capacitor with a voltage between 200 to a few thousand volts. The lamp cannot conduct electricity until the gas is ionized. The most common method to start the flash is to ionize the gas with a triggering pulse of several thousand volts. Then, the capacitor discharges quite rapidly, and the lamp emits a brief and intense light. Figure 2.5 illustrates the typical spectra of the light produced by a flashlamp with xenon and with krypton.

A fluorescent lamp is glass tube filled with low-pressure mercury vapor and argon, xenon, neon, or krypton. The inner surface of the tube is coated with a fluorescent powder, which is a blend of metallic and rare-earth phosphor salts. When the ultraviolet light emitted by the mercury vapor hits the fluorescent powder, this energy is converted to visible light with a continuous spectrum. The color of this emitted visible light can be chosen with the proper selection of the fluorescent powder. A white light closely resembling daylight illumination can be obtained.

Older fluorescent tubes contain *halophosphate*-type phosphors. Because this phosphor mainly emits yellow and blue light, and not much green and red, these tubes have very unpleasant and poor-quality color reproduction. In the absence of a reference, this mixture appears white to the eye, but the light has an incomplete

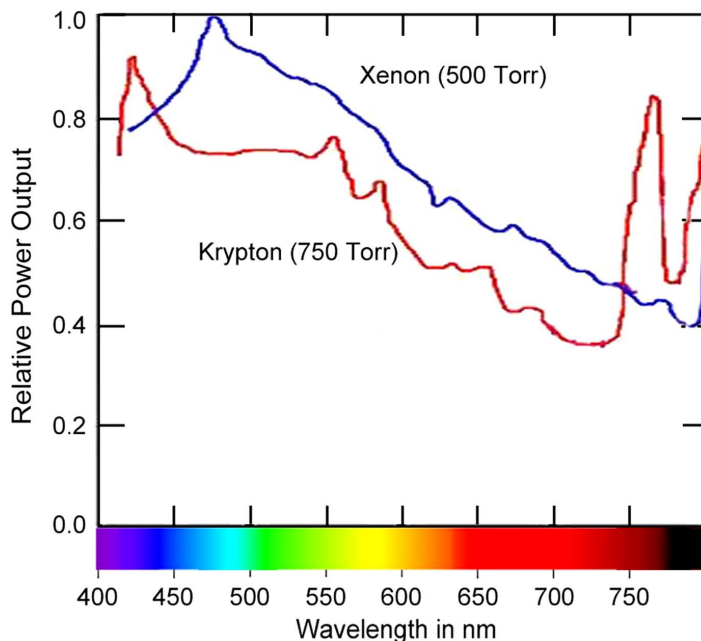


Figure 2.5 Spectra of flashlamps with xenon and with krypton.

spectrum. Since the 1990s, higher-quality fluorescent lamps use either a higher-CRI (color-rendering index, as defined in Section 2.7) halophosphate coating, or a *triphasphor* mixture, based on europium and terbium ions. The colors they emit are more evenly distributed over the visible spectrum. High-CRI halophosphate and triphosphor tubes produce a more natural color reproduction for the human eye. Figures 2.6(a) and (b) illustrate the spectral distribution for these fluorescent lamps.

2.5 Light-Emitting Diodes

A light-emitting diode (LED) is a semiconductor diode light source, traditionally used as an indicator in many electronic devices (Cassarly, 2008). Recently LEDs are becoming quite popular as light sources for many other purposes, including general illumination. Modern versions are available in low or high power. Many types of semiconductors are used to manufacture LEDs with almost any color across the visible spectrum and even in the near ultraviolet. An extensive description of LEDs and many other types of light sources is given by the IESNA (2000). Figure 2.7 illustrates the spectra of some LEDs with different colors. The half bandwidth (the width at half the maximum intensity) is 17–35 nm.

White-light LEDs are produced by two different methods, but the most common is by combining red, green, and blue LEDs (RGB LEDs). With this combination the resultant color can be tuned. Figure 2.8(a) illustrates the spectrum of light emitted by this kind of LED. While this light will appear white to the eye, any object whose colors fall between the spikes will not be faithfully rendered. The second method of

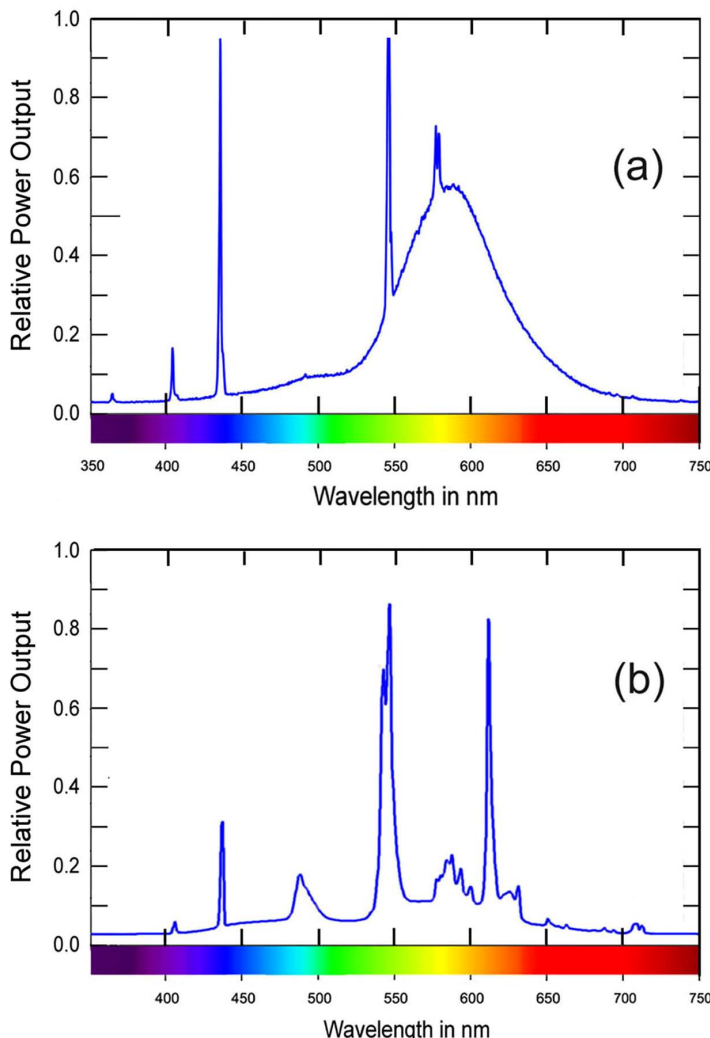


Figure 2.6 Spectra of fluorescent lamps: (a) halophosphate type and (b) triphosphor type.

producing a white-light LED is to use a phosphor material to convert blue light to a broad-spectrum white light in the same way as a fluorescent lamp converts light. LEDs with a good color rendering have been manufactured (Craford et al., 2001; Narukawa, 2004; Ohno, 2004). Figure 2.8(b) shows the spectrum of a fluorescent white-light LED. As LED technology is progressing, we can reasonably expect that in a few years LEDs will replace almost every light source or lamp we use now.

The main characteristics of LEDs that differentiate them from most common light sources are listed below.

Advantages

- (a) Luminous efficacy: LEDs produce more light per watt than do incandescent or sometimes even fluorescent light sources. The efficacy of LEDs can be

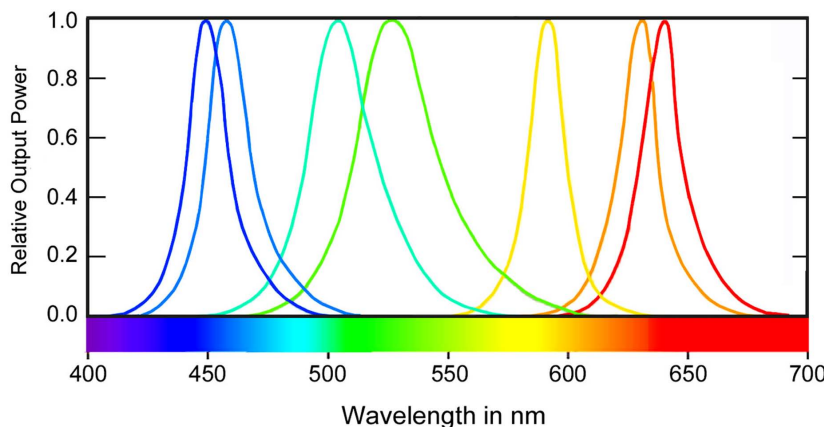


Figure 2.7 Spectra of some LEDs with different colors. The bandwidth is about 25 nm for the three colors.

greater than 100 lumens per watt, while tungsten halogen lamps provide about 20 lumens per watt, and fluorescent lamps between 60 and 100 lumens per watt. (Most of the energy supplied to tungsten incandescent lamps is wasted in generating heat; the lamp becomes very hot after several minutes. Unlike tungsten lamps, most of the energy supplied to the LED is converted to light.)

- (b) Color: LEDs can be manufactured to emit almost any desired color with a relatively narrow spectrum, and they are manufactured in almost any color within the visible spectrum. For better color rendering, di-, tri- and tetra-chromatic LEDs are also produced.
- (c) Size: LEDs can be made very small, and many different sizes and shapes are now available.
- (d) Cycling: LEDs can be turned on and off or pulsed very quickly or with a high frequency. This characteristic is especially useful for the transmission of information in a pulse-coded light beam. Another common application that benefits from this characteristic is in image displays.
- (e) Lifetime: LEDs have long useful lives—as high as 50,000 hours.

Disadvantages

- (a) Price: The price of LEDs is relatively high as compared with other light sources, but it is constantly decreasing.
- (b) Voltage sensitivity: LEDs must have a power supply with a lower tolerance in voltage and current than other light sources.
- (c) Light color: LEDs' spectra are generally more monochromatic than other light sources, but their whiteness is far from that of incandescent lamps.

Recently, a new class of LEDs has appeared, made with organic molecules instead of semiconductors. These are called *organic light-emitting diodes*, or OLEDs, as described by Howard (2004) and Boas (2010). There are some important differences between these and semiconductor LEDs, but the main one is

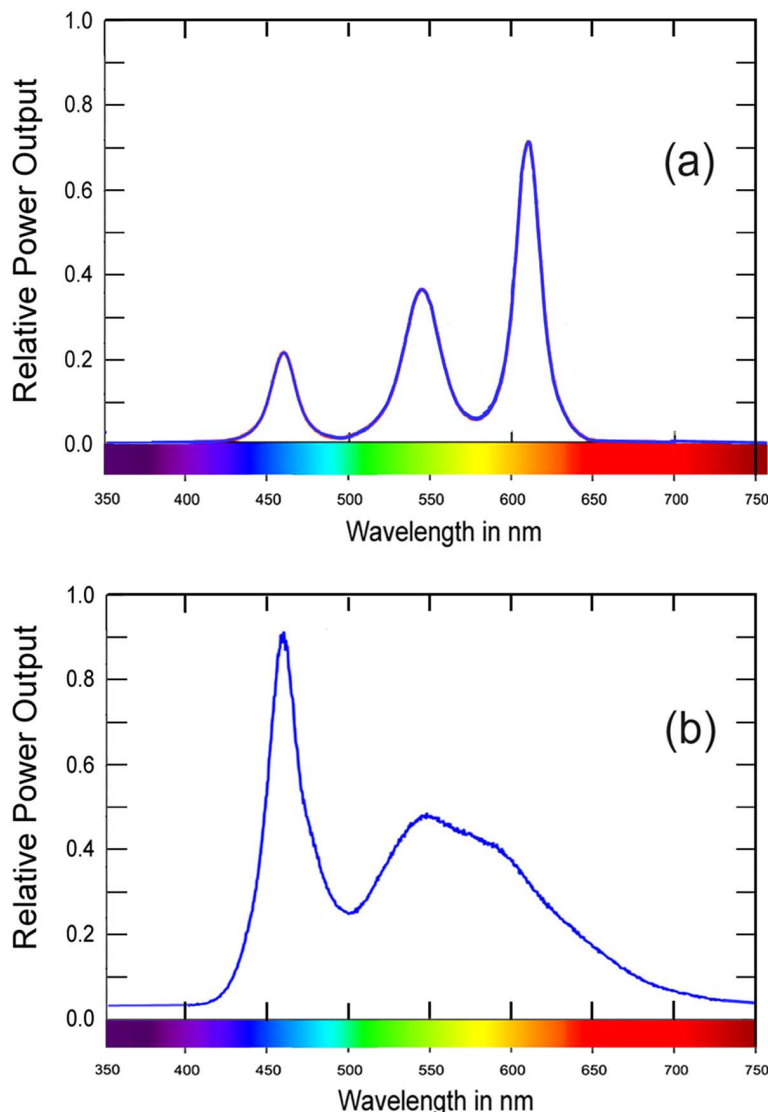


Figure 2.8 Spectra of white light LEDs: (a) trichromatic and (b) fluorescent.

that OLEDs can be made quite thin and flat, with a uniform and extended luminous flat surface. OLEDs could become the next generation of light sources for general illumination.

2.6 Television and Computer Displays

Recently, old cathode ray tubes have almost disappeared and have been replaced by newer flat screens with liquid-crystal displays (LCDs). However, the development of these displays began many years ago. A relatively early description of them

has been written by Heilmeier (1970), one of the most important contributors to the development of these displays. A more recent description of the displays can be found in many books, for example, in McDonald (1997) and Lee (2005). Liquid crystals have aroused the curiosity of researchers since the 1890s (Ferguson, 1964). They are called liquids because they flow, pour, and assume the form of their container as any liquid does. However, unlike in a liquid, the molecules form loosely ordered arrays, resembling a solid crystal. These molecules have an elongated shape, resembling small rods. There are three possible phases of liquid crystals, i.e., nematic, smectic, and cholesteric. In nematic liquid crystals, the molecules can move laterally and up and down, but their orientation (the long axis of the molecules) is relatively constant, resembling matches in a box. Smectic liquid crystals are named for the Greek word for soup. In these crystals, the molecules are in layers, one on top of the other, with their molecules aligned perpendicularly to the plane. Two adjacent layers can laterally slide over each other. In cholesteric liquid crystals, the molecules are also arranged in layers as in smectic liquid crystals, except that the molecules are oriented along the planes and not in a perpendicular direction as in smectic crystals. In these cholesteric crystals, the orientation of molecules changes slowly from one plane to the next, forming a helical pattern, resembling a screw. Any crystal can have these three phases, depending on its temperature. The molecular orientation is defined by a unit vector called the director.

The preferential orientation of the molecules causes the crystal to behave in an isotropic manner, making them double refractive. As described in any physical optics book, for example, Born and Wolf (1999), isotropic materials change an incident linearly polarized beam of light to a different state of polarization. For a more detailed description of how a polarized beam of light interacts with a liquid crystal in displays, the reader can refer to the book by McDonald (1997). We can briefly mention that the liquid crystal is a thin layer between two linear polarizers with their axes perpendicular to each other. The linearly polarized light entering the liquid crystal rotates its plane of polarization by an angle of 90 deg, so that the light can pass through the second polarizer.

As illustrated in Fig. 2.9, an electric field is applied perpendicularly to the liquid crystal by means of two thin and transparent conducting electrodes, such as tin oxide. When this electric field is applied, the rotation magnitude of the polarization plane of the light passing through the crystal decreases. Thus, the amount of light passing through the whole system can be controlled with the magnitude of the electric field. This effect is a function of wavelength, but it is not sufficient to generate the light of different colors at the output.

A full display is produced if an array of small pixels is generated, where each pixel is an independent liquid-crystal system with different electric fields applied to each pixel. A color display is made by separating each pixel into three subpixels: red, green, and blue. Each subpixel has a colored filter in front of it. To observe the image, the display is illuminated from behind with a fluorescent lamp. Some new displays use illuminating LEDs instead of a fluorescent lamp.

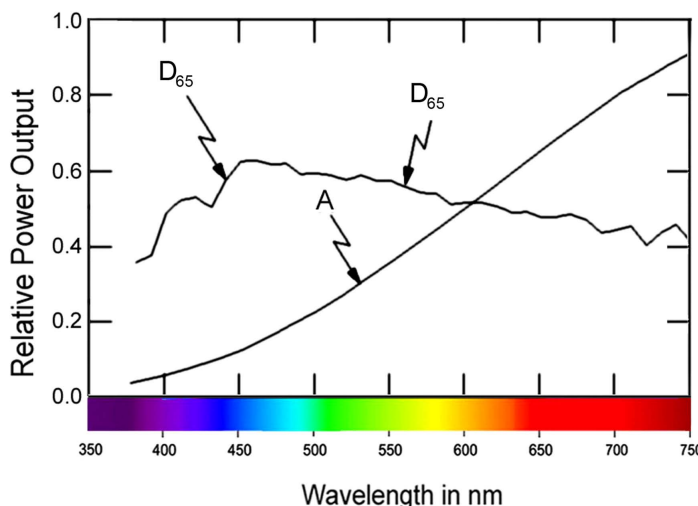


Figure 2.9 Schematics of a liquid-crystal display.

The colorimetric aspects of liquid crystal displays have been treated in detail by several authors, for example, in Chapter 14 of the book by Kang (1997) and in Chapter 7 of the book by McDonald (1997).

Research is continually carried out to obtain even better displays, such as the work on the so-called interferometric modulator displays (IMODs), which work similarly to a reflective interference filter, as described by Waldrop (2007). Another interesting new display is the previously described OLED, which has many advantages over liquid crystal displays, such as flexibility, thinness, and higher efficiency (Howard, 2004).

2.7 Standard Light Sources and Illuminants

Obviously, the most important light source is natural daylight. Unfortunately, its spectral characteristics are quite variable thanks to time, geographic location, and weather. Atmospheric transparency and clouds can change daylight in a few minutes. CCTs of daylight vary from about 2000 K in late morning to above 10,000 K in late afternoon.

Strictly speaking, standard light sources and illuminants are slightly different concepts. From a formal point of view, a standard light source exists in real life and can be physically turned off or on. On the other hand, standard illuminants are mathematical (numerical) descriptions of ideal light sources. However, some light sources are specially designed and constructed to emulate illuminants, making these terms almost equivalent for many practical purposes. In 1931 the CIE convention recommended three standard illuminants (CIE, 1932; ISO/CIE, 1991) defined by some real light sources. These standard illuminants are referred to as illuminants A, B, and C.

Illuminant A is formed by a gas-filled incandescent lamp with a coiled tungsten filament and a quartz bulb. Its CCT is 2856 K, and its spectral power distribution

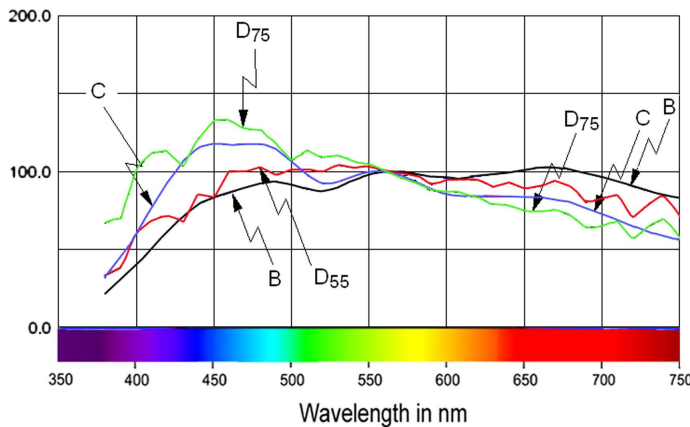


Figure 2.10 Spectral radiance of standard illuminants D₆₅, A, and F₂.

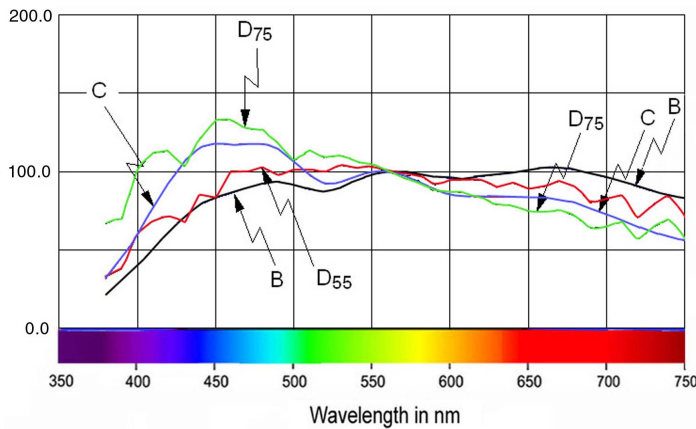


Figure 2.11 Spectral radiance of standard illuminants B, C, D₅₅, and D₇₅.

is as shown in Fig. 2.10. The second illuminant, B, now discontinued, emulates noon sunlight with the spectral power distribution and is shown in Fig. 2.11. This illuminant was produced by a double-liquid filter in front of a light source A, as shown in Table 2.1.

The third illuminant, C, emulating average daylight, is also produced by filtering a light source emulating illuminant A with a liquid filter. However, real daylight contains more ultraviolet than does illuminant C.

Due to the large fluctuations of natural daylight, illuminants B and C were considered inadequate. Instead, the CIE convention recommended a series of D illuminants with CCTs of approximately 5500 (D₅₅), 6500 (D₆₅), and 7500 (D₇₅) K, to replace illuminants B and C. As defined by the CIE Convention in 1931 (CIE, 1932), the x and y chromaticity coordinates to be studied later in this book must satisfy the following relation for D illuminants:

$$2.870y_D^2 - y_D - 3.000x_D^2 - 0.275 = 0, \quad (2.3)$$

Table 2.1 Liquid filters with 1-cm thickness to transform illuminant A to illuminant B.

Filter	Component	Quantity
First filter	Copper sulfate ($\text{CuSO}_4 \cdot 5\text{H}_2\text{O}$)	2.452 g
	Mannite [$\text{C}_6\text{H}_8(\text{OH})_6$]	2.452 g
	Pyridine ($\text{C}_5\text{H}_5\text{N}$)	30.00 cm^3
	Distilled water	1000 cm^3
Second filter	Ammonium cobalt sulfate [$\text{CoSO}_4(\text{NH}_4)_2\text{SO}_4 \cdot 6\text{H}_2\text{O}$]	27.71 g
	Copper sulfate ($\text{CuSO}_4 \cdot 5\text{H}_2\text{O}$)	16.11 g
	Sulfuric acid (H_2SO_4) (density: 1.835)	10.00 cm^3
	Distilled water	1000 cm^3

with x_D in the range of 0.250–0.380. Here, x_D and y_D are the chromaticity coordinates to be described in Chapter 5.

The standard illuminant D₆₅ (see Fig. 2.10) represents average daylight and has a color temperature of 6500 K. Its spectral power distribution is similar to that of the discontinued illuminant C, but with some important characteristics that make it closer to daylight. Illuminant D₆₅ is based on many measurements of daylight in several countries. In graphic arts and photography, the illuminants D₅₅ and D₇₅, with CCTs of 5500 and 7500 K, respectively, are sometimes used. These illuminants are obtained from the illuminant D₆₅ by changing their color temperature with a procedure suggested by the CIE convention. In the definition of illuminants, the absolute value of their spectral radiance is not important. The important factor is variation with the wavelength, so that it can be multiplied by any desired arbitrary constant, and thus the relative spectral radiances can be obtained. Illuminants F are formed by various types of fluorescent lamps. The F₂ illuminant is the most common of them, represented by a cool white fluorescent lamp (4100 K and CRI = 60). Table 2.2 gives the relative spectral radiance of illuminants A, D₆₅, and F₂ with six decimal places and 5-nm steps.

Table 2.3 gives the relative spectral radiance values for the discontinued or less-used illuminants B and C, as well as for the illuminants D₅₅ and D₇₅, with only one decimal place and 10-nm steps. All of the tabulated values for standard illuminants have been normalized by multiplying by an appropriate factor, so that their value is equal to 100 at a wavelength of 560 nm. Therefore, the relative spectral irradiance values can be larger than 100 for some wavelengths.

Good daylight simulators are very important in colorimetry and color control. Many attempts have been made to simulate these illuminants, as described by McCamy (1994). The best instruments use a high-pressure xenon arc lamp with the appropriate filters. D illuminants can be, in practice, approximated in several manners, for example, by a tungsten lamp and a bluish-colored glass filter.

2.8 Color-Rendering Index of Light Sources

In light sources for illumination or for colorimetric purposes, the color-rendering index (CRI) number, which is a measure of how faithfully colors can be perceived when illuminated with a light source relative to an ideal light source—such as a

Table 2.2 Relative spectral radiances of standard Illuminants D₆₅ and A, and the less frequently used illuminant F₂ with three decimals.

Wavelength in nm	A	D ₆₅	F ₂	Wavelength in nm	A	D ₆₅	F ₂
360	6.144620	46.638300	1.140	600	129.04300	90.006200	16.540
365	6.947200	49.363700	1.150	605	132.69700	89.802600	15.210
370	7.821350	52.089100	1.160	610	136.34600	89.599100	13.800
375	8.769800	51.032300	1.170	615	139.98800	88.648900	12.360
380	9.795100	49.975500	1.180	620	143.61800	87.698700	10.950
385	10.899600	52.311800	1.480	625	147.23500	85.493600	6.650
390	12.085300	54.648200	1.840	630	150.83600	83.288600	8.400
395	13.354300	68.701500	2.150	635	154.41800	83.493900	7.320
400	14.708000	82.754900	3.440	640	157.97900	83.699200	6.310
405	16.148000	87.120400	15.690	645	161.51600	81.863000	5.430
410	17.675300	91.486000	3.850	650	165.02800	80.026800	4.680
415	19.290700	92.458900	3.740	655	168.51000	80.120700	4.020
420	20.995000	93.431800	4.190	660	171.96300	80.214600	3.450
425	22.788300	90.057000	4.620	665	175.38300	81.246200	2.960
430	24.670900	86.682300	5.060	670	178.76900	82.277800	2.550
435	26.642500	95.773600	34.980	675	182.11800	80.281000	2.190
440	28.702700	104.865000	11.810	680	185.42900	78.284200	1.890
445	30.850800	110.936000	6.270	685	188.70100	74.002700	1.640
450	33.085900	117.008000	6.630	690	191.93100	69.721300	1.530
455	35.406800	117.410000	6.930	695	195.11800	70.665200	1.270
460	37.812100	117.812000	7.190	700	198.26100	71.609100	1.100
465	40.300200	116.336000	7.400	705	201.35900	72.979000	0.990
470	42.869300	114.861000	7.540	710	204.40900	74.349000	0.880
475	45.517400	115.392000	7.620	715	207.41100	67.976500	0.760
480	48.242300	115.923000	7.650	720	210.36500	61.604000	0.680
485	51.041800	112.367000	7.620	725	213.26800	65.744800	0.610
490	53.913200	108.811000	7.620	730	216.12000	69.885600	0.560
495	56.853900	109.082000	7.450	735	218.92000	72.486300	0.540
500	59.861100	109.354000	7.280	740	221.66700	75.087000	0.510
505	62.932000	108.578000	7.150	745	224.36100	69.339800	0.470
510	66.063500	107.802000	7.050	750	227.00000	63.592700	0.470
515	69.252500	106.296000	7.040	755	229.58500	55.005400	0.430
520	72.495900	104.790000	7.160	760	232.11500	46.418200	0.460
525	75.790300	106.239000	7.470	765	234.58900	56.611800	0.470
530	79.132600	107.689000	8.040	770	237.00800	66.805400	0.400
535	82.519300	106.047000	8.880	775	239.37000	65.094100	0.330
540	85.947000	104.405000	10.010	780	241.67500	63.382800	0.270
545	89.412400	104.225000	24.880	785	243.92400	63.843400	0.220
550	92.912000	104.046000	16.640	790	246.11600	64.304000	0.180
555	96.442300	102.023000	14.590	795	248.25100	61.877900	0.140
560	100.000000	100.000000	16.160	800	250.32900	59.451900	0.120
565	103.582000	98.167100	17.560	805	252.35000	55.705400	0.120
570	107.184000	96.334200	18.620	810	254.31400	51.959000	0.120
575	110.803000	96.061100	21.470	815	256.22100	54.699800	0.115
580	114.436000	95.788000	22.790	820	258.07100	57.440600	0.110
585	118.080000	92.236800	19.290	825	259.86500	58.876500	0.105
590	121.731000	88.685600	18.660	830	261.602000	60.312500	0.100
595	125.386000	89.345900	17.730				

Table 2.3 Relative spectral radiances for the standard illuminants B, C, D₅₅, and D₇₅.

Wavelength in nm	B	C	D ₅₅	D ₇₅
380	21.8	31.3	32.6	66.7
390	30.4	45.0	38.1	70.0
400	40.2	60.1	61.0	101.9
410	50.7	76.5	68.6	111.9
420	61.5	93.2	71.6	112.8
430	71.1	106.7	67.9	103.1
440	78.6	115.4	85.6	121.2
450	83.1	117.8	98.0	133.0
460	85.9	116.9	100.5	132.4
470	89.5	117.6	99.9	127.3
480	92.6	117.7	102.7	126.8
490	93.9	114.6	98.1	117.8
500	91.6	106.5	100.7	106.6
510	88.2	97.2	100.7	113.7
520	87.1	92.0	100.0	108.7
530	89.7	93.1	104.2	110.4
540	94.3	97.0	102.1	106.3
550	98.2	99.9	103.3	104.9
560	100.0	100.0	100.0	100.0
570	99.8	97.2	97.2	95.6
580	98.2	92.9	97.7	94.2
590	96.5	88.5	91.4	87.0
600	95.3	85.2	94.4	87.2
610	95.8	84.0	95.1	86.1
620	97.0	83.7	94.2	83.6
630	98.2	83.6	90.4	78.7
640	99.4	83.4	92.3	78.4
650	101.1	83.8	88.9	74.8
660	102.1	83.5	90.3	74.3
670	102.0	82.0	93.9	75.4
680	101.1	79.8	90.0	71.6
690	98.8	76.2	79.7	63.9
700	96.4	72.5	82.8	65.1
710	93.6	68.8	84.8	68.1
720	90.4	64.9	70.2	56.4
730	87.0	61.2	79.3	64.2
740	84.5	58.4	85.0	69.2
750	82.9	56.2	71.9	58.6
760	82.4	55.2	52.8	42.6
770	83.1	55.3	75.9	61.4

blackbody or to daylight—is quite important. The ideal or reference light source is the Planckian blackbody for light sources with a CCT < 5000 K or daylight for light sources with CCT ≤ 5000 K. A light source, such as blackbody radiation, by definition, has a CRI of 100. For this reason incandescent lamps have a CRI of 100, since they are almost blackbody radiators. A mathematical description of the CRI is given by Ohno (2004). The best possible color faithfulness is specified by a CRI of 100, while the poorest is specified by a CRI of zero. Fluorescent tubes have CRIs from 50 to 99. For example, fluorescent lamps with a low CRI have phosphors that emit too little red light. Skin appears with less red content when

Table 2.4 Correlated color temperature (CCT) and color-rendering index (CRI) of some common light sources.

Light source	CCT (K)	CRI
High-pressure sodium	2100	24
High-pressure mercury vapor	3400	49
Halophosphate cool white fluorescent	4230	64
Halophosphate daylight fluorescent	6480	77
Triphosphor fluorescent	3380	82
Incandescent/halogen lamp	3200	100
White three-chip LED	3300	80
White phosphor LED	3000	70
Illuminant A	2856	99
Illuminant D ₆₅	6500	100

compared with incandescent lighting. Since the eye is relatively less efficient at detecting red light, an improvement in the CRI, which increases red colors, may reduce the luminous efficacy.

It must be pointed out that a high CRI does not imply a good rendition of color, because the reference itself may have an imbalanced color. The color-rendering index has been criticized (Ohno, 2006) for not always correlating well with subjective color-rendering quality in practice, particularly for light sources with spiky emission spectra such as fluorescent lamps or white LEDs. A better color-rendering criterium has been recently proposed (Davies and Ohno, 2010). Table 2.4 provides some examples of CCT and CRI for some common light sources.

References

- Boas, G., "Lighting the way, developing OLEDs for the general illumination market," *Photonics Spectra*, **February**, 42–45 (2010).
- Born, M. and Wolf, E., *Principles of Optics: Electromagnetic Theory of Propagation, Interference, and Diffraction of Light*, 7th ed., Cambridge University Press, Cambridge, U.K. (1999).
- Cassarly, W. J., "High-brightness LEDs," *Opt. Photonics News*, **January**, 19 (2008).
- Craford, M. G., Holonyak, N. Jr., and Kish, F. A. Jr., "In pursuit of the ultimate lamp," *Sci. Am.* **284**, 62–77 (2001).
- CIE, *Proc., 1931 Commission Internationale de l'Éclairage*, Cambridge University Press, Cambridge, U.K. (1932).
- Davies, W. and Ohno, Y., "Color quality scale," *Opt. Eng.* **49**(3), 033602 (2010). [doi:10.1117/1.3360335].
- Eby, J. E. and Levin, R. E., "Incoherent light sources," in *Applied Optics and Optical Engineering*, Vol. 7, (Chap. 1), Kingslake, R., Ed., Academic Press, New York (1979).

- Elenbaas, W., *Light Sources*, Crane, Russak and Company, New York (1972).
- Ferguson, J. L., "Liquid crystals," *Sci. Am.* **211**, 76–85 (1964).
- Heilmeyer, G. H., "Liquid-crystal display devices," *Sci. Am.* **222**, 100–106 (1970).
- Howard, W. E., "Better displays with organic films," *Sci. Am.* **290**, 76–81 (2004).
- IESNA (Illuminating Engineering Society of North America), *The IESNA Lighting Handbook*, 9th ed., Rea, S., Ed., IESNA, Salem, MA (2000).
- ISO/CIE, *CIE Standard Colorimetric Illuminants*, Reference No. 10526, ISO/CIE, Geneva (1991).
- Kang, H. R., *Color Technology for Electronic Imaging Devices*, SPIE Press, Bellingham, WA (1997).
- LaRocca, A., *Artificial sources*, in *Handbook of Optics*, Vol. I, (Chap. 10), McGraw-Hill, New York (1995).
- Lee, H.-C., *Introduction to Imaging Science*, Cambridge University Press, Cambridge, U.K. (2005).
- McDonald, R., *Colour Physics for Industry*, 2nd ed., Society of Dyers and Colourists, West Yorkshire, U.K. (1997).
- Malacara, Z. and Morales, A., "Light sources," in *Geometrical and Instrumental Optics*, Vol. 25, Malacara, D., Ed., Academic Press, New York (1988).
- McCamy, C. S., "Simulation of daylight for viewing and measuring color," *Color Res. Appl.* **19**, 437–445 (1994).
- Narukawa, Y., "White-light LEDs," *Opt. Photonics News*, April, 25 (2004).
- Ohno, Y., "Color rendering and luminous efficacy of white LED spectra," *Proc. SPIE* **5530**, 88–98 (2004). [doi:10.1117/12.565757].
- Ohno, Y., "Optical metrology for LEDs and solid state lighting," *Proc. SPIE* **6046**, 604625 (2006). [doi:10.1117/12.674617].
- Waldrop, M. M., "Brilliant Displays," *Sci. Am.* **297**, 94–97 (2007).

Chapter 3

The Human Eye

3.1 Anatomy of the Eye

While the human eye has been the subject of interest by many researchers for several centuries, the first serious studies were carried out by von Helmholtz (1924), as described in his book, *Handbuch der Physiologischen Optik*. The eye studies in the nineteenth century culminated with the work by Gullstrand (1909). Recent developments on the eye, its color processing mechanisms, physiology, and anatomic components have been published in many books, for example by Hubel (1995), Kaiser and Boynton (1996), Rodieck (1998), Schwartz (2004), and Chalupa and Werner (2004). An interesting description of the eye's evolution in primates has been published by Jacobs and Nathans (2009).

A diagram of human eye anatomy is presented in Fig. 3.1. The main optical constants for an average adult are given in Table 3.1. The most important optical components of the eye are:

(a) *The cornea*. This is the front transparent tissue in the eye. Its normal ideal shape is nearly spherical, with a dioptric power of about 43 diopters. Any deviation

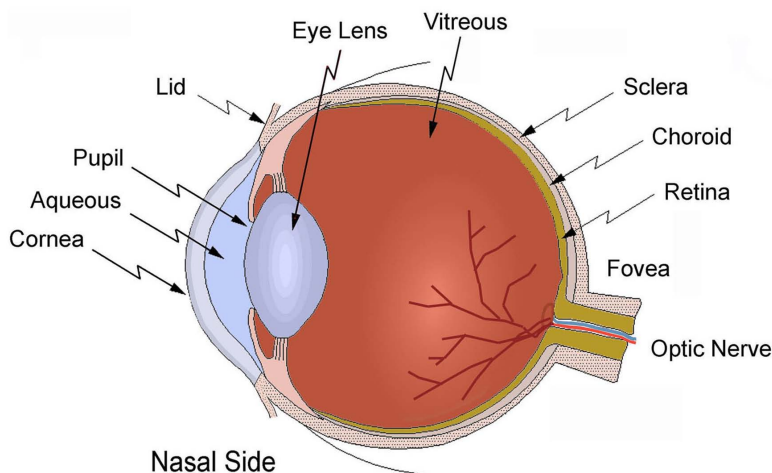


Figure 3.1 Human eye schematics.

Table 3.1 Average optical constants of the human eye.

Total length	24.75 mm
Average pupil diameter	3.5 to 4.0 mm
Effective focal length	22.89 mm
Total power (unaccommodated)	58.6 diopters
Lens power (unaccommodated)	19 diopters
Corneal power	43 diopters
Corneal radius of curvature	7.98 mm
Aqueous humor refractive index	1.336
Lens refractive index: center	1.406
Lens refractive index: edge	1.386
Vitreous refractive index	1.337

from its ideal shape produces refractive errors. If it takes on a toroidal shape, with different curvatures along two mutually perpendicular diameters, corneal astigmatism appears. The astigmatism is said to be with the rule if the curvature in the vertical diameter is larger than in the horizontal diameter and against the rule if otherwise. A small protuberance and thinning at the center makes the cornea have an almost conical shape, in a defect called keratoconus. These errors are measured with an ophthalmometer or a corneal topographer.

(b) *The pupil.* This is the circular opening in front of the eye, and it is surrounded by the iris. The pupil increases or decreases its diameter to control the amount of light entering the eye. The maximum diameter of the pupil, with low illumination levels, is around 6–8 mm, and the minimum diameter, with high illumination levels, is between 1 and 2 mm. Its average diameter is about 3.5–4 mm.

(c) *The aqueous humor.* This is the liquid between the back of the cornea and the lens.

(d) *The lens.* This is a flexible lens, also called the crystalline lens, whose optical power can be modified by means of the ciliary muscles. The ciliary muscles increase the power (accommodation) to focus on near objects and relaxes its shape to focus on distant objects. The nucleus of this lens has a higher refractive index than its external parts. The relaxed lens has a dioptric power of about 15 diopters and can be increased (accommodation amplitude) by about 15 diopters in children or about 0.5 diopters in the elderly. The lens can lose its transparency for many reasons, producing what is known as a cataract (Lerman, 1962; Van Heyningen, 1975; Pokorny et al., 1988). To correct this condition, the lens must be removed. Frequently, a plastic lens is inserted to replace the eye lens. The crystalline lens contains a yellow pigment with strong absorption in the ultraviolet region, near a wavelength of 365 nm, with almost perfect transparency 550–650 nm, as shown in Fig. 3.2. This lens pigment reduces its transparency with age.

(e) *The vitreous humor.* This is the liquid filling most of the eye globe, in the space between the lens and the retina. Sometimes, especially in medium- or high-myopic eyes, small particles float in this medium, producing small images that appear to be floating in space, as described by White and Levatin (1962).

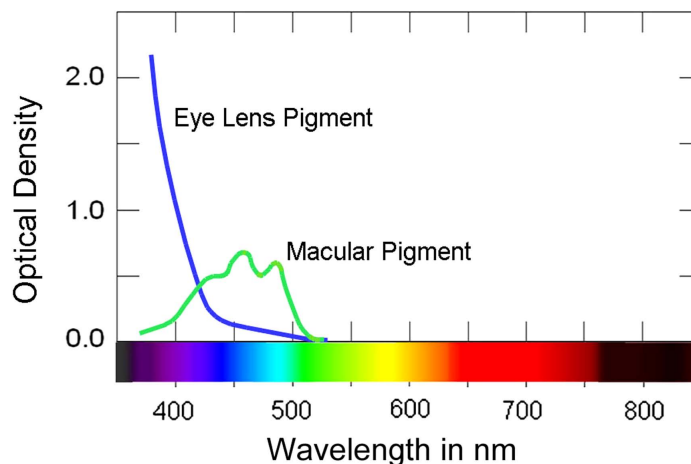


Figure 3.2 Spectral distribution of eye lens and macular pigments.

(f) *The retina*. This is the light-sensitive surface of the eye, on which the images are formed. The retina is formed by several layers. The most internal one, in contact with the vitreous humor, is formed by cells and fiber nerves, while the last layer in the back has the light-sensitive elements (Young, 1970), i.e., the rods and cones, which will be studied in more detail in the following sections.

(g) *The fovea*. There is a zone where the optic nerve enters the eye globe, producing a blind zone, with an angular diameter of about 5–7 deg, at 15 deg from the optical axis on the nasal side. The fovea is a small zone near the optical axis, where the retina becomes thinner and blood vessels are not present. It should be mentioned that, strictly speaking, the eye does not have rotational symmetry. The center of curvature of the cornea is slightly shifted from the optical axis of the crystalline lens. The fovea is also slightly shifted from the optical axis. The fovea contains only cones in a dense random array. Outside the fovea the main light-sensitive elements are the rods, which are responsible for the scotopic vision. They are much more sensitive to brightness than the cones, but they are not color sensitive and have very low spatial resolution (Rabbets, 1998; Atchison and Smith, 2000).

Using adaptive optics techniques imported from astronomers, David Williams and collaborators from the University of Rochester have been able to obtain images from a living body of cones and other retinal structures, of $\sim 5 \mu\text{m}$ diameter (Liang et al., 1997; Reiss, 1998; Williams, 1999a,b).

In a small area centered on the fovea, there is a nerve layer between the vitreous humor and the cone layer, known as the *macula lutea* (yellow spot). The yellow pigment producing its color is the macular pigment. The spectral distribution for this pigment is shown in Fig. 3.2. This pigment can be observed only under very special conditions. The macular pigment of the cones in the central retina is permanently less stimulated with blue light than the cones surrounding this zone, but this is compensated by a greater sensitivity to blue light of the cones on the macula.

The retina has a good supply of blood through the retinal artery and vein that enter the eye in the optic disk. Beginning there, many small blood vessels cover the retina, avoiding the zone of the fovea.

3.2 Eye Resolving Power and Eye Aberrations

As any other optical instrument with image-forming lenses, the eye has optical aberrations that limit its optical performance (Gubisch, 1967). The resolving power of the emmetropic eye is limited to about 1 min of arc. The three main reasons for this limitation are as follows:

- (a) *Light diffraction.* It is a well-known fact that in physical optics, the resolving power of an optical system is limited by the light-diffraction effects to an angular image size θ_{Rad} , in radians, and is equal to

$$\theta_{\text{Rad}} = \frac{1.22\lambda}{D}, \quad (3.1)$$

where D is the pupil's diameter in mm. Thus, with a simple calculation, for the center of the visible spectrum, the resolution $\theta_{\text{arc min}}$, in arc minutes, is given by

$$\theta_{\text{arc min}} = \frac{2.3}{D}. \quad (3.2)$$

We know that the eye's resolving power is 1 min of arc, so the diffraction effects are noticeable only in strong daylight if the pupil closes to less than 2.3-mm diameter.

- (b) *The size of the detector elements.* The angular size of the cones is about 1 min of arc. Thus, when the aberrations are low enough, the resolving-power limitation is due to the diameter of the cones.
- (c) *The aberrations of the optical system.* The off-axis aberrations are not very important for the human eye, since the image is always observed on axis by fast scanning through continuous movement of the eye. However, the on-axis aberrations are important and might limit the eye's resolution to more than 1 min of arc.

The axial chromatic aberration arises because the light rays with different colors focus on different focal planes along the optical axis. Köhler (1962) devised a simple and interesting experiment to show the presence of axial chromatic aberration in the eye. To repeat the experiment, with each of your hands holding a card, place them in front of each of your eyes. Each card must have a straight edge in front of the eye covering half the eye pupil. The left edge of the right-hand card must be in front of the pupil of the right eye and the right edge of the left-hand card must be in front of the pupil of the left eye. Now look at a highly colored image, for example, on a computer screen. It can be noticed that different color zones appear to have slightly different depths. This effect, called pseudostereopsis, can also be observed without the cards by some people. The effect arises because the pupils of the eyes are not always centered with the optical axis (Hunt, 1991).

The axial chromatic aberration has been studied and measured by several researchers, for example, by Wald and Griffin (1947), Bedford and Wyszecki (1957), and by Thibos et al. (1992). Powell (1981) designed a lens than can compensate for the chromatic aberration of the eye. The focus shift at the blue end of the spectrum due to this aberration is as high as 2 diopters.

The spherical aberration of the eye appears because paraxial rays and marginal rays passing through the eye are focused at different planes along the optical axis. Many different experiments have been performed to measure the spherical aberration of the eye (Koomen et al., 1949; Ivanof, 1956).

Besides the primary aberrations, the human eye has high-order and irregular aberrations due to corneal deformations, refractive index inhomogeneities, and many other causes. Ideally, the refracted wavefront coming from a point light source or point object becomes perfectly spherical and is convergent to a point image on the retina. However, the corneal irregularities and inhomogeneities produce deformations on the wavefront, causing it to deviate from its ideal spherical shape. Then, the image, instead of being a point (extremely small spot), becomes a larger spot, degrading the image quality. Many researchers (Liang et al., 1994; Liang and Williams, 1997; Prieto et al., 2000) have measured the wavefront deformations (wavefront aberrations) with a Shack–Hartmann arrangement.

3.3 Stiles–Crawford Effect

When a collimated beam of light enters the pupil of the eye, the light rays are refracted toward a common point on the retina near the optical axis. Not all rays arrive at the retina with the same incidence angle. The rays close to the optical axis are almost perpendicular to the retina, while the rays near the edge of the pupil have the largest incidence angle. The retinal angle of incidence affects the perceived luminance. The rays with the largest angle produce a smaller brightness effect on the retina. This is the Stiles–Crawford effect.

There is a small change in the perceived color when a monochromatic light beam is incident at different angles in a given zone in the retina (Enoch and Stiles, 1961). It has been customary to call this effect the Stiles–Crawford effect II. It has been shown that this color change is not only in hue but also in saturation. The changes on the perceived color are due to variations in the directional response of the three color receptors in the retina.

3.4 Eye Response to Pulsating Light

An alternation of light fields with the same or different colors can be produced by a rotating disk with apertures that permit the light to pass. The illuminated field appears to be pulsating only if the frequency is low enough—of the order of a few hertz—producing a sensation of *flicker*. When the frequency is high enough, the light pulses fuse, producing the appearance of a nonpulsating light. It is interesting that the light field seems brighter than the field when the rotating disk is stationary; that is, much brighter than the average brightness. This is known as

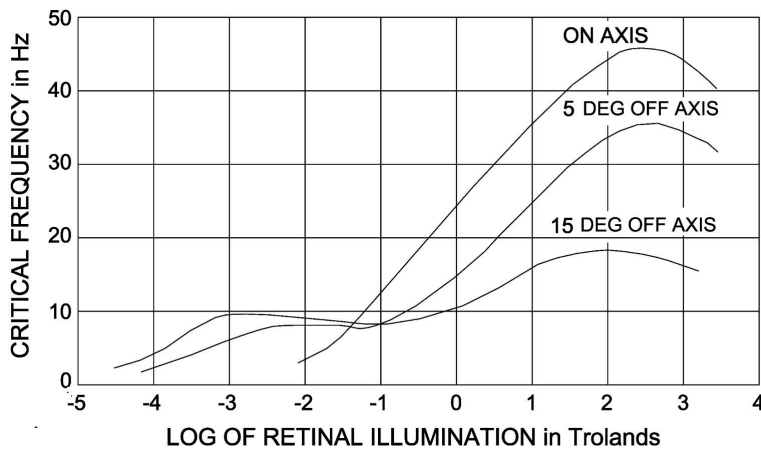


Figure 3.3 Critical flicker frequency increases linearly with the logarithm of the retinal illumination. A flickering white field with a diameter of 2 deg was used, with a constant white surround with the same luminance.

the Brücke–Bartley effect. If the speed of the rotating disk is further increased, the flickering effect returns with a smaller magnitude, but the Brücke–Bartley effect is no longer observed. With an even greater increase in the disk's rotation speed, the flickering completely disappears, and the apparent luminance of the field is equal to its time-average value, also called the Talbot luminance. This is the Plateau–Talbot law. The transition of flicker to fusion occurs at the *critical fusion frequency*, or *critical flickering frequency*.

In visual research, retinal illumination cannot be directly measured. So, conventional retinal illumination is defined as the product of the photopic luminance in the observed object, multiplied by the area of the pupil of the eye. Then, a *troland* (td) is defined as the retinal illuminance produced when a surface with a luminance of 1 cd/m^2 is viewed with an eye that has a pupil with an area of 1 mm^2 , from a distance of 1 m. The critical flickering frequency value depends on the retinal illumination. We see in Fig. 3.3 that the critical flickering frequency increases linearly with the logarithm of the retinal illumination. This is the Ferry–Porter law. There is a peak of the critical flickering frequency at about 300 td, decreasing again after this maximum. This frequency was measured with a 2-deg white-light patch that is surrounded by a 10-deg color field with the same average luminance.

If the pulses are made up of different colors, the fusion produces a color due to the color addition of these light beams. When the pulsating frequency is low enough the observer sees flicker. Let us consider two fields with different colors, separated by a common straight boundary and pulsating with the same frequency of about 10–15 Hz, but 180 deg out of phase. That is, one field is bright when the other is dark. The flickering is minimized when the two fields have the same luminance. This method was used to measure the relative color sensitivity of the

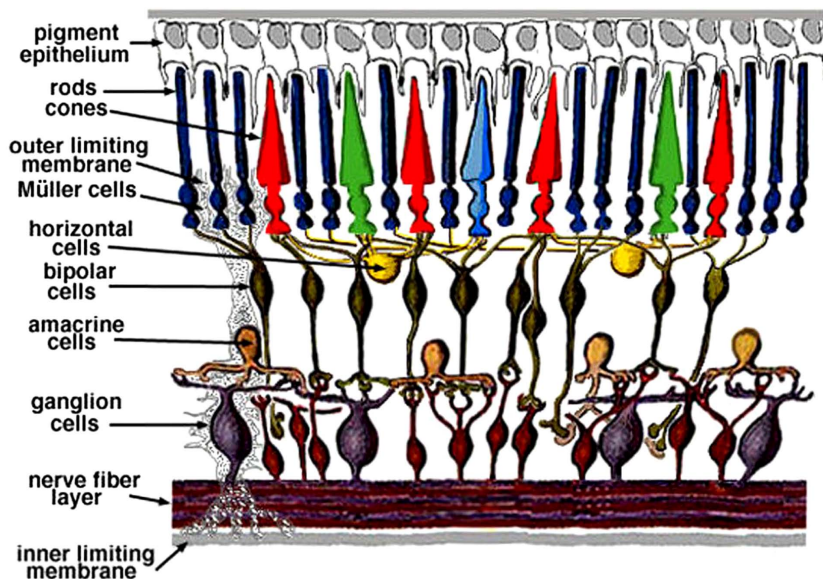


Figure 3.4 Transverse schematics of the structure of the retina in a human eye, showing the cones and rods.

eye and is known as the flicker method, which was developed by Ives (1912). This is also the principle of heterochromatic photometry methods.

With a close relation to flickering, we have the so-called afterimages, or aftereffects, that occur when looking for a prolonged period at an image and then suddenly changing the observation target to a white surface. The previously observed image appears in negative and complementary colors (Brindley, 1963; Favreau and Corballis, 1976).

3.5 Visual Detectors in the Retina

The light-sensitive elements in the retina are of two types, i.e., rods and cones. The rods are responsible for night or scotopic vision, while the cones' function is photopic or daylight color vision, with higher definition than night vision (see Fig. 3.4). There are three sets of color-sensitive elements, *L-cones* for long wavelengths, *M-cones* for medium wavelengths, and *S-cones* for short wavelengths, (approximately for red, green, and blue light, respectively). The sharpest vision occurs in the central part of the retina, called the fovea, where most cones are located, and there are no rods. The presence of rods begins at an angle of about 4 deg from the fovea centralis, as illustrated in Fig. 3.5. There are fewer S-cones than L- or M-cones.

The blue S-cones have some spatial properties that make them different from the L- and M-cones (Boynton, 1996), mainly:

- (a) They are sparsely distributed in the retina and are almost absent at the center of the fovea.

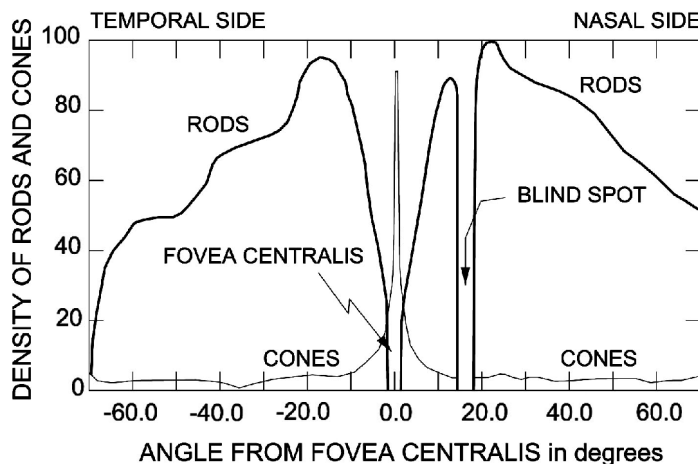


Figure 3.5 Distribution of rods and cones in the retina along a horizontal plane through the fovea.

(b) They do not contribute to the contrast discrimination, thus they are not able to detect image borders.

(c) They do not contribute to the luminance, but on the other hand, they contribute very importantly to the hue and chroma—mainly yellow–blue discrimination (Eisner and MacLeod, 1980).

(d) Genes for L- and M-cones are in the X chromosome, while the genes for the S-cones are located on an autosome (chromosome 7) (Nathans et al., 1986; Nathans, 1989).

Each of the three types of cones has an associated pigment (Rushton, 1962, 1975; MacNichol, 1964; MacLeod and Hayhoe, 1974; Bowmaker and Dartnall, 1980). A good description of these pigments is found in a chapter by Rushton (1972). The absorbance spectra for these pigments has been measured *in situ* in the outer segment using microspectrophotometry (Merbs and Nathans, 1992). In this technique the cone receptors are placed on a microscope slide. Then, the light transmission of the cones is measured by passing a very small light beam through a single cone and another reference beam outside of it (Dartnall et al., 1983). A better method to measure cone absorbance is by a physiological method in which a single cone's outer segment is drawn inside a small suction glass electrode. Then, the electrical current response to monochromatic light of different wavelengths is measured (Schnapf et al., 1987). Figure 3.6 shows the spectral absorbance of the three cone pigments. The measurement of the cone's pigment absorbance is important because the light detection efficiency is directly proportional to this absorbance. Table 3.2 shows the names and reflectance peaks of these pigments.

3.6 Observation of the Human Eye Retina

To observe the retina we must illuminate it, but unfortunately the reflectance of the retina is low, from about 0.1 to 10%, depending of the wavelength. Before

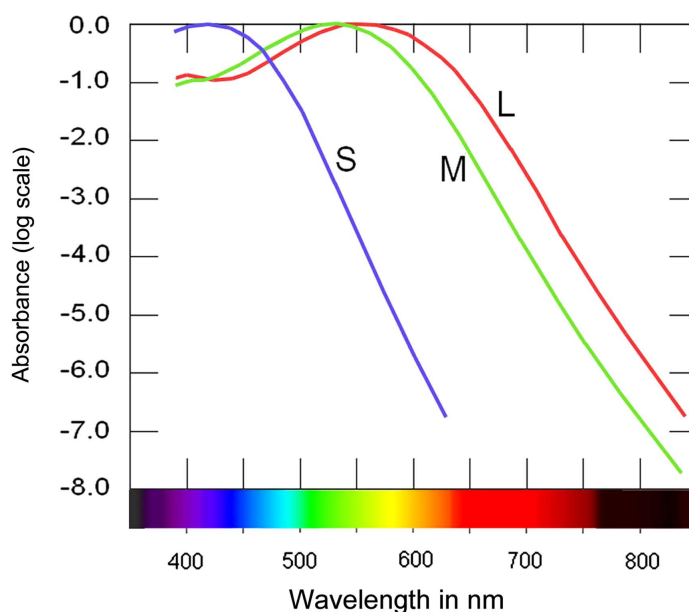


Figure 3.6 Spectral absorbance for the three cone pigments. The scales for the spectral absorbance is logarithmic.

Table 3.2 Absorbance of visual pigments.

Color	Pigment	Absorbance peak
Red	Eritrolabe	577 nm (yellow)
Green	Chrolabe	540 nm (green)
Blue	—	477 (blue-violet)

von Helmholtz (1924), during the nineteenth century, Purkinje (1923) and Brücke (1864) noticed the glow of the pupil of eyes illuminated from approximately the same direction as the observer. Using this property of the eye (reflecting the light that falls on the retina), von Helmholtz invented in 1855 an instrument to observe the human eye retina, now known as the ophthalmoscope. Jackman and Webster (1886) obtained the first photographic record of the retina.

The field, contrast, and clarity of the image were greatly improved after Helmholtz due to more elaborate ophthalmoscopes and fundus cameras. A human eye retina image is shown in Fig. 3.7, where many parts can be observed—for example, the fovea, the optic nerve entrance, the blood vessels, and many other details. The effect of the eye's aberrations is that the image is degraded in quality and the person cannot see small object details. However, there is another consequence of the presence of these aberrations, i.e., the retina cannot be observed with enough detail when a typical ophthalmoscope is employed. For this reason the cone structure cannot be observed.

The next advance in imaging the retina was the scanning-laser ophthalmoscope, invented by Webb and collaborators (Webb et al., 1980). They formed the image

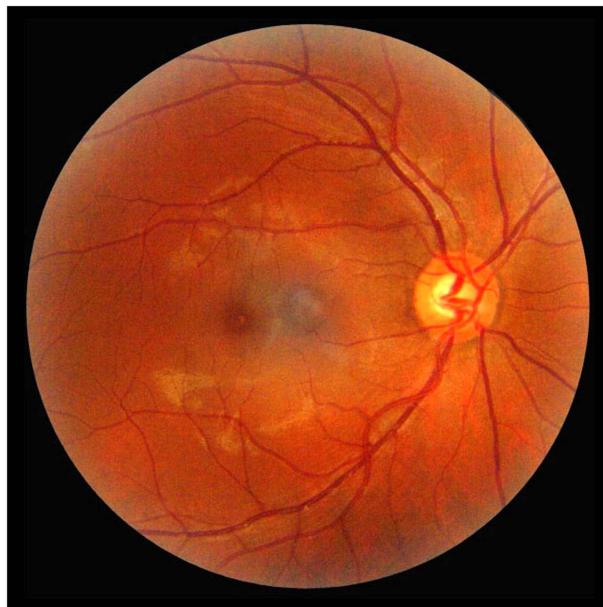


Figure 3.7 Image of a human retina taken with an ophthalmoscope.

with a confocal microscope configuration, where the microscope objective is observing the optics of the eye and the object is the retina. A laser scans the retina point by point, moving the laser in an array of parallel lines as in a television set. This arrangement has several advantages. One is that the confocal configuration allows the examination of any desired plane without light from other undesired planes interfering and reducing the contrast of the image. Another important advantage is that the amount of light needed is much less than in conventional ophthalmoscopy. The final result is an image with greater contrast and detail.

Another great advance was the adaptive optics techniques in ophthalmic instrumentation. The optical resolution in astronomical telescopes is also limited by aberrations, mainly introduced by inhomogeneities in the atmosphere due to hot air currents and turbulence in an optical effect known to astronomers as *seeing*. Astronomers compensate for the wavefront distortions introduced by the atmospheric seeing by means of a flexible mirror in front of the light beam forming the image. Since wavefront deformations are not static, but change continuously, the flexible mirror must also change its shape in a continuous manner to compensate for the wavefront deformations at all times. This is automatically done by a continuous measurement of the wavefront deformations, which are read by a computer, which in turn deforms the mirror appropriately. In this manner, the image resolution increases several times. This whole process is called *adaptive optics*.

In the human eye there is a similar situation, since the optical elements are formed by living tissues that continuously change their shape as in jellies, causing

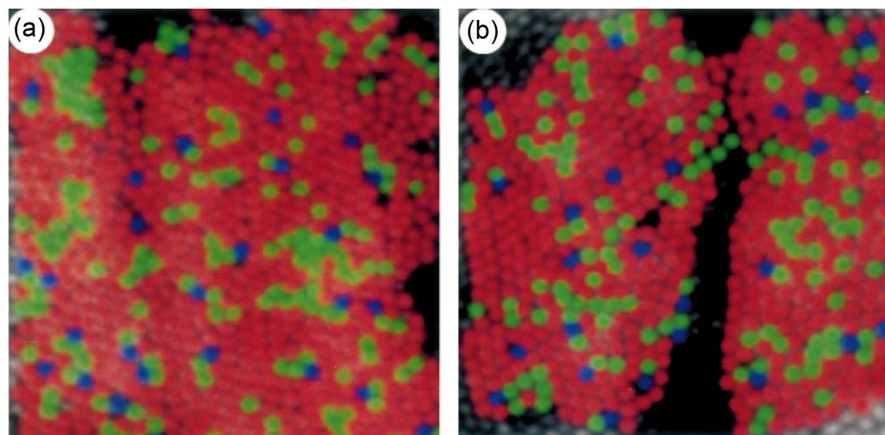


Figure 3.8 Images of a human retina taken with an ophthalmoscope with adaptive optics, by Roorda and Williams. Reprinted by permission from Macmillan Publishers Ltd: *Nature*, ©1999.

the aberration to change rapidly in a continuous manner (Hofer et al., 2001). The adaptive optics methods used by the astronomers has been used with great success to make an ophthalmoscope capable of resolving the image of the retina details to about three to five times smaller than in conventional ophthalmoscopes (Liang et al., 1997; Williams, 1999b). An image of the retina obtained with adaptive optics shows the packing arrangement of cones in the retina. These images allow the individual identification of the three types of cones, as shown in Fig. 3.8 (Roorda and Williams, 1999; Roorda et al., 2001; Carroll et al., 2009). Adaptive optics methods have been integrated with success in conventional scanning laser ophthalmoscopes (Roorda et al., 2002) and optical coherence tomography (Hermann et al., 2004), increasing their image resolution.

The contrast sensitivity of the human eye has also been the subject of many investigations. For example, Williams (1985) studied the visibility and contrast of sinusoidal interference fringes near the resolution limit.

3.7 Cone Fundamentals

The cone spectral sensitivities, also called *cone fundamentals*, involve basic understanding of color vision (Vos et al., 1990), but more than a century of research was required to discover these sensitivities. These cone fundamentals are represented by $\bar{l}(\lambda)$, $\bar{m}(\lambda)$ and $\bar{s}(\lambda)$.

Several methods have been used to obtain the sensitivities of human cones. One of these measuring techniques is based on the isolation of one type of cone in order to measure it with one of many possible procedures (Stockman et al., 1993b). A good review of this subject can be found in a chapter by Stockman and Sharpe (1999) and in an article by Boynton (1996). If a cone is illuminated with a wavelength to which it is quite sensitive, its sensitivity is suppressed for a few

minutes to all wavelengths, not merely to the one that illuminated the cone. Thus, in the isolation method a background field is illuminated with one or two wavelengths that suppress the sensitivities of two cones but spares the one of interest. Then, the desired cone sensitivity is determined by measuring the radiance necessary to detect details in an illuminated target as a function of the wavelength.

If desired, the S-cones can also be suppressed by using either relatively high spatial or temporal frequencies, to which they are insensitive. For example, high-frequency flickering reduces S-cone contributions. Sometimes the most effective method of obtaining the sensitivity of only one type of cone is to examine people that lack the unwanted cone. For example, Smith and Pokorny (1975) obtained estimations of the spectral sensitivities of the L-cones in deutanopes and of the M-cones in protanopes, using experimental conditions where the S-cones did not contribute significantly. Their measurements were later improved by Vos (1979). This approach is based on the hypothesis that in protanopia and deutanopia one of the two longer-wavelength photopigments is absent.

Another method is based on the transient chromatic adaptation produced by an abrupt change of background color (Stockman and MacLeod, 1992; Stockman et al., 1993a,b). In this experiment, 17-Hz flicker-detection spectral sensitivities were determined. An exchange of background color from blue to red was used to determine the M-cone spectral sensitivity and an exchange of background color from red to blue to determine the L-cone spectral sensitivity.

As previously noted, the cone sensitivities are directly related to the absorbance of the cone pigments located in their outer segments. However, the measured cone sensitivities are different from the pigment absorbance spectra for several reasons, mainly the presence of the macular and the crystalline pigments. The cone absorbance is directly measured, without the influence of these pigments, while the cone sensitivities are measured in the living eye, through the pigments.

The absolute sensitivity of each of the three types of cones has been measured with a high uncertainty, and only the relative spectral sensitivity for each one is well known. Thus, the cones' sensitivities can be scaled as desired, multiplying them by any desired constant. When the cones' sensitivities are plotted in a logarithmic scale, this multiplier shifts the curve up or down, preserving its shape. A common procedure is to normalize them so that the three kinds of cones show the same peak sensitivity. The spectral sensitivities for the three types of cones, or the fundamentals obtained by Stockman and Sharpe (2000a,b) for 10 deg, based on the Stiles and Burch (1959) 10-deg color-matching functions, are plotted in Fig. 3.9 in a logarithmic scale. These sensitivities, plotted in a linear scale, are illustrated in Fig. 3.10. The logarithmic scale is preferred because the tails of the curves are very important in color perception. When the spectral sensitivities of the L- and M-cones are added, using the proper scaling multipliers, the spectral relative sensitivity $V(\lambda)$ of the eye is obtained, as shown in Fig. 3.11. These results confirm that the S-cones do not play any role in luminance detection. The latest numerical values of the cones' sensitivities have been reported by Stockman and Sharpe (2000a,b) and by Stockman et al. (1999).

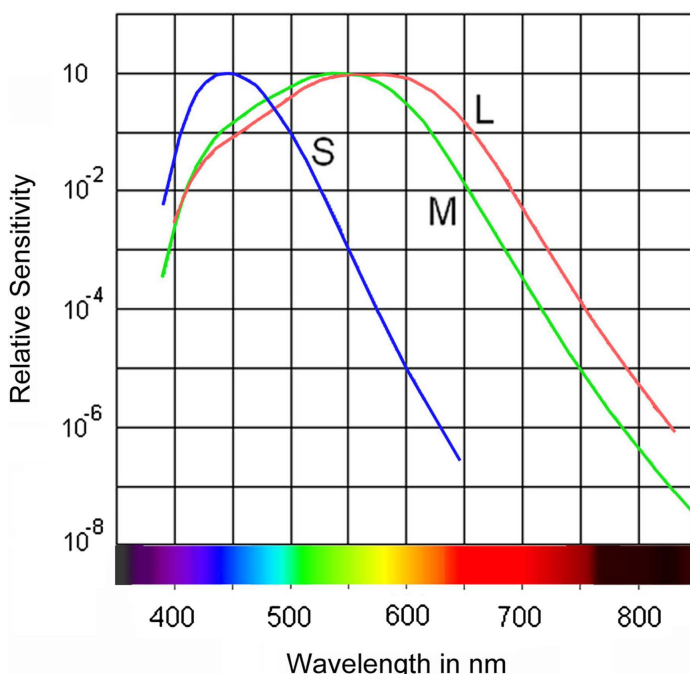


Figure 3.9 Relative spectral sensitivities (cone fundamentals) for the three types of cones in a logarithmic scale.

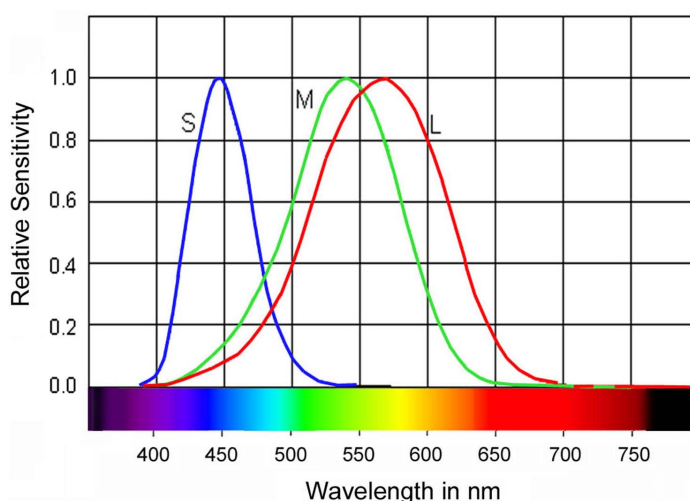


Figure 3.10 Relative spectral sensitivities (cone fundamentals) for the three types of cones in a linear scale.

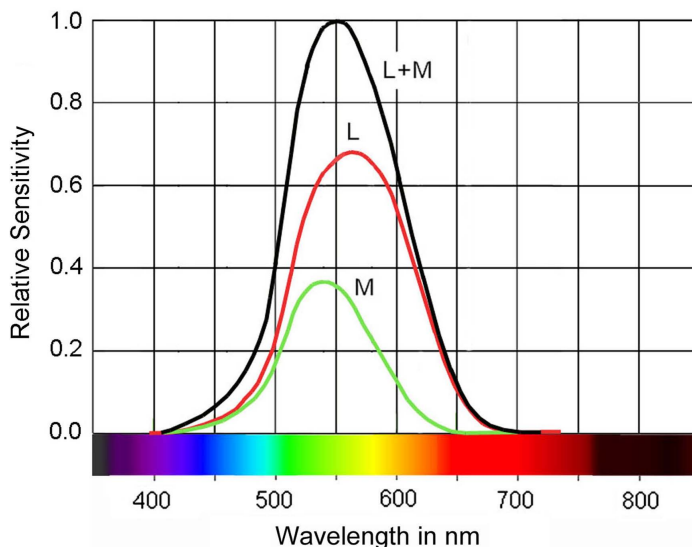


Figure 3.11 Adding the L- and M-cone sensitivities with the proper scaling constants, the $V(\lambda)$ function is obtained.

References

- Atchison, D. A. and Smith, G., *Optics of the Human Eye*, Butterworth-Heinemann, Oxford, U.K. (2000).
- Bedford, R. E. and Wyszecki, G., “Axial chromatic aberration of the human eye,” *J. Opt. Soc. Am.* **47**, 564–565 (1957).
- Bowmaker, J. K. and Dartnall, H. J. A., “Visual pigments of rods and cones in the human retina,” *J. Phys.* **298**, 501–512 (1980).
- Boynton, R. M., “History and current status of a physiologically based system on photometry and colorimetry,” *J. Opt. Soc. Am. A* **13**, 1609–1621 (1996).
- Brindley, G. S., “Afterimages,” *Sci. Am.* **209**, 85–91 (1963).
- Brücke, E., “Über den Nutzeffekt intermittierender Netzhautreizungen,” *Sitzungsber k Akad Wissensch Math-naturw Cl Wien* **49**, 128–153 (1864).
- Carroll, J., Yoon, G. Y., and Williams, D. R., “The photoreceptor mosaic in normal and defective color vision,” in *The Cognitive Neurosciences*, Gazzaniga, M. S., Ed., 4th ed., 383–394 MIT Press, Cambridge, MA (2009).
- Chalupa, L. M. and Werner, J. S., *The Visual Neurosciences*, MIT Press, Cambridge, MA (2004).
- Dartnall, H. J. A., Bowmaker, J. K., and Mollon, J. D., “Human visual pigments: microspectrophotometric results from the eyes of seven persons,” *Proc. R. Soc. London, Ser. B* **220**, 115–130 (1983).
- Eisner, A. and MacLeod, D. I. A., “Blue sensitive cones do not contribute to luminance,” *J. Opt. Soc. Am.* **70**, 121–123 (1980).

- Enoch, J. M. and Stiles, W. S., “The colour change of monochromatic light with retinal angle of incidence,” *Opt. Acta* **8**, 329–358 (1961).
- Favreau, O. E. and Corballis, M. C., “Negative after-effect in visual perception,” *Sci. Am.* **235**, 42–48 (1976).
- Gubisch, R. W., “Optical performance of the human eye,” *J. Opt. Soc. Am.* **57**, 407–415 (1967).
- Gullstrand, A., von Helmholtz, H., Ed., *Appendix II in Handbuch der Physiologischen Optik*, 3rd ed., Voss, Hamburg (1909).
- Hermann, B., Fernández, E. J., Unterhuber, A., Sattmann, H., Fercher, A. F., Drexler, W., Prieto, P. M., and Artal, P., “Adaptive-optics ultra-high-resolution optical coherence tomography,” *Opt. Lett.* **29**, 2142–2144 (2004).
- Hofer, H., Artal, P., Singer, B., Aragón, J. L., and Williams, D. R., “Dynamics of the eye’s wave aberration,” *J. Opt. Soc. Am. A* **18**, 497–506 (2001).
- Hubel, D. H., *Eye, Brain, and Vision*, W. H. Freeman, New York (1995).
- Hunt, R. W. G., *Measuring Colour*, 2nd ed., Ellis Horwood, Sussex, U.K. (1991).
- Ivanof, I., “About the spherical aberration of the eye,” *J. Opt. Soc. Am.* **46**, 901–903 (1956).
- Ives, H. E., “Studies in the photometry of lights of different colours. I. Spectral luminosity curves obtained by the equality of brightness photometer and flicker photometer under similar conditions,” *Philos. Mag.* **24**, 149–188 (1912).
- Jackman, W. T. and Webster, J. D., “On Photographing the retina of the living eye,” *The Philadelphia Photographer* **23**, 340 (1886).
- Jacobs, G. H. and Nathans, J., “The evolution of primate color vision,” *Sci. Am.* **300**, 56–63 (2009).
- Kaiser, P. K. and Boynton, R. M., *Human Color Vision*, Optical Society of America, Washington, DC (1996).
- Köhler, I., “Experiments with goggles,” *Sci. Am.* **206**, 63–72 (1962).
- Koomen, M. J., Tousey, R., and Scolnik, R., “The spherical aberration of the eye,” *J. Opt. Soc. Am.* **39**, 370–376 (1949).
- Lerman, S., “Cataracts,” *Sci. Am.* **206**, 106–114 (1962).
- Liang, J. and Williams, D. R., “Aberrations and retinal image quality of the normal human eye,” *J. Opt. Soc. Am. A* **14**, 2873–2883 (1997).
- Liang, J., Grimm, B., Goelz, S., and Bille, J. F., “Objective measurement of wave aberrations of the human eye with the use of a Hartmann–Shack wavefront sensor,” *J. Opt. Soc. Am. A* **11**, 1949–1957 (1994).
- Liang, J., Williams, D. R., and Miller, D. R., “Supernormal vision and high-resolution retinal imaging through adaptive optics,” *J. Opt. Soc. Am. A* **14**, 2884–2892 (1997).

- MacLeod, D. I. A. and Hayhoe, M., “Three pigments in normal and anomalous color vision,” *J. Opt. Soc. Am.* **64**, 92–96 (1974).
- MacNichol, E. F. Jr., “Three pigment color vision,” *Sci. Am.* **211**, 48 (1964).
- Merbs, S. L. and Nathans, J., “Absorption spectra of human cone pigments,” *Nature* **356**, 431–432 (1992).
- Nathans, J., “The genes for color vision,” *Sci. Am.* **260**, 28–35 (1989).
- Nathans, J., Piantanida, T. P., Eddy, R. L., Shows, T. B., and Hogness, S. G., “Molecular genetics of inherited variation in human color vision,” *Science* **232**, 203–210 (1986).
- Pokorny, J., Smith, V. C., and Lutze, M., “Aging of the human lens,” *Appl. Opt.* **26**, 1437–1440 (1988).
- Powell, I., “Lenses for correcting chromatic aberration of the eye,” *Appl. Opt.* **20**, 4152–4155 (1981).
- Prieto, P. M., Vargas-Martín, F., Goelz, S., and Artal, P., “Analysis of the performance of the Hartmann–Shack sensor in the human eye,” *J. Opt. Soc. Am. A* **17**, 1388–1398 (2000).
- Purkinje, J., *Beobachtungen und Versuche zur Physiologie der Sinne*, Zweites Bändchen, G. Reiner, Berlin (1923).
- Rabbets, R. B., *Clinical Visual Optics*, 3rd ed., Butterworth-Heinemann, Oxford, U.K. (1998).
- Reiss, S. M., “New advances in imaging for research?” *Opt. Photonics News January*, 24–29 (1998).
- Roorda, A. and Williams, D. R., “The arrangement of the three cone classes in the living human eye,” *Nature* **937**, 520–522 (1999).
- Roorda, A., Metha, A. B., Lennie, P., and Williams, D. R., “Packing arrangement of the three cone classes in primate retina,” *Vision Res.* **41**, 1291–1306 (2001).
- Roorda, A., Romero-Borja, F., Donnelly, W. III, Queener, H., Hebert, T., and Campbell, M., “Adaptive optics scanning laser ophthalmoscopy,” *Opt. Express* **10**, 405–412 (2002).
- Rodieck, R. W., *The First Steps in Seeing*, Sinauer Associates, Sunderland, MA (1998).
- Rushton, W. A. H., “Visual pigments in man,” *Sci. Am.* **207**, 120–132 (1962).
- Rushton, W. A. H., “Visual pigments in man,” in *Handbook of Sensory Physiology*, Dartnall, H. J. A., Ed., Springer, New York (1972).
- Rushton, W. A. H., “Visual pigment and color blindness,” *Sci. Am.* **232**, 64–77 (1975).
- Schnapf, J. L., Kraft, T. W., and Baylor, D. A., “Spectral sensitivity of human cone photoreceptors,” *Nature* **323**, 439–441 (1987).

- Schwartz, S. H., *Visual Perception: A Clinical Orientation*, 3rd ed., McGraw-Hill, New York (2004).
- Smith, V. and Pokorny, J., "Spectral sensitivity of the foveal cone photopigments between 400 and 500 nm," *Vision Res.* **15**, 161–171 (1975).
- Stiles, W. S. and Burch, J. M., "NPL colour-matching investigation: final report (1958)," *Opt. Acta* **6**, 1–26 (1959).
- Stockman, A. and MacLeod, D. I. A., "A change in color produced by an invisibly flickering light: a compressive nonlinearity in the S-cone pathway," *Invest. Ophthalmol. Visual Sci.* **33**, 756 (1992).
- Stockman, A. and Sharpe, L. T., "Cone spectral sensitivities and color matching," in *Color Vision: From Genes to Perception*, Gegenfurtner, K. R. and Sharpe, L. T., Eds., Cambridge University Press, Cambridge, U.K. (1999).
- Stockman, A. and Sharpe, L. T., "Spectral sensitivities of the middle- and long-wavelength-sensitive cones derived from measurements in observers of known genotype," *Vision Res.* **40**, 1711–1737 (2000a).
- Stockman, A. and Sharpe, L. T., "Tritanopic color matches and the middle- and long-wavelength-sensitive cone spectral sensitivities," *Vision Res.* **40**, 1739–1750 (2000b).
- Stockman, A., MacLeod, D. I. A., and Johnson, N. E., "Spectral sensitivities of the human cones," *J. Opt. Soc. Am. A* **10**, 2491–2521 (1993a).
- Stockman, A., MacLeod, D. I. A., and Vivien, J. A., "Isolation of the middle- and long-wavelength sensitive cones in normal trichromats," *J. Opt. Soc. Am. A* **10**, 2471–2490 (1993b).
- Stockman, A., Sharpe, L. T., and Fach, C., "The spectral sensitivity of the human short-wavelength-sensitive cones derived from thresholds and color matches," *Vision Res.* **39**, 2901–2927 (1999).
- Thibos, L. N., Ye, M., Zhang, X. X., and Bradley, A., "The chromatic eye—a new reduced-eye model of ocular chromatic aberration in humans," *Appl. Opt.* **31**, 3594–3667 (1992).
- Van Heyningen, R., "What happens to the human lens in cataract," *Sci. Am.* **233**, 70–81 (1975).
- von Helmholtz, H., *Handbuch der Physiologischen Optik*, Dritte Auflage; English translation of the 3rd ed., three volumes (1909–1911) by Southall, J. P. C., Optical Society of America, Washington, DC (1924).
- Vos, J. J., "Colorimetric and photometric properties of a 2-deg fundamental observer," *Color Res. Appl.* **3**, 125–128 (1979).
- Vos, J. J., Estévez, O., and Walraven, P. L., "Improved color fundamentals offer a new view on photometric additivity," *Vision Res.* **30**, 936–943 (1990).
- Wald, G. and Griflin, D. R., "The change in refractive power of the human eye in dim and bright light," *J. Opt. Soc. Am.* **37**, 321–336 (1947).

- Webb, R. H., Huges, G. W., and Pomerantzeff, O., “Flying spot TV ophthalmoscope,” *Appl. Opt.* **19**, 2991–2997 (1980).
- White, H. E. and Levatin, P., “Floaters in the eye,” *Sci. Am.* **206**, 119–127 (1962).
- Williams, D. R., “Visibility of interference fringes near the resolution limit,” *J. Opt. Soc. Am. A* **2**, 1087–1093 (1985).
- Williams, D. R., “The trichromatic cone mosaic in the human eye,” in *Color vision: From Genes to Perception*, Gegenfurtner, K. R. and Sharpe, L. T., Eds., Cambridge University Press, Cambridge, U.K. (1999a).
- Williams, D. R., “Wavefront sensing and compensation for the human eye,” in *Adaptive Optics Engineering Handbook*, Tyson, R. K., Ed., Marcel Dekker, Inc., New York (1999b).
- Young, R. W., “Visual cells,” *Sci. Am.* **223**, 80–91 (1970).

Chapter 4

Trichromatic Theory

4.1 Grassmann Laws

The bases for the addition of colors and color-matching experiments were established by Grassmann (1853), who attributed many of his ideas to Maxwell (1857, 1860). These laws express the following facts:

- (a) To specify a color, three elements are necessary and sufficient: the hue, the luminance, and the luminance of the intermixed white, which defines the saturation.
- (b) For every color, there is complementary color, which, when mixed together, produce a colorless gray.
- (c) Two lights with the same hue and saturation, when mixed, produce another color with identical hue and saturation, independent of their power spectra.
- (d) The total luminance of any mixture of light is the sum of the luminances of the lights being mixed.

These laws are the basics of all mathematical procedures later established in colorimetry. However, some important conditions must be considered:

- (a) All color matches must be made under similar conditions.
- (b) Caution must be taken to avoid the previous light exposure of the eyes affecting the state of *adaptation*, influencing the spectral sensitivity of the eye.
- (c) If a field diameter larger than 10 deg is used in a color match, a failure of the proportionality law may be found.

4.2 Maxwell's Triangle

The likely first attempts to produce some color curves describing the trichromatic theory of color were those of Maxwell (1857, 1860). As described before, the first chromaticity diagram was a circle devised by Newton. Later, Maxwell used an equilateral triangle, as illustrated in Fig. 4.1. Each of the three primary colors red (R), green (G), and blue (B) in his trichromatic theory are on each corner of the triangle. The white color is in the middle. Any other color is formed by three components— r , g , and b —represented by the distances from each of the three sides of the triangle. This triangular representation has often been used with several modifications, and it is not clear how Maxwell defined and used it (Wintringham, 1951).

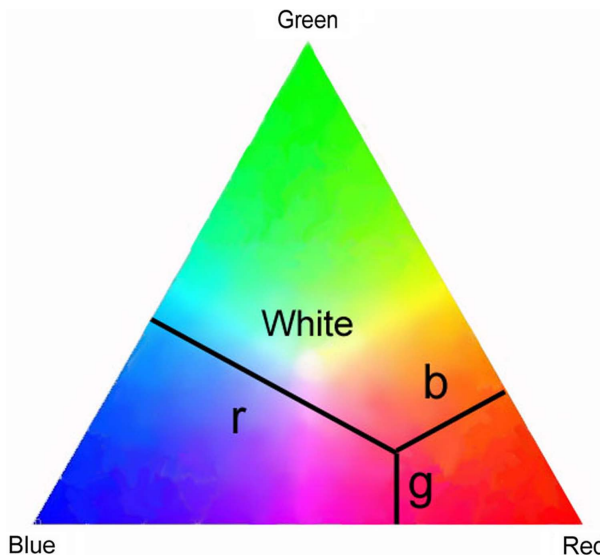


Figure 4.1 Maxwell's triangle.

4.3 Color-Matching Experiments

After Maxwell's work, the next experimental work to obtain color curves was done by König (1903) with the collaboration of Dieterici. Another important work aimed to obtain color curves was carried out by Ives (1915, 1923), who adjusted the curves previously obtained by König, thus developing the so-called König–Ives color-matching data. Several other researchers worked on these color-curve measurements during this time, but an important event came when the Optical Society of America (OSA) published a very extensive report by the OSA Colorimetry Committee (Troland, 1922). W. D. Wright, a leader in this field, describes the complete history of developments that eventually led to the CIE system in 1931 in an interesting appendix in the book by Boynton (1979).

To begin studying the CIE color system, let us consider a color-matching experiment, as shown in Fig. 4.2. Here, the color of two small regions on a screen with a split field, technically called a bipartite screen, is to be matched. The whole illuminated region subtends a visual angle of 2 deg, so that only the light receptors in the fovea at the center of the retina of the observer are illuminated. One half of the field is the *reference field*, illuminated with a spectrally pure monochromatic beam of light. The other half of the field is the *matched field*, whose color—as defined by its hue, saturation, and luminance—is to be made equal to that of the reference field. The matched field is illuminated with the combination of three pure monochromatic light beams, red (700 nm), green (546.1 nm), and blue (435.8 nm). These colors correspond to three spectrum lines in mercury vapor (see Fig. 2.4).

To begin the color-matching procedure, the spectrally pure reference field is set to have any desired radiance L_{Ref} , with a wavelength of 700 nm (red color). A perfect color match is achieved when the red light in the matched field is adjusted

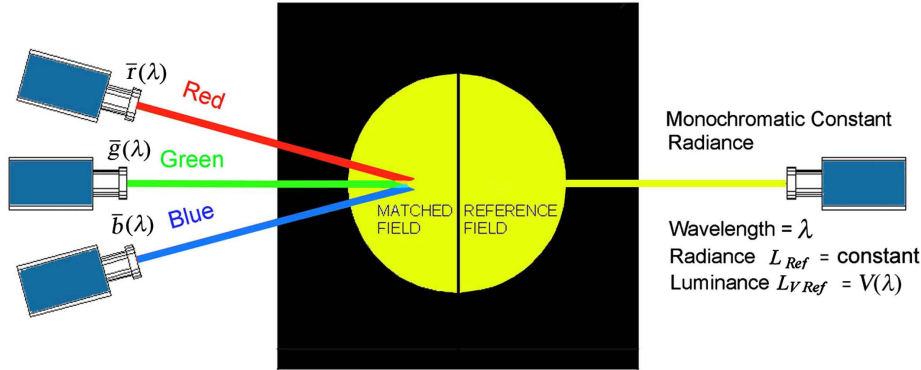


Figure 4.2 Color-matching fields with a monochromatic reference field.

to the same luminance as the reference field. The green and blue beams are set to zero luminance.

The procedure continues by decreasing the wavelength for the reference field in constant steps $\Delta\lambda$, preserving the same constant radiance L_{Ref} in this field, until all of the visible range is covered. For any monochromatic light source with wavelength λ , from (1.18), the luminance and the radiance in the reference field are related by

$$L_{VRef}(\lambda) = 683V(\lambda)L_{Ref}(\lambda), \quad (4.1)$$

where $V(\lambda)$ is the relative photopic luminous efficiency of the eye (given in Table 1.4). It must be noted here that the luminance is represented by $L_{VRef}(\lambda)$, because it has different values for different wavelengths of the monochromatic reference light source, but it is not the spectral luminance, which is defined only for polychromatic light sources. Examining Eq. (4.1), we notice that since the radiance L_{Ref} remains the same for all wavelengths used in the reference field, the corresponding luminance $L_{VRef}(\lambda)$ for all values of λ will be directly proportional to the function $V(\lambda)$.

At every wavelength step, the matching of the two fields is obtained by careful trial and error, adjusting the three colors (red, green, and blue) until both fields have the same hue, saturation, and luminance. In other words, they should look identical. As a result, in the matched field there will be three luminances— $L_{VR}(\lambda)$, $L_{VG}(\lambda)$, and $L_{VB}(\lambda)$, with corresponding radiances $L_R(\lambda)$, $L_G(\lambda)$, and $L_B(\lambda)$ —in the matched field, related by

$$\begin{aligned} L_{VR}(\lambda) &= 683V_R L_R(\lambda), \\ L_{VG}(\lambda) &= 683V_G L_G(\lambda), \\ L_{VB}(\lambda) &= 683V_B L_B(\lambda). \end{aligned} \quad (4.2)$$

The total luminance $L_{VMch}(\lambda)$ in the matched field can be expressed by the sum of the luminances of the three beams as

$$L_{VMch}(\lambda) = L_{VR}(\lambda) + L_{VG}(\lambda) + L_{VB}(\lambda). \quad (4.3)$$

After completing the matching procedure for many wavelengths in the visible spectrum, the three luminances being added, i.e., $L_{VR}(\lambda)$, $L_{VG}(\lambda)$, and $L_{VB}(\lambda)$, are known for every color. Thus, from Eqs. (4.2) and (4.3) we can write

$$L_{VMch}(\lambda) = 683 [V_R L_R(\lambda) + V_G L_G(\lambda) + V_B L_B(\lambda)]. \quad (4.4)$$

As pointed out before, $L_{VMch}(\lambda)$ is the luminance, not the spectral luminance, and it has a different value for each different wavelength (color) being matched. It is important to notice that the sum of the three radiances $L_R(\lambda)$, $L_G(\lambda)$, and $L_B(\lambda)$ is the total radiance $L_{Mch}(\lambda)$ in the matched field. However, this is not equal to the radiance L_{Ref} in the reference field, which has the same value for all wavelengths. The radiance $L_{Mch}(\lambda)$ in the matched field has a different value for every wavelength in the visible range. Equivalently, we can say that after the matching procedure, the luminances for both the reference and the matched fields are equal but are not necessarily their radiances. This is easy to understand, since the spectral distribution for the two fields is different. Thus, by equating Eqs. (4.1) and (4.4) we can find that

$$L_{VRef}(\lambda) = L_{VMch}(\lambda) = 683V(\lambda)L_{Ref} = 683 [V_R L_R(\lambda) + V_G L_G(\lambda) + V_B L_B(\lambda)], \quad (4.5)$$

where each of the three last terms represents, respectively, the luminance for the red, green, and blue components of the matched field. From this equation we can obtain

$$L_{Ref} = \frac{1}{V(\lambda)} [V_R L_R(\lambda) + V_G L_G(\lambda) + V_B L_B(\lambda)]. \quad (4.6)$$

Alternatively, we can also write

$$V(\lambda) = \frac{1}{L_{Ref}} [V_R L_R(\lambda) + V_G L_G(\lambda) + V_B L_B(\lambda)]. \quad (4.7)$$

For many different wavelengths, the values of all elements in this equation have been determined by the matching procedure. The function $V(\lambda)$ is the photopic relative luminous sensitivity of the eye, whose units are luminance over radiance, but normalized to a maximum value of 1 (this is the reason for the word “relative”). Hence, the three terms on the right-hand side of this equation are normalized values of luminance over radiance. But, since the radiance of the reference field is constant for all colors, these three elements on the right side of this equation are directly

Table 4.1 Relative luminances and radiances per stimulus unit.

Color	Wavelength (nm)	Relative luminance/stimulus unit	Relative radiance/stimulus unit
Red	700.0	1.0000 (L_R)	1.0000 (L_R)
Green	546.1	4.5907 (L_G)	0.0190 ($L_G V_R / V_G$)
Blue	435.8	0.0601 (L_B)	0.0140 ($L_B V_R / V_B$)

proportional to the luminances of each of the three added colors in the matched field. For convenience, each of these three terms can be expressed as a function of λ multiplied by a constant, as follows:

$$V(\lambda) = L_R \bar{r}(\lambda) + L_G \bar{g}(\lambda) + L_B \bar{b}(\lambda), \quad (4.8)$$

where the symbols $\bar{r}(\lambda)$, $\bar{g}(\lambda)$, and $\bar{b}(\lambda)$ are called the stimuli values or *color-matching functions*, sometimes abbreviated as CMF. These constants are defined to be unitless. Hence, the three constants L_R , L_G , and L_B must have the units of luminance over radiance. Note that they do not represent the radiances previously used, but following the usual custom in colorimetry, the same letters will be employed. The values of the products on the right-hand side of Eq. (4.8) have been determined, but not the values of the constants L_R , L_G , and L_B whose values can be selected as we choose.

The first constant is given the value $L_R = 1$. We also require that the sum of the sums of all measured values of $\bar{r}(\lambda)$, $\bar{g}(\lambda)$, and $\bar{b}(\lambda)$ are equal, as follows:

$$\sum_{i=1}^N \bar{r}(\lambda_i) = \sum_{i=1}^N \bar{g}(\lambda_i) = \sum_{i=1}^N \bar{b}(\lambda_i), \quad (4.9)$$

where N is the total number of measured values in the whole spectral range. Thus, in this manner the three numerical values of L_R , L_G , and L_B , are determined ($L_G = 4.5907$ and $L_B = 0.0601$), as well as the values of $\bar{r}(\lambda)$, $\bar{g}(\lambda)$, and $\bar{b}(\lambda)$. This scaling of the tristimulus values by means of the condition in Eq. (4.9) has the advantage that the three color-matching function values for a white light with constant energy are equal, as will be described in the next chapter.

The *relative spectral radiances* of each of the three components with respect to the red stimulus are $L_R \bar{r}(\lambda)$, $L_G \bar{g}(\lambda) V_R / V_G$, and $L_B \bar{b}(\lambda) V_R / V_B$. Table 4.1 shows the values for the relative radiances per stimulus unit and the luminances per stimulus unit.

4.4 Color-Matching Functions $\bar{r}(\lambda)$, $\bar{g}(\lambda)$, and $\bar{b}(\lambda)$

Let us consider the superimposition of three light fields with monochromatic colors red (700 nm), green (546.1 nm), and blue (435.8 nm), that have relative luminances

$L_R\bar{r}(\lambda)$, $L_G\bar{g}(\lambda)$, and $L_B\bar{b}(\lambda)$, respectively. The resulting matched field has a relative luminance $V(\lambda)$ and the same color and luminance as the reference monochromatic light field with wavelength λ . This monochromatic reference field has a constant radiance independent of its color (wavelength), but its radiance is not necessarily the same as that for the matched field formed by the superposition of the three colors.

The original matching color functions were obtained with a 2-deg field, to avoid stimulating the rods outside the fovea centralis, as defined by the CIE convention in 1931 (CIE, 1932). These color-matching functions were obtained by reconstructing relative color-matching data previously obtained by Wright (1928–29) and Guild (1931) through different experimental methods.

Wright and Guild reconstructed the color-matching functions by assuming that a linear combination of these functions must be equal to the 1924 CIE function $V(\lambda)$, as shown in Eq. (4.8). This hypothesis was reasonable, since the red, green, and blue beams add up to a field with constant radiance for all wavelengths. Unfortunately, as shown by several authors, this reconstruction of the functions is highly questionable (Sperling, 1958), because of the validity of the curve $V(\lambda)$ used in the reconstruction (Gibson and Tyndall, 1923; CIE, 1926; Judd, 1951). The reason, as explained in Chapter 2, is that the function $V(\lambda)$ has a noticeable error in the blue region. Later, Judd (1951) and Vos (1978) made some corrections to these functions, as discussed by Stockman and Sharpe (1999). Stiles and Burch (1955) also obtained these matching functions from direct measurements in 10 observers.

The 2-deg field is too small for many practical purposes, so a 10-deg field was adopted in the CIE convention in 1964, based on the work by Stiles and Burch (1959) and Speranskaya (1959). These color-matching functions $\bar{r}(\lambda)$, $\bar{g}(\lambda)$, and $\bar{b}(\lambda)$ for a 10-deg field were directly measured in 49 subjects at 392.2–714.3 nm and in nine subjects at 714.3–824.2 nm. During the measurements, the luminance of the matching field was kept high to reduce any effect from stimulation of the rods. If desired, a correction for the rod intrusion can be made, as has been shown by Stockman and Sharpe (1999). The color perception, mainly the color-matching functions with a large field, has been studied under different experimental conditions and methods (Lozano and Palmer, 1968; Gordon and Abramov, 1977; Burns and Elsner, 1985). Figure 4.3 shows the 2-deg and the 10-deg fields as seen from a distance of 250 mm.

In 1931 the color-matching functions were defined in the wavelength range from 380.0 to 780 nm at intervals of 5 nm, with their values given to five decimal places. These functions are provided in Table 4.2 and plotted in Fig. 4.4.

4.5 Tristimulus Values R , G , B

We assumed in the preceding section that the reference field was illuminated by a monochromatic beam of light with a constant radiance. Let us now assume that the reference field is illuminated by the superposition of two or more monochromatic spectral lines with wavelengths $\lambda_1, \lambda_2, \lambda_3$, etc. with relative powers P_1, P_2, P_3 , etc.,

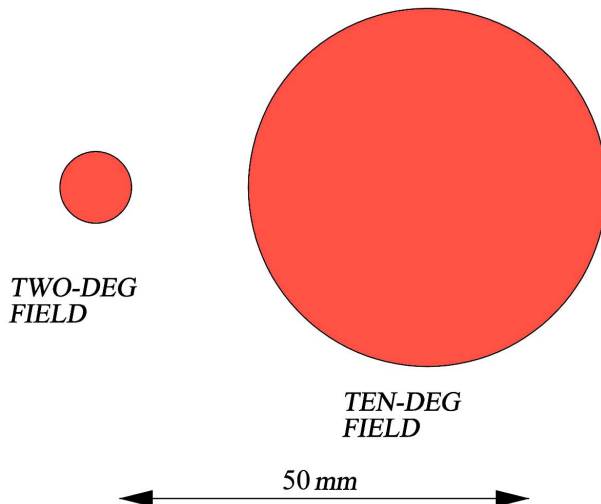


Figure 4.3 Two-deg and 10-deg fields as seen from a distance of 25 cm.

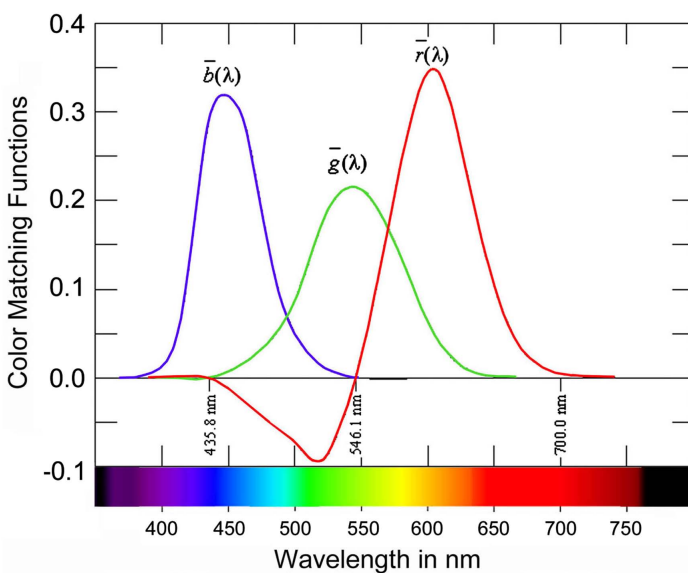


Figure 4.4 Color-matching functions $\bar{r}(\lambda)$, $\bar{g}(\lambda)$, and $\bar{b}(\lambda)$ for a 2-deg field (CIE 1931).

which are numbers whose values are directly proportional to the radiances. (See Fig. 4.5.) These relative powers are changed every time a new match is performed. To match the color component with wavelength λ_1 we need the corresponding color-matching functions $\bar{r}(\lambda_1)$, $\bar{g}(\lambda_1)$, and $\bar{b}(\lambda_1)$ to be multiplied by the relative power P_1 . To match the color component with wavelength λ_2 , we need the color-matching functions $\bar{r}(\lambda_2)$, $\bar{g}(\lambda_2)$, and $\bar{b}(\lambda_2)$, to be multiplied by the radiance P_2 ,

Table 4.2 Color-matching functions $\bar{r}(\lambda)$, $\bar{g}(\lambda)$, and $\bar{b}(\lambda)$ for a 2-deg field (CIE 1931).

Wavelength (nm)	$\bar{r}(\lambda)$	$\bar{g}(\lambda)$	$\bar{b}(\lambda)$	Wavelength (nm)	$\bar{r}(\lambda)$	$\bar{g}(\lambda)$	$\bar{b}(\lambda)$
380	0.00003	-0.00001	0.00117	585	0.27989	0.11686	-0.00093
385	0.00005	-0.00002	0.00189	590	0.30928	0.09754	-0.00079
390	0.00010	-0.00004	0.00359	595	0.33184	0.07909	-0.00063
395	0.00017	-0.00007	0.00647	600	0.34429	0.06246	-0.00049
400	0.00030	-0.00014	0.01214	605	0.34756	0.04776	-0.00038
405	0.00047	-0.00022	0.01969	610	0.33971	0.03557	-0.00030
410	0.00084	-0.00041	0.03707	615	0.32265	0.02583	-0.00022
415	0.00139	-0.00070	0.06637	620	0.29708	0.01828	-0.00015
420	0.00211	-0.00110	0.11541	625	0.26348	0.01253	-0.00011
425	0.00266	-0.00143	0.18575	630	0.22677	0.00833	-0.00008
430	0.00218	-0.00119	0.24769	635	0.19233	0.00537	-0.00005
435	0.00036	-0.00021	0.29012	640	0.15968	0.00334	-0.00003
440	-0.00261	0.00149	0.31228	645	0.12905	0.00199	-0.00002
445	-0.00673	0.00379	0.31860	650	0.10167	0.00116	-0.00001
450	-0.01213	0.00678	0.31670	655	0.07857	0.00066	-0.00001
455	-0.01874	0.01046	0.31166	660	0.05932	0.00037	0.00000
460	-0.02608	0.01485	0.29821	665	0.04366	0.00021	0.00000
465	-0.03324	0.01977	0.27295	670	0.03149	0.00011	0.00000
470	-0.03933	0.02538	0.22991	675	0.02294	0.00006	0.00000
475	-0.04471	0.03183	0.18592	680	0.01687	0.00003	0.00000
480	-0.04939	0.03914	0.14494	685	0.01187	0.00001	0.00000
485	-0.05364	0.04713	0.10968	690	0.00819	0.00000	0.00000
490	-0.05814	0.05689	0.08257	695	0.00572	0.00000	0.00000
495	-0.06414	0.06948	0.06246	700	0.00410	0.00000	0.00000
500	-0.07173	0.08536	0.04776	705	0.00291	0.00000	0.00000
505	-0.08120	0.10593	0.03688	710	0.00210	0.00000	0.00000
510	-0.08901	0.12860	0.02698	715	0.00148	0.00000	0.00000
515	-0.09356	0.15262	0.01842	720	0.00105	0.00000	0.00000
520	-0.09264	0.17468	0.01221	725	0.00074	0.00000	0.00000
525	-0.08473	0.19113	0.00830	730	0.00052	0.00000	0.00000
530	-0.07101	0.20317	0.00549	735	0.00036	0.00000	0.00000
535	-0.05316	0.21083	0.00320	740	0.00025	0.00000	0.00000
540	-0.03152	0.21466	0.00146	745	0.00017	0.00000	0.00000
545	-0.00613	0.21487	0.00023	750	0.00012	0.00000	0.00000
550	0.02279	0.21178	-0.00058	755	0.00008	0.00000	0.00000
555	0.05514	0.20588	-0.00105	760	0.00006	0.00000	0.00000
560	0.09060	0.19702	-0.00130	765	0.00004	0.00000	0.00000
565	0.12840	0.18522	-0.00138	770	0.00003	0.00000	0.00000
570	0.16768	0.17087	-0.00135	775	0.00001	0.00000	0.00000
575	0.20715	0.15429	-0.00123	780	0.00000	0.00000	0.00000
580	0.24526	0.13610	-0.00108				

and so on. So, to match the field formed by two or more wavelengths we need the combined color-matching functions, called tristimulus values and expressed as $R = P(\lambda_1)\bar{r}(\lambda_1) + P(\lambda_2)\bar{r}(\lambda_2) + P(\lambda_3)\bar{r}(\lambda_3) + \dots$, $G = P(\lambda_1)\bar{g}(\lambda_1) + P(\lambda_2)\bar{g}(\lambda_2) + P(\lambda_3)\bar{g}(\lambda_3) + \dots$, and $B = P(\lambda_1)\bar{b}(\lambda_1) + P(\lambda_2)\bar{b}(\lambda_2) + P(\lambda_3)\bar{b}(\lambda_3) + \dots$. Generalizing this result for a reference field illuminated by a light source with a continuous power spectrum where the spectral relative power per unit wavelength interval $\Delta\lambda$

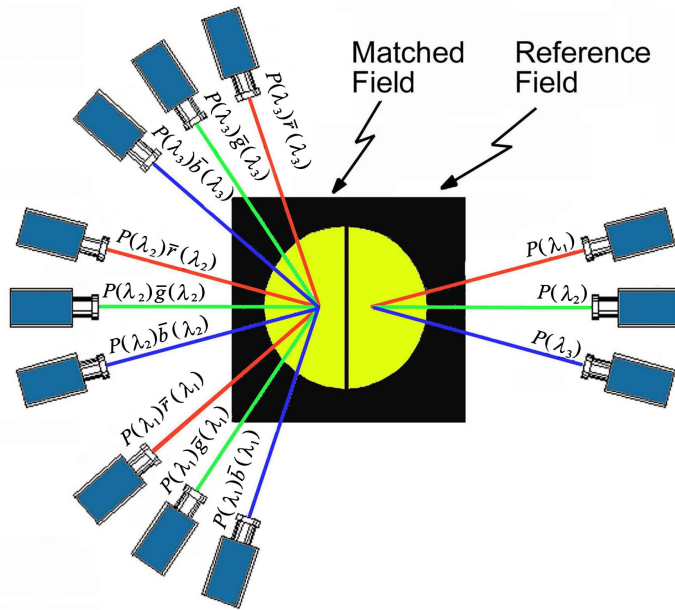


Figure 4.5 Color-matching fields with a polychromatic reference field.

is $P(\lambda)$, the required tristimulus values to match this light field is

$$R = \int_0^{\infty} P(\lambda) \bar{r}(\lambda) d\lambda, \quad (4.10)$$

$$G = \int_0^{\infty} P(\lambda) \bar{g}(\lambda) d\lambda, \quad (4.11)$$

$$B = \int_0^{\infty} P(\lambda) \bar{b}(\lambda) d\lambda, \quad (4.12)$$

or equivalently, for discrete values,

$$R = \sum_{i=0}^N P(\lambda_i) \bar{r}(\lambda_i), \quad (4.13)$$

$$G = \sum_{i=0}^N P(\lambda_i) \bar{g}(\lambda_i), \quad (4.14)$$

$$B = \sum_{i=0}^N P(\lambda_i) \bar{b}(\lambda_i). \quad (4.15)$$

If an equal energy white light is such that $P(\lambda) = 1$, we can see that the values of R , G , and B are equal. The luminances for each of these three components are $L_R R$, $L_G G$, and $L_B B$, respectively. The total luminance of the superposition is the

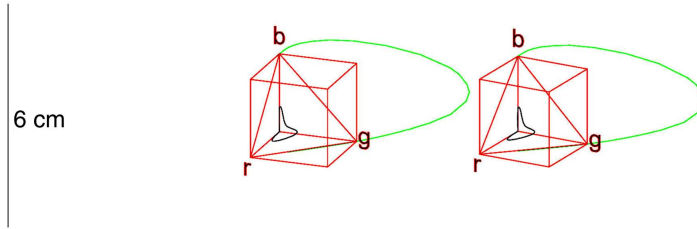


Figure 4.6 Stereo pair showing the color-matching functions in $\bar{r}(\lambda)$, $\bar{g}(\lambda)$, and $\bar{b}(\lambda)$ in \bar{r} , \bar{g} , and \bar{b} space and projection of the color-matching functions to obtain the chromaticity coordinates.

sum of these three luminances. These three tristimulus values define the light field color with its hue, saturation, and the luminance.

4.6 Chromaticity Coordinates r , g , b

In a coordinate system with three orthogonal axes r , g , b , all colors with the same hue and saturation but different luminance are represented by points on a straight line passing through the origin. The distance from the origin to a point on this line is determined by its luminance.

The monochromatic spectral colors with constant radiance are represented by points with coordinates $\bar{r}(\lambda)$, $\bar{g}(\lambda)$, $\bar{b}(\lambda)$ along a curve in this space, as shown in the stereoscopic pair of images in Fig. 4.6. This is the so-called Schrödinger (1920) spectrum bag. Notice that this curve is not entirely inside the cube, because some values of the color-matching functions are negative.

All points on this curve can be projected to a plane $r + g + b = 1$ that intersects at the coordinate axes at the points $(1, 0, 0)$, $(0, 1, 0)$, and $(0, 0, 1)$ by moving each point along a straight line radiating from the origin, as in Fig. 4.7. The points on this projected curve have coordinates $r(\lambda)$, $g(\lambda)$, $b(\lambda)$ given by

$$r(\lambda) = \frac{\bar{r}(\lambda)}{\bar{r}(\lambda) + \bar{g}(\lambda) + \bar{b}(\lambda)}, \quad (4.16)$$

$$g(\lambda) = \frac{\bar{g}(\lambda)}{\bar{r}(\lambda) + \bar{g}(\lambda) + \bar{b}(\lambda)}, \quad (4.17)$$

$$b(\lambda) = \frac{\bar{b}(\lambda)}{\bar{r}(\lambda) + \bar{g}(\lambda) + \bar{b}(\lambda)}, \quad (4.18)$$

with the following relation between them:

$$r(\lambda) + g(\lambda) + b(\lambda) = 1. \quad (4.19)$$

In Fig. 4.7, this relationship is represented as a large loop resembling a fragment of an ellipse, with all points lying in the inclined plane passing through the unit vectors. After this transformation, the projection of the points along the projected

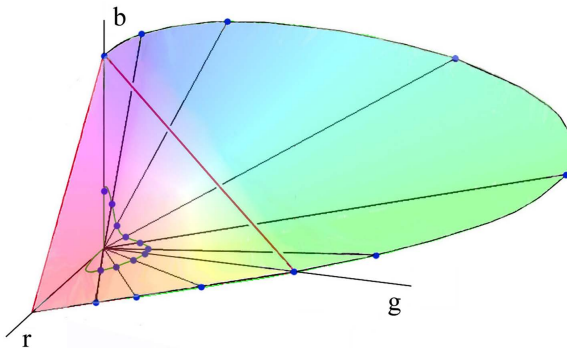


Figure 4.7 Projection of points with coordinates $\bar{r}(\lambda)$, $\bar{g}(\lambda)$, and $\bar{b}(\lambda)$ to a plane passing through points $(1, 0, 0)$, $(0, 1, 0)$, and $(0, 0, 1)$.

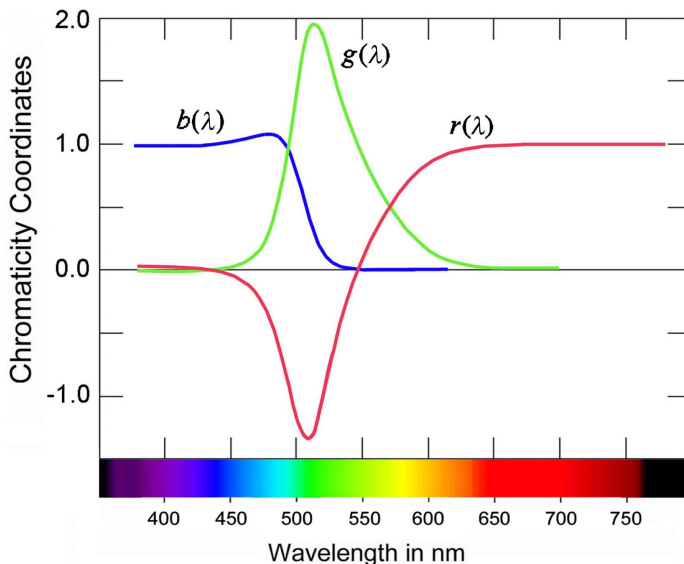


Figure 4.8 Chromaticity coordinates $r(\lambda)$, $g(\lambda)$, and $b(\lambda)$ for spectrally pure colors for a 2-deg field (CIE 1931).

curve for the spectrally pure monochromatic colors will not have constant power, nor will they have constant luminosity. The points on the plane represented by this equation can now be projected to the plane r , g by making the coordinate b equal to zero. Then, just two coordinate values called *chromaticity coordinates*, as plotted in Fig. 4.8, are sufficient to represent any color with its hue and saturation. However, with this representation in a plane, all information about the luminance is lost. The locus of all spectrally pure colors is obtained by plotting the values of $\bar{r}(\lambda)$ versus $\bar{g}(\lambda)$, as shown in Fig. 4.9. The values r , g , b defining the hue and saturation of any color are the chromaticity coordinates, which can be obtained by

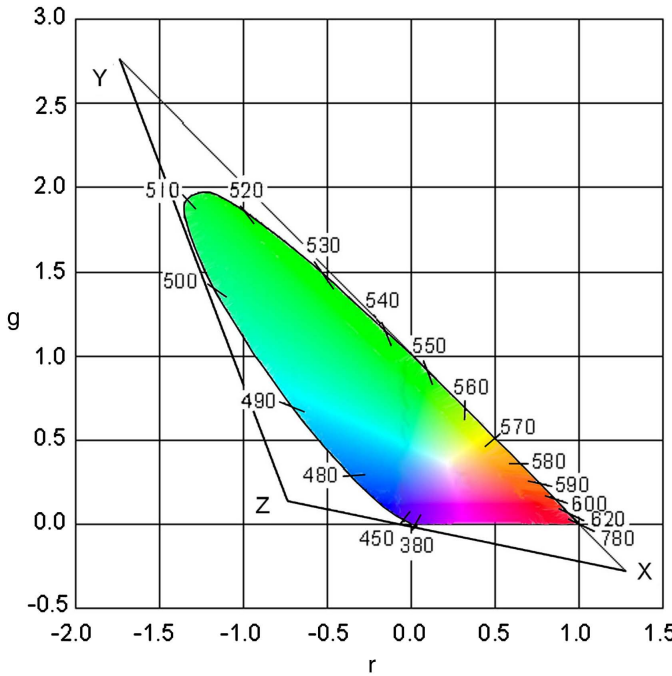


Figure 4.9 Chromaticity diagram for r versus g .

normalizing the tristimulus values, as follows:

$$r = \frac{R}{R + G + B}, \quad (4.20)$$

$$g = \frac{G}{R + G + B}, \quad (4.21)$$

and

$$b = \frac{B}{R + G + B}, \quad (4.22)$$

where

$$r + g + b = 1. \quad (4.23)$$

The values of the chromaticity coordinates $r(\lambda)$, $g(\lambda)$, and $b(\lambda)$ for spectrally pure colors, and for a 2-deg field as defined by the CIE convention in 1931, are given in Table 4.3.

It must be pointed out that these are not the only conditions that can be used in defining this transformation of units. Alternatively, instead of making the sum of the luminosities of the color-matching functions equal to that of the equal power white, as required by Eq. (4.8), they can also (Guild, 1931) be made equal

Table 4.3 Chromaticity coordinates $r(\lambda)$, $g(\lambda)$, and $b(\lambda)$ for spectrally pure colors and for a 2-deg field (from CIE 1931).

Wavelength (nm)	$r(\lambda)$	$g(\lambda)$	$b(\lambda)$	Wavelength (nm)	$r(\lambda)$	$g(\lambda)$	$b(\lambda)$
380	0.0272	-0.0115	0.9843	585	0.7071	0.2952	-0.0023
385	0.0268	-0.0114	0.9846	590	0.7617	0.2402	-0.0019
390	0.0263	-0.0114	0.9851	595	0.8087	0.1928	-0.0015
395	0.0256	-0.0113	0.9857	600	0.8475	0.1537	-0.0012
400	0.0247	-0.0112	0.9865	605	0.8800	0.1209	-0.0009
405	0.0237	-0.0111	0.9874	610	0.9059	0.0949	-0.0008
410	0.0225	-0.0109	0.9884	615	0.9265	0.0741	-0.0006
415	0.0207	-0.0104	0.9897	620	0.9425	0.0580	-0.0005
420	0.0181	-0.0094	0.9913	625	0.9550	0.0454	-0.0004
425	0.0142	-0.0076	0.9934	630	0.9649	0.0354	-0.0003
430	0.0088	-0.0048	0.9960	635	0.9730	0.0272	-0.0002
435	0.0012	-0.0007	0.9995	640	0.9797	0.0205	0.0002
440	-0.0084	0.0048	1.0036	645	0.9850	0.0152	0.0002
445	-0.0213	0.0120	1.0093	650	0.9888	0.0113	0.0001
450	-0.0390	0.0218	1.0172	655	0.9918	0.0083	0.0001
455	-0.0618	0.0345	1.0273	660	0.9940	0.0061	0.0001
460	-0.0909	0.0517	1.0392	665	0.9954	0.0047	0.0001
465	-0.1281	0.0762	1.0519	670	0.9966	0.0035	0.0001
470	-0.1821	0.1175	1.0646	675	0.9975	0.0025	0.0000
475	-0.2584	0.1840	1.0744	680	0.9984	0.0016	0.0000
480	-0.3667	0.2906	1.0761	685	0.9991	0.0009	0.0000
485	-0.5200	0.4568	1.0632	690	0.9996	0.0004	0.0000
490	-0.7150	0.6996	1.0154	695	0.9999	0.0001	0.0000
495	-0.9459	1.0247	0.9212	700	1.0000	0.0000	0.0000
500	-1.1685	1.3905	0.7780	705	1.0000	0.0000	0.0000
505	-1.3182	1.7195	0.5987	710	1.0000	0.0000	0.0000
510	-1.3371	1.9318	0.4053	715	1.0000	0.0000	0.0000
515	-1.2076	1.9699	0.2377	720	1.0000	0.0000	0.0000
520	-0.9830	1.8534	0.1296	725	1.0000	0.0000	0.0000
525	-0.7386	1.6662	0.0724	730	1.0000	0.0000	0.0000
530	-0.5159	1.4761	0.0398	735	1.0000	0.0000	0.0000
535	-0.3304	1.3105	0.0199	740	1.0000	0.0000	0.0000
540	-0.1707	1.1628	0.0079	745	1.0000	0.0000	0.0000
545	-0.0293	1.0282	0.0011	750	1.0000	0.0000	0.0000
550	0.0974	0.9051	-0.0025	755	1.0000	0.0000	0.0000
555	0.2121	0.7919	-0.0040	760	1.0000	0.0000	0.0000
560	0.3164	0.6881	-0.0045	765	1.0000	0.0000	0.0000
565	0.4112	0.5932	-0.0044	770	1.0000	0.0000	0.0000
570	0.4973	0.5067	-0.0040	775	1.0000	0.0000	0.0000
575	0.5751	0.4283	-0.0034	780	1.0000	0.0000	0.0000
580	0.6449	0.3579	-0.0028				

to the luminosity of what is called the National Physical Laboratories (NPL), England, white. The NPL white is one given by an incandescent lamp with a color temperature of about 4800 K. Wright also introduced another method to define the units of his primary stimuli (1928, 1929). This method of fixing the units has some advantages, and it is known as the *W. D. W. Method*, after Wright.

The luminosities in the r, g, b space can be found using Eq. (4.8). There is a plane in this space where the luminance is zero, given by

$$L_R r + L_G g + L_B b = 0. \quad (4.24)$$

This zero-luminance plane is called the *alychne*, and it passes through the origin of the coordinates of the r, g, b system. The normal vector to this plane, defining its orientation is 1, with components L_R, L_G , and L_B . The intersection of this plane with the plane defined by Eq. (4.23) is a straight line. Then, the projection of this line on the r, g plane is another straight line given by

$$(L_R - L_B)r + (L_G - L_B)g + L_B = 0. \quad (4.25)$$

This straight line indicates the location of purple colors (Fig. 4.9).

References

- Boynton, R. M., *Human Color Vision*, Holt, Rinehart and Winston, New York (1979).
- Burns, S. A. and Elsner, A. E., “Color matching at high illuminances: the color-match-area effect and photopigment bleaching,” *J. Opt. Soc. Am. A* **2**, 698–704 (1985).
- CIE, *Proc., 1924 Commission Internationale de l’Éclairage*, Cambridge University Press, Cambridge, U.K. (1926).
- CIE, *Proc., 1931 Commission Internationale de l’Éclairage*, Cambridge University Press, Cambridge, U.K. (1932).
- Gibson, K. S. and Tyndall, E. P. T., “Visibility of radiant energy,” *Sci. Pap. Bur. Stand.* **19**, 131–191 (1923).
- Gordon, J. and Abramov, I., “Color vision in the peripheral retina. II. Hue and saturation,” *J. Opt. Soc. Am.* **67**, 202–207 (1977).
- Grassmann, H. G., “Theory of compound colors,” *Ann. Phys. Chem.* **19**, 53–60 (1853); translation published in *Philos. Mag.* **4**, 254–264 (1854); reprinted in *Selected Papers in Colorimetry—Fundamentals*, MacAdam, D. L., Ed., SPIE Press, Bellingham, WA (1993).
- Guild, J., “The colorimetric properties of the spectrum,” *Philos. Trans. Roy. Soc. London, A* **230**, 149–187 (1931).
- Ives, H. E., “The transformation of color-mixture equations from one system to another,” *J. Franklin Inst.* **180**, 673 (1915).
- Ives, H. E., “The transformation of color-mixture equations from one system to another II. Graphical aids,” *J. Franklin Inst.* **195**, 23 (1923).

- Judd, D. B., "Report of U.S. Secretariat Committee on Colorimetry and Artificial Daylight," in *Proc., 12th Session of the Commission Internationale de l'Éclairage*, Vol. 1, 11 Bureau Central de la Commission Internationale de l'Éclairage, Paris (1951).
- König, A., *Gesammelte abhandlungen zur physiologischen optik*, Barth, Leipzig (1903).
- Lozano, R. D. and Palmer, D., "Large-field color matching and adaptation," *J. Opt. Soc. Am.* **58**, 1653–1656 (1968).
- Maxwell, J. C., "The diagram of colors," *Trans. - R. Soc. Edinbrgh* **21**, 275–298 (1857); reprinted in *Selected Papers in Colorimetry—Fundamentals*, MacAdam, D. L., Ed., SPIE Press, Bellingham, WA (1993).
- Maxwell, J. C., "On the theory of compound colours and the relations of the colours of the spectrum," *Proc. Roy. Soc. London* **10**, 404–409 (1860); reprinted in *Selected Papers in Colorimetry—Fundamentals*, MacAdam, D. L., Ed., SPIE Press, Bellingham, WA (1993).
- Schrödinger, E., "Outline of color measurement for daylight vision," *Ann. Phys.* **63**, 397–447 (1920); reprinted in *Selected Papers in Colorimetry—Fundamentals*, MacAdam, D. L., Ed., SPIE Press, Bellingham, WA (1993).
- Speranskaya, N. I., "Determination of spectrum color co-ordinates for twenty-seven normal observers," *Opt. Spectrosc.* **7**, 424–428 (1959).
- Sperling, H. G., "An experimental investigation of the relationship between colour mixture and luminous efficiency," in *Visual Problems of Colour*, Vol. 1, 249–277 Her Majesty's Stationery Office, London (1958).
- Stiles, W. S. and Burch, J. M., "Interim report to the Commission Internationale de l'Eclairage Zurich, 1955, on the National Physical Laboratory's investigation of colour-matching," *Opt. Acta* **2**, 168–181 (1955).
- Stiles, W. S. and Burch, J. M., "NPL colour-matching investigation: final report (1958)," *Opt. Acta* **6**, 1–26 (1959).
- Stockman, A. and Sharpe, L. T., "Cone spectral sensitivities and color matching," in *Color Vision: From Genes to Perception*, Gegenfurtner, K. and Sharpe, L. T., Eds., 51–85 Cambridge University Press, Cambridge, U.K. (1999).
- Troland, L. T., "Report of the committee on colorimetry for 1920–1921," *J. Opt. Soc. Am.* **6**, 527–596 (1922).
- Vos, J. J., "Colorimetric and photometric properties of a 2-deg fundamental observer," *Color Res. Appl.* **3**, 125–128 (1978).
- Wintringham, W. T., "Color television and colorimetry," *Proc. IRE* **39**, 1135–1172 (1951).
- Wright, W. D., "A re-determination of the trichromatic coefficients of the spectral colours," *Trans. Opt. Soc., London* **30**, 141–164 (1928–1929).

Chapter 5

CIE Color Specification System

5.1 The CIE Color System

In the procedure for finding color-matching functions described in Chapter 4, a practical problem appears. For some wavelengths of the monochromatic reference, after decreasing the luminance of the red beam in the matched zone to zero, the color may still look too red. The only solution in order to achieve a perfect match is to add red to the reference zone, instead of taking it from the sample, which is impossible. Mathematically, this can be considered as subtracting red light from the sample, which means that this color-matching function value is negative.

A set of three stimuli (X , Y , and Z) is defined by a linear combination of the red, green, and blue stimuli, some of which are negative. This transformation is accomplished by means of a projective transformation (Ives, 1915, 1923), transforming the system of coordinates (r, g, b) into a new system of coordinates (x, y, z) , whose properties will be defined below. The curve of spectrally pure colors $\bar{r}(\lambda)$, $\bar{g}(\lambda)$, $\bar{b}(\lambda)$ transforms into a curve of spectrally pure colors defined by $\bar{x}(\lambda)$, $\bar{y}(\lambda)$, $\bar{z}(\lambda)$ (dependence on λ omitted for simplicity):

$$\begin{bmatrix} \bar{x} \\ \bar{y} \\ \bar{z} \end{bmatrix} = \begin{bmatrix} r_x & r_y & r_z \\ g_x & g_y & g_z \\ b_x & b_y & b_z \end{bmatrix}^{-1} \bullet \begin{bmatrix} \bar{r} \\ \bar{g} \\ \bar{b} \end{bmatrix}, \quad (5.1)$$

where (r_x, g_x, b_x) are the coordinates of the point $(\bar{x} = 1, \bar{y} = 0, \bar{z} = 0)$, (r_y, g_y, b_y) are the coordinates of the point $(\bar{x} = 0, \bar{y} = 1, \bar{z} = 0)$, and (r_z, g_z, b_z) are the coordinates of the point $(\bar{x} = 0, \bar{y} = 0, \bar{z} = 1)$ as measured in the system r, g, b .

Now assume that the inverse of this matrix is A , so that we can write

$$\begin{bmatrix} \bar{x} \\ \bar{y} \\ \bar{z} \end{bmatrix} = \begin{bmatrix} a_{11} & a_{12} & a_{13} \\ a_{21} & a_{22} & a_{23} \\ a_{31} & a_{32} & a_{33} \end{bmatrix} \bullet \begin{bmatrix} \bar{r} \\ \bar{g} \\ \bar{b} \end{bmatrix}. \quad (5.2)$$

The type of linear transformation is determined by the values of these coefficients.

5.2 Color-Matching Functions $\bar{x}(\lambda)$, $\bar{y}(\lambda)$, and $\bar{z}(\lambda)$

To find the color-matching functions, we will now specify some conditions for finding the values for the elements of the transformation matrix. For convenience, it was decided that the function $\bar{y}(\lambda)$ should be equal to the luminosity function $V(\lambda)$ of the eye. So, from Eq. (4.8), the values of the matrix coefficients of the second row are $a_{21} = L_R = 1$, $a_{22} = L_G = 4.5907$, and $a_{23} = L_B = 0.0601$. Then, any color on the y axis has zero relative spectral luminance. In other words, the alychne is the y axis, with the value of $\bar{y}(\lambda)$ equal to the spectral luminous efficiency or luminosity function of the eye:

$$\bar{y}(\lambda) = V(\lambda). \quad (5.3)$$

The second condition is that the constant energy white defined by $P(\lambda) = 1$ should have equal values for the three tristimuli. Thus, in analogy with Eq. (4.9), the three sums of the three color-matching functions $\bar{x}(\lambda)$, $\bar{y}(\lambda)$, and $\bar{z}(\lambda)$ should have the same value for many equally spaced wavelengths in the visible range. If we take these three sums of the color-matching functions $\bar{r}(\lambda)$, $\bar{g}(\lambda)$, and $\bar{b}(\lambda)$ for a total of N equally spaced wavelengths in the visible range, obtained from Eq. (4.9), as equal to a quantity S , we have

$$\begin{aligned} \sum_{i=1}^N \bar{x}(\lambda_i) &= S(a_{11} + a_{12} + a_{13}) = \\ \sum_{i=1}^N \bar{y}(\lambda_i) &= S(a_{21} + a_{22} + a_{23}) = \\ \sum_{i=1}^N \bar{z}(\lambda_i) &= S(a_{31} + a_{32} + a_{33}), \end{aligned} \quad (5.4)$$

which gives

$$(a_{11} + a_{12} + a_{13}) = (a_{21} + a_{22} + a_{23}) = (a_{31} + a_{32} + a_{33}) = \sigma. \quad (5.5)$$

The value of σ is known, since the three coefficients for the second row in the matrix have already been determined.

The third condition is that the line joining point X with point Y in Fig. 4.9 be tangent to the curve on the red side. A practical advantage is that for these colors, a linear combination of tristimuli X and Y are sufficient to describe them, without any tristimulus Z . For the red-color point with a wavelength equal to 700 nm we have $\bar{r}(\lambda) = 1$, $\bar{g}(\lambda) = 0$, and $\bar{b}(\lambda) = 0$. The line joining the points X and Y pass through this last point N at the red end of the spectrum if $a_{31} = 0$, making $\bar{z}_N(\lambda) = 0$ for any values of a_{32} and a_{33} . If we want the line $X-Y$ to be tangent to the curve we, also require that for another point close to the end point, for example, the $N-1$

point,

$$\bar{z}_{N-1} = a_{32}\bar{g}_{N-1} + a_{33}\bar{b}_{N-1} = 0, \quad (5.6)$$

which gives

$$\frac{a_{33}}{a_{32}} = -\frac{\bar{g}_{N-1}}{\bar{b}_{N-1}}. \quad (5.7)$$

Thus, using Eq. (5.5) with $a_{31} = 0$ and this expression we find that

$$a_{32} = \frac{\sigma}{1 - \bar{g}_{N-1}/\bar{b}_{N-1}}, \quad (5.8)$$

and

$$a_{33} = -a_{32}\frac{\bar{g}_{N-1}}{\bar{b}_{N-1}}. \quad (5.9)$$

The fourth condition is that the \bar{y} axis must be tangent to the curve, so that no value of $\bar{x}(\lambda)$ is negative. We have

$$\bar{x}(\lambda) = a_{11}\bar{r}(\lambda) + a_{12}\bar{g}(\lambda) + a_{13}\bar{b}(\lambda), \quad (5.10)$$

and this function has a minimum that can be pushed down or pulled up by changing the value of the coefficient a_{11} . The sum of the three coefficients is equal to σ , so that we have two degrees of freedom that can be used to make the minimum of $\bar{x}(\lambda)$ equal to zero and to move the minimum position laterally. A location for this minimum is chosen so that the triangle XYZ in Fig. 4.9 has the minimum area.

Finally, using these results, the following transformation is obtained:

$$\begin{bmatrix} \bar{x} \\ \bar{y} \\ \bar{z} \end{bmatrix} = \begin{bmatrix} 2.76888 & 1.75175 & 1.13016 \\ 1 & 4.59070 & 0.06010 \\ 0 & 0.05651 & 5.59427 \end{bmatrix} \bullet \begin{bmatrix} \bar{r} \\ \bar{g} \\ \bar{b} \end{bmatrix}, \quad (5.11)$$

or in terms of L_R , L_G , and L_B ,

$$\begin{bmatrix} \bar{x} \\ \bar{y} \\ \bar{z} \end{bmatrix} = \begin{bmatrix} 2.76888L_R & 0.38159L_G & 18.801L_B \\ L_R & L_G & L_B \\ 0 & 0.012307L_G & 93.066L_B \end{bmatrix} \bullet \begin{bmatrix} \bar{r} \\ \bar{g} \\ \bar{b} \end{bmatrix}, \quad (5.12)$$

Table 5.1 Coordinate values in the r, g, b space for each of the three unit points on the x , y , and z axes, for a 2-deg field.

Point $(\bar{x}, \bar{y}, \bar{z})$	\bar{r}	\bar{g}	\bar{b}
(1, 0, 0)	0.41846	-0.09117	0.00092
(0, 1, 0)	-0.15860	0.25243	-0.00255
(0, 0, 1)	-0.08283	0.01571	0.17860

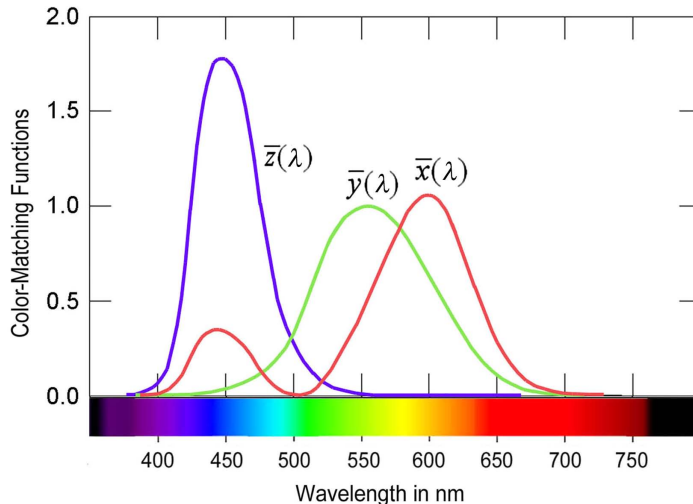


Figure 5.1 Color-matching functions $\bar{x}(\lambda)$, $\bar{y}(\lambda)$, and $\bar{z}(\lambda)$ for a 2-deg field (from CIE, 1931).

with an inverse transformation given by

$$\begin{bmatrix} \bar{r} \\ \bar{g} \\ \bar{b} \end{bmatrix} = \begin{bmatrix} 0.41846 & -1.15860 & -0.08283 \\ -0.09117 & 0.25243 & 0.01571 \\ 0.00092 & -0.00255 & 0.17860 \end{bmatrix} \bullet \begin{bmatrix} \bar{x} \\ \bar{y} \\ \bar{z} \end{bmatrix}. \quad (5.13)$$

We see that the coordinate values r, g, b corresponding to the three points in the x, y, z space ($\bar{x} = 1, \bar{y} = 0, \bar{z} = 0$), ($\bar{x} = 0, \bar{y} = 1, \bar{z} = 0$), ($\bar{x} = 0, \bar{y} = 0, \bar{z} = 1$) are as in Table 5.1. As expected, we can notice that some of the amounts of r, g , or b required to obtain these points are negative.

These color-matching functions are for a 2-deg field, so that any participation of rod vision in the measurements is avoided, as defined by the CIE (1932) convention in 1931. However, these results remain valid for field sizes of 1–4 deg angular subtense. These functions were defined in a wavelength range of 380–780 nm at wavelength intervals of 5 nm. In 1971 the CIE (1971) recommended a new extended set of values to redefine the 1931 CIE standard colorimetric observer. This new table contains interpolated values at 1-nm intervals with an extended range of 360–830 nm. Table 5.2 shows these values to six decimal places, at 5-nm intervals, which are plotted in Fig. 5.1.

Table 5.2 Color-matching functions $\bar{x}(\lambda)$, $\bar{y}(\lambda)$, and $\bar{z}(\lambda)$ for a 2-deg field (from CIE, 1932).

Wavelength (nm)	$\bar{x}(\lambda)$	$\bar{y}(\lambda)$	$\bar{z}(\lambda)$	Wavelength (nm)	$\bar{x}(\lambda)$	$\bar{y}(\lambda)$	$\bar{z}(\lambda)$
360	0.000130	0.000004	0.000606	600	1.062200	0.631000	0.000800
365	0.000232	0.000007	0.001086	605	1.045600	0.566800	0.000600
370	0.000415	0.000012	0.001946	610	1.002600	0.503000	0.000340
375	0.000742	0.000022	0.003486	615	0.938400	0.441200	0.000240
380	0.001368	0.000039	0.006450	620	0.854450	0.381000	0.000190
385	0.002236	0.000064	0.010550	625	0.751400	0.321000	0.000100
390	0.004243	0.000120	0.020050	630	0.642400	0.265000	0.000050
395	0.007650	0.000217	0.036210	635	0.541900	0.217000	0.000030
400	0.014310	0.000396	0.067850	640	0.447900	0.175000	0.000020
405	0.023190	0.000640	0.110200	645	0.360800	0.138200	0.000010
410	0.043510	0.001210	0.207400	650	0.283500	0.107000	0.000000
415	0.077630	0.002180	0.371300	655	0.218700	0.081600	0.000000
420	0.134380	0.004000	0.645600	660	0.164900	0.061000	0.000000
425	0.214770	0.007300	1.039050	665	0.121200	0.044580	0.000000
430	0.283900	0.011600	1.385600	670	0.087400	0.032000	0.000000
435	0.328500	0.016840	1.622960	675	0.063600	0.023200	0.000000
440	0.348280	0.023000	1.747060	680	0.046770	0.017000	0.000000
445	0.348060	0.029800	1.782600	685	0.032900	0.011920	0.000000
450	0.336200	0.038000	1.772110	690	0.022700	0.008210	0.000000
455	0.318700	0.048000	1.744100	695	0.015840	0.005723	0.000000
460	0.290800	0.060000	1.669200	700	0.011359	0.004102	0.000000
465	0.251100	0.073900	1.528100	705	0.008111	0.002929	0.000000
470	0.195360	0.090980	1.287640	710	0.005790	0.002091	0.000000
475	0.142100	0.112600	1.041900	715	0.004106	0.001484	0.000000
480	0.095640	0.139020	0.812950	720	0.002899	0.001047	0.000000
485	0.057950	0.169300	0.616200	725	0.002049	0.000740	0.000000
490	0.032010	0.208020	0.465180	730	0.001440	0.000520	0.000000
495	0.014700	0.258600	0.353300	735	0.001000	0.000361	0.000000
500	0.004900	0.323000	0.272000	740	0.000690	0.000249	0.000000
505	0.002400	0.407300	0.212300	745	0.000476	0.000172	0.000000
510	0.009300	0.503000	0.158200	750	0.000332	0.000120	0.000000
515	0.029100	0.608200	0.111700	755	0.000235	0.000085	0.000000
520	0.063270	0.710000	0.078250	760	0.000166	0.000060	0.000000
525	0.109600	0.793200	0.057250	765	0.000117	0.000042	0.000000
530	0.165500	0.862000	0.042160	770	0.000083	0.000030	0.000000
535	0.225750	0.914850	0.029840	775	0.000059	0.000021	0.000000
540	0.290400	0.954000	0.020300	780	0.000041	0.000015	0.000000
545	0.359700	0.980300	0.013400	785	0.000029	0.000011	0.000000
550	0.433450	0.994950	0.008750	790	0.000021	0.000007	0.000000
555	0.512050	1.000000	0.005750	795	0.000015	0.000005	0.000000
560	0.594500	0.995000	0.003900	800	0.000010	0.000004	0.000000
565	0.678400	0.978600	0.002750	805	0.000007	0.000003	0.000000
570	0.762100	0.952000	0.002100	810	0.000005	0.000002	0.000000
575	0.842500	0.915400	0.001800	815	0.000004	0.000001	0.000000
580	0.916300	0.870000	0.001650	820	0.000002	0.000001	0.000000
585	0.978600	0.816300	0.001400	825	0.000002	0.000001	0.000000
590	1.026300	0.757000	0.001100	830	0.000001	0.000000	0.000000
595	1.056700	0.694900	0.001000				

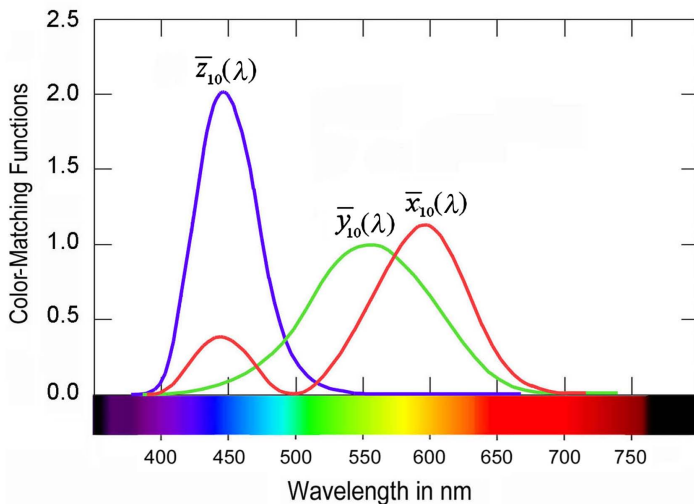


Figure 5.2 Color-matching functions $\bar{x}_{10}(\lambda)$, $\bar{y}_{10}(\lambda)$, and $\bar{z}_{10}(\lambda)$ for a 10-deg field (from CIE, 1964).

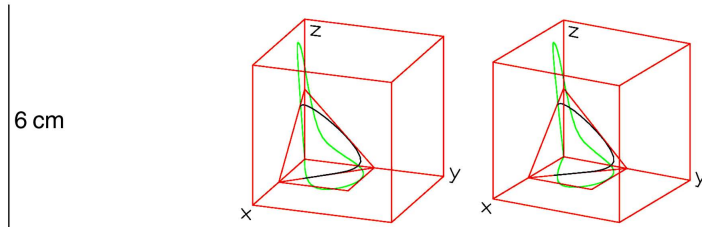


Figure 5.3 Stereo image pair representing the color-matching functions in x , y , z space and projection to $x + y + z = 1$ plane.

The CIE (1964) recommended another slightly different set of color-matching functions, which is more accurate for fields larger than 4 deg. These functions were measured for a field of ten degrees. These functions—defined in the wavelength range of 360–830 nm—are plotted in Fig. 5.2 and tabulated in Table 5.3. The precision of the larger field functions is generally considered more satisfactory for most practical applications. The difference between a large and a small field can be clearly observed in a very large uniform field, where the appearance to the observer clearly shows a central spot with a slightly different color. This central zone is known as the Maxwell spot, which has a diameter of about four degrees; when the eye looks to a different point, the Maxwell spot moves with the eye. This spot is more clearly seen with a moderate luminance of the field. This is due to the presence of the macular pigment in the central portion of the retina.

It is interesting to notice that the spectral relative luminous efficiency of the eye $V(\lambda)$ is not defined for large fields, but only for a 3-deg field. Then, $\bar{y}_{10}(\lambda)$ is slightly different from $V(\lambda)$, with the most noticeable difference being in the blue region. The color-matching functions in the x , y , z space are represented in the stereoscopic image pair in Fig. 5.3.

Table 5.3 Color-matching functions $\bar{x}_{10}(\lambda)$, $\bar{y}_{10}(\lambda)$, and $\bar{z}_{10}(\lambda)$ for a 10-deg field (from CIE, 1964).

Wavelength (nm)	$\bar{x}_{10}(\lambda)$	$\bar{y}_{10}(\lambda)$	$\bar{z}_{10}(\lambda)$	Wavelength (nm)	$\bar{x}_{10}(\lambda)$	$\bar{y}_{10}(\lambda)$	$\bar{z}_{10}(\lambda)$
360	0.000000	0.000000	0.000001	600	1.123990	0.658341	0.000000
365	0.000001	0.000000	0.000004	605	1.089100	0.593878	0.000000
370	0.000006	0.000001	0.000026	610	1.030480	0.527963	0.000000
375	0.000033	0.000004	0.000146	615	0.950740	0.461834	0.000000
380	0.000160	0.000017	0.000705	620	0.856297	0.398057	0.000000
385	0.000662	0.000072	0.002928	625	0.754930	0.339554	0.000000
390	0.002362	0.000253	0.010482	630	0.647467	0.283493	0.000000
395	0.007242	0.000768	0.032344	635	0.535110	0.228254	0.000000
400	0.019110	0.002004	0.086011	640	0.431567	0.179828	0.000000
405	0.043400	0.004509	0.197120	645	0.343690	0.140211	0.000000
410	0.084736	0.008756	0.389366	650	0.268329	0.107633	0.000000
415	0.140638	0.014456	0.656760	655	0.204300	0.081187	0.000000
420	0.204492	0.021391	0.972542	660	0.152568	0.060281	0.000000
425	0.264737	0.029497	1.282500	665	0.112210	0.044096	0.000000
430	0.314679	0.038676	1.553480	670	0.081261	0.031800	0.000000
435	0.357719	0.049602	1.798500	675	0.057930	0.022602	0.000000
440	0.383734	0.062077	1.967280	680	0.040851	0.015905	0.000000
445	0.386726	0.074704	2.027300	685	0.028623	0.011130	0.000000
450	0.370702	0.089456	1.994800	690	0.019941	0.007749	0.000000
455	0.342957	0.106256	1.900700	695	0.013842	0.005375	0.000000
460	0.302273	0.128201	1.745370	700	0.009577	0.003718	0.000000
465	0.254085	0.152761	1.554900	705	0.006605	0.002564	0.000000
470	0.195618	0.185190	1.317560	710	0.004553	0.001768	0.000000
475	0.132349	0.219940	1.030200	715	0.003145	0.001222	0.000000
480	0.080507	0.253589	0.772125	720	0.002175	0.000846	0.000000
485	0.041072	0.297665	0.570600	725	0.001506	0.000586	0.000000
490	0.016172	0.339133	0.415254	730	0.001045	0.000407	0.000000
495	0.005132	0.395379	0.302356	735	0.000727	0.000284	0.000000
500	0.003816	0.460777	0.218502	740	0.000508	0.000199	0.000000
505	0.015444	0.531360	0.159249	745	0.000356	0.000139	0.000000
510	0.037465	0.606741	0.112044	750	0.000251	0.000098	0.000000
515	0.071358	0.685660	0.082248	755	0.000178	0.000070	0.000000
520	0.117749	0.761757	0.060709	760	0.000126	0.000050	0.000000
525	0.172953	0.823330	0.043050	765	0.000090	0.000035	0.000000
530	0.236491	0.875211	0.030451	770	0.000065	0.000025	0.000000
535	0.304213	0.923810	0.020584	775	0.000046	0.000018	0.000000
540	0.376772	0.961988	0.013676	780	0.000033	0.000013	0.000000
545	0.451584	0.982200	0.007918	785	0.000024	0.000010	0.000000
550	0.529826	0.991761	0.003988	790	0.000018	0.000007	0.000000
555	0.616053	0.999110	0.001091	795	0.000013	0.000005	0.000000
560	0.705224	0.997340	0.000000	800	0.000009	0.000004	0.000000
565	0.793832	0.982380	0.000000	805	0.000007	0.000003	0.000000
570	0.878655	0.955552	0.000000	810	0.000005	0.000002	0.000000
575	0.951162	0.915175	0.000000	815	0.000004	0.000001	0.000000
580	1.014160	0.868934	0.000000	820	0.000003	0.000001	0.000000
585	1.074300	0.825623	0.000000	825	0.000002	0.000001	0.000000
590	1.118520	0.777405	0.000000	830	0.000002	0.000001	0.000000
595	1.134300	0.720353	0.000000				

5.3 Tristimulus Values X, Y, Z

By analogy with Eqs. (4.10)–(4.12) it is easy to see that the tristimulus values for a nonmonochromatic light source with spectral relative power $P(\lambda)$ are given by

$$X = \int_0^{\infty} P(\lambda) \bar{x}(\lambda) d\lambda, \quad (5.14)$$

$$Y = \int_0^{\infty} P(\lambda) \bar{y}(\lambda) d\lambda, \quad (5.15)$$

$$Z = \int_0^{\infty} P(\lambda) \bar{z}(\lambda) d\lambda. \quad (5.16)$$

As described in Chapter 1, the maximum photopic relative luminous efficiency of the human eye is about 683 lm/W at a wavelength of 555 nm. Thus, from Eq. (1.19), for a polychromatic light source, the luminance of a light source \bar{L}_V in lumens is given by

$$\bar{L}_V = 683 \int_0^{\infty} V(\lambda) L(\lambda) d\lambda = 683Y, \quad (5.17)$$

where $L(\lambda)$ is the spectral radiance of the light source. This means that, as desired, the luminosity is given only by the tristimulus value Y . From Eq. (1.20), the luminous efficacy σ of a light source in lumens per watt is given by

$$\sigma = 683 \frac{Y}{L}, \quad (5.18)$$

where L is the radiance.

5.4 Chromaticity Coordinates x, y, z

As in the case of the r, g, b space, the chromaticity coordinates for spectrally pure colors are found by projecting all points with coordinates equal to the color-matching functions $\bar{x}(\lambda)$, $\bar{y}(\lambda)$, and $\bar{z}(\lambda)$ to a plane passing through the points $(1, 0, 0)$, $(0, 1, 0)$, $(0, 0, 1)$ (as illustrated in Fig. 5.4), by normalizing the color-matching functions for that wavelength, as follows:

$$x(\lambda) = \frac{\bar{x}(\lambda)}{\bar{x}(\lambda) + \bar{y}(\lambda) + \bar{z}(\lambda)}, \quad (5.19)$$

$$y(\lambda) = \frac{\bar{y}(\lambda)}{\bar{x}(\lambda) + \bar{y}(\lambda) + \bar{z}(\lambda)}, \quad (5.20)$$

$$z(\lambda) = \frac{\bar{z}(\lambda)}{\bar{x}(\lambda) + \bar{y}(\lambda) + \bar{z}(\lambda)}. \quad (5.21)$$

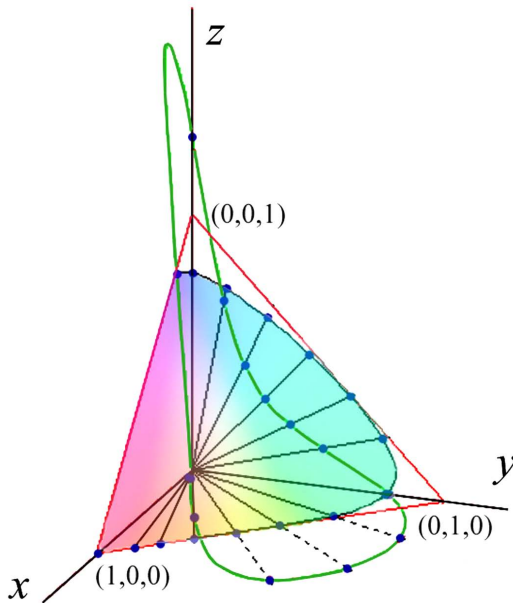


Figure 5.4 Projection of points with coordinates $x(\lambda)$, $y(\lambda)$, $z(\lambda)$ to a plane passing through points $(1, 0, 0)$, $(0, 1, 0)$, $(0, 0, 1)$.

For the case of a nonmonochromatic (with several wavelengths) color, the corresponding chromaticity coordinates are

$$x = \frac{X}{X + Y + Z}, \quad (5.22)$$

$$y = \frac{Y}{X + Y + Z}, \quad (5.23)$$

$$z = \frac{Z}{X + Y + Z}. \quad (5.24)$$

These chromaticity coordinates, illustrated in Fig. 5.5, are not linearly independent of each other, since they are related by

$$x + y + z = 1. \quad (5.25)$$

The numerical values of the chromaticity coordinates $x(\lambda)$, $y(\lambda)$, and $z(\lambda)$ for spectrally pure monochromatic colors, for a field of 2 deg, given to four decimal places, are given in Table 5.4.

Table 5.5 shows the numerical values of the chromaticity coordinates $x_{10}(\lambda)$, $y_{10}(\lambda)$, and $z_{10}(\lambda)$ for the spectrally pure monochromatic colors, for a field of 10 deg, given to four decimal places.

The values of the chromaticity coordinates r , g , and b for each of the three stimuli X , Y , and Z , defined by the points $(1, 0, 0)$, $(0, 1, 0)$, and $(0, 0, 1)$ in the

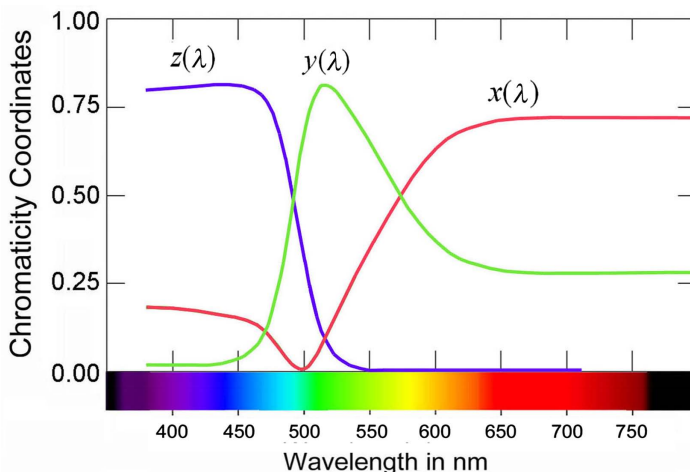


Figure 5.5 Chromaticity coordinates $x(\lambda)$, $y(\lambda)$, $z(\lambda)$ for spectrally pure colors for a 2-deg field (from CIE, 1931).

x - y color space are obtained by normalizing the values in Table 5.1, as shown in Table 5.6.

A representation of x versus y values is known as the CIE chromaticity diagram, shown in Fig. 5.6, with all spectrally pure colors represented along the horseshoe-like curve. A straight line joining the extremes of this curve represents the purple colors, formed by a combination of red with blue in different proportions. The luminosity cannot be represented in this diagram, only the saturation and the hue of the color, as is shown in Fig. 5.7. So, the point with coordinates $x = 0.33$ and $y = 0.33$ represents not only the white color, but also the black and all gray colors. In the same manner, any other point can have any luminosity. A complete specification for any given color would be given by the chromaticity coordinates x and y and the luminosity Y .

An approximate color representation of this chromaticity diagram is shown in Fig. 5.8. For several reasons, this color representation cannot be made perfectly faithful either in printed paper or in a computer display. One reason is that the primary colors used to produce this figure are colors located at the corners of a triangle in the CIE diagram. Thus, only colors inside this triangle can be accurately displayed. Even if an infinite number of spectral colors could be used in the display, another practical problem arises, i.e., the luminance cannot be made constant over the whole diagram. The reason is that the alychne, that is, the straight line representing the purple colors, has zero luminance; hence, all of the points on the CIE chromaticity diagram would have zero luminosity. A diagram with any nonzero constant luminosity must leave out the colors that are in the neighborhood of the alychne. A solution to this last problem would be to produce the color diagram with nonconstant luminance, as is frequently done.

In this diagram we can see that Hering's (1964) ideas of opponent colors (Krantz, 1975; Billock and Tsou, 2010)—that red and green as well as blue and yellow are opposite colors—is confirmed, since they are pairs on the opposite side

Table 5.4 Chromaticity coordinates $x(\lambda)$, $y(\lambda)$, and $z(\lambda)$ for spectrally pure colors and for a 2-deg field (from CIE, 1932).

Wavelength (nm)	$x(\lambda)$	$y(\lambda)$	$z(\lambda)$	Wavelength (nm)	$x(\lambda)$	$y(\lambda)$	$z(\lambda)$
380	0.1741	0.0050	0.8209	585	0.5448	0.4544	0.0008
385	0.1740	0.0050	0.8210	590	0.5752	0.4242	0.0006
390	0.1738	0.0049	0.8213	595	0.6029	0.3965	0.0006
395	0.1736	0.0049	0.8215	600	0.6270	0.3725	0.0005
400	0.1733	0.0048	0.8219	605	0.6482	0.3514	0.0004
405	0.1730	0.0048	0.8222	610	0.6658	0.3340	0.0002
410	0.1726	0.0048	0.8226	615	0.6801	0.3197	0.0002
415	0.1721	0.0048	0.8231	620	0.6915	0.3083	0.0002
420	0.1714	0.0051	0.8235	625	0.7006	0.2993	0.0001
425	0.1703	0.0058	0.8239	630	0.7079	0.2920	0.0001
430	0.1689	0.0069	0.8242	635	0.7140	0.2859	0.0001
435	0.1669	0.0086	0.8245	640	0.7190	0.2809	0.0001
440	0.1644	0.0109	0.8247	645	0.7230	0.2770	0.0000
445	0.1611	0.0138	0.8251	650	0.7260	0.2740	0.0000
450	0.1566	0.0177	0.8257	655	0.7283	0.2717	0.0000
455	0.1510	0.0227	0.8263	660	0.7300	0.2700	0.0000
460	0.1440	0.0297	0.8263	665	0.7311	0.2689	0.0000
465	0.1355	0.0399	0.8246	670	0.7320	0.2680	0.0000
470	0.1241	0.0578	0.8181	675	0.7327	0.2673	0.0000
475	0.1096	0.0868	0.8036	680	0.7334	0.2666	0.0000
480	0.0913	0.1327	0.7760	685	0.7340	0.2660	0.0000
485	0.0687	0.2007	0.7306	690	0.7344	0.2656	0.0000
490	0.0454	0.2950	0.6596	695	0.7346	0.2654	0.0000
495	0.0235	0.4127	0.5638	700	0.7347	0.2653	0.0000
500	0.0082	0.5384	0.4534	705	0.7347	0.2653	0.0000
505	0.0039	0.6548	0.3413	710	0.7347	0.2653	0.0000
510	0.0139	0.7502	0.2359	715	0.7347	0.2653	0.0000
515	0.0389	0.8120	0.1491	720	0.7347	0.2653	0.0000
520	0.0743	0.8338	0.0919	725	0.7347	0.2653	0.0000
525	0.1142	0.8262	0.0596	730	0.7347	0.2653	0.0000
530	0.1547	0.8059	0.0394	735	0.7347	0.2653	0.0000
535	0.1929	0.7816	0.0255	740	0.7347	0.2653	0.0000
540	0.2296	0.7543	0.0161	745	0.7347	0.2653	0.0000
545	0.2658	0.7243	0.0099	750	0.7347	0.2653	0.0000
550	0.3016	0.6923	0.0061	755	0.7347	0.2653	0.0000
555	0.3373	0.6589	0.0038	760	0.7347	0.2653	0.0000
560	0.3731	0.6245	0.0024	765	0.7347	0.2653	0.0000
565	0.4087	0.5796	0.0017	770	0.7347	0.2653	0.0000
570	0.4441	0.5547	0.0012	775	0.7347	0.2653	0.0000
575	0.4788	0.5202	0.0010	780	0.7347	0.2653	0.0000
580	0.5125	0.4866	0.0009				

of the white point. In other words, a mixture of red and green or a mixture of yellow and blue, if combined in the proper proportions, may produce a white color.

5.5 Dominant Wavelength and Correlated Color Temperature

Let us consider a point A in the CIE diagram, as shown in Fig. 5.9. Now, let us trace a line from the point W, representing white, to the curve representing

Table 5.5 Chromaticity coordinates $x_{10}(\lambda)$, $y_{10}(\lambda)$, and $z_{10}(\lambda)$ for a 10-deg field (from CIE, 1964).

Wavelength (nm)	$x_{10}(\lambda)$	$y_{10}(\lambda)$	$z_{10}(\lambda)$	Wavelength (nm)	$x_{10}(\lambda)$	$y_{10}(\lambda)$	$z_{10}(\lambda)$
380	0.1813	0.0197	0.7990	585	0.5654	0.4345	0.0000
385	0.1809	0.0195	0.7995	590	0.5900	0.4100	0.0000
390	0.1803	0.0193	0.8003	595	0.6116	0.3884	0.0000
395	0.1795	0.0190	0.8015	600	0.6306	0.3694	0.0000
400	0.1784	0.0187	0.8029	605	0.6471	0.3529	0.0000
405	0.1771	0.0184	0.8045	610	0.6612	0.3388	0.0000
410	0.1755	0.0181	0.8064	615	0.6730	0.3269	0.0000
415	0.1732	0.0178	0.8090	620	0.6827	0.3173	0.0000
420	0.1706	0.0178	0.8115	625	0.6897	0.3102	0.0000
425	0.1679	0.0187	0.8134	630	0.6955	0.3045	0.0000
430	0.1650	0.0203	0.8147	635	0.7010	0.2990	0.0000
435	0.1622	0.2249	0.8153	640	0.7059	0.2941	0.0000
440	0.1590	0.0252	0.8152	645	0.7102	0.2897	0.0000
445	0.1554	0.0300	0.8146	650	0.7137	0.2863	0.0000
450	0.1510	0.0364	0.8126	655	0.7156	0.2844	0.0000
455	0.1459	0.0452	0.8088	660	0.7158	0.2832	0.0000
460	0.1389	0.0589	0.8021	665	0.7179	0.2821	0.0000
465	0.1295	0.0779	0.7926	670	0.7187	0.2813	0.0000
470	0.1152	0.1090	0.7758	675	0.7193	0.2806	0.0000
475	0.0957	0.1591	0.7452	680	0.7198	0.2802	0.0000
480	0.0728	0.2292	0.6980	685	0.7200	0.2800	0.0000
485	0.0452	0.3273	0.6275	690	0.7202	0.2798	0.0000
490	0.0210	0.4401	0.5389	695	0.7203	0.2797	0.0000
495	0.0073	0.5625	0.4302	700	0.7203	0.2796	0.0000
500	0.0056	0.6745	0.3199	705	0.7203	0.2797	0.0000
505	0.0219	0.7526	0.2255	710	0.7202	0.2798	0.0000
510	0.0495	0.8023	0.1481	715	0.7201	0.2799	0.0000
515	0.0850	0.8169	0.0980	720	0.7199	0.2801	0.0000
520	0.1252	0.8102	0.0646	725	0.7197	0.2803	0.0000
525	0.1664	0.7922	0.0414	730	0.7194	0.2805	0.0000
530	0.2070	0.7963	0.0267	735	0.7192	0.2808	0.0000
535	0.2436	0.7399	0.0165	740	0.7189	0.2811	0.0000
540	0.2786	0.7113	0.0101	745	0.7186	0.2814	0.0000
545	0.3132	0.6813	0.0055	750	0.7183	0.2817	0.0000
550	0.3473	0.6501	0.0026	755	0.7179	0.2820	0.0000
555	0.3812	0.6182	0.0007	760	0.7176	0.2824	0.0000
560	0.4142	0.5859	0.0000	765	0.7172	0.2828	0.0000
565	0.4469	0.5531	0.0000	770	0.7168	0.2831	0.0000
570	0.4790	0.5210	0.0000	775	0.7165	0.2835	0.0000
575	0.5096	0.4903	0.0000	780	0.7160	0.2839	0.0000
580	0.5386	0.4614	0.0000				

Table 5.6 Chromaticity coordinates (on the inclined plane passing through the unit vectors) r , g , and b for each of the three stimuli X , Y , and Z , for a 2-deg field.

Point (x, y, z)	r	g	b
(1, 0, 0)	1.275	-0.278	0.003
(0, 1, 0)	-1.738	2.765	-0.028
(0, 0, 1)	-0.743	0.141	1.602

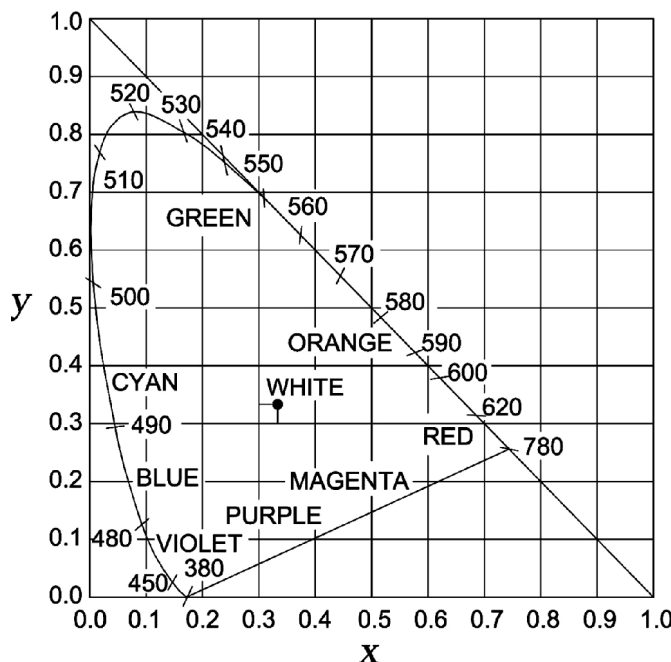


Figure 5.6 Cromaticity x - y diagram for a 10-deg field (from CIE, 1964).

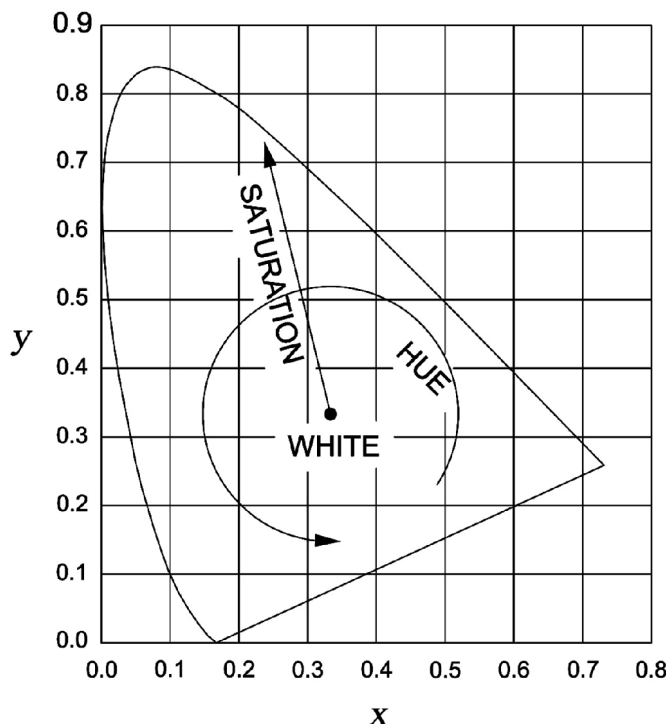


Figure 5.7 Hue and saturation variation in the chromaticity diagram.

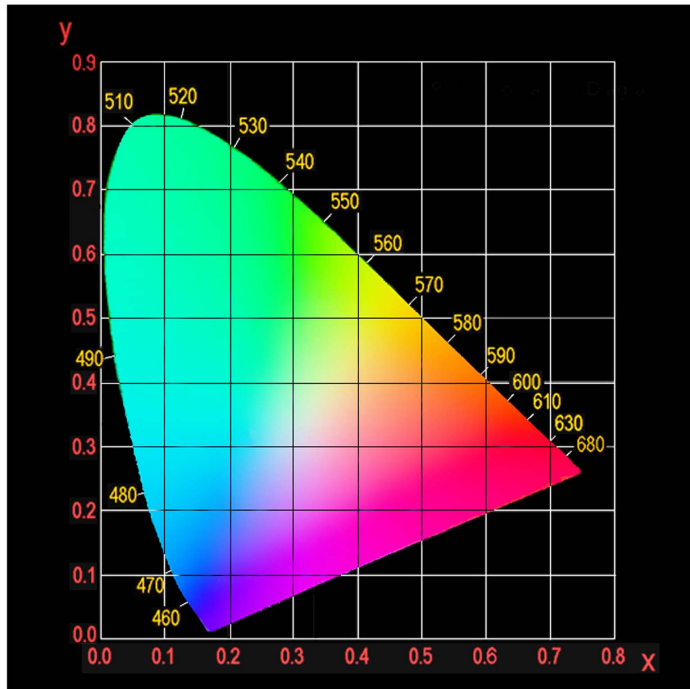


Figure 5.8 Color chromaticity x - y diagram for a 2-deg field (from CIE, 1932).

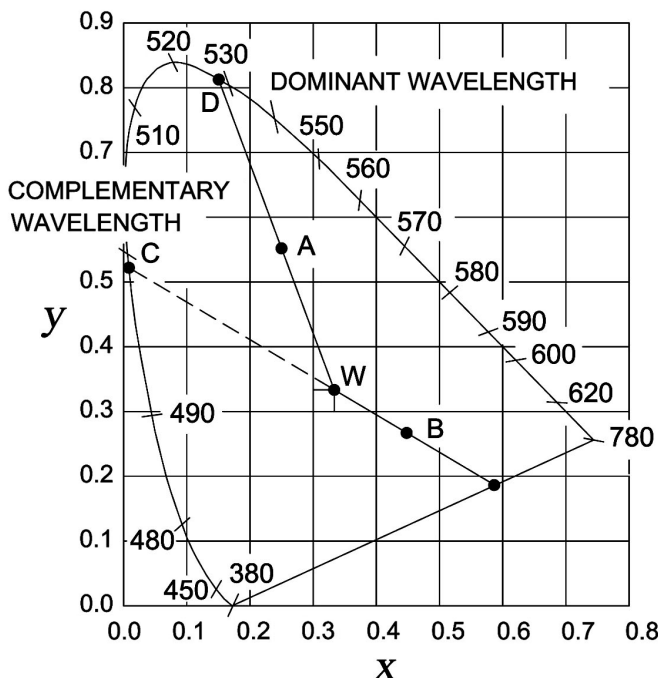


Figure 5.9 Dominant and complementary wavelengths in the chromaticity diagram.

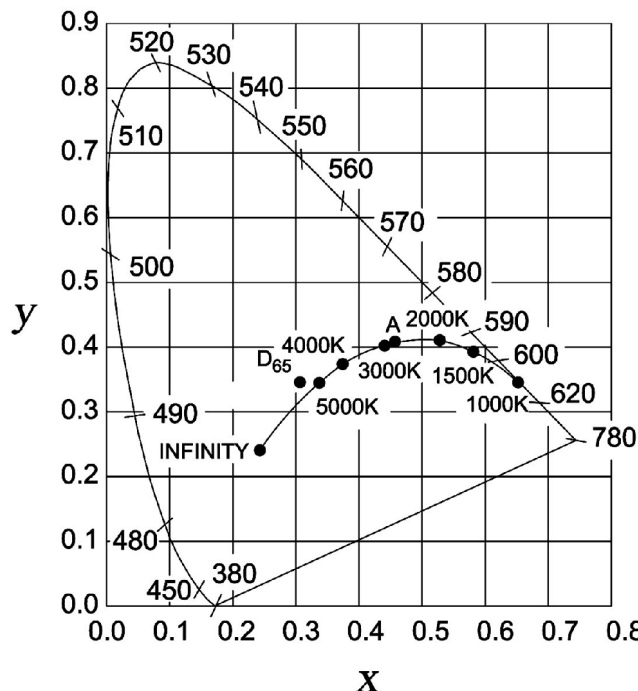


Figure 5.10 Colors of blackbody light sources for different temperatures.

the spectrally pure colors, passing through point A. Crossing point D between this line and this curve indicates the *dominant wavelength* of color A, which is approximately related to the hue of this color. *Excitation purity* p , closely related to the *saturation* of color A, is given by

$$p = \frac{WA}{WD}, \quad (5.26)$$

where WA is the distance between points W and A, and WD is the distance between points W and D. As we will see in Section 6.2, colors with a given dominant wavelength but different excitation purity can have slightly different hues.

Let us now consider point B on the chromaticity diagram. The line from the white point W to point B does not pass through the spectrally pure colors curve, but through the straight purple line. In this case no dominant wavelength is defined. Instead, we define the *complementary wavelength* defined by crossing point C of this line with the spectrally pure colors curve. Again, in this case the *excitation purity* of color B is given by

$$p = \frac{WB}{WC}, \quad (5.27)$$

where WB is the distance between points W and B, and WC is the distance between the points W and C. It is interesting to see in the CIE diagram in Fig. 5.10 that

the location of the chromaticity coordinates of blackbody radiators is at different temperatures. This curve will be referred to here as the Planckian locus. As described in Chapter 2, if a colored body has the same chromaticity coordinates as a blackbody at a certain temperature T , the color temperature of this colored body or light source is T . Strictly speaking, the color temperature is defined only for colored bodies whose color lies on the Planckian locus. However, if the colored body does not have exactly the same chromaticity coordinates as a blackbody radiator, but they are close, as in the case of a D₆₅ illuminant, we may speak of its *correlated color temperature*, which is defined as the temperature of a blackbody whose chromaticity most resembles a colored body. However, it should be pointed out that this concept loses its meaning if the color of the colored body is far from the Planckian locus.

For a spectrally pure (monochromatic) light source with wavelength λ_0 , the relative spectral power can be written as $P(\lambda) = P_0\delta(\lambda - \lambda_0)$, where δ is the Dirac delta function, and P_0 is the relative power of the monochromatic light source. Thus, the tristimulus values X , Y , and Z for a spectrally pure (monochromatic) light source can be written as

$$\begin{aligned} X &= \int_0^\infty P_0\delta(\lambda - \lambda_0)\bar{x}(\lambda)d\lambda = P_0\bar{x}(\lambda_0), \\ Y &= \int_0^\infty P_0\delta(\lambda - \lambda_0)\bar{y}(\lambda)d\lambda = P_0\bar{y}(\lambda_0), \\ Z &= \int_0^\infty P_0\delta(\lambda - \lambda_0)\bar{z}(\lambda)d\lambda = P_0\bar{z}(\lambda_0), \end{aligned} \quad (5.28)$$

or in terms of the luminous efficiency of the eye $V(\lambda)$ and the chromaticity coordinates $x(\lambda)$, $y(\lambda)$, $z(\lambda)$, using Eq. (5.3), as

$$X = P_0 \frac{\bar{x}(\lambda)}{\bar{y}(\lambda)} V(\lambda) = P_0 \frac{x(\lambda)}{y(\lambda)} V(\lambda), \quad (5.29)$$

$$Y = P_0 V(\lambda), \quad (5.30)$$

$$Z = P_0 \frac{z(\lambda)}{y(\lambda)} V(\lambda) = P_0 \frac{\bar{z}(\lambda)}{\bar{y}(\lambda)} V(\lambda). \quad (5.31)$$

Thus, the tristimulus value Y for this monochromatic luminous object with unit relative power is equal to the normalized luminous efficiency of the eye $V(\lambda)$, which, as $\bar{y}(\lambda)$, has a wavelength peak of about 550 nm.

The CIE diagram was originally obtained in 1931 for a field diameter of 2 deg, but in 1964 it was obtained for a field diameter of 10 deg for the reasons described in Chapter 4. These two diagrams are quite similar, as shown in Fig. 5.11.

Any color with its hue, saturation, and luminance can be specified by the tristimulus values X , Y , and Z , or by the chromaticity coordinates x and y plus the tristimulus value Y . If x , y , and Y are known, the values of X and Z values can

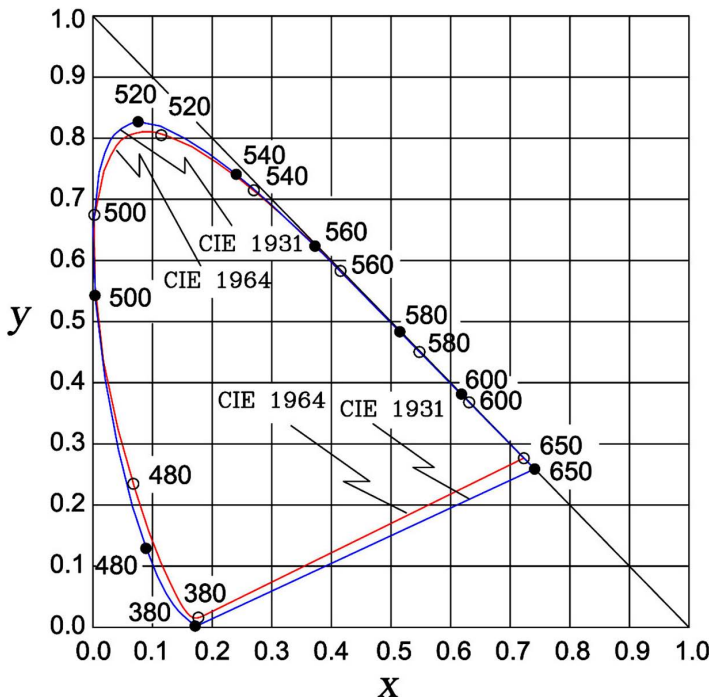


Figure 5.11 Two CIE chromaticity diagrams, shown for 2 deg and for 10 deg, for comparison.

be obtained with

$$X = \frac{x}{y} Y \quad (5.32)$$

$$Z = \left(\frac{1}{y} - \frac{x}{y} - 1 \right) Y. \quad (5.33)$$

5.6 The Color of a Transparent or Opaque Body

When a transparent or opaque body is illuminated by a light source, its color parameter's hue and saturation can be specified independently of the luminance of the light source illuminating the body. However, the color of the light source, i.e., its light spectral radiance or power spectrum, greatly influences the perceived color. Printed or painted colors absorb part of the illuminating energy at some characteristic wavelengths; thus, they necessarily reflect less than 100% of the illuminating light.

Let us consider an illuminating light source with a certain power spectrum represented by its relative spectral power $P(\lambda)$. This light passes through a colored transparent object, or it is reflected by a colored opaque body. As defined in Chapter 1, the spectral transmittance $\tau(\lambda)$ of this filter, or the spectral reflectance $\rho(\lambda)$ of this object, is defined by the ratio of the exiting to the entering radiant

fluxes, per unit wavelength interval. Then, the observed spectral radiance on the illuminated object is directly proportional to the product of the spectral transmittance or reflectance and the illuminating spectral irradiance $W(\lambda)$. For example, neglecting the proportionality constant, for the case of an opaque object, the observed spectral radiance is

$$L(\lambda) = \rho(\lambda)W(\lambda). \quad (5.34)$$

Then, the color of an object can be defined as the perceived color when illuminated by a standard white-light source. The natural theoretical choice is a white-light source with a constant spectral irradiance $W(\lambda) = 1$. However, this is not practical because this light source does not exist in nature; a better choice for this reference light source is an available standard illuminant. Then, a perfectly white opaque object with $\rho(\lambda) = 1$ will reflect light with a power spectrum equal to that of the chosen illuminant. Thus, this white body has the maximum *luminous reflectance* that an opaque body may have, defined to be equal to 100. The minimum luminous reflectance is that of a blackbody, which is equal to zero. Thus, the tristimulus values defining the color of an opaque object are

$$X = 100 \frac{\sum_{i=1}^N P_{st}(\lambda_i)\rho(\lambda_i)\bar{x}(\lambda_i)}{\sum_{i=1}^N P_{st}(\lambda_i)\bar{y}(\lambda_i)}, \quad (5.35)$$

$$Y = 100 \frac{\sum_{i=1}^N P_{st}(\lambda_i)\rho(\lambda_i)\bar{y}(\lambda_i)}{\sum_{i=1}^N P_{st}(\lambda_i)\bar{y}(\lambda_i)}, \quad (5.36)$$

$$Z = 100 \frac{\sum_{i=1}^N P_{st}(\lambda_i)\rho(\lambda_i)\bar{z}(\lambda_i)}{\sum_{i=1}^N P_{st}(\lambda_i)\bar{y}(\lambda_i)}, \quad (5.37)$$

where these values have been normalized so that the luminous reflectance of a perfectly white object is 100 and $P_{st}(\lambda)$ is the relative spectral power of the standard illuminant being used, and $\rho(\lambda)$ is the spectral reflectance of the colored opaque body. Both of these spectra are in a scale from zero to 1.0. For the case of a colored filter or a transparent colored object, the spectral reflectance $\rho(\lambda)$ is replaced by the spectral transmittance $\tau(\lambda)$. It must be noted that the tristimulus Y value is equal to the luminous reflectance (or luminous transmittance) of an opaque (or transparent) colored body. The denominator in these expressions represents the luminance of the illuminating light beam.

The tristimulus values X_n , Y_n , and Z_n for a white opaque object with a unit spectral reflectance [$\rho(\lambda) = 1$], also called a perfect diffuser, when illuminated

Table 5.7 Tristimulus values X_n , Y_n , Z_n for a white opaque object with a constant unit spectral reflectance; the last column lists the values of the denominator in Eqs. (5.38)–(5.40).

Illuminant		X_n	Y_n	Z_n	x_n	y_n	Denominator
A	2 deg	109.850	100.000	35.585	0.448	0.407	2157.94
	10 deg	111.144	100.000	35.201	0.451	0.406	2275.83
D_{65}	2 deg	95.053	100.000	108.900	0.313	0.329	2113.41
	10 deg	94.812	100.000	107.327	0.314	0.331	2324.08
F_2	2 deg	99.187	100.000	67.397	0.372	0.375	292.83
	10 deg	103.281	100.000	69.031	0.379	0.367	309.66

with an standard illuminant, are

$$X_n = 100 \frac{\sum_{i=1}^N P_{st}(\lambda_i) \bar{x}(\lambda_i)}{\sum_{i=1}^N P_{st}(\lambda_i) \bar{y}(\lambda_i)}, \quad (5.38)$$

$$Y_n = 100, \quad (5.39)$$

$$Z_n = 100 \frac{\sum_{i=1}^N P_{st}(\lambda_i) \bar{z}(\lambda_i)}{\sum_{i=1}^N P_{st}(\lambda_i) \bar{y}(\lambda_i)}, \quad (5.40)$$

which have the values given in Table 5.7.

If none of the incident luminous energy is absorbed in an opaque or transparent body, the body appears white. The appearance of any color other than white requires the absorption of part of the incident light energy in some spectral regions. The spectral reflectance (or the spectral transmittance) defines the dominant wavelength, the purity, and the luminous reflectance or transmittance of the body. If we select some particular values of any two of these three quantities, there will be an infinite number of different spectral reflectances or the spectral transmittances that give us the desired two values. For example, given the luminous reflectance (or the luminous transmittance) value and the dominant wavelength, there will be an infinite number of spectral reflectance (or spectral transmittance) curves with an infinite number of purity values.

To better understand these important concepts, let us assume that we illuminate a colored reflecting diffuse surface with a standard illuminant, for example, D_{65} . If the surface is perfectly reflecting [$\rho(\lambda) = 1$] in a certain narrow-wavelength interval, the reflected beam will have the power spectrum as illustrated in Fig. 5.12. Let us further assume that the reflected light has a dominant wavelength λ_0 . Another power spectrum, represented by the dotted line in Fig. 5.12, has the same luminance and the same dominant wavelength. As easily observed and previously proven by MacAdam (1935a,b), the power spectrum with the straight boundaries has the highest purity (smallest saturation). Figure 5.13 shows the spectra of four light sources with the same dominant wavelength. These light sources have the

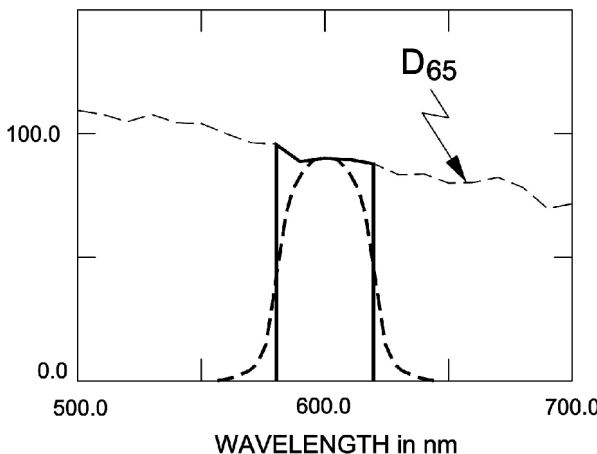


Figure 5.12 Two spectral curves with the same dominant wavelength and the same luminance.

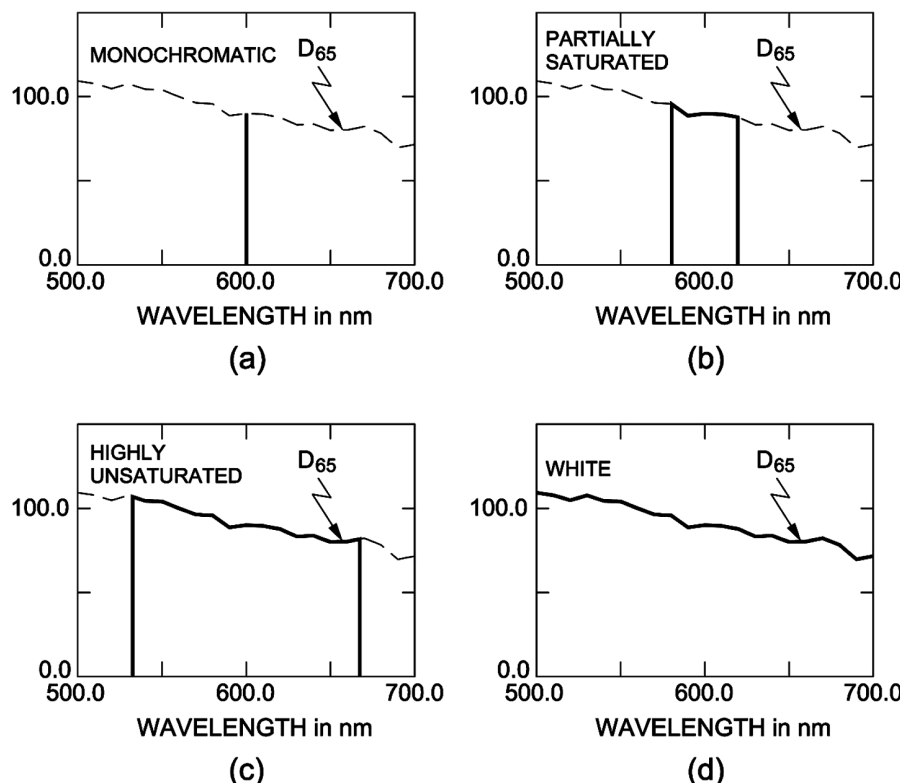


Figure 5.13 Four spectral curves: (a) a spectrally pure color; (b) a partially saturated color with straight boundaries; (c) a highly unsaturated color with straight boundaries; and (d) a white color.

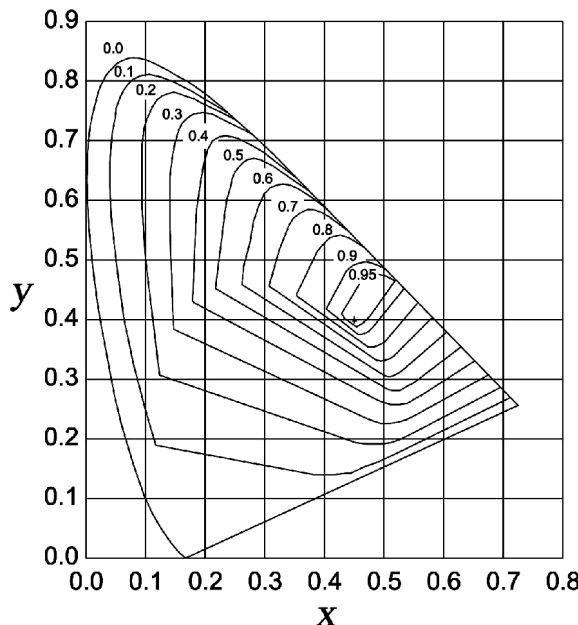


Figure 5.14 Locus of points with maximum possible purity of reflected (or transmitted) light, or MacAdam limits, in nonfluorescent objects in an incandescent tungsten lamp with a color temperature of 2854 K (illuminant A).

maximum possible purity for the power spectrum bandwidth given in each of the four cases, with increasing luminance levels.

A consequence of the former analysis is that given a constant fixed luminance, for any dominant wavelength there is a maximum possible purity value. When the maximum luminous reflectance value is equal to 100, only the white color is possible.

Following a slightly different line of thought, the thin dotted power spectrum in Fig. 5.12 can be narrowed, preserving the same dominant wavelength so that the two spectra have the same purity (instead of the same luminance). Thus, they will have the same position on the chromaticity diagram. The color with the power spectrum having straight boundaries has the maximum possible luminance.

The maximum attainable purity for a given dominant wavelength and a given luminance depends on the type of the illuminant, as illustrated in Fig. 5.14 for an incandescent tungsten lamp with CIE illuminant A (2854 K), and in Fig. 5.15 for artificial daylight with CIE illuminant C. The important conclusion is that the gamut of all physically attainable colors is gradually reduced as the reflectance (luminosity) of the color becomes larger. An approximate color representation of this possible gamut of color for different daylight illuminances is shown in Fig. 5.16. The boundary of this gamut of colors for each reflectance value is frequently called the MacAdam limit.

If we represent the luminance along the z axis, perpendicular to both the x and y axes, the closed curves representing the MacAdam limits for different luminances

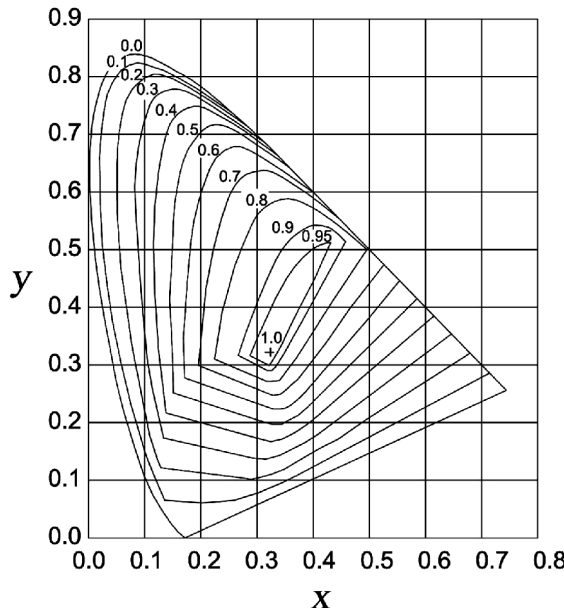


Figure 5.15 Locus of points with maximum possible purity of reflected (or transmitted) light, or MacAdam limits, in nonfluorescent objects in artificial daylight (illuminant D₆₅).

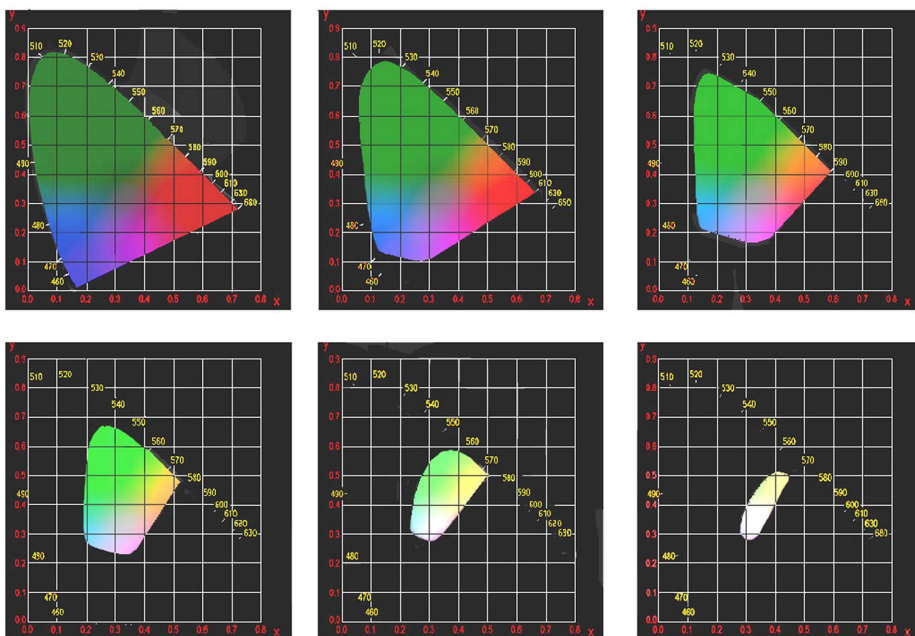


Figure 5.16 Gamut of possible colors for different values of the luminance with artificial daylight illumination.

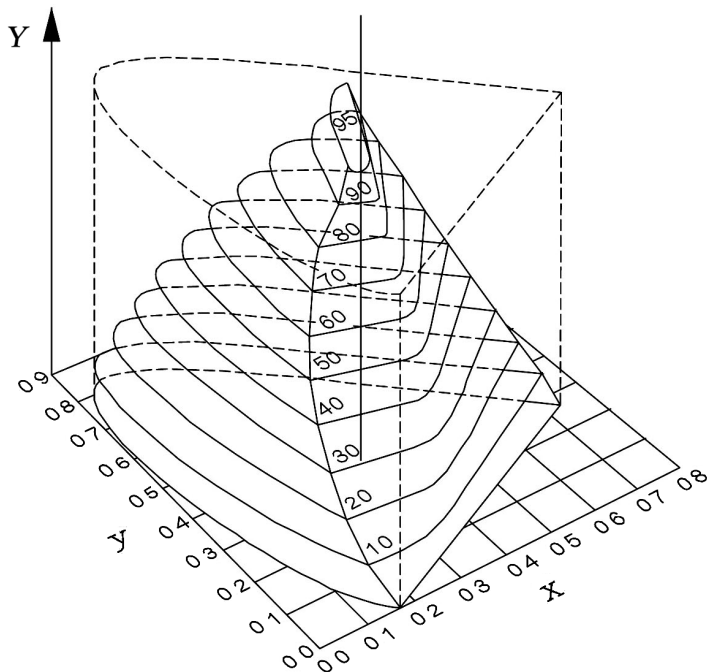


Figure 5.17 CIE (x, y, z) color solid described in this chapter.

in Fig. 5.14 will be at different heights z , forming a space volume. This is the CIE color-space solid with the CIE illuminant D_{65} shown in Fig. 5.17.

MacAdam (1950) showed the curves on the CIE chromaticity diagram with the maximum possible luminous efficiency in lumens per watt, as shown in Fig. 5.18. As expected, we see that the maximum possible luminous efficiency in the whole diagram corresponds to a monochromatic spectral color with a wavelength of 555 nm with 683 lm/W.

5.7 Color Discrimination Mechanisms

Individual cones send a signal about the rate at which they absorb photons, without regard to the wavelength of photons. The wavelength only determines the rate of absorption by each type of cone, but once it is absorbed, the signal is the same. In other words, the signal provided by the cone output does not contain any color information. The color sensation is determined by the relative proportions in the signals provided by the three types of detectors, with the light filtered by the cone pigments. The close analogy with a tristimulus colorimeter, as described in Chapter 8, is evident.

Each cone output, as schematically shown in Fig. 5.19, enters a gain control system. This gain control is largely responsible for the process called *adaptation*, which is the ability of the eye to adjust to various levels of illumination or darkness. Thanks to this process, the eye's luminance-sensing capability has a dynamic range of many orders of magnitude. The adaptation is made at each cone so that color

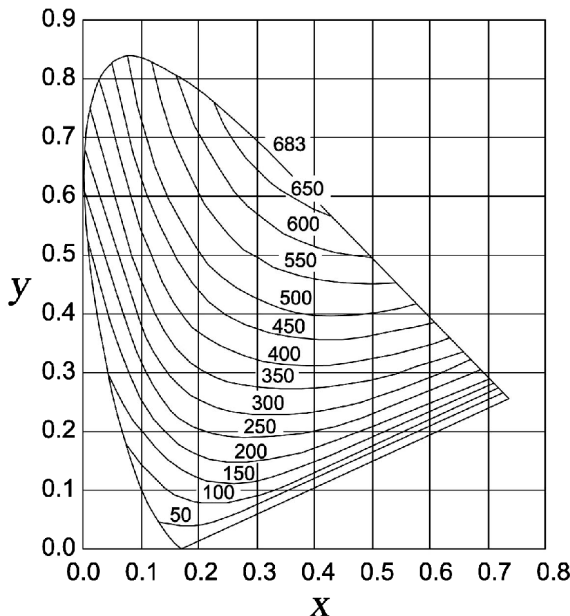


Figure 5.18 Locus of points with maximum attainable luminous efficiency (lumens per watt) for colors in the CIE chromaticity diagram.

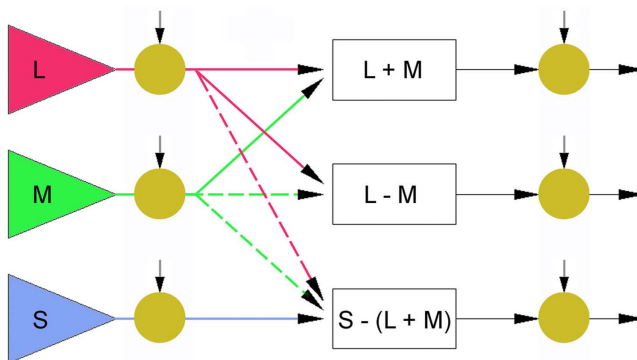


Figure 5.19 Color discrimination mechanism based on color–color opposition. The signals from the cones combine to produce three outputs: $(L-M)$, $S-(L+M)$, and $(L+M)$. These outputs can be active or inhibitory signals, represented by the dashed lines. Also, two stages of gain control act to produce the adaptation mechanism.

compensations can be made. This is the reason why we see the correct colors we expect with many different types of illumination.

In Section 1.3 we stated that at the end of the nineteenth century, Ewald Hering proposed the opponent theory of colors. He noted that two opposing colors, for example, red and green, cannot be observed as a mixture, and thus a reddish green or a greenish red do not exist. He also noted that a chromatic afterimage always has a complementary color. For example, a red stimulus elicits a green afterimage.

Hering's (1964) ideas were not taken seriously until Svaetichin (1956) discovered by means of electrophysiological experiments that some eye detectors are activated by a certain wavelength but inhibited by the wavelength corresponding to the opponent color.

Modern theories of color perception are based on opponent color mechanisms. The color-discrimination mechanism is schematically illustrated in Fig. 5.19. In a simple manner, the mechanism can be explained by considering that the three classes of cones in the retina are connected to produce spectrally opponent neurons. The L- and M-cones are connected, the L-cones with an excitatory output and the L-cones with an inhibitory output, to produce L-M opponent cells. The S-cones are connected with the L- and M-cones to produce S-(L+M) opponent cells. Noncolor opponent cells (L+M) are also produced with the sum of the L- and M-cones.

The (L+M) output carries luminance information as expected, since the S-cones do not contribute to brightness. The (L-M) and the S-(L+M) outputs carry all of the necessary information about color, hue, and saturation. Some researchers believe that luminance information is also contained in these outputs.

After these outputs, a second gain-control stage is found to complement the adaptation process. For more details on these color discrimination processes, see the chapter by Pokorni and Smith (2004) and the book by Schwartz (2004).

5.8 Use of Cone Sensitivities as Color-Matching Functions

The magnitudes of the three cone signals can be thought of as color-matching functions for the three colors, as defined by the three types of cones. For example, the spectral sensitivities of the three types of cones—also known as cone fundamentals $\bar{l}(\lambda)$, $\bar{m}(\lambda)$, and $\bar{s}(\lambda)$ —could in principle be obtained with a linear transformation from the three color-matching functions $\bar{x}(\lambda)$, $\bar{y}(\lambda)$, and $\bar{z}(\lambda)$ or from the three color-matching functions \bar{r} , \bar{g} , \bar{b} or vice versa. Let us assume that the transformation matrix is

$$\begin{bmatrix} \bar{l}(\lambda) \\ \bar{m}(\lambda) \\ \bar{s}(\lambda) \end{bmatrix} = \begin{bmatrix} l_r & l_g & l_b \\ m_r & m_g & m_b \\ s_r & s_g & s_b \end{bmatrix} \bullet \begin{bmatrix} \bar{r}(\lambda) \\ \bar{g}(\lambda) \\ \bar{b}(\lambda) \end{bmatrix}. \quad (5.41)$$

The units for the three cones' spectral sensitivities can be arbitrarily chosen. The scaling factors only define the magnitudes for the units of each of the three tristimuli in the l , m , s space. They do not need to be directly proportional to the luminosity, radiance, or to anything else. Any choice is equally valid. A possibility is to make their sums for all wavelength values equal, as in Eq. (4.9), so that we have a white color with equal values of the tristimuli. Another possibility is to normalize the peak value for the spectral sensitivities of the three cones as equal to 1. A change in the scaling factors would change the geometry of the linear transformation, resulting in a different set of tristimulus values, but the color matching would still be valid.

The color-matching functions are measured through the macular and lens pigments. So, when determining the elements of this matrix, the absorption of these

pigments should be taken into account. The effects of the pigments are different if the 2-deg or the 10-deg color-matching functions are used. For example, from 10 deg to 2 deg it is assumed that the macular pigment optical density changes from a peak of 0.095 to a peak of 0.35, and that the lens photopigment optical density changes from 0.38 to 0.50 for L- or M-cones or from 0.30 to 0.40 for S-cones.

Using the preceding concepts, Stockman et al. (1993) described a transformation to obtain the cone fundamentals from the Stiles and Burch (1955) color-matching functions, as follows:

$$\begin{bmatrix} \bar{l} \\ \bar{m} \\ \bar{s} \end{bmatrix} = \begin{bmatrix} 0.214808 & 0.751035 & 0.045156 \\ 0.022882 & 0.940534 & 0.076827 \\ 0.000000 & 0.016500 & 0.999989 \end{bmatrix} \bullet \begin{bmatrix} \bar{r} \\ \bar{g} \\ \bar{b} \end{bmatrix}. \quad (5.42)$$

The inverse transformation is given by

$$\begin{bmatrix} \bar{r} \\ \bar{g} \\ \bar{b} \end{bmatrix} = \begin{bmatrix} 5.088288 & -4.064546 & 0.082501 \\ -0.123959 & 1.163679 & -0.083805 \\ 0.002045 & -0.019201 & 1.001394 \end{bmatrix} \bullet \begin{bmatrix} \bar{l} \\ \bar{m} \\ \bar{s} \end{bmatrix}. \quad (5.43)$$

When adding $\bar{l}(\lambda)$ and $\bar{m}(\lambda)$ with weights equal to 0.68273 for $\bar{l}(\lambda)$ and 0.35235 for $\bar{m}(\lambda)$, the function $V(\lambda)$ is obtained, as follows:

$$V(\lambda) = 0.68273\bar{l}(\lambda) + 0.35235\bar{m}(\lambda), \quad (5.44)$$

which proves that the contribution to luminance of the S-cones is zero, since the cones' sensitivities $\bar{s}(\lambda)$ are not needed to obtain an almost perfect fit to $V(\lambda)$.

In an analogous manner, the 1964 CIE color-matching functions $\bar{x}_{10}(\lambda)$, $\bar{y}_{10}(\lambda)$, and $\bar{z}_{10}(\lambda)$, for a field of 10 deg, can be obtained from a linear transformation [proposed by Stockman et al. (1993)] of the $\bar{l}(\lambda)$, $\bar{m}(\lambda)$, and $\bar{s}(\lambda)$ cones' spectral sensitivities by means of the transformation

$$\begin{bmatrix} \bar{l} \\ \bar{m} \\ \bar{s} \end{bmatrix} = \begin{bmatrix} 0.236157 & 0.826427 & -0.045710 \\ -0.431117 & 1.206922 & 0.090020 \\ 0.040557 & -0.019683 & 0.486195 \end{bmatrix} \bullet \begin{bmatrix} \bar{x}_{10} \\ \bar{y}_{10} \\ \bar{z}_{10} \end{bmatrix}. \quad (5.45)$$

These transformations are not as accurate as desired, due to many uncertainties in the measurements, but they are continually being improved. More recent determination of the cone fundamentals and of the transformation matrices have been recently described by Stockman et al. (1999) and Stockman and Sharpe (2000), who have substantially improved these values and proposed a new set of values for 2-deg as well as 10-deg field-cone sensitivities. They have even proposed a new set of values for the luminosity function of the eye $V(\lambda)$. The processes involved in human vision are quite complicated (Neissner, 1968; Michael, 1969), and it is outside the scope of this book to cover all of these aspects with detail.

References

- Billock, V. A. and Tsou, B. H., "Impossible color: hues that can't exist," *Sci. Am.* **302**, 72–77 (2010).
- CIE, *Proc., 1931 Commission Internationale de l'Éclairage*, Cambridge University Press, Cambridge, U.K. (1932).
- CIE, *1963 Vienna Session Committee Report E-1.4.1*, Vol. B, pp. 209–220 CIE, Paris (1964).
- CIE, Publication CIE No. 15, *Colorimetry*, Central Bureau, Paris (1971).
- Hering, E., *Outlines of a Theory of the Light Sense*, Hurvich, L. M. and Jameson, D., Eds., (translation), Harvard University Press, Cambridge, MA (1964).
- Ives, H. E., "The transformation of color-mixture equations from one system to another," *J. Franklin Inst.* **180**, 673 (1915).
- Ives, H. E., "The transformation of color-mixture equations from one system to another II. Graphical aids," *J. Franklin Inst.* **195**, 23 (1923).
- Krantz, D. H., "Color measurement and color theory: II Opponent-colors theory," *J. Math. Psychol.* **12**, 304–327 (1975).
- MacAdam, D. L., "The theory of the maximum visual efficiency of colored materials," *J. Opt. Soc. Am.* **25**, 249–252 (1935a).
- MacAdam, D. L., "Maximum visual efficiency of colored materials," *J. Opt. Soc. Am.* **25**, 361–367 (1935b).
- MacAdam, D. L., "Maximum attainable luminous efficiency of various chromaticities," *J. Opt. Soc. Am.* **40**, 120 (1950).
- Michael, C. R., "Retinal processing of visual images," *Sci. Am.* **220**, 104–114 (1969).
- Neissner, U., "The processes of vision," *Sci. Am.* **219**, 204–214 (1968).
- Pokorni, J. and Smith, V. C., "Chromatic discrimination," in *The visual neurosciences*, Chalupa, L. M. and Werner, J. S., Eds., MIT Press, Cambridge, MA (2004).
- Schwartz, S. H., *Visual Perception: A Clinical Orientation*, McGraw-Hill, New York (2004).
- Stiles, W. S. and Burch, J. M., "Interim report to the Commission Internationale de l'Eclairage, Zurich, 1955, on the National Physical Laboratory's investigation of colour matching," *Opt. Acta* **2**, 168–181 (1955).
- Stockman, A. and Sharpe, L. T., "Spectral sensitivities of the middle- and long-wavelength-sensitive cones derived from measurements in observers of known genotype," *Vision Res.* **40**, 1711–1737 (2000).
- Stockman, A., MacLeod, D. I. A., and Johnson, N. E., "Spectral sensitivities of the human cones," *J. Opt. Soc. Am. A* **10**, 2491–2521 (1993).

- Stockman, A., Sharpe, L. T., and Fach, C., “The spectral sensitivity of the human short-wavelength-sensitive cones derived from thresholds and color matches,” *Vision Res.* **39**, 2901–2927 (1999).
- Svaetichin, G., “Spectral response curves from single cones,” *Acta Physiol. Scand. Suppl.* **39**, 17–46 (1956).

Chapter 6

Uniform Color Systems

6.1 Introduction

A small displacement in the CIE color space X , Y , Z will not produce the same change in the perceived color at any point or any direction of change. Similarly, any displacement in the CIE chromaticity diagram will not produce a constant change in hue and saturation. The minimum displacement needed to detect a color change in the CIE diagram is represented by the MacAdam (1942, 1943) ellipses shown in Fig. 6.1, where they are drawn 10 times larger for clarity. We can see that very small changes can be detected near the blue end. On the other hand, purity (saturation) changes in the green region are difficult to detect.

Ellipsoids in a 3D space that include small differences in lightness (luminance) have also been obtained by Brown and MacAdam (1949) and by Brown (1957).

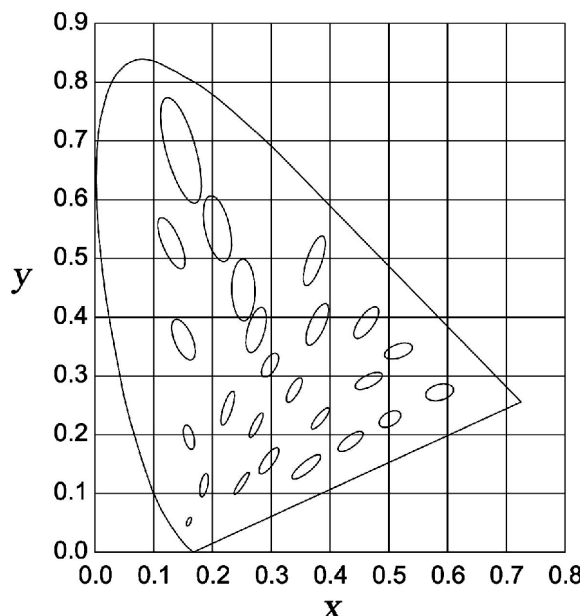


Figure 6.1 Color discrimination with McAdam ellipses. Equally noticeable color differences for 25 points are shown. Ellipses are 10 times larger.

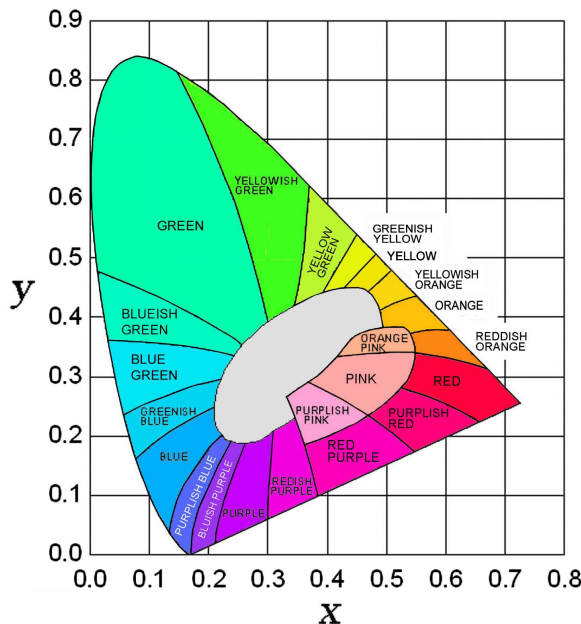


Figure 6.2 Names for some colors in the CIE chromaticity diagram [from Kelly (1943)].

However, these ellipsoids have been difficult to use, and attempts made to develop algebraic expressions for them have been unsuccessful.

Ideally, the CIE color space is modified by means of a linear transformation obtaining a representation on which the minimum perceived color changes in a transparent colored body, or in an opaque colored body, are almost equal at any point and in any direction, which transforms the ellipses into circles with a constant diameter. However, Silverstein (1943) has shown that this transformation is impossible.

Several color systems have been designed to obtain an approximately uniform color space. MacAdam (1971, 1974) proposed one system that nearly transformed the ellipses into circles. However, since the transformation is not linear, graphic rules for color addition do not work on this diagram. One other disadvantage is that there is no definite location for the white point. Another provisionally accepted system is the CIE (1960) chromaticity diagram in which the ellipses transform into a system with a smaller range of sizes, as we will see later in this chapter.

6.2 Hue and Chroma in the CIE Diagram

The measurements of hue, brightness, or saturation, as opposed to tristimulus values, are more in the realm of psychology than in the field of physics. Direct measurements are difficult to make; however, indirect measurements can be made, for example, by counting only perceptible intervals, as pointed out by Richardson (1960), but this is not a simple problem (Judd, 1962). The names of different colors that Kelly (1943) indicated in a CIE diagram (Fig. 6.2) are all defined by their hue and chroma.

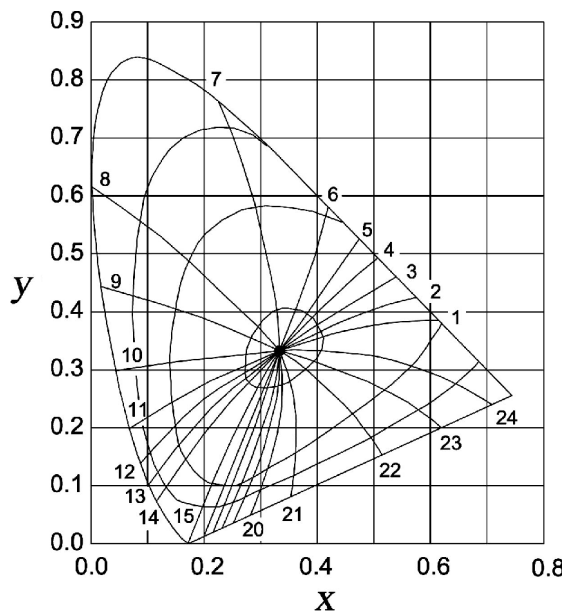


Figure 6.3 Locus of constant hue and constant chroma in the CIE chromaticity diagram.

We have seen in Section 5.4 that a straight line in the CIE diagram going from the white point to a point for a spectrally pure color is the locus of colors with the same dominant wavelength. However, the locus of points with the same hue is not a straight line, since colors with the same dominant wavelength but a different chroma can have slightly different hues. According to Schrödinger (1920) the shortest path to neutral (white or gray) from any highly saturated color is that which passes through colors with the same hue. Let us imagine the CIE diagram completely covered by MacAdam ellipses (nonoverlapping). Then, the color path length between any two points can be defined as the number of ellipses being crossed from one point to the other. Thus, the color path length in a given direction starting from a point in the diagram is a function of the direction. Similarly to the propagation of a ray of light in an anisotropic media, the straight line is not necessarily the minimum color path length. Many efforts have been made to obtain the loci of constant hue in the CIE diagram, as described by Judd (1972). An example is the constant hue curves derived by Muth and Persels (1971) and shown in Fig. 6.3. The approximate shape for the constant chroma curves (Newhall, 1943) for a given value of the luminosity is closed curves around the neutral color (gray), also shown in Fig. 6.3.

6.3 The Munsell System

Around 1900, many years before the CIE convention, Albert H. Munsell, an artist, empirically prepared a set of color charts with an almost uniform color representation (Munsell, 1905, 1912). In the Munsell color space, the colors are represented in a cylinder with zero-saturation colors (black, gray, and white) along

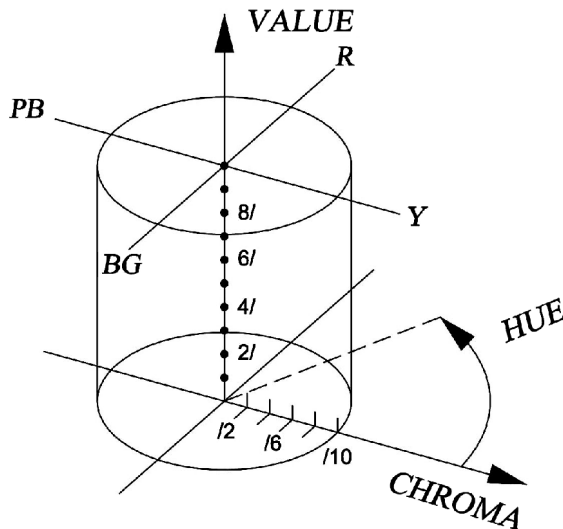


Figure 6.4 Munsell color space.

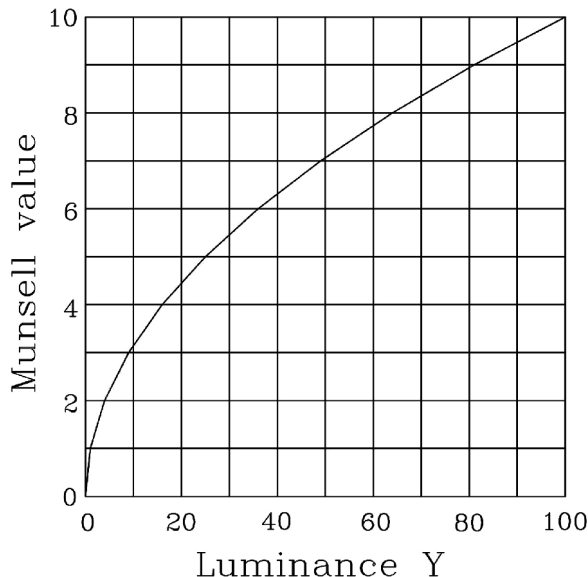


Figure 6.5 The magnitude of the Munsell value is equal to the square root of the luminance.

the axis of the cylinder. The coordinate's configuration in this space is illustrated in Fig. 6.4. The lowest extreme of the cylinder axis corresponds to black, while the highest extreme corresponds to white. The position along this axis, with 10 steps from zero to nine, is called the *value*, representing the perceived lightness that is nonlinear with the luminance Y . To account for this nonlinearity, the value was originally taken as the square root of the luminance (Fig. 6.5), although it was later redefined to improve the relation between the value and the luminance.

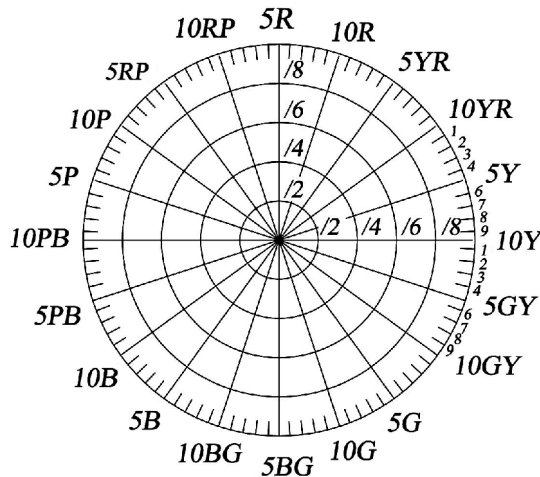


Figure 6.6 Organization of the colors in a Munsell circle with a constant value.

The chroma represents the saturation of the color. It increases in a perpendicular direction to the axis, toward the edge of the cylinder, with values from zero to eight, with monochromatic and purple colors around the periphery.

The hue of the color is represented by the angle. The Munsell circle is divided into the following 10 angular sectors with an angle of 36 deg: yellow (Y), yellow-red (YR), red (R), red-purple (RP), purple (P), purple-blue (PB), blue (B), blue-green (BG), green (G), and green-yellow (GY). Each of these sectors is divided in 10 subsectors with an angle of 3.6 deg. Figure 6.6 shows a Munsell circle in the CIE diagram. In this system, the different colors are specified by *hue value/chroma* as in the following example: 4 YR 7/3, which means a yellow-red color in subsection 4 (hue = 4 YR) with lightness (value) = 7 and chroma = 3. Figure 6.7 shows a circle of colors with the same Munsell value.

In this system there are many planes with colors—one for each hue. A 3D representation of all colors in Munsell color space is formed by a series of radial planes with constant hue, as illustrated in Fig. 6.8. Thus, on each radial plane all colors have the same hue, but with chroma increasing outward from the central axis and the value increasing with height. It is interesting to note that not all planes have the same shape; they bulge outward for blue and purple colors at low values, and for yellow colors at high values. Only black is considered for the lowest value, while white represents the highest. We will see later in this chapter that these characteristics are also present in other uniform color spaces. Figure 6.9 is a close representation of the colors for four Munsell planes with different hues.

The original Munsell system was later modified to correct some obvious errors in the location of some colors. The new color designations and coordinates are known as *Munsell Renotations*, and the system is the *Munsell Renotation System*.

The Munsell system is an almost perfectly uniform color system, where each color is separated from its closest neighbor by equal perceptual distances (Fig. 6.10) in comparison to the location of the same colors in the CIE *x-y* diagram.

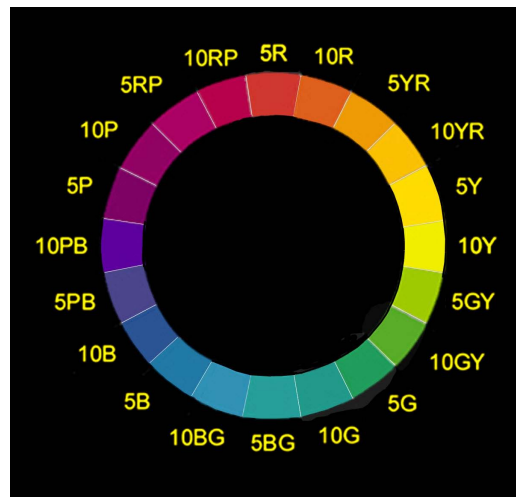


Figure 6.7 A circle of Munsell colors for a given Munsell value.

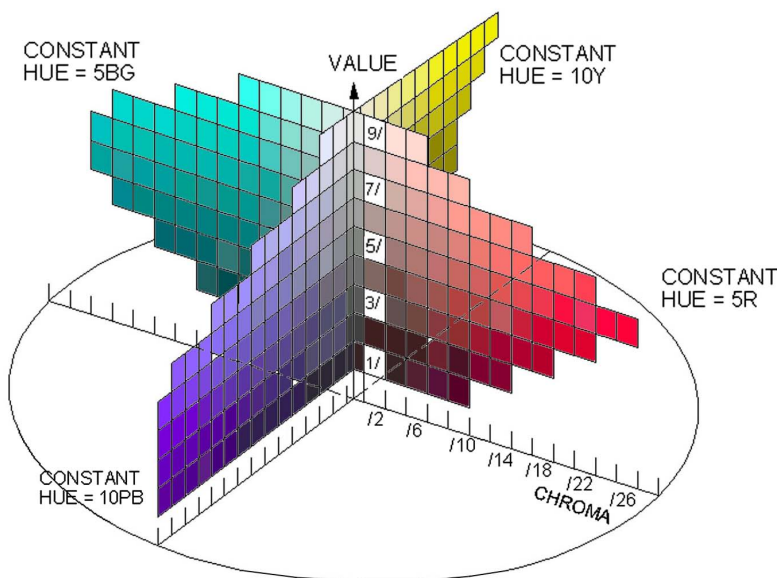


Figure 6.8 Four constant hue planes in the Munsell color space.

We can observe that the curves joining the dots in the CIE x, y diagram resemble the constant chroma curves in Fig. 6.3. An important practical disadvantage is that the Munsell colors are defined only for a 2-deg observer and a C illuminant. Another problem with this system is that no analytical expressions to convert the Munsell system to the CIE system, or vice versa, exist; however, lookup table programs to perform these conversions have been proposed (Newhall, 1943; Rheinboldt and Menard, 1960). As described in the book *Munsell Book of Color*

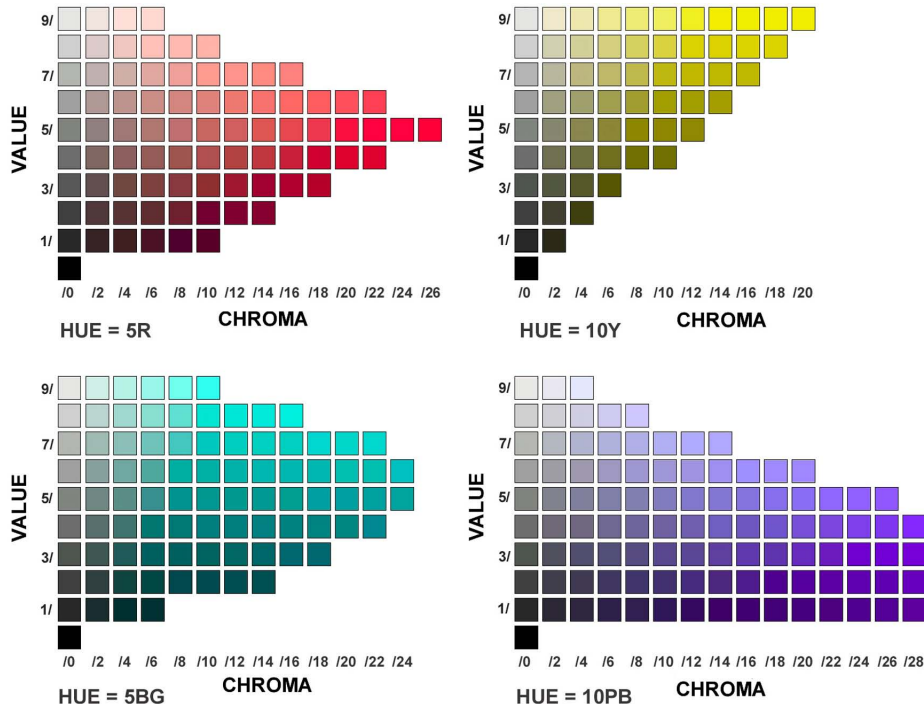


Figure 6.9 Approximate representation of the Munsell colors for four different hues.

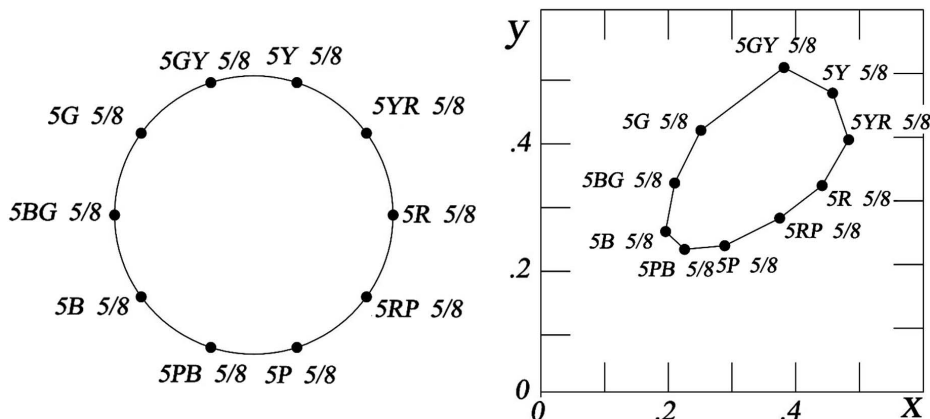


Figure 6.10 Relative location in a circle of some perceptually equally spaced Munsell colors, compared with their separation in a CIE x - y diagram.

(X-Rite, 2007), originally published by Munsell Color in Baltimore in 1976, there is a collection of 1257 chips representing some Munsell colors (Parkkinen et al., 1989).

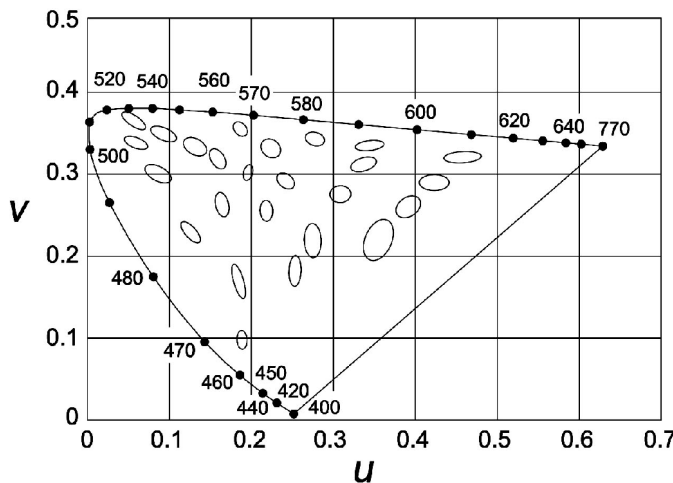


Figure 6.11 The Luv chromaticity diagram (CIE, 1960). MacAdam ellipses are 10 times larger.

Many attempts have been made to analytically define a color system that closely resembles the Munsell System, but without complete success. Some of these systems will be described in the following sections.

6.4 The 1960 CIE Luv Color Space

An almost uniform chromaticity diagram with coordinates Luv proposed by the CIE convention in 1960 (CIE, 1960) is based on the work of several researchers (MacAdam, 1937, 1971). This diagram was the result of an extensive search for a uniform color space by the Committee on Uniform Color Scales of the OSA established in 1947. The history of the activities of this committee is given in Nickerson (1977). This space is defined by

$$u = \frac{4X}{X + 15Y + 3Z} = \frac{4x}{-2x + 12y + 3}, \quad (6.1)$$

$$v = \frac{6Y}{X + 15Y + 3Z} = \frac{6y}{-2x + 12y + 3}, \quad (6.2)$$

with its inverse transformation

$$x = \frac{6u}{6u - 16v + 12}; \quad y = \frac{4v}{6u - 16v + 12}. \quad (6.3)$$

In this diagram, shown in Fig. 6.11, the MacAdam ellipses are more uniform in size and their eccentricities are smaller. A color representation of this diagram is shown in Fig. 6.12.

Since this is a linear projective transformation, a great advantage is that a straight line in the x, y chromaticity diagram converts into another straight line in the u, v

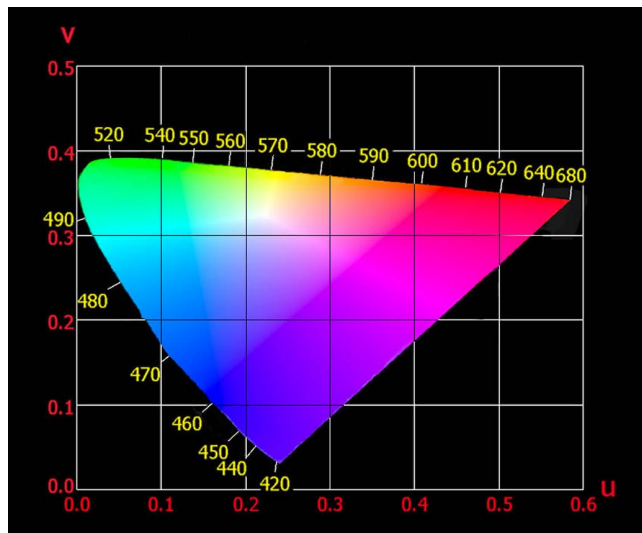


Figure 6.12 A color Luv chromaticity diagram (CIE, 1960).

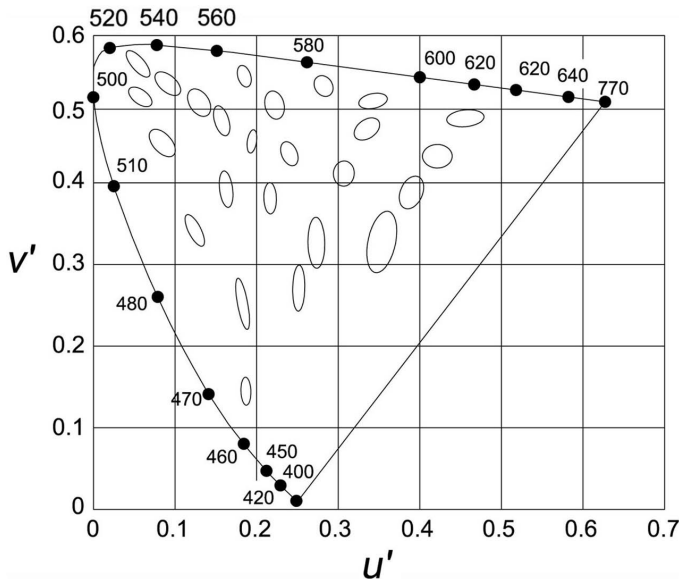


Figure 6.13 The $L'u'v'$ chromaticity diagram (CIE, 1960). MacAdam ellipses are ten times larger.

diagram. This property is important, because it preserves the usual graphic rules for the addition of colors, as will be described with detail in Chapter 7.

In 1976, the CIE made a slight improvement to this diagram by defining a new chromaticity diagram, shown in Fig. 6.13, with coordinates u' , v' defined by

$$u' = u, \quad (6.4)$$

$$v' = 1.5v, \quad (6.5)$$

thus, obtaining

$$u' = \frac{4X}{X + 15Y + 3Z} = \frac{4x}{-2x + 12y + 3}, \quad (6.6)$$

$$v' = \frac{9Y}{X + 15Y + 3Z} = \frac{9y}{-2x + 12y + 3}. \quad (6.7)$$

While this color space is not used alone, it is nearly always an intermediate step in the use of the CIE $L^*u^*v^*$ color space, which will be described next.

6.5 The 1976 CIE $L^*u^*v^*$ Color Space

In 1976, the CIE convention recommended the $L^*u^*v^*$ color space, abbreviated as CIELUV, for use in television and video display industries. This space is a modification of the u' , v' , defined by

$$L^* = 116f\left(\frac{Y}{Y_n}\right) - 16, \quad (6.8)$$

$$u^* = 13L^*(u' - u_n), \quad (6.9)$$

$$v^* = 13L^*(v' - v_n). \quad (6.10)$$

As pointed out before, the perceived lightness L is not linear with the luminance Y . Here, it is defined by the nonlinear cubic root function

$$\begin{aligned} f(s) &= 7.787s + \frac{16}{116} \quad \text{for } s \leq 0.008856, \\ &= s^{1/3} \quad \text{for } s > 0.008856. \end{aligned} \quad (6.11)$$

Equation (6.11) improves the original square-root function. There is no discontinuity either in the value of the function or the slope at the point where both definitions join, as shown in Fig. 6.14. The values of u_n and v_n are the coordinates for a nominal white color, which can be calculated using the tristimulus values X_n , Y_n , and Z_n corresponding to the perfect diffuser when illuminated with a standard illuminant such as D₆₅. Therefore, the standard illuminant location in the u^* , v^* diagram is always the origin.

We see that the expressions for the coordinates u^* and v^* are multiplied by the value of the luminance L^* . So, in a u^* , v^* diagram, a color with a certain hue and chroma is not uniquely represented with the same values of u^* , v^* for all possible values of the luminance. The only exceptions are the neutral colors (white, gray, and black), which are at $u^* = v^* = 0$, since those coordinate values depend on the value of L^* . However, the property that a straight line in the x , y diagram transforms into a straight line in the u^* , v^* diagram is valid if L^* is constant. A sketch of the CIE $L^*u^*v^*$ color solid is given in Fig. 6.15. The locus of all monochromatic colors for all possible luminance values is a cone with a vertex at the origin, since

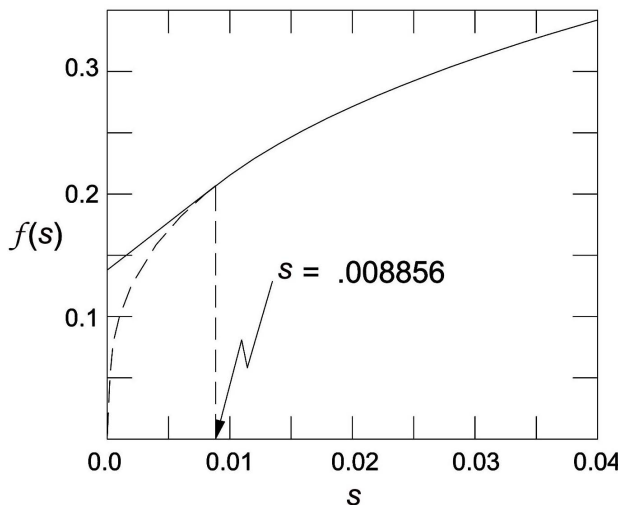


Figure 6.14 Function $f(s)$ for CIE $L^*u^*v^*$ and CIE $L^*a^*b^*$ color space.

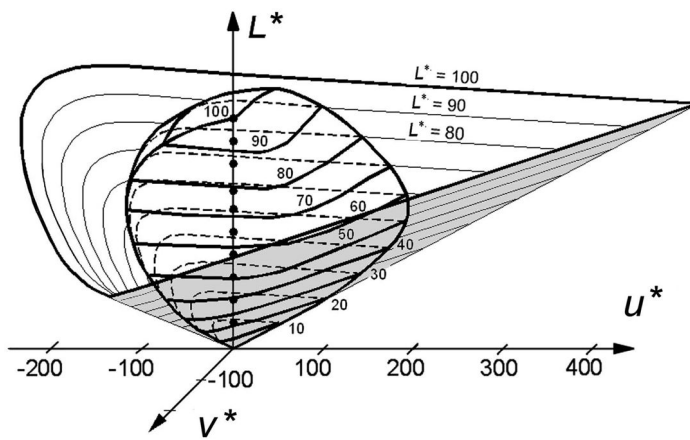


Figure 6.15 The $L^*u^*v^*$ color solid (CIE, 1976).

the coordinates u^* , v^* are multiplied by the luminance. The reason for this conic shape is that as the luminance decreases, the color differences are more difficult to perceive—that is, the MacAdam ellipses grow in size, and thus all colors converge to the black point when the luminance becomes zero.

If the transformation equations are applied to the CIE horseshoe-shaped locus of the monochromatic colors for many values of the luminance, a conical surface with a vertex at the zero-luminance black color is obtained. However, as described in Section 5.6, as the luminance increases, the maximum possible purity for a given dominant wavelength decreases, reaching the MacAdam limit. These limits shrink the gamut of possible colors for a given luminance, becoming a point for the maximum possible value of the luminance, representing the white color. Then,

as expected, for the minimum and maximum values of the luminosity—zero and 100, respectively—only the neutral colors (black and white) are possible.

The CIELUV color-difference equation is

$$\Delta E_{uv}^* = \left[(\Delta L^*)^2 + (\Delta u^*)^2 + (\Delta v^*)^2 \right]^{1/2}, \quad (6.12)$$

where

$$\begin{aligned}\Delta L^* &= L^* - L_{ref}^*, \\ \Delta u^* &= u^* - u_{ref}^*, \\ \Delta v^* &= v^* - v_{ref}^*,\end{aligned} \quad (6.13)$$

where the subscript *ref* stands for the reference or target value. A positive value of ΔL^* means that the measured color is lighter than the reference and negative otherwise. A positive value of Δu^* means that the sample is too red or too green if it is negative. A positive value of Δv^* means that the sample is too yellow or too blue if it is negative.

Sometimes, instead of specifying the color by L^* , u^* , and v^* , the quantities L^* , C^* , and h^* are used, where

$$C^* = \left(u^{*2} + v^{*2} \right)^{1/2} \quad (6.14)$$

is the saturation or chroma, and

$$h^* = \arctan \left[\frac{v^*}{u^*} \right] \quad (6.15)$$

is the hue angle with a zero value along the u^* axis.

6.6 The Hunter *L a b* Color Space

For many years, R. S. Hunter tried to design a good uniform color system by using the Munsell colors as a reference. His most successful color space was the *L a b* (Hunter and Harold, 1987). He represented the lightness L , as in the Munsell system, by the square root of the luminance Y along the z axis in a Cartesian system of coordinates. The maximum value of the lightness, equal to 100, is for a perfect white, while the minimum value, equal to zero, is used for black.

Hunter based his system on the fact discovered by Hering (1964) and later confirmed by the CIE diagram that red and green are opposite colors, as are blue and yellow. The a value represents the redness on the positive side and the greenness on the negative side. In the same manner, the b value represents the yellowness on the positive side and the blueness on the negative side.

By subtracting the value of the tristimulus X from the value of Y and also the value of Y from the value of Z , an opponent-color-type system was obtained. The equations used for transforming from the CIE x , y system to the Hunter *L a b*

system are

$$L^* = 100 \left(\frac{Y}{Y_n} \right)^{1/2}, \quad (6.16)$$

$$a = 1.785 X_n \frac{\left[\left(\frac{X}{X_n} \right) - \left(\frac{Y}{Y_n} \right) \right]}{\left(\frac{X}{X_n} \right)^{1/2}}, \quad (6.17)$$

$$b = 0.5929 Z_n \frac{\left[\left(\frac{Y}{Y_n} \right) - \left(\frac{Z}{Z_n} \right) \right]}{\left(\frac{Y}{Y_n} \right)^{1/2}}, \quad (6.18)$$

where the opposite colors are on the opposite sides of a line passing through the perfect white with tristimulus values X_n, Y_n, Z_n . This reference white can be for the 2-deg or the 10-deg observer and for any desired standard illuminant as well. The constants in front of the expression for a and b have been chosen so that the color system is as uniform as possible.

It can be easily shown that there is a line in the CIE x, y diagram that transforms into the red axis (a -axis). This line can be found by setting $b = 0$ in Eq. (6.18), obtaining $Y/Y_n = Z/Z_n$; then, this result is used in Eqs. (5.22) through (5.25). We then find a line that passes through the reference white point, as described by the expression

$$x = 1 - \left(\frac{1 - x_n}{y_n} \right) y. \quad (6.19)$$

In a similar manner, we set $a = 0$ in Eq. (6.17), obtaining $X/X_n = Y/Y_n$, and then use Eqs. (5.22) through (5.24). The result is a line on the CIE x, y diagram corresponding to the b axis that passes through both the origin and the point for the reference white illuminant, as given by

$$x = \left(\frac{x_n}{y_n} \right) y. \quad (6.20)$$

As described above, the positive part of the a axis represents the amount of red-purple color, and the negative part of the a axis represents the amount of green-cyan color. The positive part of the b axis represents the amount of yellow, and the negative part of the b axis represents the amount of blue. These lines are illustrated in a CIE x, y diagram in Fig. 6.16.

A similar color space with opponent colors was designed by Adams and later modified by Nickerson (1977). During the 1973 CIE meeting, David MacAdam proposed to modify the existing opponent color systems to improve some of their deficiencies. Then, the CIE $L^*a^*b^*$ color system, described in the next section, was proposed. However, it was difficult to decide between the $L^*a^*b^*$ system and the previously described $L^*u^*v^*$ system. Thus, after an extensive study both systems were accepted in 1976.

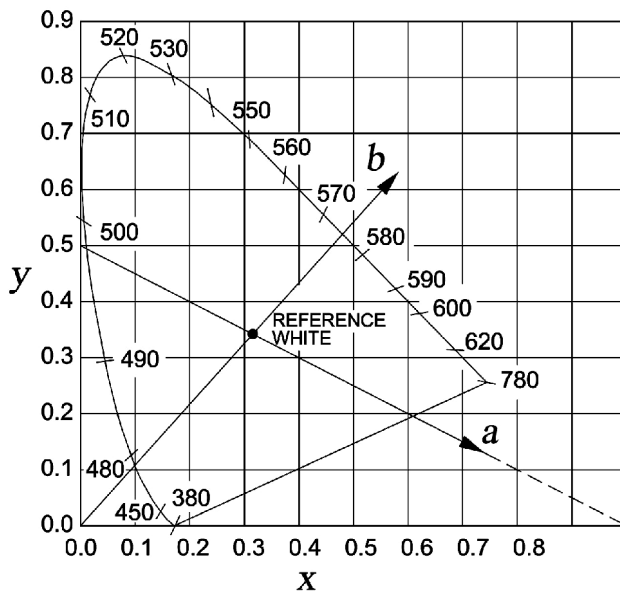


Figure 6.16 The a and b axes shown in the CIE 1964 chromaticity diagram (CIE, 1976).

6.7 The 1976 CIE $L^*a^*b^*$ Color Space

In 1976, the CIE convention recommended the CIE $L^*a^*b^*$, or CIELAB, color space, mainly for use in the plastic, textile, and paint industries. As in the Hunter space, the luminance is represented along the z axis in a Cartesian system of coordinates, with values from zero for black to 100 for a perfectly white body [constant reflectance $R(\lambda) = 1$]. The positive a^* axis represents the amount of purplish red, while the negative a^* axis represents the amount of green. The positive b^* axis represents the amount of yellow and the negative b^* axis represents the amount of blue. The maximum possible magnitude of the values on these axes is a function of the luminance, between ± 100 and ± 200 for a^* and b^* , respectively.

The transformation equations used for passing from the CIE x, y, z system to the CIE $L^*a^*b^*$ system are

$$\begin{aligned} L^* &= 116 \left(\frac{Y}{Y_n} \right)^{1/3} - 16 \quad \text{for } \frac{Y}{Y_n} > 0.008856, \\ &= 903.3 \left(\frac{Y}{Y_n} \right) \quad \text{for } \frac{Y}{Y_n} \leq 0.008856, \end{aligned} \quad (6.21)$$

$$a^* = 500 \left[f \left(\frac{X}{X_n} \right) - f \left(\frac{Y}{Y_n} \right) \right], \quad (6.22)$$

$$b^* = 200 \left[f \left(\frac{Y}{Y_n} \right) - f \left(\frac{Z}{Z_n} \right) \right], \quad (6.23)$$

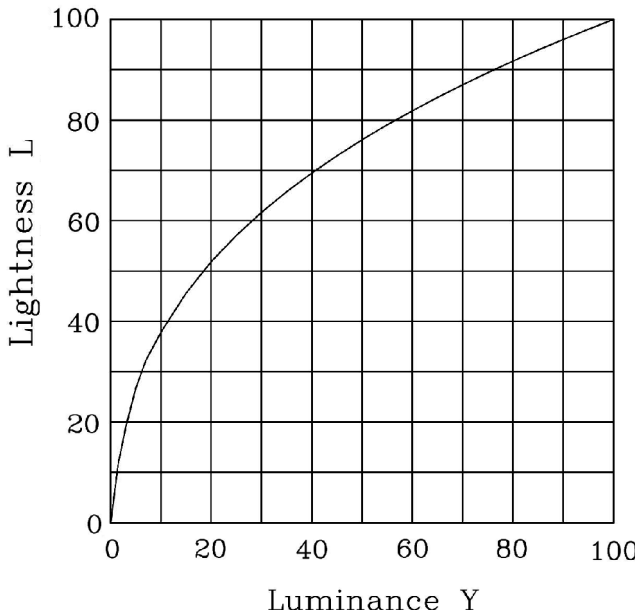


Figure 6.17 Plot of the lightness in the CIELAB system versus the luminance.

where as in the Lab and the $L^*u^*v^*$ systems, the lightness L^* is not linear with the luminance Y as shown in Fig. 6.17. As was shown in the previous section, the function $f(s)$ is defined by

$$\begin{aligned} f(s) &= 7.787s + \frac{16}{116} \quad \text{for } s \leq 0.008856, \\ &= s^{1/3} \quad \text{for } s > 0.008856. \end{aligned} \quad (6.11)$$

Also, as before, the tristimulus values X_n , Y_n , and Z_n correspond to the perfect diffuser when illuminated with the selected standard illuminant and observer (see Section 5.6). As in the preceding systems, the standard illuminant location in the a^*b^* diagram is the origin.

At the point $a^* = b^* = 0$, which is the L^* axis, the neutral color has a well-defined location, but any other color does not have a unique location, as a^*b^* is independent of the value of L^* . The lines in the x , y diagram that transform into the a^* and b^* axes are the same as for the Hunter system, as illustrated in Fig. 6.16.

When the transformation equations are applied to the CIE locus of the monochromatic colors for many values of the luminance, the curves in Fig. 6.18 are obtained. We can observe that the purple line is transformed into a curve in the a^*b^* plane. When these curves are plotted in a 3D space with the lightness in the third axis, a conical surface with its vertex at the black point is obtained. However, as described in Section 5.6, when the luminance increases, the allowed gamut of color for any given luminance decreases for high values of the luminance, producing the MacAdam limits. This gamut of possible colors for a given luminance becomes

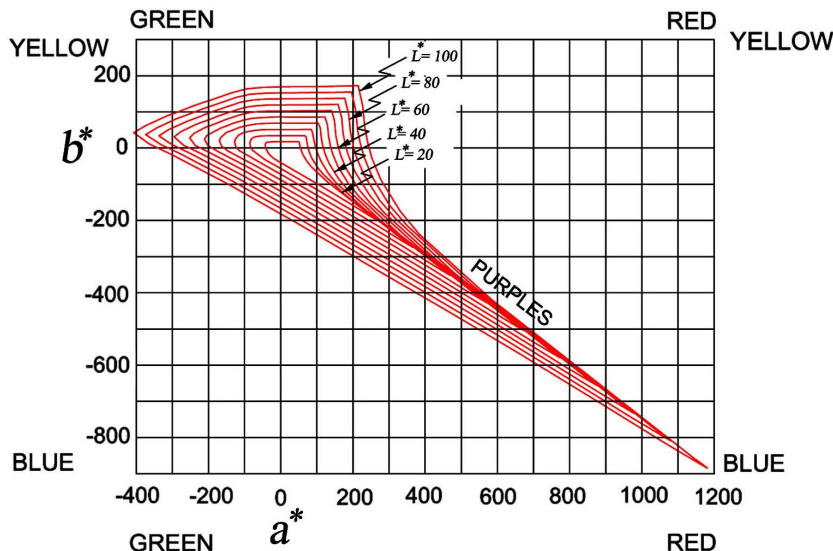


Figure 6.18 Locus of spectrally pure and purple colors for different values of lightness in the a^*b^* plane.

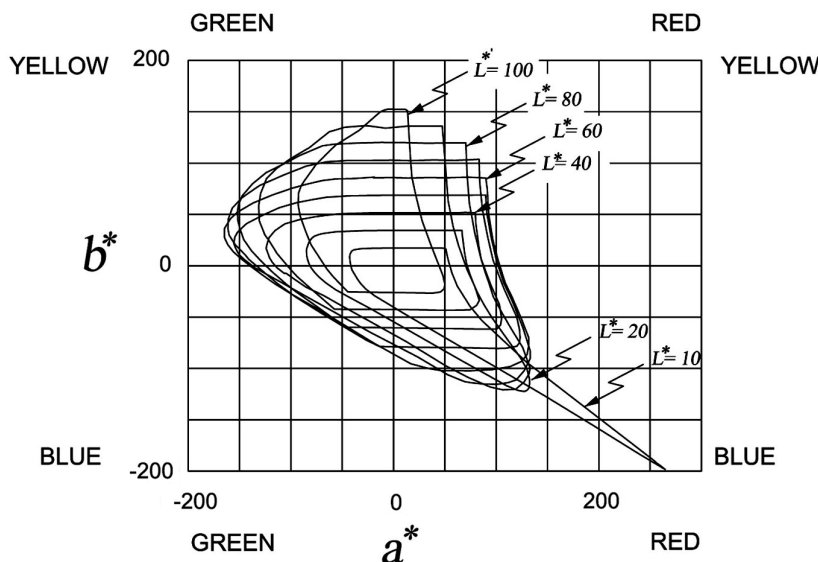


Figure 6.19 Gamut of all possible colors for different value of the luminance in the a^*b^* plane.

a point for the maximum value of the luminance, representing white. Thus, the minimum and maximum values of the lightness, which are 0 and 100, respectively, are possible only for neutral colors (black and white).

The size and shape of the regions representing the gamut of colors for different values of the luminance have an irregular shape and are plotted in Fig. 6.19. The

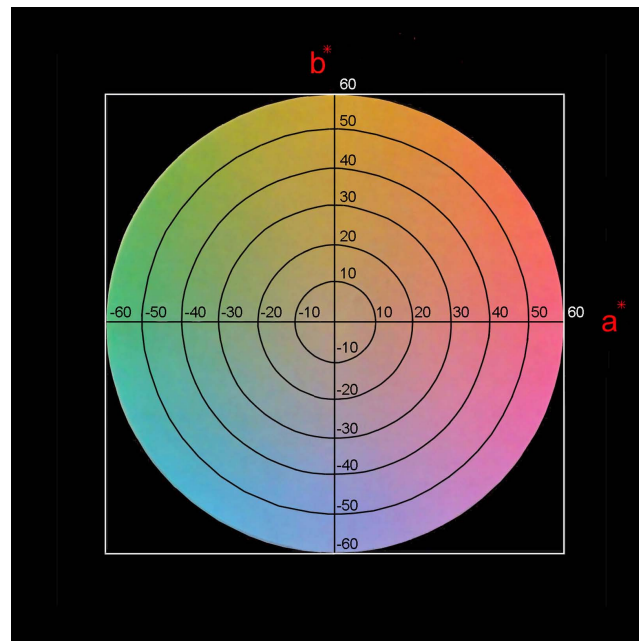


Figure 6.20 Color diagram representing in crude approximation the distribution of colors in the a^*b^* plane. In this plane all colors have the same luminance.

maximum area of this region is close to a luminance equal to about 50. As in the CIE diagram, this zone of real colors is not a circle (see Figs. 5.16 and 5.17), but has an irregular shape. In a rough approximation, the circular representation of the colors in this system is seen in Fig. 6.20.

We have seen that in this color system a line in the x, y diagram does not transform into a straight line but into a curved line. Hence, the usual graphic rules for the addition of colors are not preserved. A sketch of the CIE $L^*a^*b^*$ color solid can be found in Fig. 6.21. The locus of all monochromatic colors for all possible luminance values has an approximately conic shape with the smallest cross section at the origin. We can observe that for constant values of the luminance the locus of the purple colors is not a straight line as in the CIE $L^*u^*v^*$ system. In the CIE $L^*u^*v^*$ color system, the coordinates a^*b^* are linearly dependent on the luminance, producing a conically shaped color solid in the vicinity of the black point, that is, near zero luminance. For the reasons described in Section 6.4, for large values of luminance, all possible colors are in a small area around the gray point, as defined by the MacAdam limits, and finally become a single point for the white color. Thus, as in the CIE $L^*u^*v^*$ color solid, the CIE $L^*a^*b^*$ color solid also shrinks to a small spot for large and small values of luminance.

Instead of specifying the color by $L^*, a^*,$ and b^* , the quantities L^*, C_{ab}^* , and h_{ab}^* in polar coordinates can be used in the so-called CIELCH system, where

$$C_{ab}^* = \left(a^{*2} + b^{*2} \right)^{1/2} \quad (6.24)$$

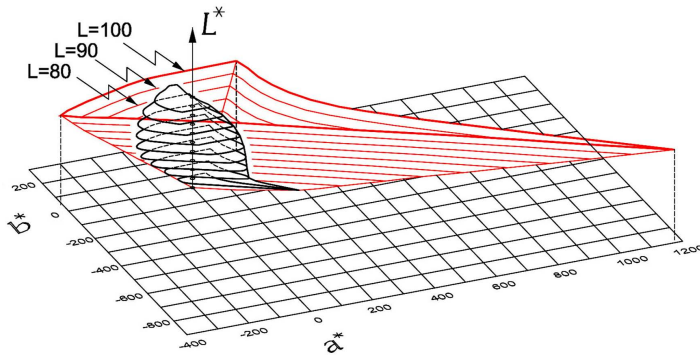


Figure 6.21 The $L^*a^*b^*$ color solid (CIE, 1976). For the sake of clarity, the L^* scale has been amplified by a factor of 10 with respect to the a^* and b^* axes.

is the saturation or chroma, and

$$h_{ab}^* = \arctan\left(\frac{b^*}{a^*}\right) \quad (6.25)$$

is the hue angle with a zero value along the a^* axis.

An evaluation of the uniformity of this system is shown in Fig. 6.22, where the locations of some perceptually equally spaced Munsell colors are represented in the CIELAB color a^*b^* plane. As pointed out before, in a perfectly uniform color system, this diagram would be a circle. As a consequence, the tolerance volume is not a sphere but an ellipsoid with different dimensions for hue, chroma, and luminance. Another consequence of the lack of uniformity in this system is that the tolerance ellipsoids do not have a constant size, as will be described in the next section. Due to the orientation of the ellipsoids, in this system an average observer is most sensitive to hue differences, less sensitive to chroma differences, and least sensitive to luminance differences.

6.8 Color-Difference Equation in the CIE $L^*a^*b^*$ Color Space

The CIELAB color-difference equation is the distance in the CIELAB diagram between the reference color and the measured color, given by

$$\Delta E_{ab}^* = \left[(\Delta L^*)^2 + (\Delta a^*)^2 + (\Delta b^*)^2 \right]^{1/2}, \quad (6.26)$$

where

$$\begin{aligned} \Delta L^* &= L^* - L_{ref}^*, \\ \Delta a^* &= a^* - a_{ref}^*, \\ \Delta b^* &= b^* - b_{ref}^*, \end{aligned} \quad (6.27)$$

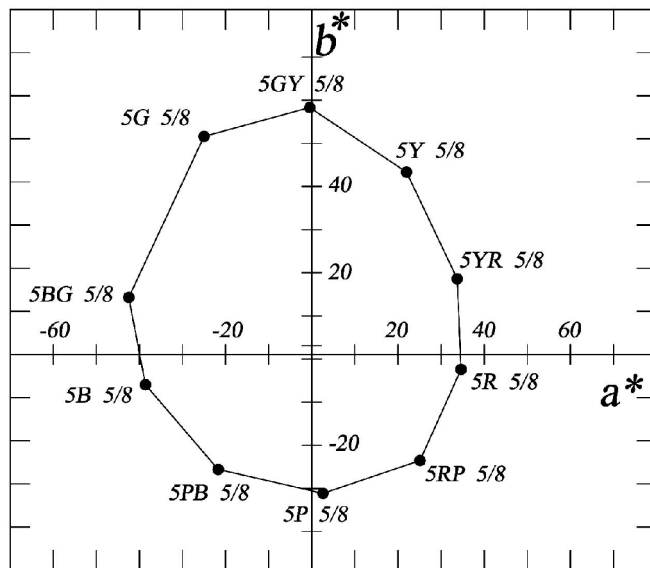


Figure 6.22 Relative location of some Munsell perceptually equally spaced colors in the CIELAB a^*b^* diagram.

where the subscript *ref* stands for reference or target value. A positive value of ΔL^* means that the measured color is lighter than the reference, and a negative value means it is darker than the reference. A positive value of Δa^* means that the sample is too red, and the sample is too green if Δa^* is negative. A positive value of Δb^* means that the sample is too yellow, or it is too blue if Δb^* is negative.

In the CIELCH system the chroma difference may be written as

$$\Delta C_{ab}^* = C_{ab}^* - C_{ab\text{ ref}}^*, \quad (6.28)$$

where a positive value indicates a higher chroma than the reference, and a negative value indicates a lower chroma than the reference. The hue difference is not calculated by the angle difference. It is given by the part that remains after taking lightness and chroma differences into account, as given by

$$\Delta h_{ab}^* = \left[(\Delta E_{ab}^*)^2 - (\Delta L_{ab}^*)^2 - (\Delta C_{ab}^*)^2 \right]^{1/2}, \quad (6.29)$$

which can also be written as

$$\Delta h_{ab}^* = \left[(\Delta a^*)^2 + (\Delta b^*)^2 + (\Delta C_{ab}^*)^2 \right]^{1/2}, \quad (6.30)$$

and is illustrated in Fig. 6.23. This quantity is positive if the hue angle is greater than that of the reference and negative if the hue angle is otherwise.

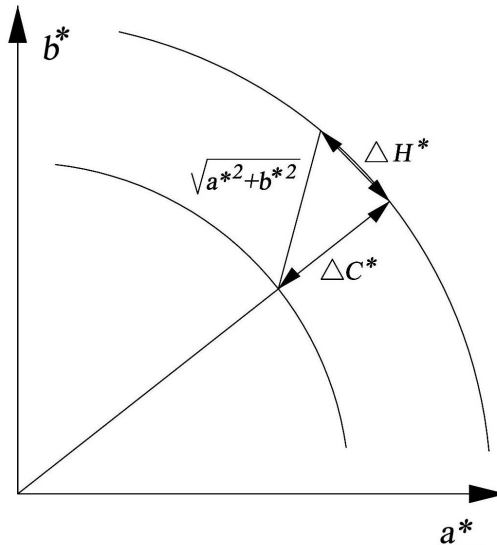


Figure 6.23 Distance between the measured point and the reference point in the $L^*a^*b^*$ diagram.

The distance in this diagram is not the only factor to be taken into account, since the tolerance is not the same for all colors or in all directions, as previously stated. The dimensions of the tolerance ellipsoids should be taken into account when deciding which color distance between the reference and the sample colors is acceptable.

In 1984, the Colour Measurement Committee (CMC) of the Society of Dyers and Colourists in Great Britain suggested the following color-difference formula, known as the CMC($l: c$) equation (Robertson, 1990):

$$\Delta E_{ab}^* = \left[\left(\frac{\Delta L^*}{LS_L} \right)^2 + \left(\frac{\Delta C_{ab}^*}{cS_C} \right)^2 + \left(\frac{\Delta h_{ab}^*}{S_H} \right)^2 \right]^{1/2}, \quad (6.31)$$

where ΔL^* is the lightness difference, ΔC_{ab}^* is the chroma difference, and Δh_{ab}^* is the hue difference. The semiaxes of the tolerance ellipsoids represented by this equation have the dimensions LS_L , cS_C , and S_H , where S_L is a function of the luminance L , given by

$$S_L = \begin{cases} \frac{0.04097L^*}{1 + 0.01765L^*} & \text{if } L^* \geq 16, \\ 0.511 & \text{if } L^* < 16; \end{cases} \quad (6.32)$$

the quantity S_C is a function of the chroma C , given by

$$S_C = \frac{0.0638C_{ab}^*}{1 + 0.0131C_{ab}^*} + 0.638; \quad (6.33)$$

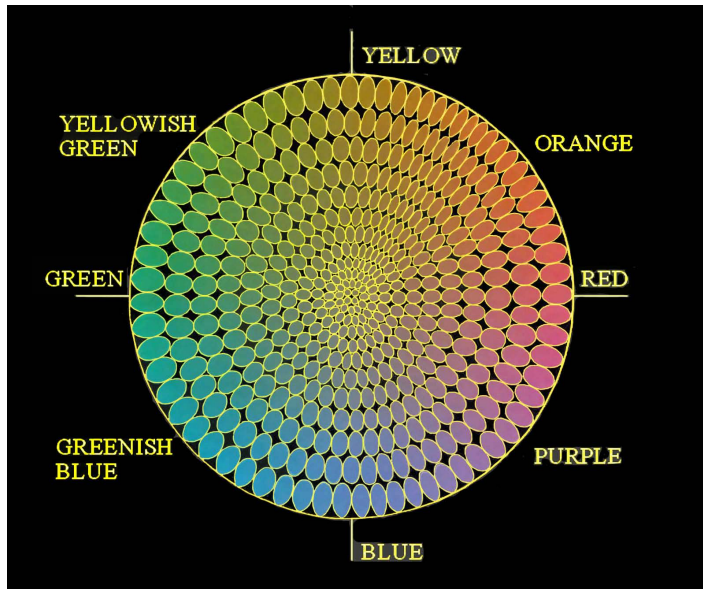


Figure 6.24 MacAdam ellipses plotted in the a^*b^* plane for $L^* = 50$.

S_H is a function of the chroma C_{ab}^* and of the hue h_{ab}^* , given by

$$S_H = S_C (TF + 1 - F), \quad (6.34)$$

where

$$F = \sqrt{\frac{(C_{ab}^*)^4}{(C_{ab}^*)^4 + 1900}}, \quad (6.35)$$

and

$$T = 0.56 + 0.2 |\cos(h_{ab} + 168 \text{ deg})| \quad \text{if } 164 \text{ deg} > h_{ab} > 345 \text{ deg}, \quad (6.36)$$

$$T = 0.38 + 0.4 |\cos(h_{ab} + 35 \text{ deg})| \quad \text{otherwise.}$$

The constants l and c in Eq. (6.31) are correction constants that can be chosen according to the kind of sample to be measured. The two parameters, the lightness l and the chroma c , allow the weight of the difference to be based on the ratio $l:c$, which is more appropriate for the desired application. Values of 2:1 are commonly used for acceptability and 1:1 for imperceptibility.

In this color-difference equation, the tolerance ellipsoids are assumed to be radially oriented, as shown with the MacAdam ellipses in Fig. 6.24, which is only an approximate truth. These ellipsoids are oriented with their largest dimension along the radial (chroma) direction. We can see that they are longer and narrower

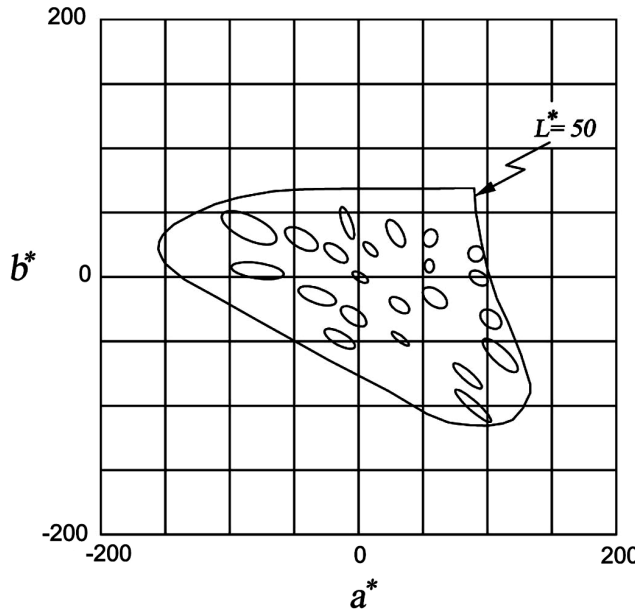


Figure 6.25 Tolerance ellipsoids in the $L^*a^*b^*$ system.

in the orange region than in the green and blue regions. Their size decreases with the chroma and changes with the luminance. The actual shapes of the MacAdam ellipsoids in the CIE $L^*a^*b^*$ diagram are illustrated in Fig. 6.25 for $l = c = 1$.

Another color-difference equation was proposed by the CIE in 1994, based on the CMC(l, c) equation, as follows:

$$\Delta E_{94}^* = \left[\left(\frac{\Delta L^*}{k_L S_L} \right)^2 + \left(\frac{\Delta C_{ab}^*}{k_C S_C} \right)^2 + \left(\frac{\Delta h_{ab}^*}{k_H S_H} \right)^2 \right]^{1/2}, \quad (6.37)$$

where ΔL^* , ΔC^* , and Δh^* are the lightness, chroma, and hue differences. S_L , S_C , and S_H are the weighting functions, whose best estimated values are

$$\begin{aligned} S_L &= 1, \\ S_C &= 1 + 0.045C_{ab\ ref}^*, \\ S_H &= 1 + 0.015C_{ab\ ref}^*, \end{aligned} \quad (6.38)$$

where $C_{ab\ ref}^*$ is the chroma of the reference color. The quantities k_L , k_C , and k_H are the parametric factors, for which

$$k_L = k_C = k_H = 1 \quad (6.39)$$

for most applications, although for the textile industry the following values are preferred:

$$k_L = 2; \quad k_C = k_H = 1. \quad (6.40)$$

The luminance axis is assumed to be constant, while the other two axes are functions only of the chroma value, and the hue value is not used. The human eye can perceive CIELAB color differences on the order of ± 1 .

6.9 MacLeod and Boynton Chromaticity Diagram

We have seen that a combination of three beams of light with different colors can match any color reference field if the proper amount of each color (including negative values, if necessary), given by the color-matching functions, is added. These color-matching functions can be expressed in one of several color systems, for example $\bar{x}(\lambda)$, $\bar{y}(\lambda)$, and $\bar{z}(\lambda)$. In the 3D color space, any given color is represented by points along a straight line passing through the origin of coordinates and the point defined by the three values of the color-matching functions. Different points on this line represent the same color (hue and saturation) but different luminances, according to each point's distance from the origin of the coordinates. However, if two different colors are represented by points on two different lines in the color space, and they have the same distance to the origin, they do not necessarily have the same luminance.

A chromaticity diagram is a plane where different colors (different hue and saturation) are represented, but the luminance is, in general, different for different points on the diagram. The chromaticity diagram is generated by the intersection of the lines passing through the origin, defining all colors with any desired plane in the color space. As previously described, the CIE chromaticity diagram was defined by passing a plane through the points $(1, 0, 0)$, $(0, 1, 0)$, and $(0, 0, 1)$ in the color space defined by the matching functions $\bar{x}(\lambda)$, $\bar{y}(\lambda)$, and $\bar{z}(\lambda)$. The matching functions are chosen so that the luminance is the same for all colors having the same value of the chromaticity coordinate $y(\lambda)$ in the chromaticity diagram.

It was previously stated that the S-cones play an important role in color definition, but that their influence is negligible in sensing the luminance. Therefore, the luminance is completely determined by the L- and M-cones. Using this fact, MacLeod and Boynton (1979) proposed a color space where the color-matching functions are the cone sensitivities $\bar{l}(\lambda)$, $\bar{m}(\lambda)$, and $\bar{s}(\lambda)$. Then, the plane for the chromaticity diagram was taken as the plane that intersects the L-cone axis at the point $(1, 0, 0)$ and the M-cone axis at the point $(0, 1, 0)$, but the S-cone axis never intersects it, as illustrated in Fig. 6.26. The color sensitivities are scaled by multiplying them by a constant, so that the maximum values of $\bar{l}(\lambda)$ and $\bar{m}(\lambda)$ in the chromaticity diagram are equal to 1, as illustrated in Fig. 6.27. In this chromaticity diagram, the luminance will not change along the S-cone axis, since it does not play any role in the luminance.

6.10 Derrington, Krauskopf, and Lennie (DKL) Color Space

Derrington et al. (1984) introduced an opponent modulation color space also based on cones sensitivities, like the just-described color space defined by MacLeod and Boynton (1979). The three color-matching functions (or color-space coordinates)

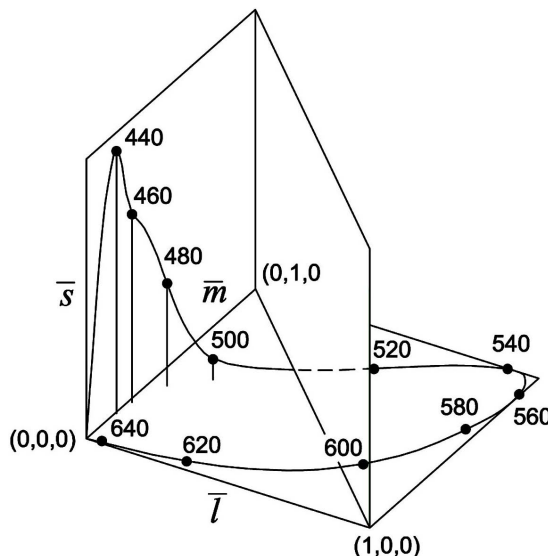


Figure 6.26 MacLeod and Boynton color space.

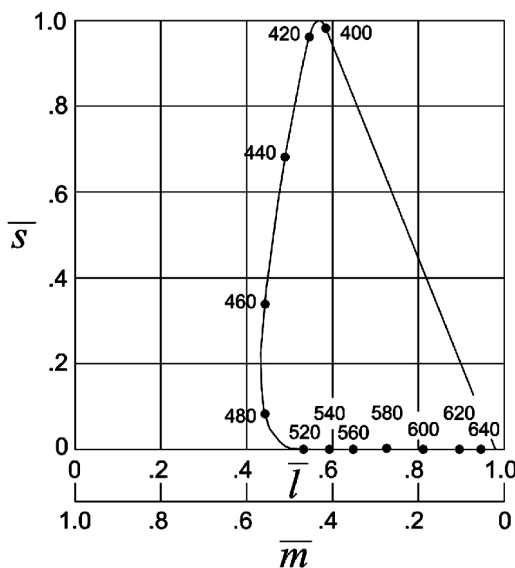


Figure 6.27 MacLeod and Boynton chromaticity diagram.

are defined in close analogy to the color-discrimination mechanism in the human eye, as described in Section 5.7. The color coordinates in this DKL space are $(L-M)$, $[S-(L+M)]$, and $(L+M)$, as illustrated in Fig. 6.28. Along the vertical axis $(L+M)$, called the luminance axis, only the luminance changes, without any change in the chromaticity. On the other hand, all colors represented in the horizontal plane, called the isoluminant plane, have the same luminance. The chromaticity

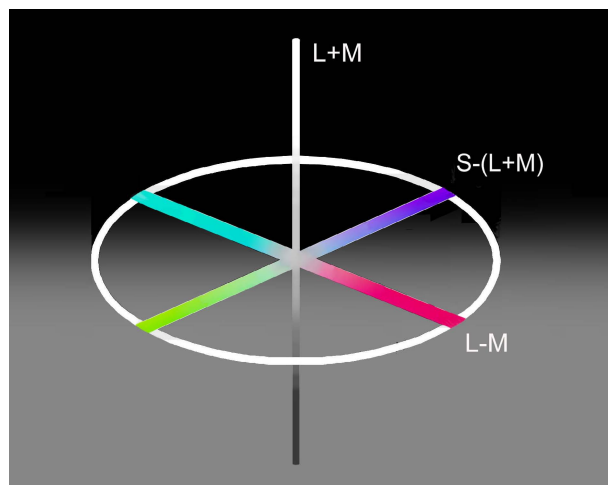


Figure 6.28 Derrington, Krauskopf, and Lennie (DKL) color space.

changes along the $(L-M)$ axis without changing the excitation of the S -cones. Along the $S-(M+L)$ axis the chromaticity changes, but without changing the excitation of the M - or L -cones. The three axes intersect at a neutral gray color.

6.11 Other Color Spaces

While the color spaces described above are those most frequently used, they are not the only ones used. There are many other color spaces that have been used, mainly for specialized purposes, such as color spaces specifically designed for color printers, color displays, photographic cameras, etc. A good description of these color spaces can be found in the books by Kang (1997) and by Dubois (2010). A detailed historical description of many color spaces from antiquity to the present is also described in the book by Kuehni (2003). In conclusion, the search for perfectly uniform color systems is of great practical interest and is still a subject of research.

References

- Brown, W. R. J., “Color discrimination of twelve observers,” *J. Opt. Soc. Am.* **47**, 137–143 (1957).
- Brown, W. R. J. and MacAdam, D. L., “Visual sensitivities to combined chromaticity and luminance differences,” *J. Opt. Soc. Am.* **49**, 808–834 (1949).
- CIE, “Brussels session of the International Commission on Illumination,” *J. Opt. Soc. Am.* **50**, 89–90 (1960).
- Derrington, A. M., Krauskopf, J., and Lennie, P., “Chromatic mechanism in lateral geniculate nucleus of macaque,” *J. Physiol.* **357**, 241–265 (1984).

- Dubois, E., *The Structure and Properties of Color Spaces and the Representation of Color Images*, Morgan and Claypool Publishers, San Rafael, CA (2010).
- Hering, E., Hurvich, L. M. and Jameson, D., Eds., *Outlines of a Theory of the Light Sense*, Harvard University Press, Cambridge, MA (1964) (translation).
- Hunter, R. S. and Harold, R. W., *The Measurement of Appearance*, 2nd ed., John Wiley & Sons, New York (1987).
- Judd, D. B., “The unsolved problem of colour perception,” *Palette* **10**, 30–35 (1962); reprinted in *Selected Papers in Colorimetry—Fundamentals*, MacAdam, D. L., Ed., SPIE Press, Bellingham, WA (1993).
- Judd, D. B., “Perceptually uniform spacing of equiluminous colors and the loci of constant hue,” in *Proc., Symposium on Color Metrics*, 147–159 (1972); reprinted in *Selected Papers in Colorimetry—Fundamentals*, MacAdam, D. L., Ed., SPIE Press, Bellingham, WA (1993).
- Kang, H. R., *Color Technology for Electronic Imaging Devices*, SPIE Press, Bellingham, WA (1997).
- Kelly, K. L., “Color designations for lights,” *J. Opt. Soc. Am.* **33**, 627–632 (1943).
- Kuehni, R. G., *Color Space and Its Divisions: Color Order from Antiquity to Present*, Wiley Interscience, New York (2003).
- MacAdam, D. L., “Projective transformations of I.C.I. color specifications,” *J. Opt. Soc. Am.* **27**, 294–299 (1937).
- MacAdam, D. L., “Visual sensitivities to color differences in daylight,” *J. Opt. Soc. Am.* **32**, 247–274 (1942).
- MacAdam, D. L., “The graphical representation of small color differences,” *J. Opt. Soc. Am.* **33**, 632–636 (1943).
- MacAdam, D. L., “Geodesic chromaticity diagram based on variances of color matching by 14 normal observers,” *Appl. Opt.* **10**, 1–7 (1971).
- MacAdam, D. L., “Uniform color scales,” *J. Opt. Soc. Am.* **64**, 1691–1702 (1974).
- MacLeod, D. I. A. and Boynton, R. M., “Chromaticity diagram showing cone excitation by stimuli of equal luminance,” *J. Opt. Soc. Am.* **69**, 1183–1186 (1979).
- Munsell, A. H., *A Color Notation*, G. H. Ellis Co., Boston (1905).
- Munsell, A. H., “A pigment color system and notation,” *Am. J. Psychol.* **23**, 236–244 (1912).
- Muth, E. J. and Persels, C. G., “Constant-brightness surfaces generated by several color-difference formulas,” *J. Opt. Soc. Am.* **61**, 1152–1154 (1971).
- Newhall, S. M., “Final report of the O.S.A. Subcommittee on the spacing of the Munsell colors,” *J. Opt. Soc. Am.* **33**, 385–418 (1943).
- Nickerson, D., “History of the OSA committee on uniform color scales,” *Optics News* **3**, 8–17 (1977).

- Parkkinen, J. P. S., Hallikainen, J., and Jaaskelainen, T., “Characteristic spectra of Munsell colors,” *J. Opt. Soc. Am. A* **6**, 318–322 (1989).
- Rheinboldt, W. C. and Menard, J. P., “Mechanized conversion of colorimetric data to Munsell rennotations,” *J. Opt. Soc. Am* **50**, 802–807 (1960).
- Richardson, L. F., “Measurability of sensations of hue, brightness, or saturation,” in *Discussion on vision*, IOP, London (1960); reprinted in *Selected Papers in Colorimetry—Fundamentals*, MacAdam, D. L., Ed., SPIE Press, Bellingham, WA (1993); reprinted in *Sources of Color Science*, MIT Press, Cambridge, MA (1970) pp. 241–243.
- Robertson, A. R., “Historical development of CIE recommended color difference equations,” *Color Research & Application* **15**, 167–170 (1990).
- Schrödinger, E., “Grundlinien einer Theorie der Farbenmetrik im Tagessehen,” *Ann. Phys.* **62**, 603–622 (1920).
- Silverstein, L., “Investigations of the intrinsic properties of the color domain. II,” *J. Opt. Soc. Am.* **33**, 1–9 (1943).
- X-Rite, *Munsell Book of Color*, X-Rite, Inc., Grand Rapids, MI (2007).

Chapter 7

Color Mixtures and Colorants

7.1 Color Addition

Additive mixing of color takes place when two or more light beams with different colors are superimposed on a screen or directly on the retina of the observing eye. One example is theater stage illumination where several colored light projectors illuminate the same region. Another example is the well-known rotating top with a disc of colors. If all colors of the spectrum are in the disc, a neutral gray color is observed when the top is rotating. A third example is in color television screens, or in computer screens. Extremely small red, green, and blue dots are produced on the screen. The relative intensities of these colors produce a wide range colors for the eye.

The CIE chromaticity diagram is a useful tool for predicting the color produced by different color additive mixtures. Consider two light fields with spectral powers $P_1(\lambda)$ and $P_2(\lambda)$. If the tristimulus values are (X_1, Y_1, Z_1) and (X_2, Y_2, Z_2) , the total tristimulus values are

$$\begin{aligned} X_T &= X_1 + X_2 \\ &= \sum_{i=1}^N P_1(\lambda_i) \bar{x}(\lambda_i) + \sum_{i=1}^N P_2(\lambda_i) \bar{x}(\lambda_i), \end{aligned} \quad (7.1)$$

$$\begin{aligned} Y_T &= Y_1 + Y_2 \\ &= \sum_{i=1}^N P_1(\lambda_i) \bar{y}(\lambda_i) + \sum_{i=1}^N P_2(\lambda_i) \bar{y}(\lambda_i), \end{aligned} \quad (7.2)$$

$$\begin{aligned} Z_T &= Z_1 + Z_2 \\ &= \sum_{i=1}^N P_1(\lambda_i) \bar{z}(\lambda_i) + \sum_{i=1}^N P_2(\lambda_i) \bar{z}(\lambda_i). \end{aligned} \quad (7.3)$$

The chromaticity coordinates for the addition of the two fields are (x_T, y_T, z_T) , given by

$$x_T = \frac{X_1 + X_2}{X_1 + Y_1 + Z_1 + X_2 + Y_2 + Z_2}$$

$$= \frac{\sum_{i=1}^N [P_1(\lambda_i) + P_2(\lambda_i)] \bar{x}(\lambda_i)}{\sum_{i=1}^N [P_1(\lambda_i) + P_2(\lambda_i)] [\bar{x}(\lambda_i) + \bar{y}(\lambda_i) + \bar{z}(\lambda_i)]}, \quad (7.4)$$

$$\begin{aligned} y_T &= \frac{Y_1 + Y_2}{X_1 + Y_1 + Z_1 + X_2 + Y_2 + Z_2} \\ &= \frac{\sum_{i=1}^N [P_1(\lambda_i) + P_2(\lambda_i)] \bar{y}(\lambda_i)}{\sum_{i=1}^N [P_1(\lambda_i) + P_2(\lambda_i)] [\bar{x}(\lambda_i) + \bar{y}(\lambda_i) + \bar{z}(\lambda_i)]}, \end{aligned} \quad (7.5)$$

$$\begin{aligned} z_T &= \frac{Z_1 + Z_2}{X_1 + Y_1 + Z_1 + X_2 + Y_2 + Z_2} \\ &= \frac{\sum_{i=1}^N [P_1(\lambda_i) + P_2(\lambda_i)] \bar{z}(\lambda_i)}{\sum_{i=1}^N [P_1(\lambda_i) + P_2(\lambda_i)] [\bar{x}(\lambda_i) + \bar{y}(\lambda_i) + \bar{z}(\lambda_i)]}. \end{aligned} \quad (7.6)$$

Now, if we define the weight w_j of a colored light beam j , plotted in Fig. 7.1 as

$$\begin{aligned} w_j &= \sum_{i=1}^N [\bar{x}(\lambda_i) + \bar{y}(\lambda_i) + \bar{z}(\lambda_i)] P_j(\lambda_i) \\ &= X_j + Y_j + Z_j, \end{aligned} \quad (7.7)$$

we can show that

$$x_j = \frac{\sum_{i=1}^N P_j(\lambda_i) \bar{x}(\lambda_i)}{w_j}, \quad (7.8)$$

$$y_j = \frac{\sum_{i=1}^N P_j(\lambda_i) \bar{y}(\lambda_i)}{w_j}, \quad (7.9)$$

$$z_j = \frac{\sum_{i=1}^N P_j(\lambda_i) \bar{z}(\lambda_i)}{w_j}. \quad (7.10)$$

Thus, with these definitions, the chromaticity coordinates for the combination of two colored light beams become

$$x_T = \frac{w_1 x_1 + w_2 x_2}{w_1 + w_2}, \quad (7.11)$$

$$y_T = \frac{w_1 y_1 + w_2 y_2}{w_1 + w_2}, \quad (7.12)$$

$$z_T = 1 - x_T - y_T. \quad (7.13)$$

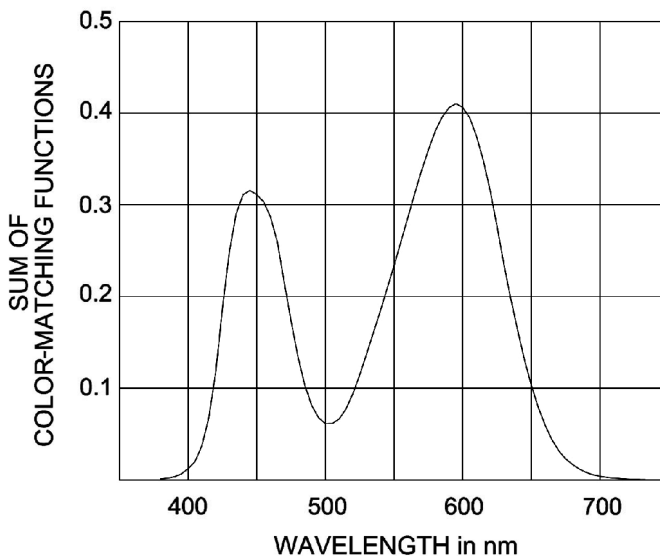


Figure 7.1 Weight w_i for a colored light beam with spectral power $P_j(\lambda)$ (sum of color-matching functions).

Table 7.1 Chromaticity coordinates x, y for some light sources.

Source	x	y
Fluorescent lamp 4800 K	0.35	0.37
Sun 6000 K	0.32	0.33
Red phosphor (europium yttrium vanadate)	0.68	0.32
Green phosphor (zinc cadmium sulfide)	0.28	0.60
Blue phosphor (zinc sulfide)	0.15	0.07

This result can be interpreted as a lever in equilibrium, where each of the two colors with weights w_1 and w_2 is on either end of the resultant color at the equilibrium point, as illustrated in Fig. 7.2. The conclusion is that any color in the line joining the two added colors can be reproduced with the proper weight for these components. Generalizing this result, we conclude that with three colors—A, B, and C—in the chromaticity diagram, as shown in Fig. 7.3, any color inside the triangle can be faithfully reproduced. To find this resultant color, a first step is to find the result for the combination of A with B and then combine it with the color C. Figure 7.4 shows how three colors combine by color addition. Unfortunately, these rules do not apply for the CIELAB uniform color system.

7.2 RGB Color System for Cathode Ray Tubes

A common example of color addition is in color television screens and computer monitors (Allebach, 1992; Smith, 1950; Kang, 1997), where three phosphors are used with the chromatic coordinates given in Table 7.1. Thus, all colors inside the triangle can be reproduced, but none of the colors outside of the triangle can be

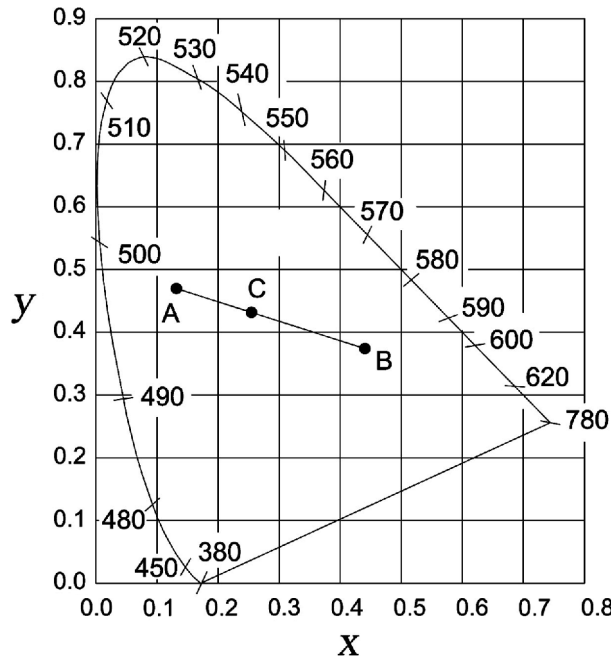


Figure 7.2 Lever in equilibrium, with weights w_1 and w_2 on each end and resultant color at the equilibrium point.

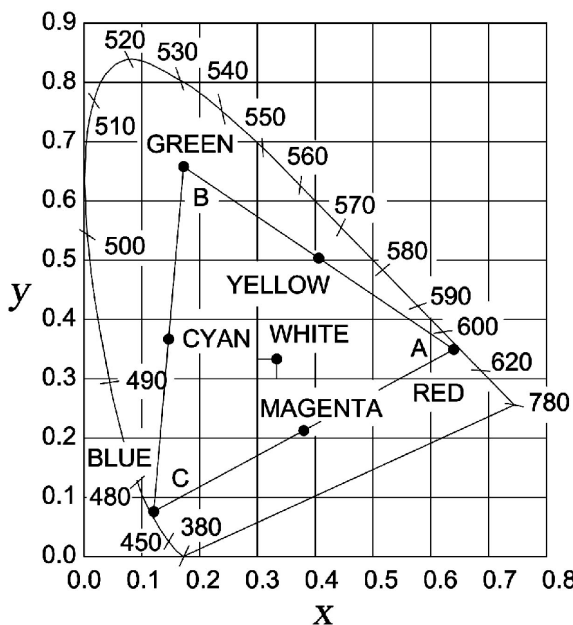


Figure 7.3 The CIE chromaticity diagram with three colors A, B, and C.

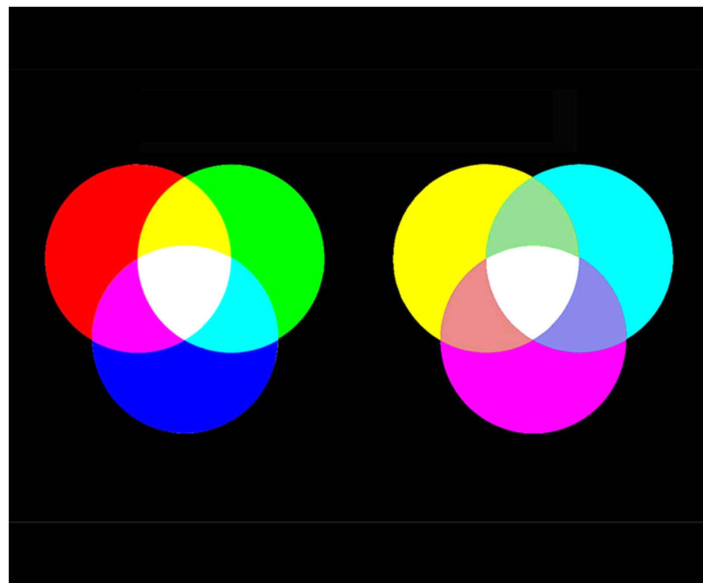


Figure 7.4 Three colors (red, green, and blue) combined by color addition.

reproduced. The larger the triangle is, the greater the gamut of colors produced. Thus, primaries with high purity seem desirable. Unfortunately, an increase in the purity of a light source can only be achieved by reducing the spectral width, thus decreasing the radiance.

A linear transformation can be performed as described in Section 5.1 in order to transform the CIE XYZ system to an RGB system, defined by the phosphor colors. This transformation must take into account the color coordinates for each of the three phosphor colors as well as the white point coordinates for the selected observer and illuminant. To convert from the tristimulus values X, Y, Z to the R, G, B system, and vice versa for a computer display using the color coordinates given in Table 7.2, we can use the linear transformation given by

$$\begin{bmatrix} R \\ G \\ B \end{bmatrix} = \begin{bmatrix} 2.7465 & -1.1477 & -0.4252 \\ -1.1155 & 2.0222 & -0.0330 \\ 0.1403 & -0.3392 & 1.1237 \end{bmatrix} \bullet \begin{bmatrix} X \\ Y \\ Z \end{bmatrix}, \quad (7.14)$$

and its inverse transformation, given by

$$\begin{bmatrix} X \\ Y \\ Z \end{bmatrix} = \begin{bmatrix} 0.4770 & 0.2995 & 0.1717 \\ 0.2628 & 0.6571 & 0.0801 \\ 0.0197 & 0.1609 & 0.8926 \end{bmatrix} \bullet \begin{bmatrix} R \\ G \\ B \end{bmatrix}. \quad (7.15)$$

The white point in this transformation is for the illuminant D_{65} and the 10-deg observer. The R, G, B values are in the range from 0 to 100. Thus, the white color generated by the set of values $R = G = B = 100$, with this matrix transformation,

Table 7.2 Some common CRT phosphors and light sources for image displays and their x , y coordinates.

Source	Red		Green		Blue	
	x	y	x	y	x	y
NTSC	0.68	0.32	0.28	0.60	0.15	0.07
Computer	0.628	0.346	0.268	0.588	0.150	0.070
SMPTE*	0.63	0.34	0.31	0.60	0.16	0.07
High-brightness LEDs	0.70	0.30	0.17	0.70	0.13	0.08

* Society of Motion Picture and Television Engineers.

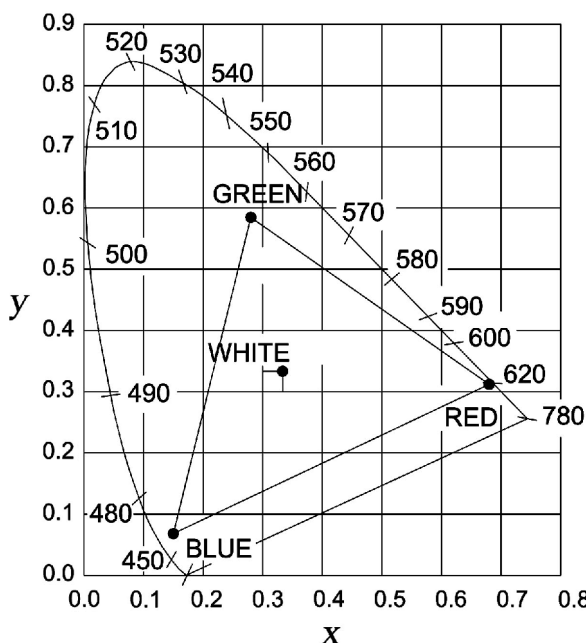


Figure 7.5 Colors that can be displayed in a color television (NTSC) are inside the triangle formed by the chromaticity coordinates of the three phosphors.

must be adjusted so that it is equal to the white color as observed by a 10-deg observer with a D₆₅ illuminant. Only the colors inside the triangle formed by these three points with coordinates x , y in Table 7.1 can be displayed in a color television, as shown in Fig. 7.5.

Several different cathode-ray tube (CRT) phosphors are used in display systems. The color coordinates for some of them are listed in Table 7.2, where the first entry [National Television System Committee (NTSC)] has the same coordinate values as the third entry in Table 7.1.

The RGB system is a device-dependent color model, since different devices detect or reproduce a given RGB value differently. This is because the spectral characteristics of phosphors or dyes differ from manufacturer to manufacturer.

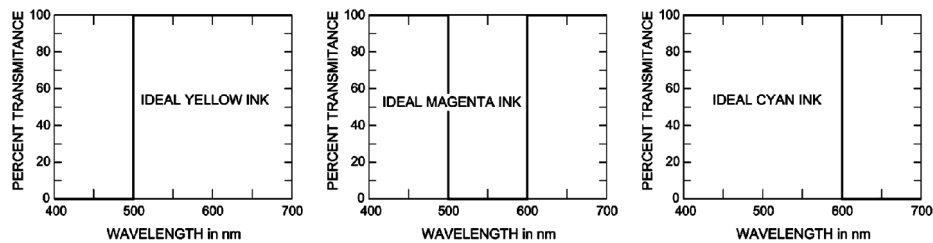


Figure 7.6 Spectral characteristics of three ideal filters that can be used to reproduce color by subtraction.

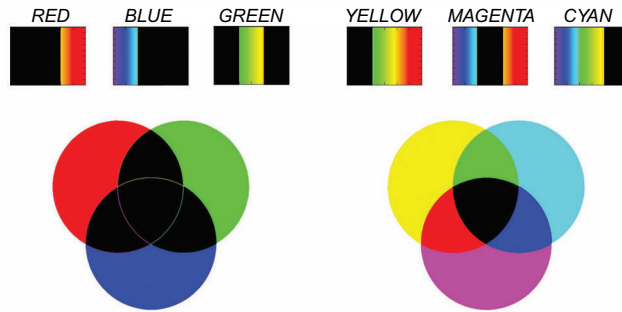


Figure 7.7 Three colored filters (cyan, magenta, and yellow) combined by color subtraction.

7.3 Color Subtraction

If a colored light field is observed through a colored filter, some color components will be removed. If the spectral radiance for the light field is $P(\lambda)$ and the spectral transmittance of the filter is $\tau(\lambda)$, the effective final relative spectral power is the product $P(\lambda)\tau(\lambda)$. It is easy to see that if $P(\lambda)$ and $\tau(\lambda)$ do not have any wavelength ranges aside from zero in common, the final color is black. So, the process of color subtraction must be done with continuous nonmonochromatic colors, frequently white.

In most color-printing processes, the primary colors used are cyan, magenta, and yellow. Figure 7.6 shows the spectral characteristics of three filters—cyan, magenta, and yellow—that can be used to reproduce color by the subtractive process. Ideally, each colorant will transmit two-thirds of the visible spectrum and absorb one-third. Figure 7.7 illustrates how these three filters, whose spectral transmissions are in the upper part, combine with this process.

The subtraction process selectively removes some parts of the visible spectrum. For example, the yellow filter removes the blue color, transmitting the green and red colors. The magenta filter removes the green light, transmitting the red and blue colors. The cyan filter eliminates the red light, transmitting the blue and green. Thus, by adjusting the transparency of these filters, the amounts of red, green, and blue color can be controlled. Mathematically, we may express the relationship

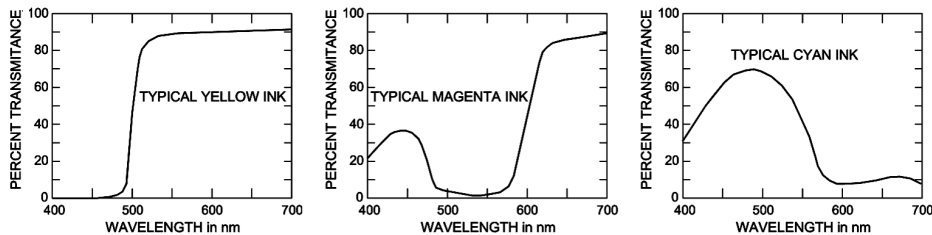


Figure 7.8 Three practical filter transmissions for color subtraction.

between these filters by the following set of equations:

$$\begin{aligned} \text{cyan} &= \text{white} - \text{red}, \\ \text{magenta} &= \text{white} - \text{green}, \\ \text{yellow} &= \text{white} - \text{blue}. \end{aligned} \quad (7.16)$$

With these colors we have what is known as the cyan/magenta/yellow (CMY) system. However, these ideal filters do not exist, so a more practical set of CMY filters is shown in Fig. 7.8. Ideally, cyan, magenta, and yellow are sufficient to generate a wide range of colors by the subtractive process. For example, equal amounts of these three colors should produce black, but in practice, a dark brown color is generated. For this reason, a fourth real black ink is added in many printing processes to obtain a truer color (designated as “K”). This is called the CMYK system.

Predicting colors obtained by color subtraction is not as simple as with color addition. As shown in Fig. 7.9, cyan, yellow, and magenta are obtained inside a triangle where three curved lines are formed. The subtractive color process is used, for example, in color photography, where several layers with different colors are superimposed. Color subtraction is also used in some printers where three or four inks are mixed.

7.4 Metamerism

We have seen that the perceived color of an opaque object, as defined by the tristimulus values in Eqs. (5.35)–(5.37) depends not only on its intrinsic color given by its spectral reflectance $\rho(\lambda)$, but also on the relative spectral power $P(\lambda)$ of the illuminating beam. A color match with any given illuminating light source is obtained when the tristimulus values X , Y , and Z are the same for the two samples being compared.

However, a perfect match with a light source does not guarantee a color match with another light source, or by another observer, unless their spectral reflectances are exactly equal. An example is shown in Fig. 7.10, where two hypothetical objects appear to have the same color under illumination with illuminant D_{65} , but not with any other light. This phenomenon is called *metamerism*. When two

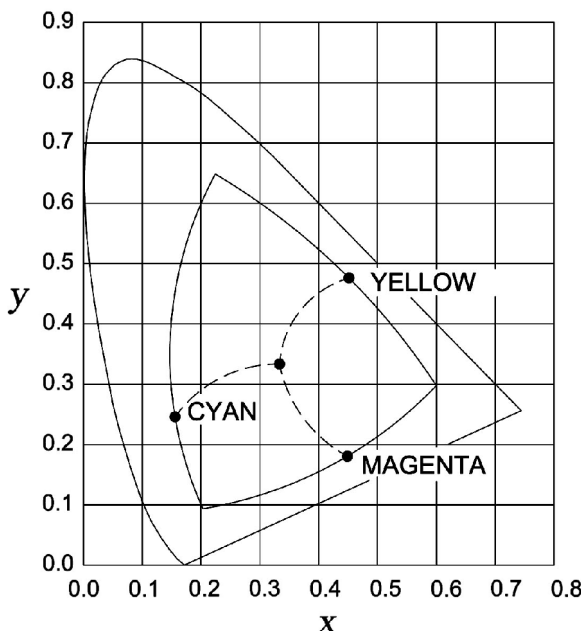


Figure 7.9 Colors obtained by subtraction using cyan, magenta, and yellow.

colors with different spectral powers appear to have the same color, they are said to be a *metameric* pair. The term metamerism was apparently proposed by Wilhelm Ostwald, a German chemist. In the field of chemistry, the word metamerism is frequently used to describe structural isomerism. A typical example of metamerism appears when a part of a car body is repainted. If the color match was made under daylight, the repair can probably be detected under street lamp illumination unless the same type of paint was used. Metameric pairs have the following properties:

- (a) Their two spectral distributions have at least three wavelengths that have the same values.
- (b) Two different light source illuminations could make them to appear different, but not necessarily.
- (c) Two different observers could possibly see them differently, but not necessarily. The CIE standard observer and two real-life observers could all have different color-matching functions.

A good color match under any illumination conditions can be obtained only if the spectral reflectance curves for the two samples are identical. In principle, the presence of metamerism in two colored samples can be detected only by examination of their spectral reflectances. However, in practice, the use of three different lamps is sufficient to detect any important metamerism. The three recommended lamps for this purpose are all daylight illuminants such as D₆₅, the color-matching lamp by Westinghouse, and the Philips Color 84 lamp, which has three peaks in its spectrum.

When displaying a color image in a computer or television screen, it is impossible to display exactly the same spectral distribution present in the object. The aim is to display a metameric color. If we know the spectral power distribution of the monitor's phosphors, we may calculate the appropriate weights on the monitor's phosphors to produce the metameric color that closely resembles the real object.

7.5 Colorants

The word *colorant* is a general term describing any substance used for modifying the color of an object by changing its spectral transmittance or its spectral reflectance. Colorants can be either *dyes* or *pigments*. Technically speaking, the difference is that dyes are soluble in the host material, typically water, while pigments are not. Another difference is that dyes do not scatter light, and they look transparent. On the other hand, pigments scatter light and thus, are opaque. This difference between a dye and a pigment may not be so clear sometimes, as treated in more detail by Kuehni (2005) and as illustrated in Fig. 7.11. Still another difference is that dyes are absorbed by the colored substrate, while pigments require a binder to stick to the surface. With suitable chemical treatment, a soluble dye can be converted into an insoluble pigment. Unfortunately, in common language, the differences between a dye and a pigment are not taken into consideration, and confusion is frequent. Definitions given in dictionaries or used in some industries do not necessarily coincide with these ideas.

Dyes are used for coloring transparent materials, such as liquids, films, and plastics, including translucent materials, such as textiles and paper. They give coloration to these materials without affecting the surface structure. Pigments are formed by crystalline particles that have low solubility in most solvents—only in properly selected organic solvents—but not in water. The interaction of light with pigments is understood only with a study of their absorbance and scattering properties.

7.6 Color Matching and Color Management

To make a color match with three lights is simple, since only an additive process takes place, as in color television. It is a little bit more difficult to make only the color subtraction process take place, but it can be done without much complication, as in color photography. However, an extremely practical problem—calculating the resultant color after mixing three paints in different proportions—is difficult. The reason for this is that both additive and subtractive processes take place in addition to many other factors that have to be considered. Most materials are colored either with dyes or with pigments.

When two or more liquid dyes or paints are mixed, the color combination mechanisms cannot be characterized as purely additive or subtractive, because we actually have a combination of the two processes, as illustrated in Fig. 7.12. The colors of the two side-by-side contiguous color elements [(a) and (b)] combine at

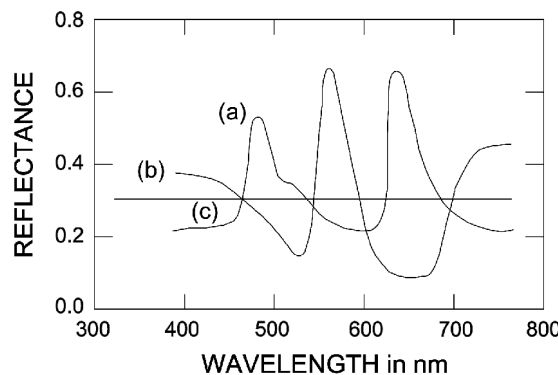


Figure 7.10 Spectral reflectance of two hypothetical objects that have the same color (gray) illumination with illuminant D₆₅.

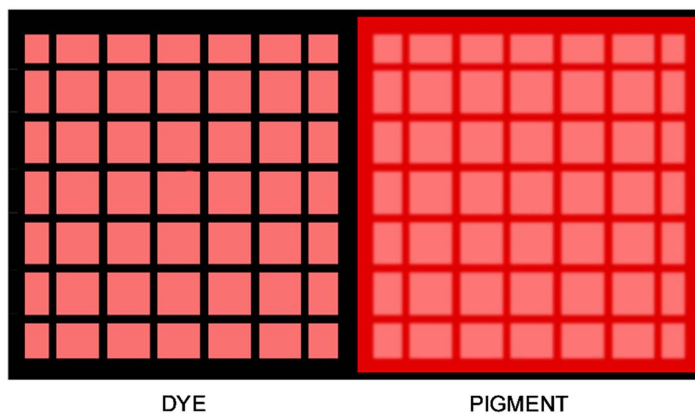


Figure 7.11 Illustration of the difference between (a) a dye and (b) a pigment covering an object.

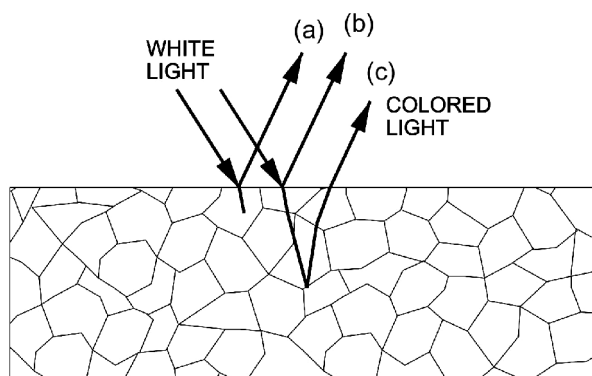


Figure 7.12 Combined addition and subtraction processes.

the eye with an addition process. If the two elements are slightly transparent—as they nearly always are—and one is on top of the other, the two colors of the two particles mix with a subtractive process [(b) and (c)].

Many approaches can be used for solving this color-matching problem with several dyes or pigments (Allen, 1980; Volz, 1995), for example:

- (a) *The trial-and-error method.* The closest pigment to the reference sample is selected. Then, if the pigment lacks red, green, or yellow, some pigment with the missing color is added. If the mixture of pigments is too light or too dark, some black or white pigment is added. Then, the whole process is iterated several times until a satisfactory match is obtained. This is the most intuitive approach, but also the least practical, accurate, and scientific approach. It is highly dependent on the experience of the person doing the color matching. It is quite important in this method to use noonday sunlight or a light source that closely resembles it. There are commercial cabinets with standard light sources for this purpose.
- (b) *Using a colorimeter to measure the tristimulus values.* A better approach than trial and error for characterizing the pigment mixtures of each of the basic pigments to be used involves measuring the color with any color system. After making a mixture, the proportion of pigments being used and the final measured color are recorded. This process is repeated for many combinations of pigments in many different proportions until a good database of all combinations is developed and stored in a computer for future reference. This process is more rational than the trial-and-error method and produces more reliable results. The great disadvantage is that the database has to be previously generated and is valid only for those particular measured pigments, not for any other set.
- (c) *Using the Kubelka–Munk theory.* While this is not the simplest approach, it is the most scientific. It also has many practical restrictions, as will be explained. The color of a mixture of dyes or pigments is determined by the resultant reflectance $R(\lambda)$. This reflectance and the transmittance $T(\lambda)$ of a translucent sample are functions of the light-absorption coefficient $K(\lambda)$ and the light-scattering coefficient $S(\lambda)$ in the sample shown by Kubelka and Munk (1931). The absorption of light depends on the concentration of the colorant. The light scattering depends only on the microscopic structure of the colored material if dyes are used, but also on the colorant concentration when pigments are used. The Kubelka–Munk equations are quite complex for translucent materials, but they become much simpler when the material is opaque. In that case, the light transmission is zero and the Kubelka–Munk equation becomes

$$\frac{K(\lambda)}{S(\lambda)} = \frac{[1 - R(\lambda)]^2}{2R(\lambda)}, \quad (7.17)$$

which shows that the spectral reflectance is a function only of the ratio of the absorption and the scattering coefficients. It has been found that this expression

is quite accurate if the refractive index is close to that of air, which is true for most opaque samples. From this relation we can obtain the following expression for the reflectance $R(\lambda)$:

$$R(\lambda) = 1 + \frac{K(\lambda)}{S(\lambda)} - \left\{ \left[1 + \frac{K(\lambda)}{S(\lambda)} \right]^2 - 1 \right\}^{1/2}. \quad (7.18)$$

In conclusion, the spectral reflectance $R(\lambda)$ is a function only of the ratio $K(\lambda)/S(\lambda)$ of the absorption and scattering coefficients. In other words, if the ratio $K(\lambda)/S(\lambda)$ of the absorption and scattering coefficients for two samples is identical for all wavelengths, their spectral reflectance $R(\lambda)$ is also identical, producing a reasonable color match with an accuracy of about $7\text{--}8 \Delta E_{ab}$. [See Chapter 2 in Kang (1997) and McDonald (1997)]. In the case of dyes applied to textiles, the scattering coefficient is a constant with value equal to one.

An important aspect of the Kubelka–Munk theory is that when a mixture of several dyes or pigments is used for coloring the material, the absorption and scattering coefficients of the mixture are calculated from the coefficients for each pigment only by their sum, as

$$K(\lambda) = \sum_{i=0}^N c_i K_i(\lambda), \quad (7.19)$$

and

$$S(\lambda) = \sum_{i=0}^N c_i S_i(\lambda), \quad (7.20)$$

where c_i is the colorant concentration. If the absorption coefficient $K(\lambda)$ and the scattering coefficient $S(\lambda)$ as functions of the wavelength for each colorant in a mixture are known, the spectral reflectance $R(\lambda)$ of this mixture can be calculated from the colorant concentrations. Conversely, if the spectral reflectance is known, the colorant concentrations can be obtained by an iterative mathematical procedure. More details on the Kubelka–Munk theory and their methods can be found in the classic book by Judd and Wyszecki (1975) and also in more recent books, such as Kuehni (2005).

The methods for color management are quite important in almost any industrial plant, but they become especially important in the case of graphic arts, press technologies, printers, and electronic displays. They have been treated in detail in many books by several authors. The general principles and rules when mixing dyes or pigments are described in the books by Kuehni (1975, 2005). The application of computer methods to the dye coloring of textiles is described in Chapter 5 of the book edited by McDonald (1997) and in Park (1993). The color-matching prediction for pigmented materials is presented by Nobbs in Chapter 6 of McDonald (1997). The subjects of color management in multimedia devices and

digital image processing are in the books by MacDonald and Luo (1999), Koschan and Abidi (2008), and Westland and Ripamonti (2004). Color management in computer software, including some popular programs, is treated by Fraser et al. (2005). Digital color in the graphic arts is described by Bruno (1986), Kang (1999), and Yule et al. (2001). Color technology for electronic imaging devices has been fully described by Kang (1997, 2006).

References

- Allebach, J. P., "Processing digital color images: from capture to display," *Phys. Today* **45**, 32–39 (1992).
- Allen, E., "Colorant formulation and shading," in Grum, F. and Bartleson, C. J., Eds., in *Optical Radiation Measurements: Color Measurement*, Vol. 2, Academic, New York (1980).
- Bruno, M. H., *Principles of Color Proofing: A Manual on the Measurement and Control on Time and Color Reproduction*, Gama Communications, Salem, NH (1986).
- Fraser, B., Murphy, C., and Bunting, F., *Real World Color Management*, 2nd ed., Peachpit Press, Berkeley, CA (2005).
- Judd, D. B. and Wyszecki, G., *Color in Business, Science, and Industry*, 3rd ed., John Wiley & Sons, New York (1975).
- Kang, H. R., *Color Technology for Electronic Imaging Devices*, SPIE Press, Bellingham, WA (1997).
- Kang, H. R., *Digital Color Halftoning*, SPIE Press, Bellingham and IEEE Press, New York (1999).
- Kang, H. R., *Computational Color Technology*, SPIE Press, Bellingham, WA (2006) [doi:10.11117/3.660835].
- Koschan, A. and Abidi, M., *Digital Color Image Processing*, John Wiley & Sons, New York (2008).
- Kubelka, P. and Munk, F., "Ein Beitrag zur Optik der Farbanstriche," *Z. Tech. Phys. (Leipzig)* **12**, 593 (1931).
- Kuehni, R. G., *Computer Colorant Formulation*, D. C. Heath, Lexington, MA (1975).
- Kuehni, R. G., *Color: An Introduction to Practice and Principles*, John Wiley & Sons, New York (2005).
- MacDonald, L. W. and Luo, M. R., Eds., *Colour Imaging: Vision and Technology*, John Wiley and Sons, Ltd., Chichester, U.K. (1999).
- McDonald, R., Ed., *Colour Physics for Industry*, 2nd ed., The Society of Dyers and Colourists, Bradford, U.K. (1997).
- Park, J., *Instrumental Color Formulation: A Practical Guide*, The Society of Dyers and Colourists, Bradford, U.K. (1993).

- Smith, N., "Color television," *Sci. Am.* **182**, 13 (1950).
- Volz, H. G., *Industrial Color Testing: Fundamentals and Techniques*, John Wiley & Sons, New York (1995).
- Westland, S. and Ripamonti, C., *Computational Colour Science Using MATLAB*, John Wiley and Sons, Ltd., Chichester, U.K. (2004).
- Yule, J. A., Field, G. G., and Yule, J. A. C., *Principles of Color Reproduction*, 2nd ed., Graphic Arts Technical Foundation, Sewickley, PA (2001).

Chapter 8

Color Measurements and Color Defects

8.1 Introduction

The measurement of color is a very important issue with applications in many types of industrial activities, mainly in the textile, paper, leather, and graphic arts industries. The subject of color measurement is so important that many articles (Kippman, 1993), books (Grum and Bartleson, 1980; Pearson, 1980; Berger-Schunn, 1994), and standards are devoted to this topic.

8.2 Visual Chromatic Defects

Color deficiency was first studied by John Dalton (Hunt et al., 1995) in 1798, because Dalton himself was color-blind; in fact, color deficiency problems are sometimes known as Daltonism. His studies were based solely on color naming and subjective descriptions by different observers. After Dalton, color vision deficiencies were investigated by John William Strutt Rayleigh, who developed a precise color-matching test, still known as the Rayleigh Matching Test (Thomas and Mollon, 2004), which was the basis for an instrument called the *anomaloscope*. In this test, a yellow light must be matched with a mixture of red and green light. By measuring the matching proportions of red and green, it is possible to detect different types of red-green color deficiencies. Following Rayleigh, color defects have been studied with more detail by many other researchers (Pitt, 1944). An excellent review of color deficiencies is in a chapter by Sharpe et al. (1999).

The names for the different manifestations of color defects are formed by the Greek roots *protos* (first), *deutan* (second), and *tritan* (third), for the order in which they were discovered. *Trichromats* are those people with normal color vision, i.e., they have three normal color receptors. *Anomalous trichromats* also have three color receptors, but one of them is deficient. A person can be *protanomalous*, *deuteranomalous*, or *tritanomalous* if the L-, M-, or S-cones are defective, respectively. This defect may be caused by a shift from the normal spectral sensitivity of the L- or M-cones. These spectral shifts can be produced by hybrid LM- or ML-pigments that may appear due to genetic inheritance. Anomalous trichromats are more common than *dichromats*.

Table 8.1 Relative abundance of visual chromatic defects.

Type of visual defect	Visual defect	Abundance in men	Abundance in women
Trichromats	None		
Anomalous trichromats	Protanomalous	1.08% ²	0.03% ²
	Deuteranomalous	4.63% ²	0.36% ²
	Tritanomalous	0.0% ³	0.0% ³
Dichromats	Protanopes	1.01% ²	0.02% ²
	Deutanopes	1.27% ²	0.01% ²
	Tritanopes	0.005% ³	0.005% ³
Monochromats		0.003% ¹	0.002% ¹

¹ The incidence of monochromats is the lowest of all chromatic defects.

² Abundancies are from Sharpe et al. (1999).

³ The incidence of tritan defects has not been clearly determined.

Table 8.2 X and Y chromosomes in protan and deutan defects; X is a normal chromosome and X* is an abnormal chromosome.

Type of defect	Men	Women
Normal	XY	XX
Affected and carrier	X*Y	X*X*
Not affected carrier		X*X

Dichromats can be *protanopes*, *deutanopes* (Judd, 1945, 1949), or *tritanopes*, depending on which cone is absent or completely deficient (Rushton, 1975). In protanopes the L-cones are absent (Rushton, 1963), while in deutanopes the M-cones are absent. Dicromats require only two primary colors in a matching experiment to match any given color. Table 8.1 shows the relative abundance of chromatic defects.

In protanopes (protanomalous) and deutanopes (deuteranomalous), color deficiency is hereditary and associated with the X chromosome, as illustrated in Table 8.2. Protan and deutan defects are the most common, also known as red–green color deficiencies.

According to Wright (1952) the incidence of tritanopia (Alpern, 1976), also called the blue–green defect, is extremely low: between one person in 13,000 and one person in 65,000. The ratio of men to women is very close to 1: between 1 and 1.6. The transmission of tritan defects is not linked to the X chromosome, making it quite different from protan and deutan defects. Most frequently, this is an acquired deficiency. The congenital form seems to be less frequent than one person in a million.

One kind of monochromat is the so-called S-cone monochromat, first described by Blackwell and Blackwell (1957, 1961) and later by Alpern et al. (1971). Monochromats have rods, but only S-cones, and they lack M- and L-cones. Reitner et al. (1991) speculated that some kind of color vision is possible for these people. This defect is linked to the X chromosome.

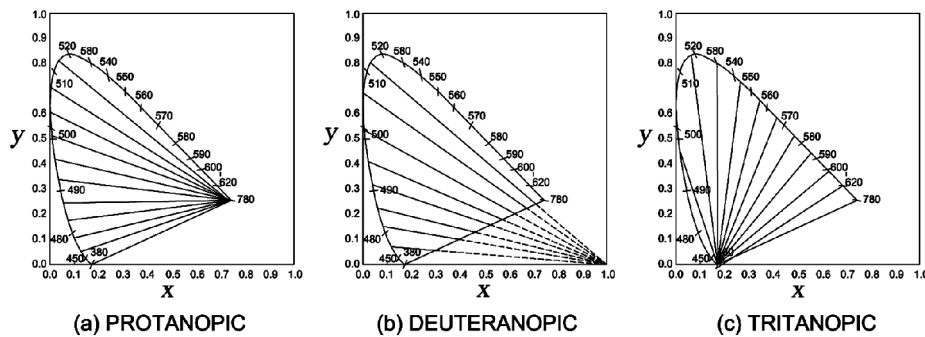


Figure 8.1 Lines of constant hue for protanopes, deutanopes, and tritanopes.

Completely color-blind people are extremely rare (Lewis and Mandelbaum, 1943). Their visual functions have been studied by Hecht et al. (1938), Walls and Heath (1954), and Vienot et al. (1995).

In 1855, Maxwell pointed out that if two different colors appear identical to a color-deficient person, and we plot the two points corresponding to these two colors in a chromaticity diagram, then the line joining these two points is the locus of colors that appear identical to this person. If we repeat this process for many colors, we may find many straight lines in the chromaticity diagram, which indicate the chromaticity confusions of a color-deficient person. The intersection point of all these lines indicates the color of the nonfunctioning primary process in this person. The mathematics of this theory have been studied in detail by Judd (1945, 1949). Figure 8.1 shows the lines of constant hue for the three types of color-deficient people, i.e., protanopes, deutanopes, and tritanopes. The color-matching conditions for these people are obviously different from those of normal-color-vision people (Walraven et al., 1966; Walraven, 1974; Breton and Cowan, 1981).

A metamer pair of colors, as described in Section 7.5, is a pair that has the same color but different spectral power. Therefore, if we have a metamer pair, it will still be a metamer pair for a color-deficient person.

There are many possible tests that can be used to detect color defects (Working Group 41, 1981; Birch, 2003), for example, with the Rayleigh test described above or with color charts designed to identify and detect color deficiencies. The most popular test is probably the *Ishihara Pseudoisochromatic Test*, first introduced by J. Spilling in 1917 and later improved by Ishihara (1954). One of these plates is illustrated in Fig. 8.2. People with normal color vision will see a number 74 in this pattern, while color-deficient people will see a number 21. Ishihara plates are quite popular, but it is important to know that they can detect only red–green deficiencies.

Another common method to detect color vision deficiencies is by means of the *D-15 color arrangement tests*. The subject being examined arranges a collection of 15 colored disks in a certain order. People with color defects cannot arrange the disks in the correct order. There are several variations of this test. A good review on

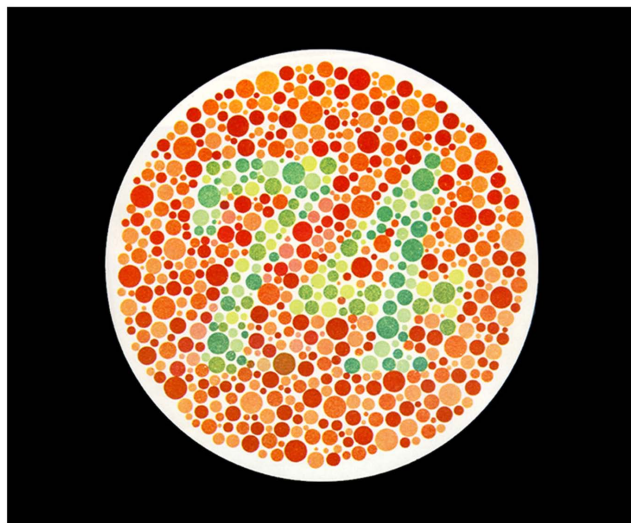


Figure 8.2 Ishihara pseudoisochromatic (Ishihara, 1954) test pattern to detect color vision deficiencies.

the subject on the psychophysics methods for color detection deficiencies is found in a chapter by Sharpe et al. (1999)

8.3 Whiteness and White Standards

By definition, white is a color with high luminance and low purity. Most observers have a personal bias to classify the whiteness of several samples, but the exact order greatly depends on the illumination conditions and the environment. The ideal theoretical definition of white is that which diffuses light perfectly and has a spectral reflectance equal to one for all wavelengths in the visible spectrum (CIE, 1986). Unfortunately, this is not a practical definition, as described in the section on illuminants in Chapter 2.

Magnesium oxide, and more commonly, barium sulfate, have been defined as working standard whites. These whites are prepared by pressing high-grade BaSO₄ powder into tablets. Recently, polytetrafluoroethylene (PTFE), or pressed PTFE powder, also commercially known as Halon, Spectralon, or G-80 tetrafluorethylene resin (Weidner and Hsia, 1981) has been used. Another popular standard white is made out of ceramic tiles.

Several definitions specifying the whiteness of a material have been proposed (Judd, 1936; Ganz, 1976, 1979; Ganz et al., 1995). The whiteness of a material is defined by its closeness to the ideal pure white, which has a 100% reflectance and a purity of zero (MacAdam, 1934).

Obviously, the observed color depends not only on the spectral reflectance on the colored body, but also on the color of the illuminating light source. Table 8.3 shows the chromaticity coordinates and the color temperature for a white surface when illuminated by common illuminants and light sources, assuming a 100% reflection.

Table 8.3 Color temperature and chromaticity coordinates for a white surface, using different illuminants.

Source	CIE 1931 (2 deg)		CIE 1964 (10 deg)		Color temperature (K)
	x	y	x	y	
Illuminant A	0.4476	0.4074	0.4512	0.4059	2856
Illuminant B	0.3484	0.3516	0.3498	0.3527	4874
Illuminant C	0.3101	0.3162	0.3104	0.3191	6774
Illuminant D ₅₅	0.3324	0.3475	0.3341	0.3487	5503
Illuminant D ₆₅	0.3127	0.3290	0.3138	0.3310	6504
Illuminant E	0.333	0.333	0.333	0.333	5400
Direct sun light	0.336	0.350	—	—	5335
Overcast sky	0.313	0.327	—	—	6500
North sky	0.277	0.293	—	—	10000

The CIE formula to specify the *whiteness* W of a sample when illuminated by a D₆₅ illuminant with a 10-deg field (CIE, 1964) (see Section 4.4) is

$$W = Y + 800(0.3138 - x) + 1700(0.3310 - y). \quad (8.1)$$

In this formula, if $x = 0.3138$ and $y = 0.3310$, the sample is neutral (gray) and its whiteness is W and its luminance is Y . The *tint* (shade) T is given by

$$T = 900(0.3138 - x) - 650(0.3310 - y). \quad (8.2)$$

If T is positive, the sample is greenish, and if T is negative, the sample is reddish. These formulas have the limits of application: $Y > 70$ and $T < \pm 3$.

8.4 Pantone® Colors, GretagMacbeth ColorChecker®, and Spectralon® Standards

A company established in New Jersey, called Pantone, Inc., proposed a proprietary color space called the Pantone matching system (PMS). The primary product of this company is the Pantone Guide, formed by a fan of 6×2 -in cardboard sheets printed with a large series of colors. These colored sheets allow designers of commercial products to match any specific color to a Pantone color before entering production. The company has been so successful that even the colors of some flags are defined by a Pantone color.

The Goe™ System, introduced by Pantone in 2007, consists of over 2000 colors. Each of these colors has RGB and LAB values associated with each color. The commercial use of these colors is not free.

A company called Macbeth that now belongs to X-Rite produced a color-calibration target that consists of a cardboard sheet with an array of 24 colored squares. This calibration target is known as the GretagMacbeth ColorChecker, as shown in Fig. 8.3. Six of these colors are typical primary colors: red, green, blue, cyan, magenta, and yellow; six colors form a uniform gray lightness scale. The rest of the colors are approximations of colors frequently found in nature and daily life.



Figure 8.3 Gretag Macbeth ColorChecker®. Courtesy X-Rite, Inc.

Another frequently used and useful color reference is a set of small discs, about one inch in diameter, made with a highly diffusing and almost constant color, commercially known with the name of Spectralon. They are produced by a company called Labsphere, Inc., which provides the Spectralon Diffuse Reflectance Standards. These standards have a NIST traceable calibration for their spectral reflectance.

8.5 Optical Configurations to Measure Reflectance

When a light beam illuminates a mirror, the light is entirely reflected at an angle following the law of reflection, as shown in Fig. 8.4(a). This is called specular reflection. If the illuminated surface is not completely polished but partially diffuse, as in the case of a white piece of paper, the beam is reflected in many directions, but with a strong preferential direction, as shown in Fig. 8.4(b). When the surface diffuses more light, like a glossy white paper, as shown in Fig. 8.4(c), the light is reflected in all directions, but still has a preferential direction. Finally, if the surface is perfectly diffusing, as in Fig. 8.4(d), the light enters the volume of the material and the reflected light does not have any preferential direction. In practice, the latter surface can be approximated by a compressed pellet of barium sulfate powder.

When measuring the color of an object, it is quite important that we measure only the diffusely reflected light and none of the specularly reflected light. Only the diffusely reflected light will be colored by the object. The specularly reflected light can be avoided by using asymmetric illumination and measuring directions, as shown in Fig. 8.5. If the illumination is normal, and the observation is at a 45-angle,

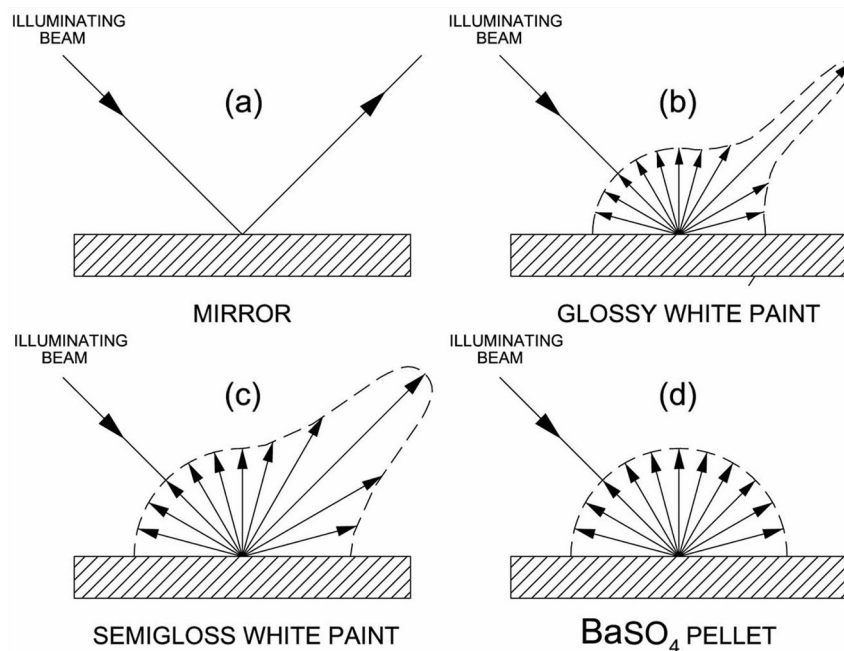


Figure 8.4 Light reflection of four types of surfaces, (a) a mirror, (b) a glossy white paint, (c) a semigloss white paint, and (c) a BaSO₄ pellet.

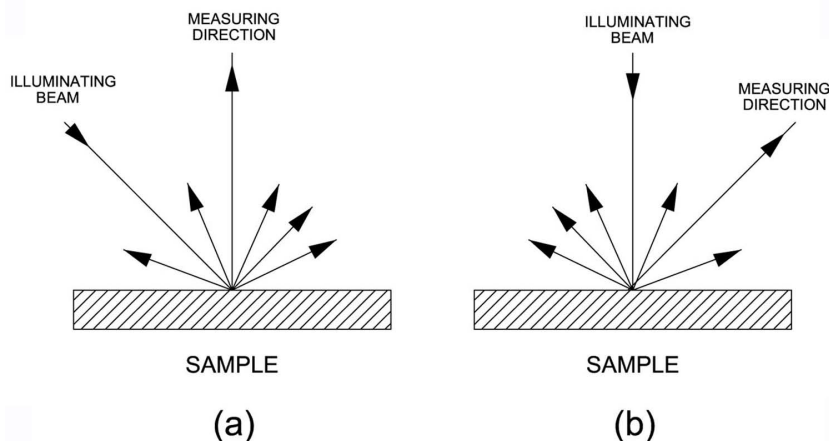


Figure 8.5 Asymmetric illumination configurations to measure color: (a) 45/0 and (b) 0/45.

we have the 0/45-deg configuration. On the other hand, if the illumination is at 45 deg and the observation is in the perpendicular direction, we have the 45-deg/0-deg method. The problem with these two arrangements is that the measurement can be affected by polarization effects, depending on the texture of the object. A solution to this problem is to illuminate from several directions. For example, if the illuminating beam is in the shape of an annular cone, the measurement is made at the axis of the cone (Fig. 8.6).

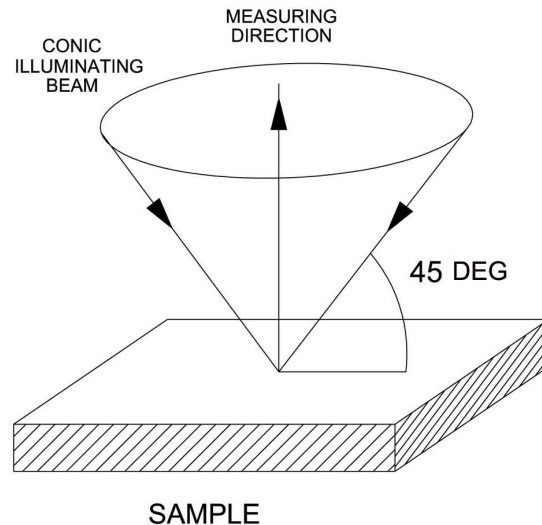


Figure 8.6 Annular illumination to measure color.

The CIE recommended two illumination configurations, using a diffusely illuminating white sphere, called an integrating sphere. In the so-called normal/diffuse (0/d) method, the illuminating beam goes directly to the measured object, and the measurement is made from the surface of the integrating sphere. A more common procedure, called the diffuse/normal (d/n) method, illuminates the surface of the integrating sphere, which in turn illuminates the object from all directions (Fig. 8.7). The measurement is then performed from a hole in the integrating sphere. If all specularly reflected light needs to be avoided, a hole is made at the symmetrical location of the measuring hole. If this hole is covered with a small white surface, some specularly reflected light is added to the measurement. These two measurements can give an estimate of the gloss of the object, which can be defined by

$$\text{gloss} = \frac{\text{specular flux}}{\text{diffuse flux} + \text{specular flux}}, \quad (8.3)$$

which, as a function of λ , can be shown to be

$$\text{gloss}(\lambda) = \frac{P_2(\lambda) - P_1(\lambda)}{P_2(\lambda)}, \quad (8.4)$$

where $P_1(\lambda)$ and $P_2(\lambda)$ are the relative spectral powers at the wavelength λ for the first and second measurements, respectively.

The integrating sphere must contain light baffles to prevent light from going directly from the light source, or from the integrating sphere, to the detector. This integrating sphere can be made with any efficient white-diffusing material, as described in Section 8.3.

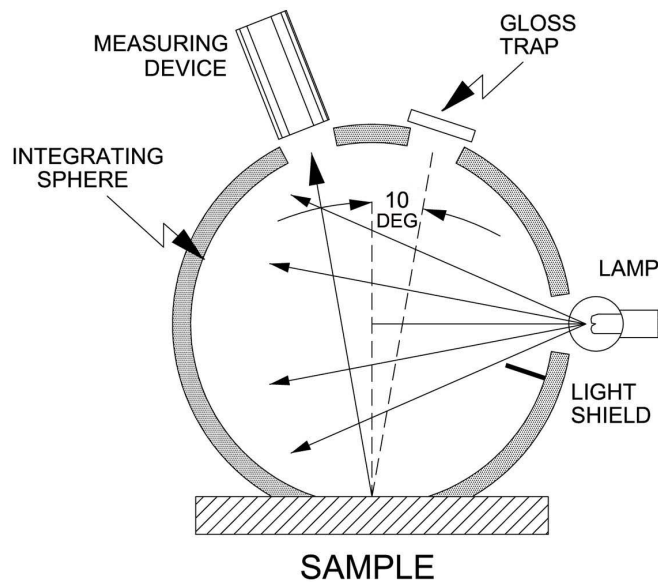


Figure 8.7 Illumination configuration d/10 using an integrating sphere to measure color.

When measuring the reflectance color of an object, several effects can introduce errors into the results (Zwinkels, 1989; Berns and Reniff, 1997). For example, the presence of specularly reflected light from the illuminating light source on the object to be measured can affect the result.

Another source of error could be any fluorescence in the colored object. Fluorescent samples absorb short-wavelength light, mainly violet and ultraviolet, and emit it at longer wavelengths, mainly in the visible. The presence of the light emitted by the fluorescence effect changes the measured color of the object. This makes it necessary to determine whether a sample to be measured is fluorescent or not. This is done by illuminating the sample in a light boot with ultraviolet light before measuring its color. As described by McDonald (1997), once they have been identified, fluorescent bodies are measured with two different measurements. One is made in the normal way, as with any nonfluorescent body. Using a second monochromator, a second measurement is taken by illuminating with monochromatic light, and then the reflected light is measured for all wavelengths. In this manner, sufficient information is obtained to separate the spectra of the reflected and the fluorescence emitted light. Due to fluorescence, reflectance values as high as 300% are uncommon.

The spectrum of the light source illuminating the colored body whose spectral reflectance is to be measured is not important since it is defined by the ratio of the reflected spectral radiance to the incident spectral radiance. It is only important that the light source emits all wavelengths of the visible spectrum except when measuring fluorescent samples. In this case, the amount of short-wavelength light

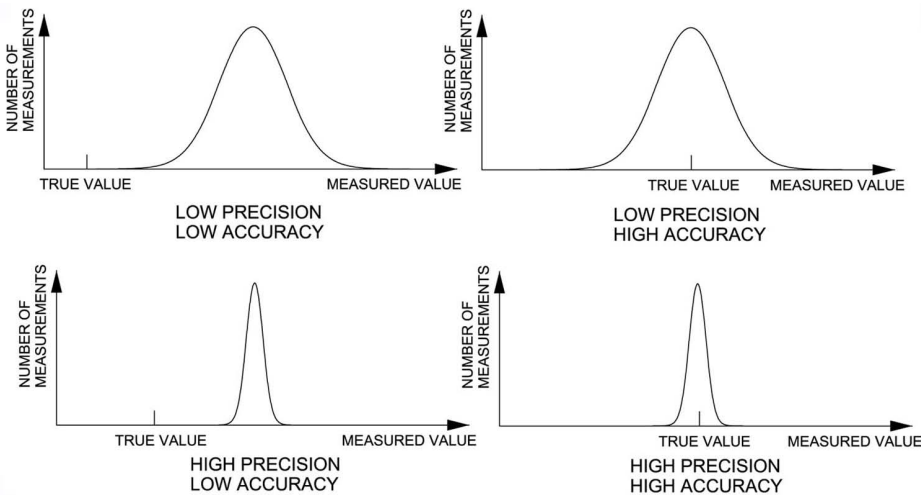


Figure 8.8 Accuracy and precision in measuring instruments.

producing the fluorescence is important because light sources with different short-wavelength spectrums produce different spectral reflectances.

Metallic or pearlescent objects are especially prone to introduce errors in color when measuring reflectance. The color of these objects is highly dependent on the angles of illumination and observation. Therefore, an instrument called a spectrogoniometer is used to take measurements of several different angles. The two CIE-recommended measuring configurations cannot be used with these metallic or pearlescent colors.

8.6 Precision and Accuracy of Measuring Instruments

Any measuring instrument has two types of errors—random and systematic—that should be reduced to a minimum. Systematic, or bias, errors arise because of approximations and simplifications made during the measuring procedure, or when some important parameters or variables are ignored. For example, warm-up time may be a source of systematic errors. Random errors occur due to the presence of unpredictable parameters that may have different values and signs every time a measurement is taken. Random errors can be reduced by averaging several measurements, but this averaging does not reduce systematic errors. An instrument with low systematic errors has high accuracy, and an instrument with low random errors has high precision. These errors are graphically represented in Fig. 8.8.

Precision has two classifications—*repeatability* and *reproducibility*. Repeatability is an evaluation of variations in the measured values with a given instrument and sampled over a specific period. The sampling can be done over a short time (a few seconds or minutes), or over a long time (days or months). The samples are evaluated by taking many measurements of a stable colored body over a short period without moving the instrument or the sample. This is important if color differences

Table 8.4 Classification of errors in measuring instruments and a rough estimation of their maximum acceptable value in colorimeters.

Type of error	Related characteristics		Acceptable value in colorimeters	
Systematic	Accuracy			0.5–1.0%
Random	Precision	Reproducibility		0.5–1.0%
		Repeatability	Short term Long term	0.05–0.1% 0.5–1.0%

are to be evaluated for quality control. Repeatability should be on the order of 0.1 CIELAB color difference.

Reproducibility is an evaluation of variations in the measured values with changing conditions such as the operator, the laboratory, the temperature, or any other condition that might be subject to change. The values are assessed with many measurements over a long period. A good reproducibility value in a colorimeter is about 0.2, but not higher than 0.5. This is important for color matching because two objects whose color is to be matched are normally measured at different times.

Accuracy is evaluated by comparing measurements with a standard reference or with other instruments in a procedure called calibration. The accuracy procedure is not as reliable as the repeatability or the reproducibility procedures. See Table 8.4 for the classification of these errors.

8.7 Spectrocolorimeters

A good description of some commercial color-measuring instruments may be found in Chapter 2 of the book by McDonald (1997). In a spectrocolorimeter, the spectral reflectance values $\rho(\lambda)$ are measured at equal wavelength separations in the visible range, or scanned across the whole visible range. At each selected wavelength in the visible range, the spectral radiance values of the reflected light are divided by the spectral radiance values of the illuminating light using a perfect white diffuser. Alternatively, if a perfect standard white diffuser is not available, a white or gray sample whose spectral reflectance is known with sufficient accuracy can be used. However, an important condition is that the color of this reference is as constant as possible over time.

The light source used to illuminate the reference sample as well as the sample to be measured must have certain characteristics. The most important one is that its spectral distribution covers the whole visible spectra (near infrared to near ultraviolet). It does not need to be perfectly white, as long as its spectral distribution is clearly determined. Frequently, a pulsed xenon lamp is used. If tungsten light is used, two problems may occur. The first is that there is not enough light in the ultraviolet and near ultraviolet, which may cause the signal-to-noise ratio in this region to be too low. The second problem is that as the lamp heats up, its spectral distribution rapidly changes. Therefore, the measurements must be taken when the temperature becomes stable enough.

Let us assume that the spectral reflectance for the white or gray reference sample is $\rho_{ref}(\lambda)$ and that for the colored body is $\rho(\lambda)$. Thus, if the measured reflected spectral radiance on the white reference sample is $L_{ref}(\lambda)$, and the measured spectral radiance on the colored surface is $L(\lambda)$, the spectral reflectance $\rho(\lambda)$ is given by

$$\rho(\lambda) = \left(\frac{L(\lambda)}{L_{ref}(\lambda)} \right) \rho_{ref}(\lambda). \quad (8.5)$$

Once the reflectance $\rho(\lambda)$ has been determined, the tristimulus values and the chromaticity coordinates can be calculated using the color-matching functions. By definition, the color of an object is obtained when the object is illuminated with a light source emulating the D₆₅ illuminant. Thus, the spectral reflectance is multiplied by the power spectrum of this illuminant.

The small amount of stray light going directly from the integrating sphere to the light detector should be subtracted from the measurements. To measure the spectral radiance $L_{black}(\lambda)$ of this light, a blackbody is measured. This blackbody is formed by a light trap constructed with a cavity in a hollow body with a small hole to observe its black-painted interior. Both calibrations with a white or gray reference and a black reference should be done before using the instrument.

Thus, the true spectral reflectance $\rho(\lambda)$ of the measured sample is

$$\rho(\lambda) = \left[\frac{L(\lambda) - L_{black}(\lambda)}{L_{ref}(\lambda) - L_{black}(\lambda)} \right] \rho_{ref}(\lambda). \quad (8.6)$$

This is the complete computational procedure for calculating the color in a spectroradiometer. Every spectroradiometer must have its own *white reference tile* from which to obtain the white reference reflectance $\rho_{ref}(\lambda)$. The absolute value for this reflectance is stored in the instrument. During the white calibration, its spectrum is adjusted so that it matches the stored spectrum within the specified tolerance. Each instrument has its own tile and cannot be interchanged with the tile from another instrument. Colored reference tiles are also convenient for checking the color measured by the instrument. Green or cyan tiles are frequently used. The spectral reflectance of the reference tile must have several well-defined inflection points to be able to detect any spectral shifts in the instrument. Since the color of ceramic tiles changes with temperature due to an effect known as thermochromism, the temperature must be carefully controlled within ±2 °C.

To measure the spectral radiance values $L_{ref}(\lambda)$ for the white reference sample and the spectral radiance $L(\lambda)$ for the colored surface, the spectrum must be formed by means of a grating or prism spectrometer. Then, the complete spectrum values can be measured by means of a scanning slit with a photometer behind it. This is a scanning spectrophotometer. Alternatively, a 1D CCD array can be used. Some common arrangements for spectrophotometers are shown in Fig. 8.9.

The measured spectral reflectance of the measured color object is used with the color-matching functions to obtain the tristimulus values X, Y, and Z. Then,

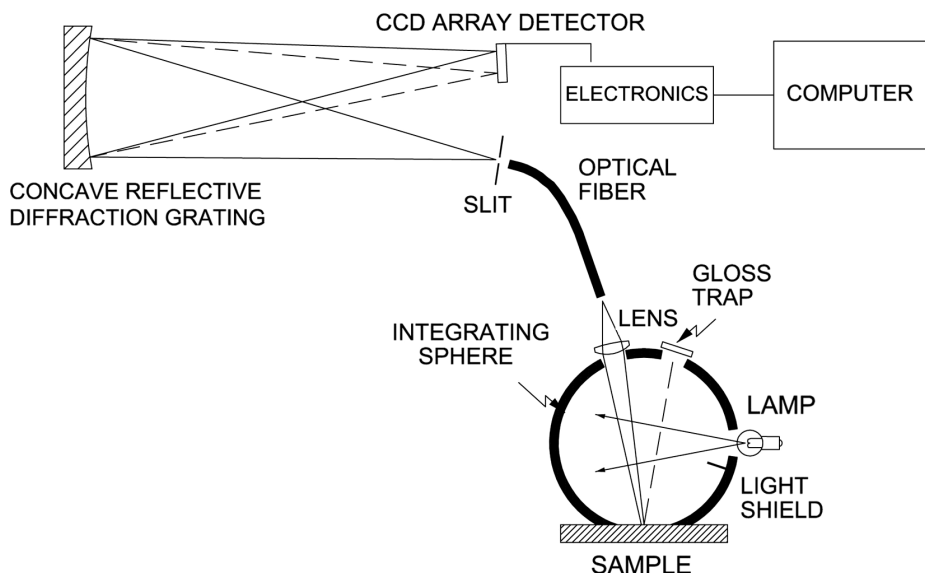


Figure 8.9 Common optical arrangements for spectrophotometers.

these values can be converted to a different system, such as the $L^*a^*b^*$ system or any other. The complete typical procedure for calculating the color in a spectrophotometer is illustrated in the block diagram presented in Fig. 8.10.

If the spectral reflectance of the reference sample and the spectral reflectance of the sample to be measured are measured at different times, the lamp's spectral distribution may be slightly different due to many possible practical reasons. To reduce the error being introduced, the two measurements have to be taken as close in time as possible, or better yet, simultaneously. Several procedures have been devised to achieve this. One of them involves taking both measurements simultaneously using two spectrophotometers. Another method takes the two measurements by rapidly switching between the sample to be measured and the reference by means of a small reflecting rotating mirror.

8.8 Tristimulus Photocolorimeters

Tristimulus photocolorimeters take three photoelectric measurements with three different colored filters. These instruments work similarly to the visual process in the human eye, where three different color detectors (cones) are used. In general, these filters are quite complicated since all of the spectral responses—taking into account the filter's transmittance and the detector's spectral response—must be equal to the color-matching functions \bar{x}_λ , \bar{y}_λ , and \bar{z}_λ . Since each of the three photometers measures the integrated light for all wavelengths, the three measurements are proportional to the tristimulus values X , Y , and Z . A practical problem is that filters with spectral transmissions equal to the color-matching functions do not exist. Thus, they have to be specially designed and synthesized with the superposition of three or four filters.

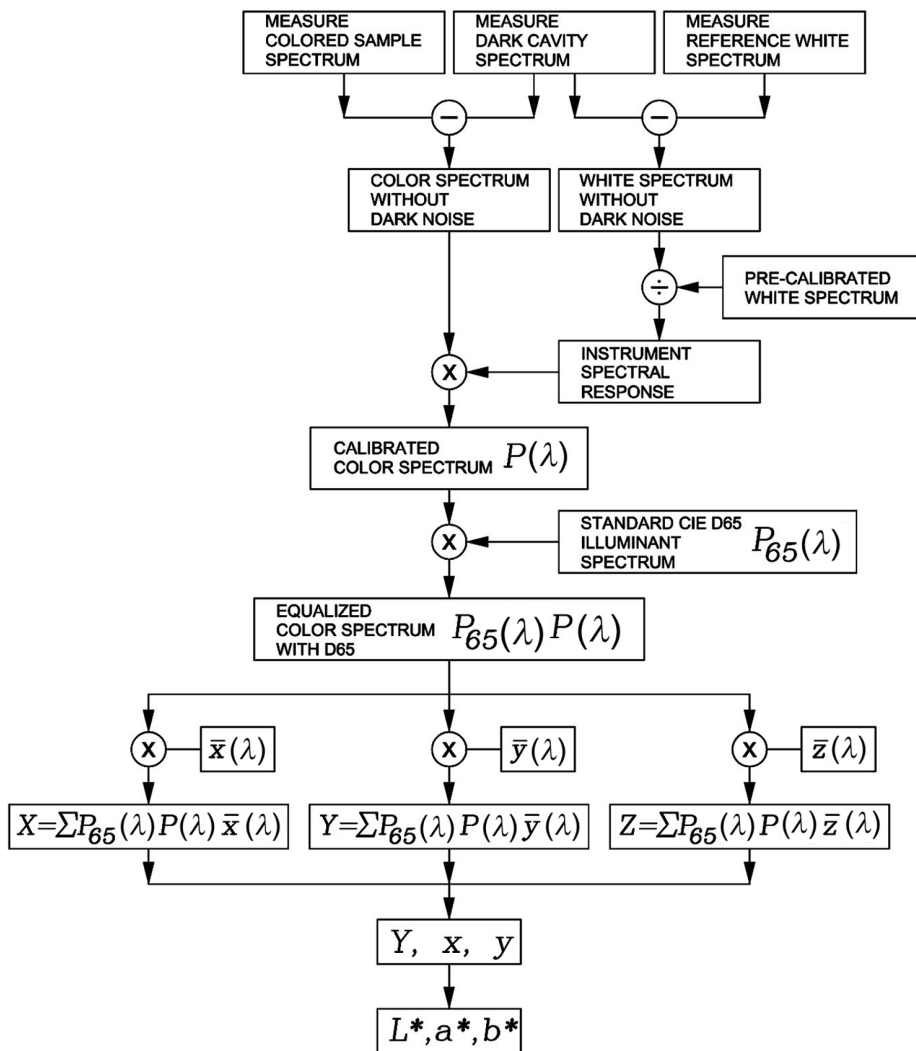


Figure 8.10 Procedure used to find the tristimulus values after measuring the spectral reflectance of a colored body.

We cannot “match” all colors in this way, but we can obtain enough information to identify all colors in nature. The important requirement is that the three spectral transmittances for the three filters form a set of color-matching functions. In Chapter 3, we saw that the human eye works in an almost identical manner.

Tristimulus colorimeters were very popular before the advent of modern minicomputers and microprocessors. Their accuracy was extremely poor, but the results were acceptable for color difference measurements. These colorimeters cannot detect the presence of metamerism in two samples with the same color. Color television and CCD cameras have also been used by some authors to measure color, for example, by Corbalán et al. (2000).

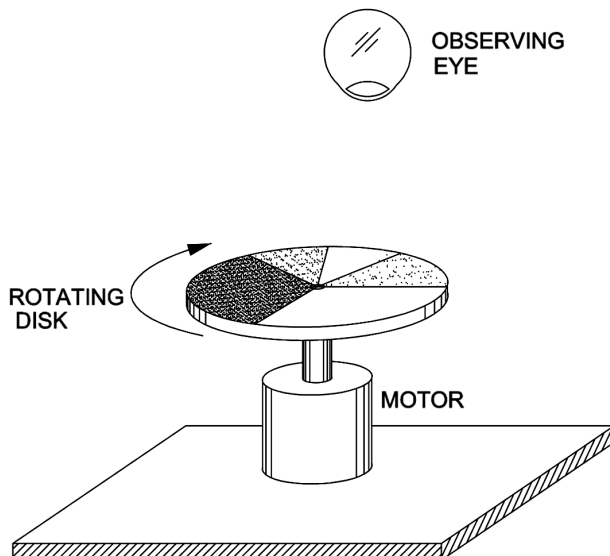


Figure 8.11 Disk colorimeter.

8.9 Visual Colorimeters

A visual colorimeter is a color-matching device with a split color field. Half of the field is covered by the body of the color to be measured, illuminated by a reference white-light source. The other half of the field is formed by a white surface, illuminated by three light sources whose colors are well determined—typically, red, green, and blue. The luminance of the three lights is varied until a good color match with the other half of the field is obtained. The three lights' brightness is manually adjusted on each lamp until a close match is obtained. The brightness of the incandescent tungsten lamps should be adjusted by means of diaphragms, since a change in the electrical current not only changes the brightness but also changes the color temperature.

The adjustment of this colorimeter is not simple and requires skill. This adjustment process can be simplified with other complex arrangements. For example, the white-light source illuminating the colored body to be measured can be substituted by three colored lamps with the same colors as the lamps illuminating the white reference field. This arrangement adds flexibility to the system, making the adjustment simpler for unskilled operators.

Many variations of this basic arrangement have been devised to construct visual colorimeters for different applications. The disk colorimeter presents an interesting method for finding the needed proportions of a colorant for a given mixture (Fig. 8.11). This instrument takes advantage of the eye's slow response by superimposing onto it several colors painted on angular sectors of a motorized rotating disk. It is assumed that the color of the reference sample is obtained by a color-addition process. This hypothesis is more valid for pigments than for dyes. The contribution of each pigment to the resultant color is directly proportional to

the magnitude of the angle in the painted sector. With this method, the hue and saturation of the sample color can be matched, but not necessarily the luminosity, unless the sample and the disk are illuminated with different light intensities.

References

- Alpern, M., "Tritanopia," *Am. J. Opt. Phys. Opt.* **53**, 340–349 (1976).
- Alpern, M., Lee, G. B., Maaseidvaag, F., and Miller, S. S., "Colour vision in blue-cone 'Monochromacy,'" *J. Phys.* **212**, 211–233 (1971).
- Berger-Schunn, A., *Practical Color Measurement*, John Wiley & Sons, New York (1994).
- Berns, R. S. and Reniff, L., "An abridged technique to diagnose spectrophotometric errors," *Color Res. Appl.* **22**, 51–60 (1997).
- Birch, J., "Colour vision examination," in *Investigative Techniques and Ocular Examination*, Doshi, S. and Harvey, W., Eds., Elsevier Health Sciences, Maryland Heights, MO (2003).
- Blackwell, H. R. and Blackwell, O. M., "Blue cone monochromacy: a new color vision defect," *J. Opt. Soc. Am.* **47**, 338–338 (1957); (abstract only).
- Blackwell, H. R. and Blackwell, O. M., "Rod and cone receptor mechanisms in typical and atypical congenital achromatopsia," *Vision Res.* **1**, 62–107 (1961).
- Breton, M. E. and Cowan, W. B., "Deuteranomolous color matching in the deutanopic eye," *J. Opt. Soc. Am.* **71**, 1220–1223 (1981).
- CIE, *Colorimetry*, CIE Publication No. 15.2-1986, 2nded., Commission Internationale de l'Eclairage, Vienna (1986).
- Corbalán, M., Millan, M. S., and Ysuel, M., "Color measurement in standard CIELAB coordinates using a 3CCD camera: correction for the influence of the light source," *Opt. Eng.* **39**, 1470–1476 (2000). [doi:10.1117/1.602519].
- Ganz, E., "Whiteness formulas: a selection," *Appl. Opt.* **18**, 1073–1078 (1979).
- Ganz, E., "Whiteness: photometric specification and colorimetric evaluation," *Appl. Opt.* **15**, 2039–2058 (1976).
- Ganz, E., Kurt, H., and Pauli, A., "Whiteness and tint formulas of the Commission Internationale de l'Eclairage: approximations in the $L^*a^*b^*$ color space," *Appl. Opt.* **34**, 2998–2999 (1995).
- Grum, F. and Bartleson, C. J., Eds., in *Optical Radiation Measurements: Color Measurement*, Vol. 2, Academic, New York (1980).
- Hecht, S., Shlaer, S., Smith, E. L., Haig, C., and Peskin, J. C., "The visual functions of a completely color blind person," *Am. J. Phys.* **123**, 94–95 (1938).
- Hunt, D. M., Dulai, K. S., Bowmaker, J. K., and Mollon, J. D., "The chemistry of John Dalton's color blindness," *Science* **267**, 984–988 (1995).
- Ishihara, S., *Tests for Colour Blindness*, Kanehara Shuppan, Tokyo (1954).

- Judd, D. B., "Standard response functions for protanopic and deutanopic vision," *J. Opt. Soc. Am.* **35**, 199–221 (1945).
- Judd, D. B., "Standard response functions for protanopic and deutanopic vision," *J. Opt. Soc. Am.* **39**, 505–509 (1949).
- Judd, D. B., "A method for determining whiteness in paper," *Pap. Trade J.* **103**, 38–44 (1936); reprinted in *Selected Papers in Colorimetry—Fundamentals*, MacAdam, D. L., Ed., SPIE Press, Bellingham, WA (1993).
- Kippman, H., "Color measurement methods and systems in printing technology and graphic arts," *Proc. SPIE* **1912**, 278–1998 (1993). [doi:10.1177/12.146].
- Lewis, S. D. and Mandelbaum, J., "Achromatopsia: report of three cases," *Arch. Ophthalmol.* **30**, 225–231 (1943).
- MacAdam, D. L., "The specification of whiteness," *J. Opt. Soc. Am.* **24**, 188–191 (1934).
- McDonald, R., *Colour Physics for Industry*, 2nd ed., Society of Dyers and Colourists, West Yorkshire, U.K. (1997).
- Pearson, M., "Modern color measuring instruments," in *Optical Radiation Measurements: Color Measurement*, Vol. 2, Grum, F. and Bartleson, C. J., Eds., Academic, New York (1980).
- Pitt, F. H. G., "The nature of normal trichromatic and dichromatic vision," *Proc. R. Soc. London* **B1-32**, 101–117 (1944).
- Reitner, A., Sharpe, L. T., and Zrenner, E., "Is colour vision possible with only rods and blue-sensitive cones?" *Nature* **352**, 798–800 (1991).
- Rushton, W. A. H., "A cone pigment in the protanope," *J. Physiol.* **168**, 345–359 (1963).
- Rushton, W. A. H., "Visual pigment and color blindness," *Sci. Am.* **232**, 64–77 (1975).
- Sharpe, L. T., Stockman, A., Jägle, H., and Nathans, J., "Opsin genes, cone photopigments, color vision, and color blindness," in *Color Vision: From Genes to Perception*, Gegenfurtner, K. R. and Sharpe, L. T., Eds., Cambridge University Press, Cambridge, U.K. (1999).
- Thomas, P. B. M. and Mollon, J. D., "Modelling the Rayleigh match," *Visual Neurosci.* **21**, 477–482 (2004).
- Vienot, F., Brettel, H., Ott, L., Ben, M. B. A., and Mollon, J. D., "What do colour-blind people see? [letter]," *Nature* **376**, 127–128 (1995).
- Walls, G. L. and Heath, G. G., "Typical total color blindness reinterpreted," *Acta Ophthalmol.* **32**, 253–297 (1954).
- Walraven, P. L., "A closer look at the tritanopic confusion point," *Vision Res.* **14**, 1339–1343 (1974).

- Walraven, P. L., Van Hout, A. M. J., and Leebeek, H. J., "Fundamental response curves of a normal and a deuteranomalous observer derived from chromatic adaptation," *J. Opt. Soc. Am.* **56**, 125–127 (1966).
- Weidner, V. R. and Hsia, J. J., "Reflection properties of pressed polytetra-fluorethylene powder," *J. Opt. Soc. Am.* **71**, 856–861 (1981).
- Working Group 41, *Procedures for Testing Color Vision*, National Academy Press, Washington, DC (1981).
- Wright, W. D., "The characteristics of tritanopia," *J. Opt. Soc. Am.* **42**, 509–521 (1952).
- Zwinkels, J. C., "Errors in colorimetry caused by the measuring instrument," *Text. Chem. Colorist* **21**, 23–29 (1989).

General References

Books

American Society for Testing and Materials (ASTM), *ASTM Standards on Color and Appearance Measurement*, 3rd ed., ASTM, New York (1991).

Abney, W. D. W., *Researches in Colour Vision*, Longmans, London (1913).

Berger-Schunn, A., *Practical Color Measurement*, John Wiley & Sons, New York (1994).

Berns, R. S., Billmeyer, F. W., and Saltzman, M., *Billmeyer and Saltzman's Principles of color technology*, Wiley, New York (2000).

Billmeyer, F. W. Jr., and Saltzman, M., *Principles of Color Technology*, 2nd. ed., John Wiley & Sons, New York (1981).

Byrne, A., David, R. H., and Hilbert, D. R., Eds., *Readings on Color: The Science of Color*, MIT, Cambridge, MA (1997).

Boynton, R. M., *Human Color Vision*, Holt, Rinehart and Winston, New York (1979).

CIE, *Colorimetry*, CIE Publication No. 15.2-1986, 2nd. ed., CIE, Vienna (1986).

DeCusatis, C., *Handbook of Applied Photometry*, AIP Press, New York (1999).

Doherty, P. and Rathjen, D., *The Magic Wand and Other Bright Experiments on Light and Color*, John Wiley & Sons, New York (1995).

Fairchild, M. D., *Color Appearance Models*, Addison-Wesley, New York (1997).

Fortner, B., Meyer, T. E., and Meyer, T., *Number by Colors: A Guide to Using Color to Understand Technical Data*, Springer, Berlin (1997).

Gegenfurtner, K. R. and Sharpe, L. T., Eds., *Color Vision: From Genes to Perception*, Cambridge University Press, Cambridge, UK (1999).

Giorgianni, E. J. and Madden, T. E., *Digital Color Management: Encoding Solutions*, Addison-Wesley, New York (1998).

Hunt, R. W. G., *Measuring Colour*, 2nd ed., Ellis Horwood, Sussex, UK (1991).

Hunt, R. W. G., *The Reproduction of Colour*, Fountain Press, London (1996).

- Hunter, R. S. and Harold, R. W., *The measurement of appearance*, 2nd Ed., John Wiley & Sons, New York (1987).
- Judd, D. B. and Wyszecki, G., *Color in Business, Science and Industry*, 3rd ed., John Wiley & Sons, New York (1975).
- Kaiser, P. K. and Boynton, R. M., *Human Color Vision*, 2nd ed., Optical Society of America, Washington, DC (1996).
- LeGrand, Y., *Light, Colour and Vision*, 2nd ed., Chapman and Hall, London (1968).
- MacAdam, D. L., *Color Measurement: Theme and Variations*, 2nd ed., Springer, Berlin (1985).
- MacAdam, D. L., Ed., *Selected Papers in Colorimetry—Fundamentals*, SPIE Press, Bellingham, WA (1993).
- Minnaert, M. G. J., *The Nature of Light and Color in the Open Air*, Dover, New York (1954).
- Minnaert, M. G. J. and Seymour, L., *Light and Color in the Outdoors*, Springer, Berlin (1993).
- Mueller, C. G., and Rudolph, M., *Light and Vision*, Time-Life International, New York (1963).
- Nassau, K., Ed., *The Physics and Chemistry of Color: The Fifteen Causes of Color*, John Wiley & Sons, New York (1983).
- Nassau, K., Ed., *Color for Science, Art and Technology*, Elsevier Science B. V., Amsterdam, The Netherlands (1998).
- Parsons, J. H., *An Introduction to Colour Vision*, 2nd ed., Cambridge University Press, Cambridge, UK (1924).
- Rood, O. N., *Modern Chromatics, with Applications to Art and Industry*, Appleton, New York (1879).
- Sanguine, S. J. and Horne, R. E. N., Eds., *The Colour Image Processing Handbook*, Chapman and Hall, London (1998).
- Stiles, W. S., *Mechanisms of Colour Vision*, Academic, London (1978).
- Tilley, R. J. D., *Color and the Optical Properties of Materials: An Exploration of the Relationships Between Light, the Optical Properties of Materials and Color*, John Wiley & Sons, New York (2000).
- Volz, H. G. and Teague, B. (Trans.), *Industrial Color Testing: Fundamentals and Techniques*, John Wiley & Sons, New York (1995).
- Williamson, S. J., and Herman, Z. C., *Light and color in nature and art*, John Wiley & Sons, New York (1983).

Wyszecki, G., and Stiles, W. S., *Color Science: Concepts and Methods, Quantitative Data and Formulae*, 2nd ed., John Wiley & Sons, New York (1982).

From *Scientific American*

- Beck, J., "The perception of surface color," *Sci. Am.*, **233**, 62–75 (1975).
- Brindley, G. S., "Afterimages," *Sci. Am.*, **209**, 85–91 (1963).
- Brou, P., Sciascia, T. R., Linette, L., and Jerome, Y. L., "The colors of things," *Sci. Am.*, **255**, 80–87 (1986).
- Clevenger, S., "Flower pigments," *Sci. Am.*, **209**, 84–92 (1963).
- Evans, R. M., "Maxwell's color photograph," *Sci. Am.*, **205**, 112–128 (1961).
- Favreau, O. E. and Corballis, M. C., "Negative after effects in visual perception," *Sci. Am.*, **235**, 42–48 (1976).
- Gregory, R. L., "Visual illusions," *Sci. Am.*, **219**, 66–76 (1968).
- Horridge, A., "The compound eye of insects," *Sci. Am.*, **237**, 108–120 (1977).
- Kohler, I., "Experiments with goggles," *Sci. Am.*, **206**, 63–72 (1962).
- Land, E. H., "Experiments in color vision," *Sci. Am.*, **200**, 84–99 (1959).
- Land, E. H., "The retinex theory of color vision," *Sci. Am.*, **237**, 108–128 (1977).
- Lerman, S., "Cataracts," *Sci. Am.*, **206**, 106–114 (1962).
- Levine, J. S., and MacNichol, E. F., Jr., "Color vision in Fishes," *Sci. Am.*, **246**, 108–117 (1982).
- MacNichol, E. F., Jr., "Three pigment color vision," *Sci. Am.*, **211**, 48–56 (1964).
- Michael, C. R., "Retinal processing of visual images," *Sci. Am.*, **220**, 104–114 (1969).
- Milne, L. J. and Milne, M. J., "How animals change color," *Sci. Am.*, **186**, 64–67 (1952).
- Nathans, J., "The genes for color vision," *Sci. Am.*, **260**, 28–35, (1989)
- Nassau, K., "The causes of color," *Sci. Am.*, **243**, 124–152 (1980).
- Neisser, U. "The processes of vision," *Sci. Am.*, **219**, 204–214 (1968); reprinted in *Lasers and Light*, Schawlow, A. L., Ed., W. H. Freeman, San Francisco (1969).
- Newman, E. A., and Hartline, P. H., "The infrared vision of snakes," *Sci. Am.*, **246**, 98–107 (1982).
- Nijhout, H. F., "The color patterns of butterflies and moths," *Sci. Am.*, **245**, 104–115 (1981).
- Pettigrew, J. D., "The neurophysiology of binocular vision," *Sci. Am.*, **227**, 84–95 (1972).

- Rushton, W. A. H., "Visual pigments in man," *Sci. Am.*, **207**, 120–132 (1962).
- Rushton, W. A. H., "Visual pigment and color blindness," *Sci. Am.*, **232**, 64–77 (1975).
- Smith, N., "Color television," *Sci. Am.*, **182**, 13–15 (1950).
- Thimann, K. V., "Autumn colors," *Sci. Am.*, **182**, 40 (1950).
- Timberge, N., "Defense by color," *Sci. Am.*, **197**, 48–54 (1957).
- Van Heyningen, R., "What happens to the human lens in cataract," *Sci. Am.*, **233**, 70–81 (1975).
- Wallach, H., "The perception of neutral colors," *Sci. Am.*, **208**, 107–116 (1963).
- White, H. E. and Levatin, P., "Floaters in the eye," *Sci. Am.*, **206**, 119–127 (1962).
- Wolfe, J. M., "Hidden visual processes," *Sci. Am.*, **248**, 72–85 (1983).
- Young, R. W., "Visual cells," *Sci. Am.*, **223**, 80–91 (1970).

Review Articles

- Boynton, R. M., "Color vision," *Annu. Rev. Psychol.*, **39**, 69–100, 1988.
- Boynton, R. M., "History and current status of a physiologically based system of photometry and colorimetry," *J. Opt. Soc. Am. A*, **13**, 1609–1621 (1996).
- Luria, S. M., "Color vision," *Phys. Today*, **19**, 34–41 (1966).
- MacAdam, D. L., "Color photography," *Phys. Today*, **20**, 27–39 (1967).
- MacAdam, D. L., "Color essays," *J. Opt. Soc. Am.*, **65**, 483–493 (1975).
- Mollon, J. D., "Color vision," *Annu. Rev. Psychol.*, **33**, 41–85 (1982).
- Robertson, A. R., "Color perception," *Phys. Today*, **45**, December, Pags. 24–29 (1992).
- Wald, G., "Human vision and the spectrum," *Science*, **101**, 653–658 (1945).
- Wintringham, W. T., "Color television and colorimetry," *Proc. IRE*, **39**, 1135–1172 (1951).

Internet Sites

International Commission on Illumination

This is the official site of the International Commission on Illumination (CIE). It contains the information on all color standards.

<http://www.cie.co.at>

Efg's Color Library

This page contains a very large amount of color information, with many web addresses, classified in three subjects: (a) General Color Information, (b) Color Science/Theory, and (c) Color and Computers.

<http://www.efg2.com/Lab/Library/Color/>

Color and Vision Research Laboratories, Institute of Ophthalmology, London

These Web pages provide a very good library of easily downloaded standard data sets relevant to color and vision research. The focus of this site is primarily scientific and technical.

<http://www.cvrl.org/>

The Coloring Info Pages

This site contains some interesting information. Of special interest are some calculators to convert coordinates between different color systems.

<http://www.colorpro.com/info/>

Color Science

This web page by the Department of Physics and Astronomy of the Stephen F. Austin State University has a lot of interesting educational information about color science.

<http://www.physics.sfasu.edu/astro/color.html>

Coordinate Converter

This is a web page by the Lappeerants University of Technology in Finland. It has several interesting demonstrations and color coordinate converters, and it includes some links to other color sites.

<http://www.it.lut.fi/research/color/coordinates/coordinates.html>

Linocolor

This page is by the Linocolor Company. It has some interesting educative color pages.

<http://www.linocolor.com/>

Index

A

absolute temperature, 16
absorption filters, 18
accuracy, 156
adaptation, 59, 97
adaptive optics, 43, 50
addition of colors, 59
additive mixing of color, 131
alychné, 72, 76
anomaloscope, 147
aqueous humor, 42
autosome, 48

B

bandpass filters, 18
blackbody, 16
blackbody radiation, 23
blackbody radiators, 90
blackbody spectral radiance, 25
Boltzmann's constant, 23
brightness, 12
Brücke–Bartley effect, 46

C

candela, 11
Celsius temperature, 16
cholesteric liquid crystals, 32
chroma, 3, 48, 104, 107, 120
chroma difference, 121, 122, 124
chromatic aberration, 44
chromatic adaptation, 7, 52
chromaticity coordinates, 68, 69, 71, 82, 85, 86
CIE chromaticity diagram, 84

CIE color space, 103
CIE color specification system, 75
CIE diagram, 90
CIE illuminant, 95
CIE $L^*a^*b^*$ color solid, 119
CIE $L^*a^*b^*$ color space, 116, 120
CIE $L^*a^*b^*$ color system, 115
CIE $L^*u^*v^*$ color solid, 112
CIE $L^*u^*v^*$ color space, 112
CIE XYZ system, 135
CIELAB, 116
CIELAB uniform color system, 133
CIELCH system, 119, 121
CIELUV, 112
CIELUV color-difference equation, 114
CIE $L\ u\ v$ color space, 110
ciliary muscles, 42
CMYK, 138
color addition, 131
color defects, 147
color discrimination, 97, 99
color management, 140
color matching, 59, 140
color measurement, 147
color mixtures, 131
color saturation, 3
color sensitivity of the eye, 14
color spaces, 127
color subtraction, 137
color television, 133
color temperature, 16, 18, 23, 24, 151
color-blind people, 149

color-difference equation, 114, 120, 124
 color-matching experiments, 60
 color-matching functions, 63, 66, 76, 79, 81, 99
 color-rendering index (CRI), 35
 colorants, 131, 140
 colored filter, 137
 colorimeter, 142
 colorimeter, tristimulus, 97
 colorimeter, visual, 161
 colorimetry, 59, 63
 Colour Measurement Committee (CMC), 122
 complementary wavelength, 89
 computer displays, 31
 cone absorbance, 52
 cone fundamentals, 51, 99
 cone sensitivities, 99
 cones, 44
 confocal microscope, 50
 constant chroma curves, 105
 cornea, 41
 corneal astigmatism, 42
 correlated color temperature (CCT), 24, 33, 38, 85, 90
 critical flickering frequency, 46
 critical fusion frequency, 46
 crystalline lens, 42
 cyan/magenta/yellow (CMY) system, 138

D

D-15 color arrangement tests, 149
 Daltonism, 147
 daylight color vision, 47
 Derrington, Krauskopf, and Lennie (DKL) color space, 125
 deuteranomalous, 147
 deutanopes, 148
 deutanopia, 52
 dichromats, 147
 dominant wavelength, 85, 89
 dyes, 140

E

electromagnetic spectrum, 1
 emmetropic eye, 44
 error classification, 157
 excitation purity, 89
 eye aberrations, 44
 eye resolving power, 44
 eye, anatomy of, 41
 eye, human, 41
 constants, 42

F

Ferry–Porter law, 46
 filters, 18
 flashlamp, 27
 flicker, 45
 fluorescence, 155
 fluorescent lamp, 24, 26
 fovea, 43
 fovea centralis, 47, 64
 fundus cameras, 49

G

gas discharge lamp, 26
 Grassmann laws, 59

H

halogen lamp, 26
 heterochromatic photometry, 47
 hue, 2, 3, 48, 90, 104, 107
 hue difference, 124
 Hunter *L a b* color space, 114
 Hunter space, 116

I

illuminance, 10
 illuminants, 23, 33
 incandescent temperature lamp, 24
 integrating sphere, 154
 interference filters, 18
 irradiance, 9
 Ishihara plates, 149
 Ishihara pseudoisochromatic test, 149
 isoluminant, 126

K

Kelvin temperature, 16
keratoconus, 42
Kubelka–Munk theory, 142

L

L-cones, 148
Land's theory, 7
lens, eye, 42
light diffraction, 44
light source, purity of a, 135
light sources, 23, 133
light-emitting diode (LED), 28
lightness, 12
lightness difference, 122, 124
liquid crystals, 32
lumens, 82
luminance, 11, 62, 82, 90
luminosity function, 76
luminous efficacy, 12, 29
luminous exitance, 10
luminous flux, 10, 25
luminous intensity, 11
luminous power efficiency, 25
luminous reflectance, 14, 92
luminous sensitivity, 13
luminous transmittance, 14
lux, 10

M

M-cones, 47, 148
MacAdam ellipses, 103, 105, 110
MacAdam limits, 117
Macbeth color checker, 151
MacLeod and Boynton chromaticity diagram, 125
macula lutea, 43
matched field, 60
Maxwell spot, 80
Maxwell triangle, 59
McCollough effect, 8
metallic objects, 156
metameric color, 140
metameric pair, 139, 149
metamerism, 138

microspectrophotometry, 48

monochromat, 148
monochromatic color, 2
monochromator, 155
Munsell circle, 107
Munsell color space, 107
Munsell colors, 114
Munsell renotation system, 107
Munsell renotations, 107
Munsell system, 105

N

neutral colors, 112
Newton's color experiment, 4

O

opaque body, 91
ophthalmometer, 42
ophthalmoscopes, 49
opponent colors, 84
opposing colors, 98
organic light-emitting diode (OLED), 30

P

Pantone colors, 151
pearlescent objects, 156
photocolorimeters, tristimulus, 159
photometric units, 8, 10
photopic curve, 15
photopic relative luminous sensitivity, 62
photopic vision, 47
photopigments, 14, 52, 100
pigments, 140
Planck's constant, 23
Planckian locus, 90
polychromatic light, 13
power spectrum, 23
precision, 156
protanomalous, 147
protanopes, 148
protanopia, 52
pseudostereopsis, 44
pulsating light, 45

pulsed xenon lamp, 157
pupil, 42

R

radiant exitance, 9
radiant flux, 8
radiant incidence, 9
radiant intensity, 9
radiometric units, 8
random errors, 156
Rayleigh matching test, 147
reference field, 60
reflectance, 14
reflectance measurements, 152
relative luminance, 63
relative luminous efficiency, 15, 82
relative photopic luminous efficiency, 61
relative radiance, 63
relative spectral luminous efficiency, 13
relative spectral radiances, 37, 63
repeatability, 156
reproducibility, 156
retina, 43, 47, 48
retinex theory, 7
RGB color system, 133
RGB LED, 28
RGB system, 135

S

S-cones, 47, 147
saturation, 3, 89, 90, 120
scanning-laser ophthalmoscope, 49
scotopic curve, 16
scotopic vision, 47
seeing, 50
sodium lamp, 27
spatial resolution, 43
spectral illuminance, 10
spectral irradiance, 9, 92
spectral luminance, 12, 62
spectral luminous efficiency, 12, 13
spectral luminous intensity, 11
spectral luminous reflectance, 14

spectral luminous transmittance, 14
spectral radiance, 25, 82
spectral radiant intensity, 9
spectral reflectance, 14, 93, 139, 156, 158
spectral reflection, 17
spectral reflectivity, 23
spectral relative luminous efficiency, 80
spectral transmission, 17
spectrally pure colors, 1, 70, 75
spectrally pure monochromatic colors, 69
Spectralon standards, 151
spectrocolorimeters, 157
spectrogoniometer, 156
specular reflection, 152
spherical aberration, 45
standard illuminant, 35, 37, 93
standard light sources, 33
standard observer, 11
Stiles–Crawford effect, 45
stimuli, 75
stimuli values, 63
systematic errors, 156

T

television displays, 31
thermochromism, 158
transmittance, 14
transparent body, 91
trichromatic, 59
trichromatic theory, 7, 59
trichromats, 147
 anomalous, 147
tristimuli, 76
tristimulus colorimeter, 97
tristimulus photocalorimeters, 159
tristimulus values, 64, 70, 82, 92, 93, 158
tritanomalous, 147
tritanopia, 148
troland, 46
Tungsten lamps, 24

U

uniform color scales, 110
uniform color systems, 103

V

visual chromatic defects, 147, 148
visual colorimeters, 161
visual detectors, 47
vitreous humor, 42

W

wavefront deformations, 50

white reference tile, 158

white standards, 150

whiteness, 150

Wien's displacement law, 23

Wratten filters, 18

Y

yellow–blue discrimination, 48

Z

zero-luminance plane, 72



Daniel Malacara obtained his B.Sc. in Physics in 1961 from the National University of Mexico and his Ph.D. in Optics in 1965 from the University of Rochester. At that time, he joined the Institute of Astronomy of the National University of México, and in 1972 he joined the *Instituto Nacional de Astrofísica, Óptica y Electrónica*. He promoted the creation of the *Centro de Investigaciones en Óptica* and served as its first General Director from 1980 to 1989. He was the Rudolf and Hilda Kingslake Professor at the University of Rochester in 1989 and 1990.

Dr. Malacara's central field of activity is optical testing and optical instrumentation. His scientific contributions include more than one hundred papers in well-known optics journals, and he has been the author and editor of several books in optics. His most widely acknowledged book, *Optical Shop Testing*, has been translated into several languages. He is a fellow of both SPIE, and the Optical Society of America (OSA). He has been vice president of the International Commission for Optics (ICO), a topical Editor for *Applied Optics*, and he has been a co-organizer of many international scientific meetings. In 1986 he received the Mexican National Prize for Technology; in 1994, SPIE's Conrady Award; and, in 1997, the ICO Galileo Galilei Prize.

Color Vision and Colorimetry

THEORY AND APPLICATIONS

Second Edition

Daniel Malacara

In 1671, Isaac Newton demonstrated color dispersion by positioning a triangular prism in a narrow beam of sunlight and projecting bands of differently colored lights onto a white surface. The spectrum had been discovered. Since that historic experiment, color has been the subject of intensive study.

The second edition has been rewritten, updated, and enlarged, now including description of LEDs, new types of displays, explanation of color-formation techniques, and new studies on the eye. It continues to provide a number of concepts, definitions, and tools useful to students who wish to develop a basic understanding of colorimetry and color vision. The history of color is described, along with the main methods used to measure color and their associated color systems, and the human eye and its color detectors are explained in detail. Those who have experience in the field will find a compendium of data and other information, including the mathematical procedure for transforming the r, g, b system to the CIE x, y, z system, as well as many tables with colorimetric data and standards for working in color-measuring systems. Numerous references throughout and at the end of the book provide a considerable bibliography for readers looking to deepen their knowledge of this fascinating subject.

Contents:

- The Nature of Color
- Light Sources and Illuminants
- The Human Eye
- Trichromatic Theory
- CIE Color Specification System
- Uniform Color Systems
- Color Mixtures and Colorants
- Color Measurements and Color Defects

ISBN 978-0-8194-8397-3



9 0 0 0 0

9 780819 483973



P.O. Box 10
Bellingham, WA 98227-0010

ISBN: 9780819483973
SPIE Vol. No.: PM204